AIIM

Association for Information and Image Management
1100 Wayne Avenue, Suite 1100
Silver Spring, Maryland 20910
301/587-3202

Centimeter

Inches

MANUFACTURED TO AIIM STANDARDS
BY APPLIED IMAGE, INC.

1 of 3

CONF-930412--

BNL-48880

MESON INTERFEROMETRY IN RELATIVISTIC HEAVY ION COLLISIONS

Brookhaven National Laboratory
April 16–17, 1993

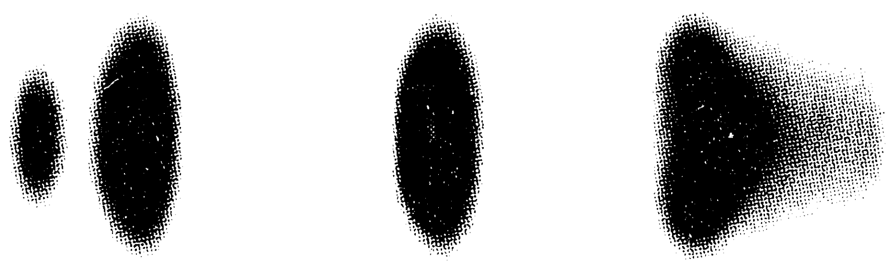

Organizers:

George Bertsch (NINT)
Carl Dover (BNL)
Miklos Gyulassy (Columbia)

Transparencies shown at
a Workshop
held
April 16–17, 1993
at
Brookhaven National Laboratory

sponsored jointly by
the National Institute of Nuclear Theory
Seattle, Washington
and
the Nuclear Theory Group, BNL

Cover: An arcists representation of baryon density in Si+Au at 14.6 GeV-A/C.

This manuscript has been authored under contract number DE-AC02-76CH00016 with the U.S. Department of Energy. Accordingly, the U.S. Government retains a non-exclusive, royalty-free license to publish or reproduce the published form of this contribution, or allow others to do so, for U.S. Government purposes.

TABLE OF CONTENTS

Recent HBT Results from CERN Experiment NA44

Tom Humanic
Ohio State University

THE NA44 COLLABORATION

Brookhaven Nat. Lab., Cern, Columbia Univ.,
Creighton Univ., Hiroshima Univ., Los Alamos Nat. Lab.,
Lund Univ., Tbilisi State Univ., Tsukuba Nat. Lab.,
Niels Bohr Inst., Pittsburgh Univ., Tokyo Univ.,
Tsukuba Univ., OHIO STATE UNIV.,
TEXAS A+M

H.Atherton, H.Bøggild, J.Boissevain, K.Bussmann,
M.Cherney, E.Chesi, G.DiTore, J.Dodd, J.Downing,
S.Esumi, C.W.Fabjan, A.Franz, K.H.Hansen, T.Humanic,
T.Ikemoto, B.Jacak, R.Jayanti, H.Kalechofsky,
T.Kobayashi, R.Kuatadze, Y.Y.Lee, M.Leltchouk, D.Linker,
B.Lörstad, N.Maeda, A.Medvedev, Y.Miake,
A.Miyabayashi, M.Murray, S.Nagamiya, S.Nishimura,
E.Noteboom, S.U.Pandey, P.Peters, F.Piuz,
V.Polychronakos, M.Potekhin, G.Poulard, D.Rahm,
J.M.Rieubland, A.Sakaguchi, M.Sarabura, K.Shigaki,
J.Simon-Gillo, W.Sondheim, T.Sugitate, J.Sullivan, Y.Sumi,
J.Sunier, H.Sletten, H.Tam, H.vanHecke, D.Williams,
G. VILKELIS, K. WOLF, W.Willis, T.Zhu

EXPERIMENT NA44

$\sigma_p / p = 0.2\%$

$\Delta p / p = \pm 10\%$ (p - BITE)

$\Delta\Omega = 0.8$ MSR

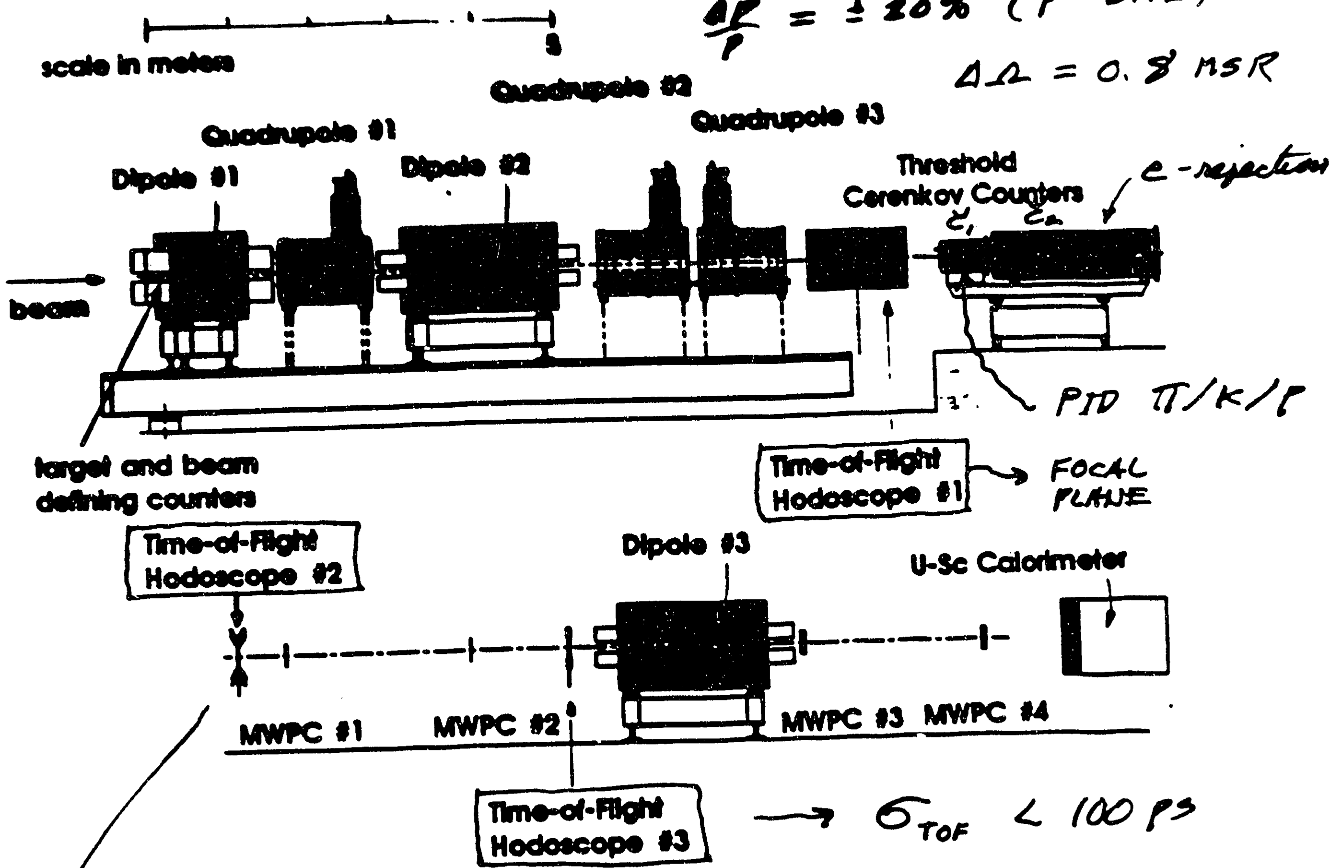

$\rightarrow \sigma_{TOF} < 100$ ps

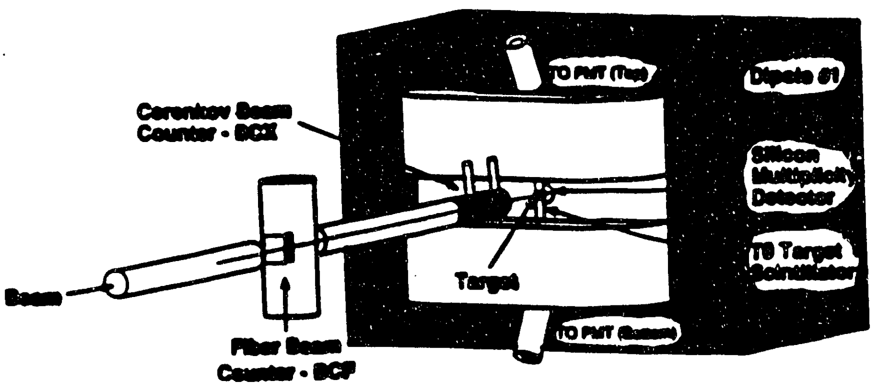

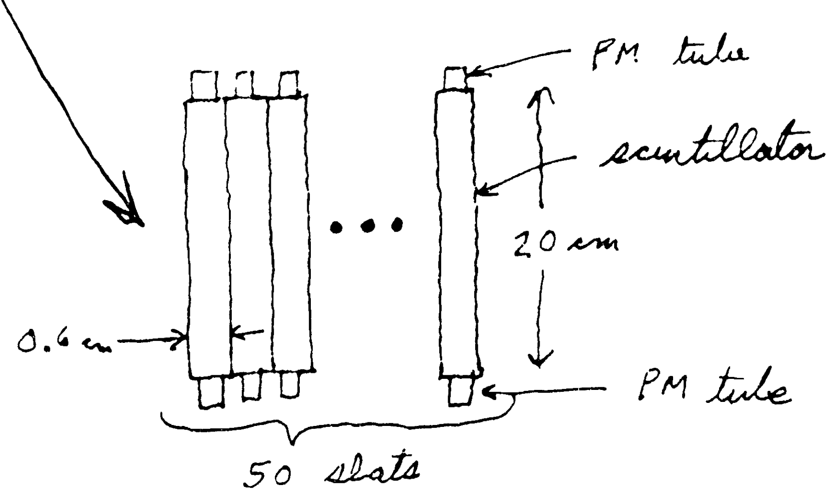

Picket - fence TOF hodoscope

Quadrupole Configuration for the Normal Setting.

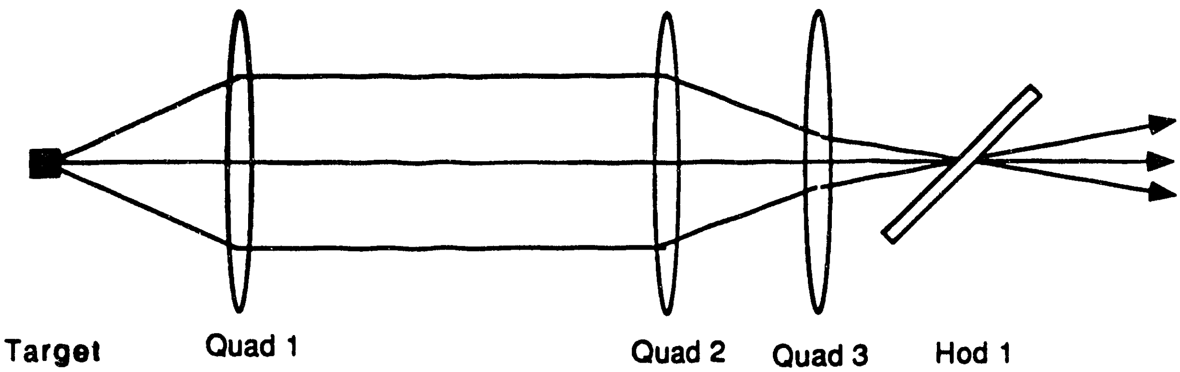

Figure 1: Quadrupole configuration in the horizontal plane.

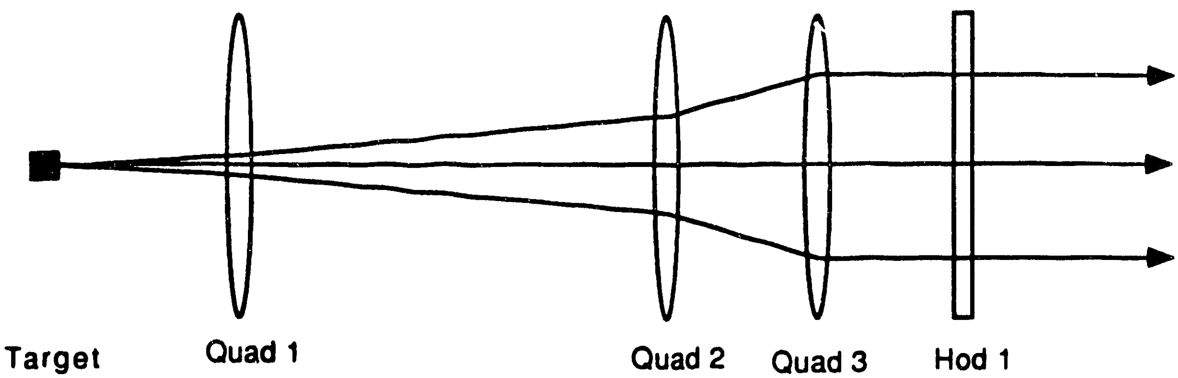

Figure 2: Quadrupole configuration in the vertical plane.

NA44 Acceptances

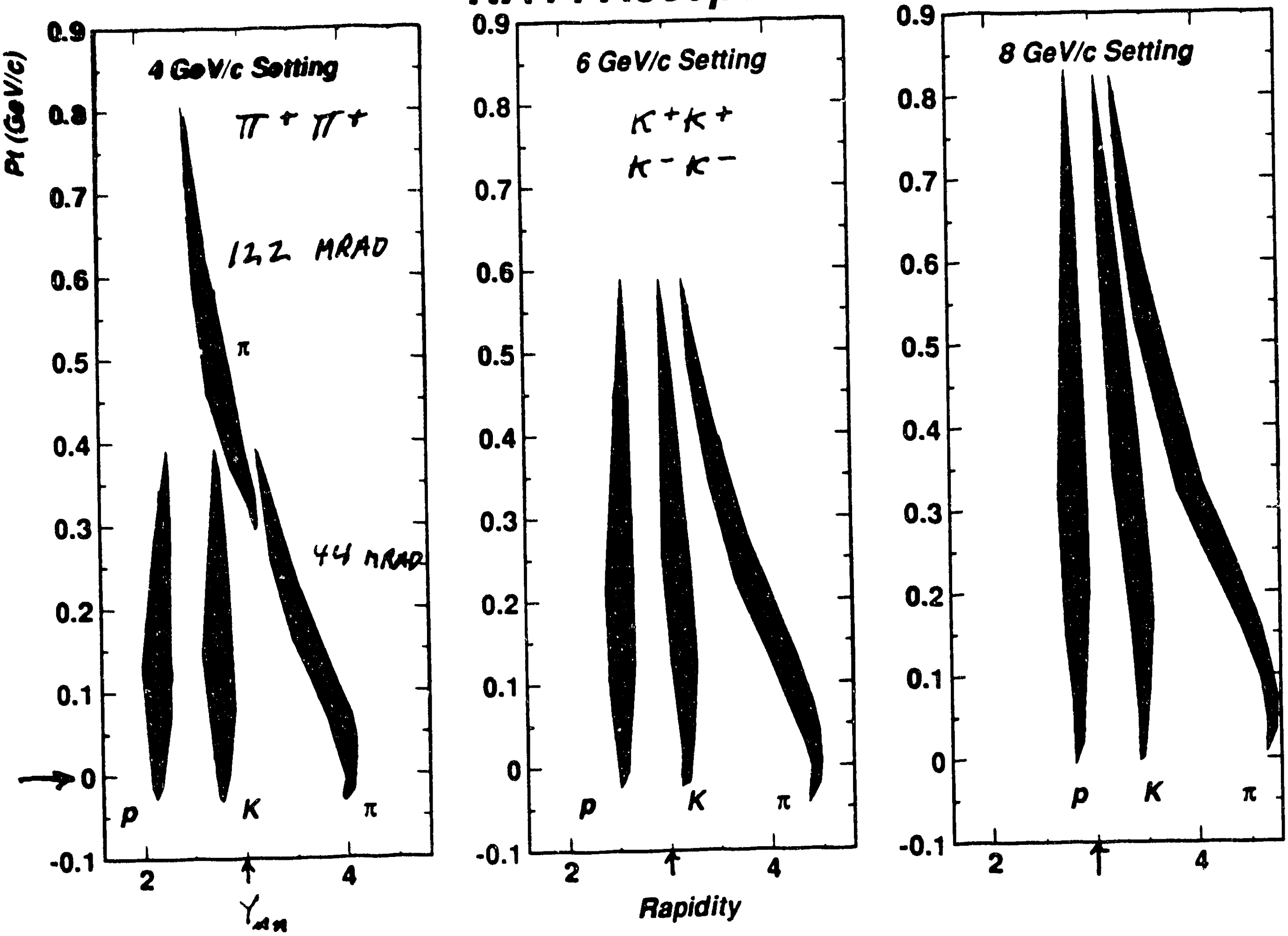

Particle Identification in Experiment NA44

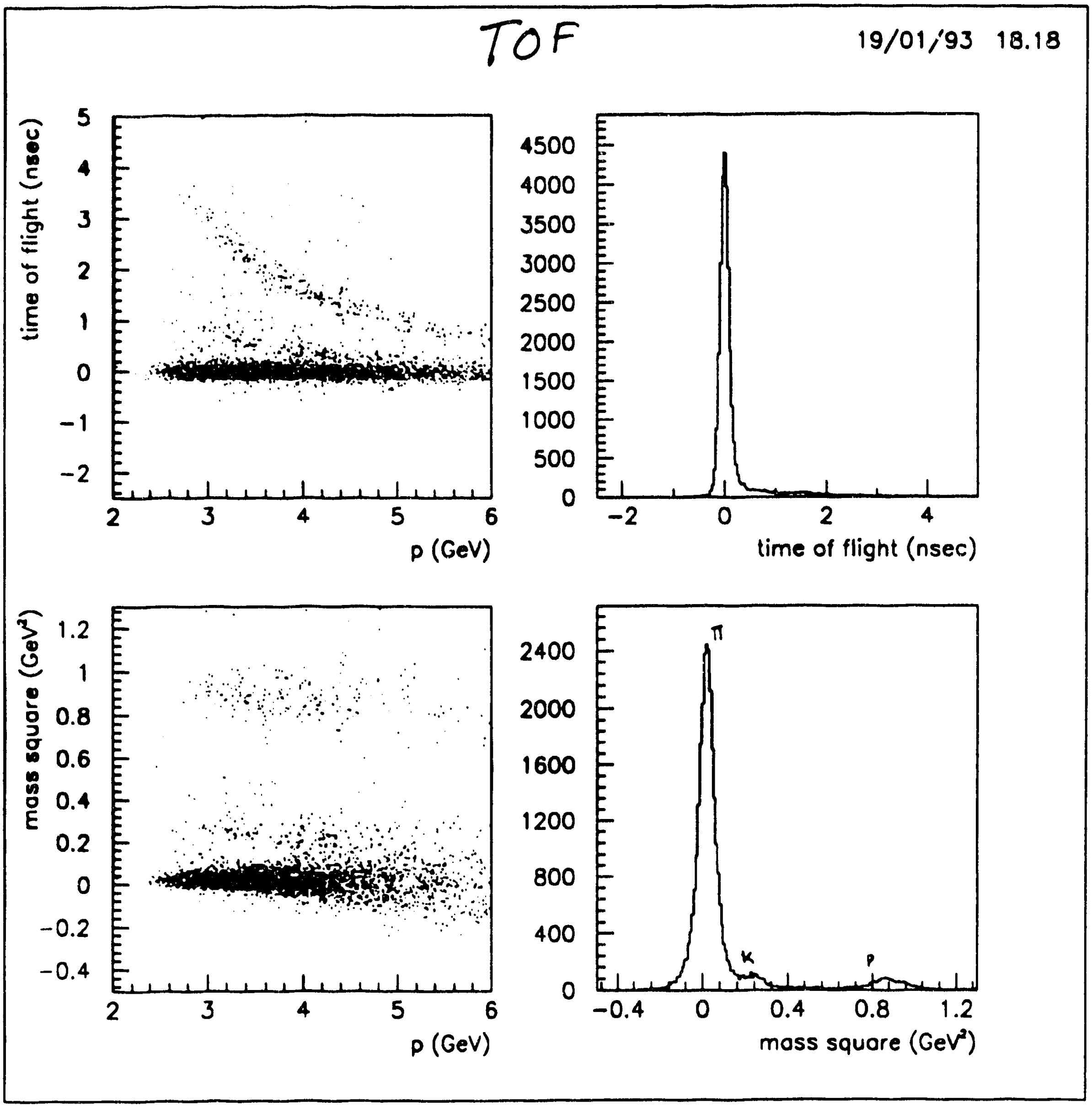

$m^2 = p^2\left(\frac{1-\beta^2}{\beta^2}\right)$

TOF & P INFORMATION

$\longrightarrow m^2$

Čerenkovs

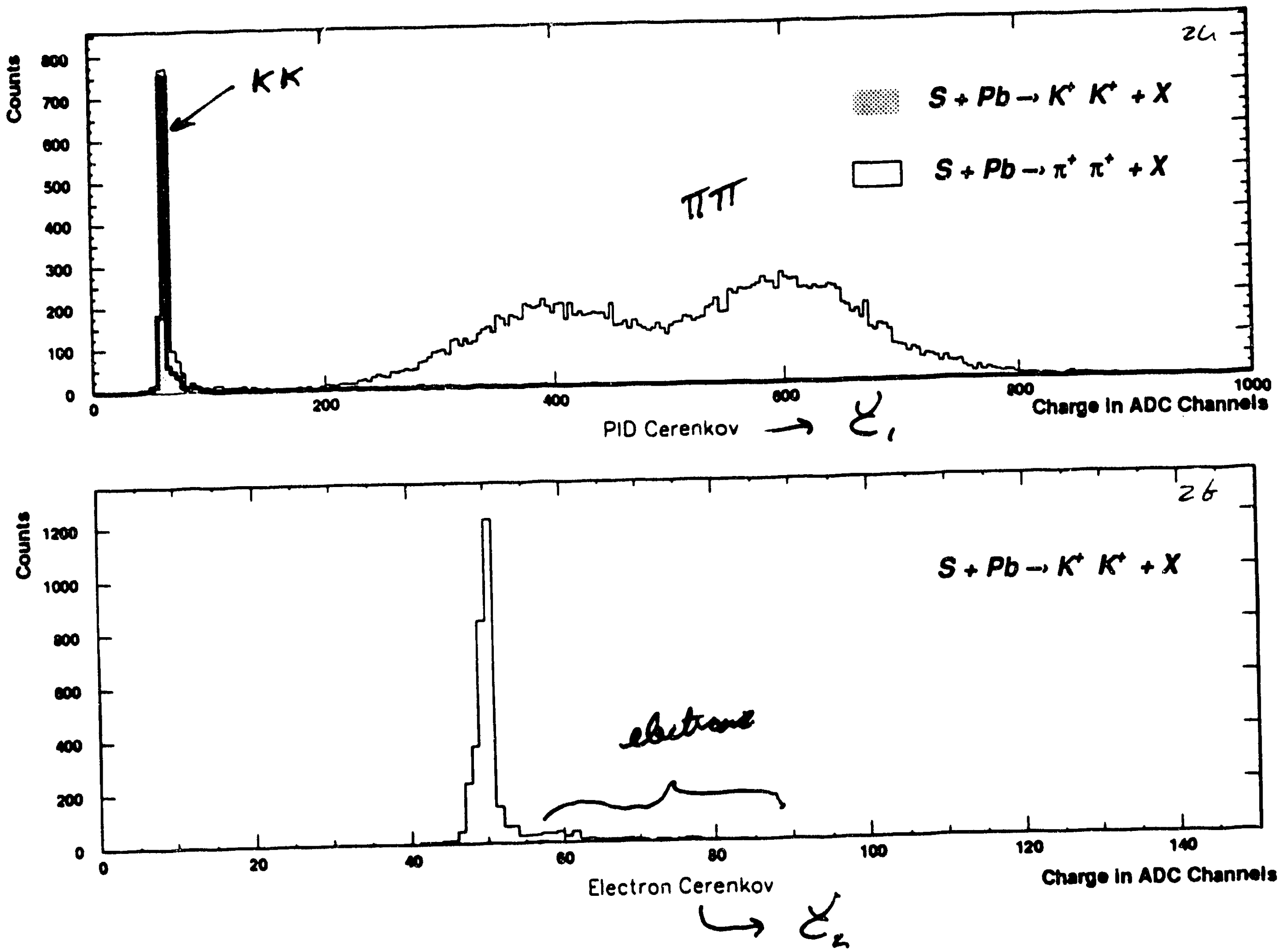

2a
Counts
800
700
600
500
400
300
200
100
0
KK
S + Pb → K⁺ K⁺ + X
S + Pb → π⁺ π⁺ + X
ππ
0
200
400
600
800
1000
Charge in ADC Channels
PID Cerenkov → Č1
2b
Counts
1200
1000
800
600
400
200
0
S + Pb → K⁺ K⁺ + X
electrons
0
20
40
60
80
100
120
140
Charge in ADC Channels
Electron Cerenkov → Č2

Cutting on τ, produces clean K, P

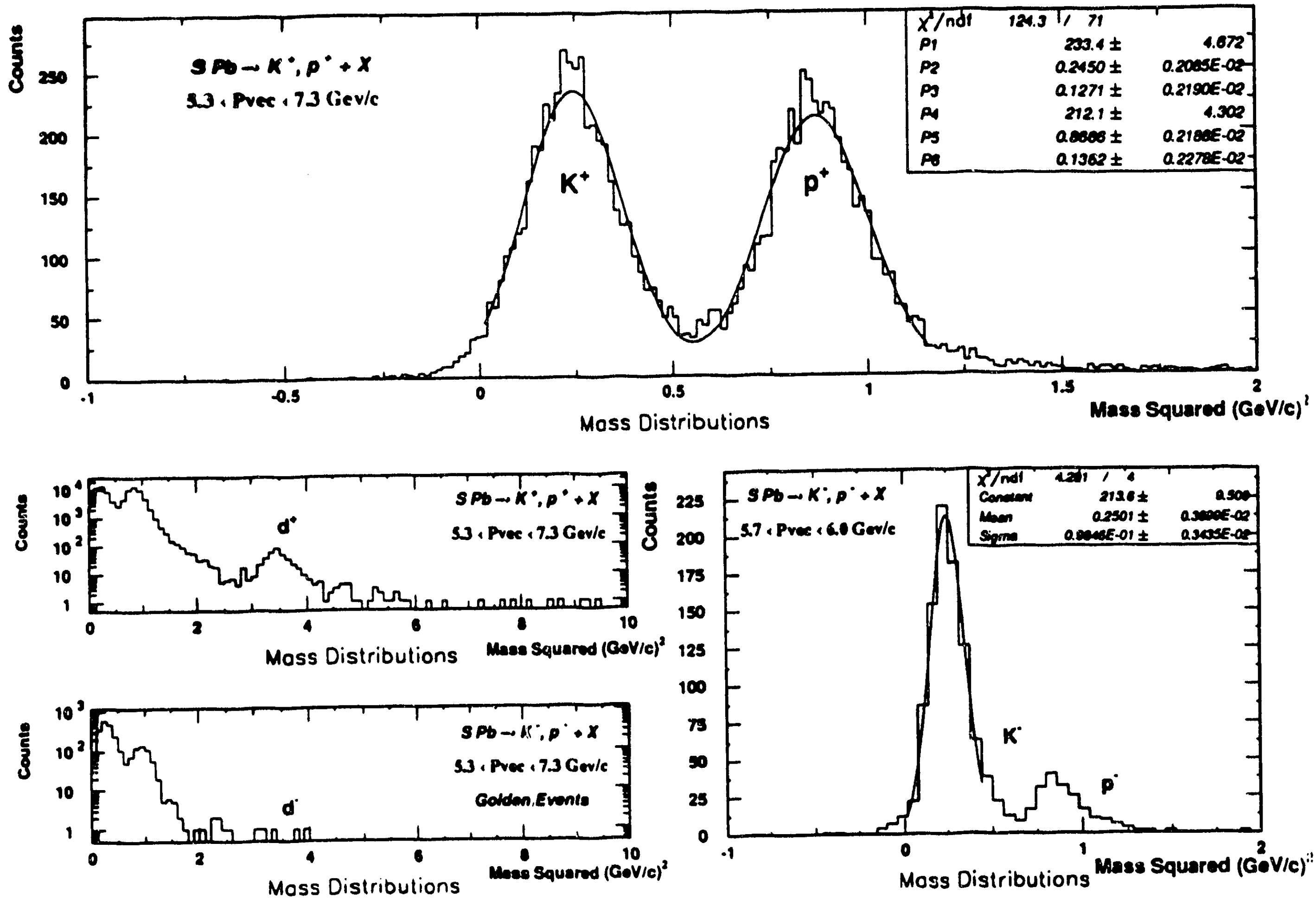

Effect of 2 particles in spectrometer on centrality of collision

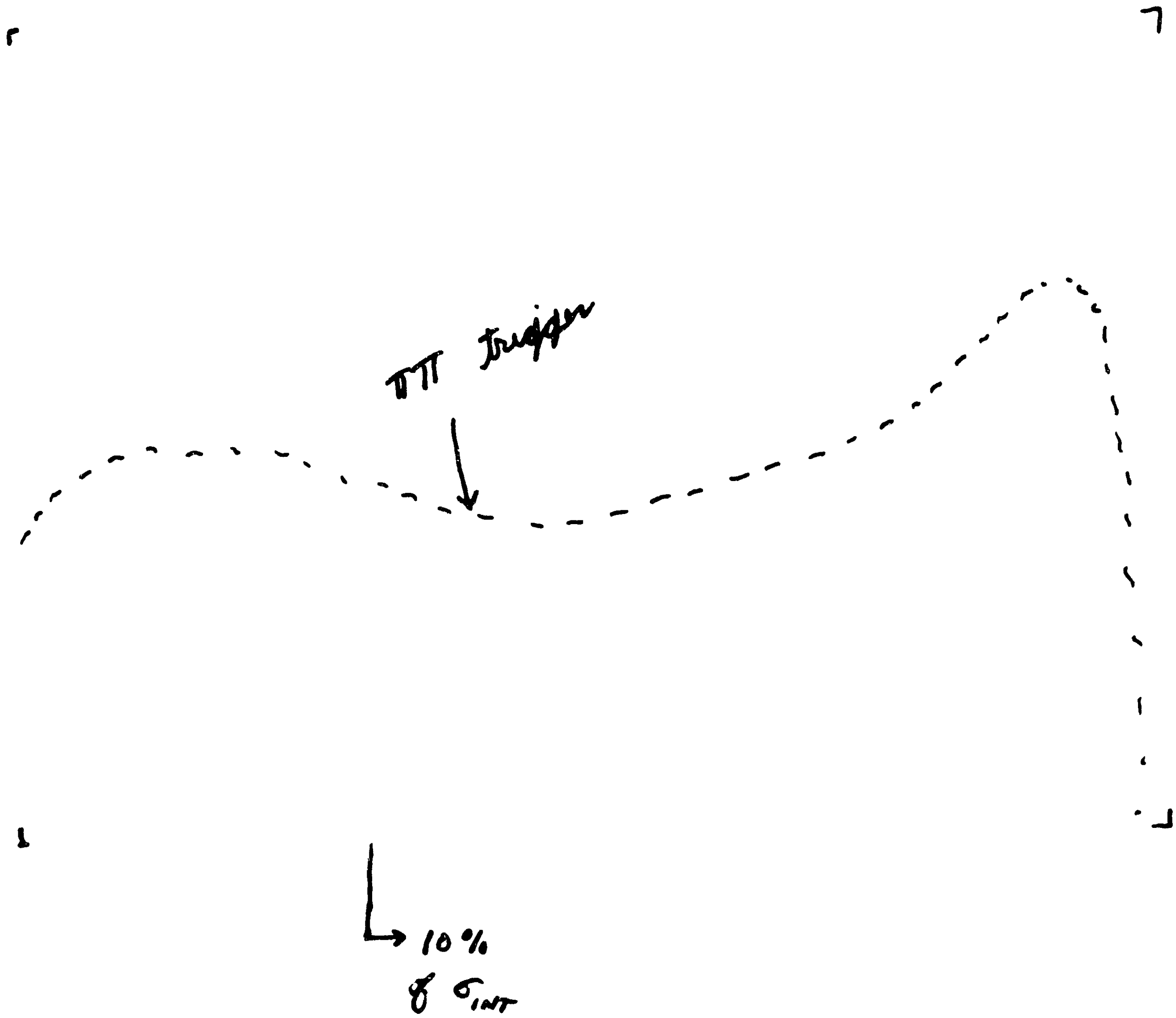

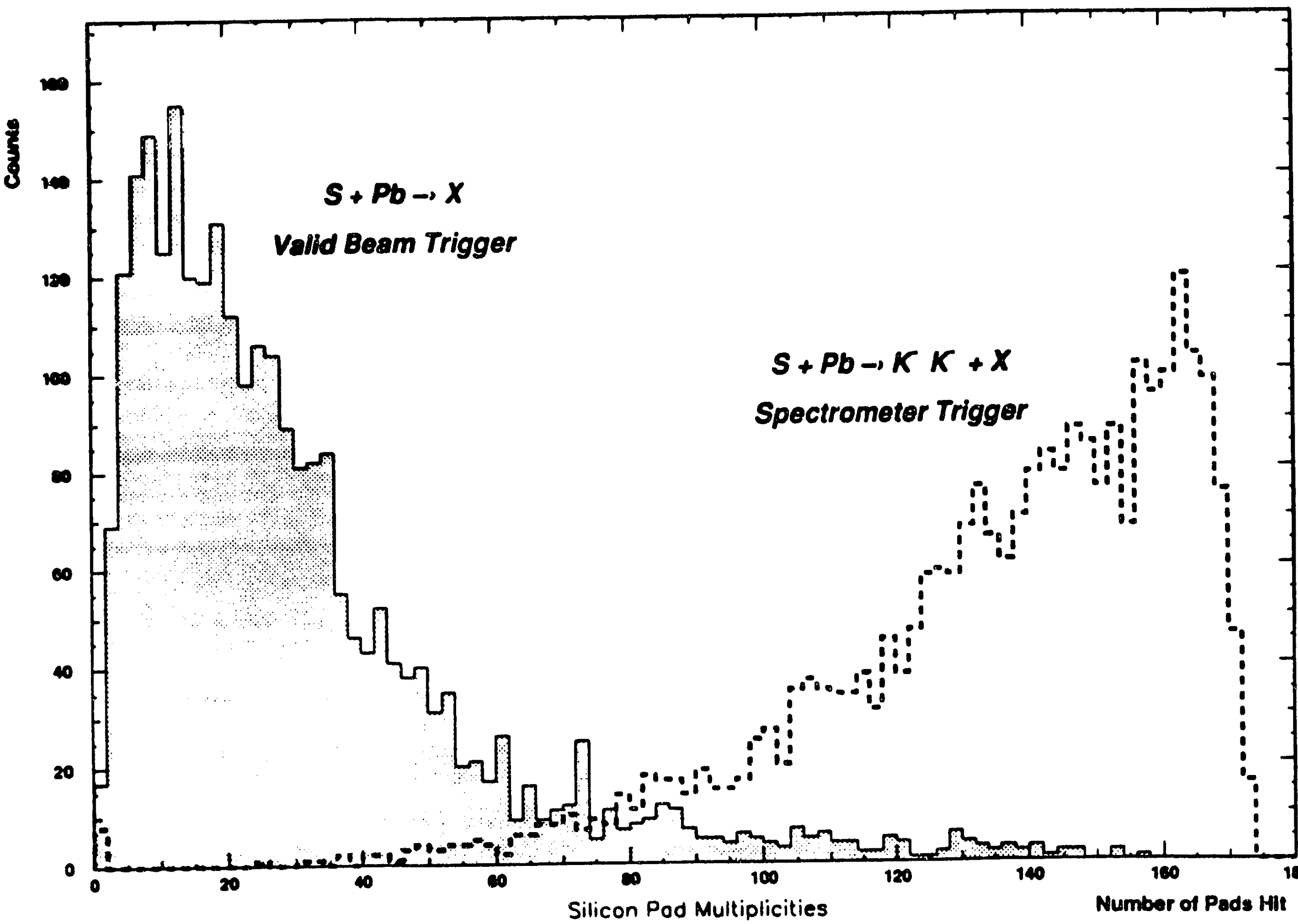

Counts
160
140
120
100
80
60
40
20
0
S + Pb → X
Valid Beam Trigger
S + Pb → K K + X
Spectrometer Trigger
0
20
40
60
80
100
120
140
160
180
Silicon Pad Multiplicities
Number of Pads Hit

NA44 Preliminary Results

$\longrightarrow$ HBT

$$p + Pb \rightarrow \begin{cases} \pi^+ \pi^+ \\ K^+ K^+ \end{cases}$$

$$S + Pb \rightarrow \begin{cases} \pi^+ \pi^+ \leftarrow \text{(44 AND 122 MRAD SETTINGS)} \\ K^+ K^+ \\ K^- K^- \end{cases}$$

• EXPERIMENTAL DEFINITION OF $C(Q)$

$$C(Q) \equiv \frac{A(Q)}{B(Q)}$$

$A(Q) \equiv$ MEASURED DISTRIBUTION
(REQUIRE TWO PARTICLES IN TRIGGER)

$B(Q) \equiv$ BACKGROUND DISTRIBUTION FROM MIXED EVENTS.

FITTING FUNCTIONS :

$$C(Q_{inv}) \equiv N\left[1 + \lambda e^{-Q_{inv}^2 R_{inv}^2}\right]$$

$$C(Q_{inv}) \equiv N\left[1 + \lambda e^{-2 Q_{inv} R_{inv}}\right]$$

$$C(Q_{TO}, Q_{TS}, Q_L) \equiv N\left(1 + \lambda e^{-Q_{TO}^2 R_{TO}^2 - Q_{TS}^2 R_{TS}^2 - Q_L^2 R_L^2}\right)$$

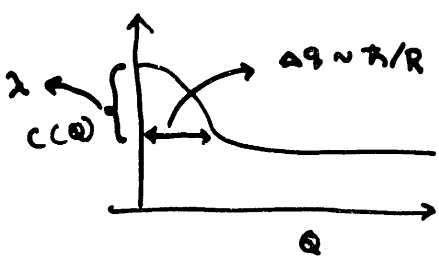

DATA ANALYSIS

RAW DATA

↓

CALIBRATIONS

↓

TRACK RECONSTRUCTION → MOMENTA (Straight line trajectory from magnet, minimize χ^2)

↓

DATA QUALITY CUTS

↓

HBT STUDY, ERROR ANALYSIS MONTE CARLO CORRECTIONS, FITS

DATA ANALYSED

200 GeV S + Pb] → $\pi^+\pi^+ + X$ (Also K^+ & K^-)

$\sqrt{s} = 20$ GeV

44mrad & 122mrad

~~200 GeV~~ P + Pb] → $\pi^+\pi^+ + X$ (K^+ & K^-)

450 GeV

44mrad.

$\pi^+ \pi^+$ results
(small angle → 44 MRAD)

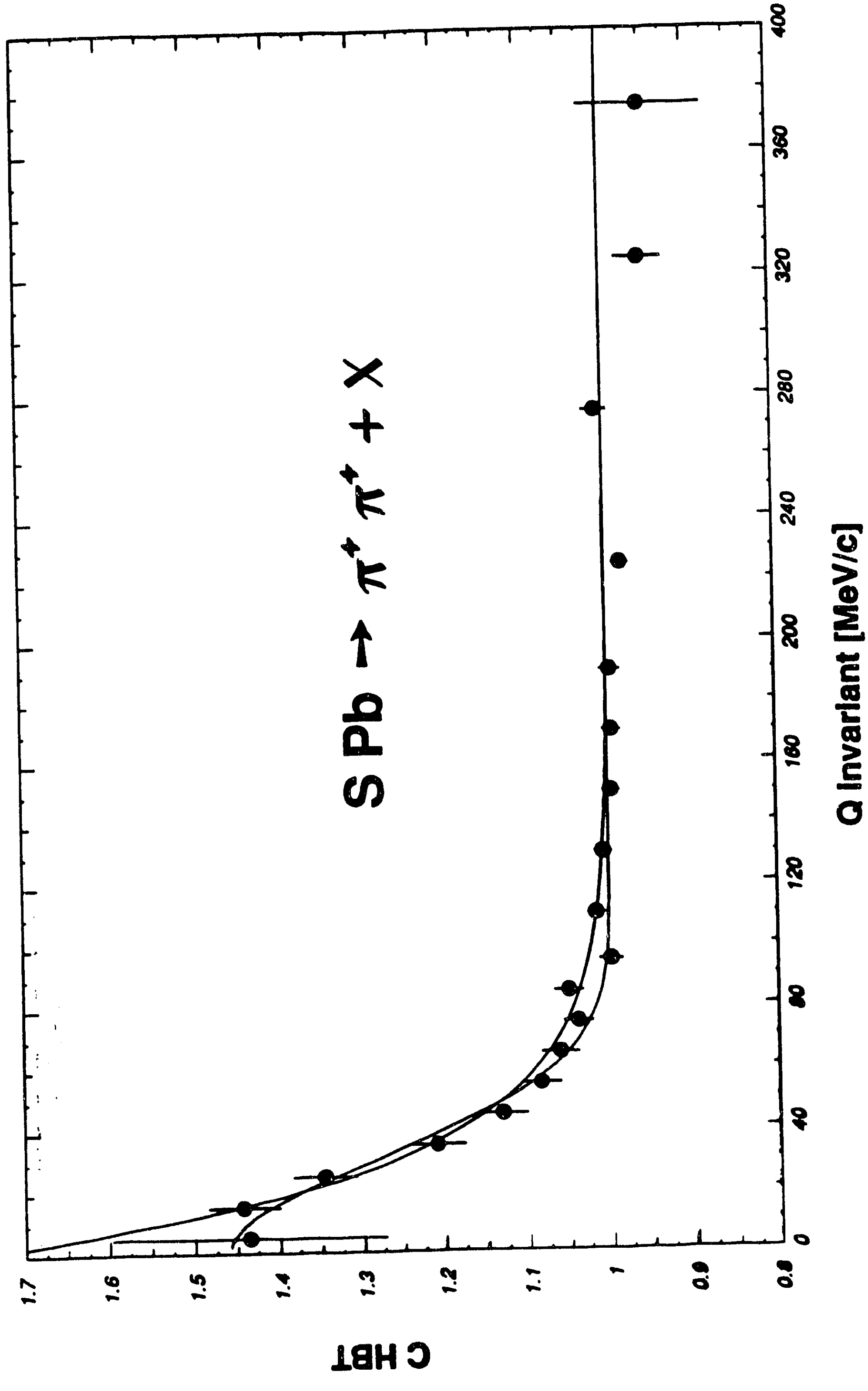

Figure 3: C_{HBT} as a function of Q_{inv}. The systematic and statistical errors have been added in quadrature.

Table 1: Table of experimental results and corrections

Q_{inv} (MeV/c)	C_{raw}	SPC correction	Acceptance correction	C_{corr}	Coulomb correction	C_{HBT}^{data}	$\delta C_{statistic}$	$\delta C_{systematic}$
5	1.169	1.220	0.514	0.733	1.565	1.148	0.031	0.126
15	1.143	1.224	0.710	0.994	1.161	1.154	0.011	0.032
25	1.136	1.226	0.720	1.003	1.074	1.077	0.008	0.029
35	1.080	1.224	0.706	0.933	1.037	0.968	0.007	0.026
45	1.034	1.223	0.702	0.887	1.020	0.905	0.007	0.023
55	1.004	1.220	0.701	0.858	1.012	0.868	0.008	0.017
65	0.992	1.217	0.698	0.842	1.009	0.849	0.008	0.016
75	0.970	1.214	0.701	0.826	1.007	0.831	0.008	0.012
85	0.979	1.210	0.705	0.835	1.005	0.840	0.008	0.012
95	0.942	1.206	0.700	0.796	1.005	0.799	0.008	0.007
110	0.946	1.200	0.713	0.809	1.003	0.812	0.006	0.006
130	0.942	1.189	0.716	0.802	1.003	0.805	0.007	0.004
150	0.937	1.179	0.720	0.796	1.002	0.797	0.007	0.004
170	0.946	1.170	0.718	0.795	1.002	0.796	0.008	0.004
190	0.945	1.160	0.726	0.797	1.001	0.797	0.009	0.004
225	0.934	1.139	0.739	0.785	1.001	0.785	0.007	0.004
275	0.947	1.108	0.768	0.805	1.001	0.807	0.012	0.004
325	0.901	1.080	0.790	0.769	1.001	0.770	0.022	0.004
375	0.890	1.054	0.798	0.749	1.000	0.749	0.059	0.004

Table 2: Fitted results of Gaussian and exponential parametrizations

Parametrization	Normalization	λ	R_{inv} (fm)	χ^2/N_{dof}
Gaussian	0.800 ± 0.002	0.46 ± 0.04	4.50 ± 0.31	18.1/16
Exponential	0.794 ± 0.004	0.77 ± 0.08	3.54 ± 0.33	12.0/16

for the Gaussian parametrization and

$$C_{HBT}^{exp}(Q_{inv}) = A(1 + \lambda e^{-2Q_{inv}R_{inv}}) \tag{14}$$

for the exponential parametrization. The fitted parameters are listed in Table 2 and shown together with the data in Fig. 3, where a renormalization to the Gaussian fitting result has been applied (i.e. divided by 0.80). If the standard Gamow correction is used instead of the Coulomb wave-function correction applied here, the resulting parameters for the Gaussian fit are $\lambda = 0.52 \pm 0.04$, $R_{inv} = 4.12 \pm 0.20$ fm.

It is seen that the Gaussian fit deviates from the data mainly around 80 MeV, whilst the exponential fit is excellent.

The Gaussian fit [1] allows comparison with other experiments and models, despite its larger χ^2. The value in Table 2 is much larger than that obtained in experiments on hadron collisions, consistent with the picture that we are measuring a geometrical effect related to the large dimensions of the nuclear system. However, it is not much larger than

1) It is important to note that the R_{inv} in the Gaussian is very often introduced in such a way that the value is $\sqrt{2}$ larger than in this paper. We have decided to adhere to the definition used in Ref. [18].

- ASSUME SOURCE SIZE $\rho(r) \propto e^{-r^2/2R^2}$ (1 DIM GAUSSIAN)
  (GAUSSIAN OF WIDTH R)

THE CORRESPONDING CORRELATION FUNCTION

$$C(Q) = 1 + e^{-Q^2R^2} \qquad \left\{ Q^2 = Q^\mu Q_\mu = Q_x^2 + Q_y^2 + Q_z^2 - Q_0^2 \right\}$$

TO ACCOUNT FOR THE CHAOTICITY OF THE SOURCE, PARAMETER λ IS INTRODUCED

$$C(Q) = A\left[1 + \lambda e^{-Q^2R^2}\right] \qquad \begin{cases} \lambda = 0 & \text{COHERENT SOURCE} \\ \lambda = 1 & \text{INCOHERENT} \end{cases}$$

A : OVERALL NORMALIZATION

- A BETTER REPRESENTATION OF THE CORRELATION FUNCTION IS

$$C(Q) = 1 + \lambda e^{-(Q_{TO}^2 R_{TO}^2 + Q_{TS}^2 R_{TS}^2 + Q_L^2 R_L^2)}$$

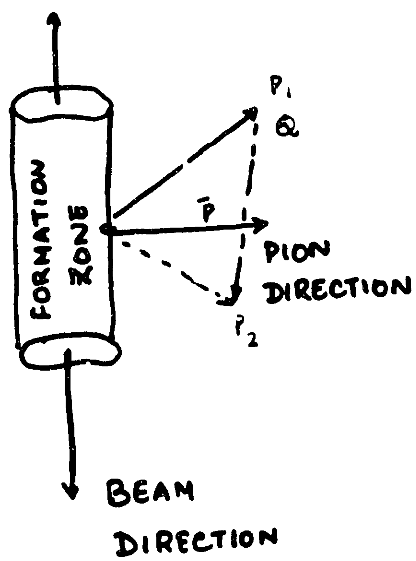

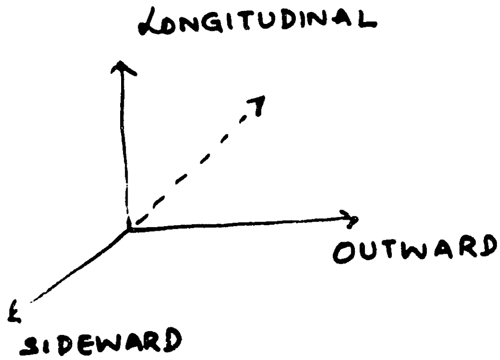

Preliminary

→ Projections ←

05/03/93 09.59

Two-pion correlation for S-Pb collisions

Horizontal

C2

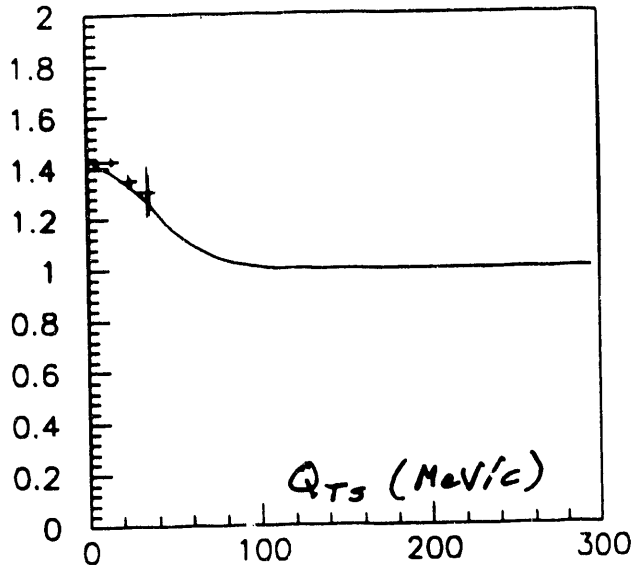

HOR C2(QTS) AVE. ON QTO, QL

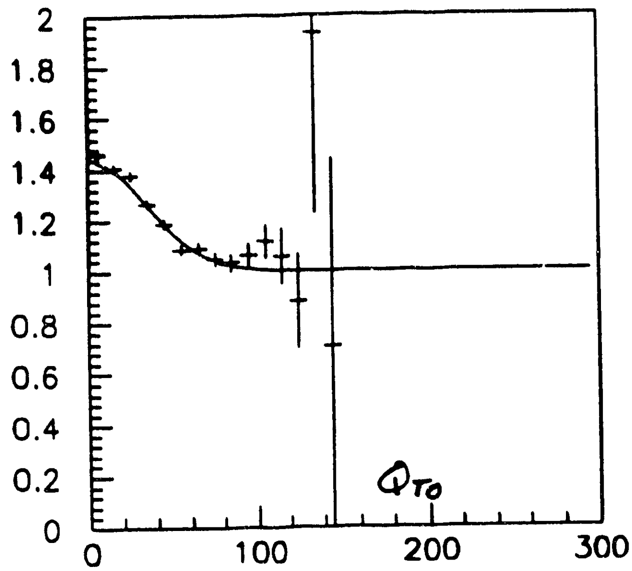

HOR C2(QTO) AVE. ON QTS, QL

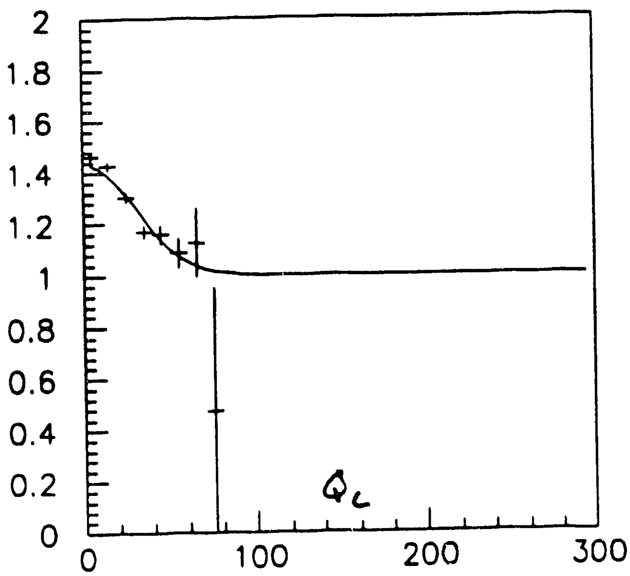

HOR C2(QL) AVE. ON QTS, QTO

Preliminary

05/03/93 09.59

→ Projections ←

Two-pion correlation for $\boxed{\text{S-Pb collisions}}$ Vertical

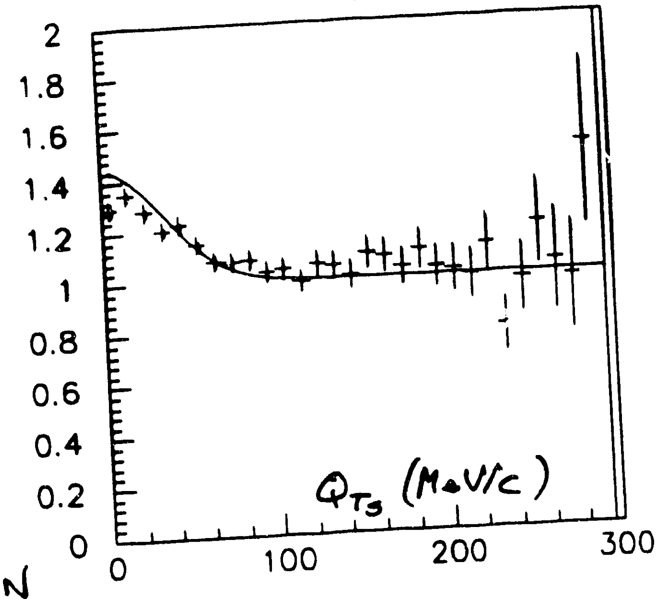

C_2

VER C2(QTS) AVE. ON QTO, QL

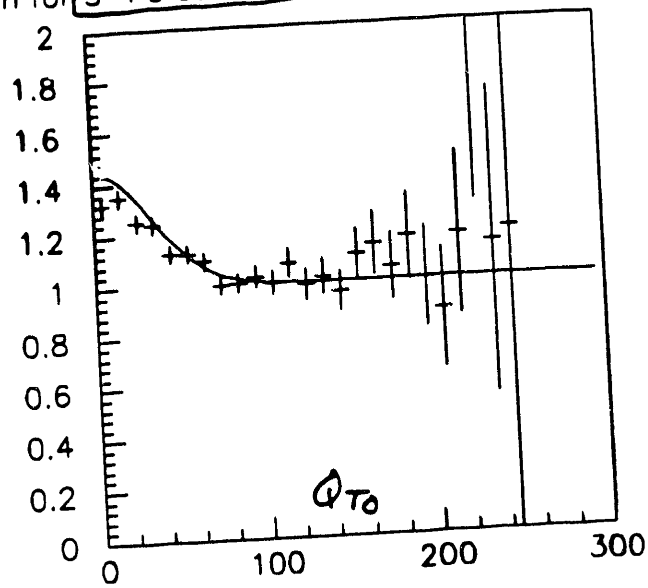

VER C2(QTO) AVE. ON QTS, QL

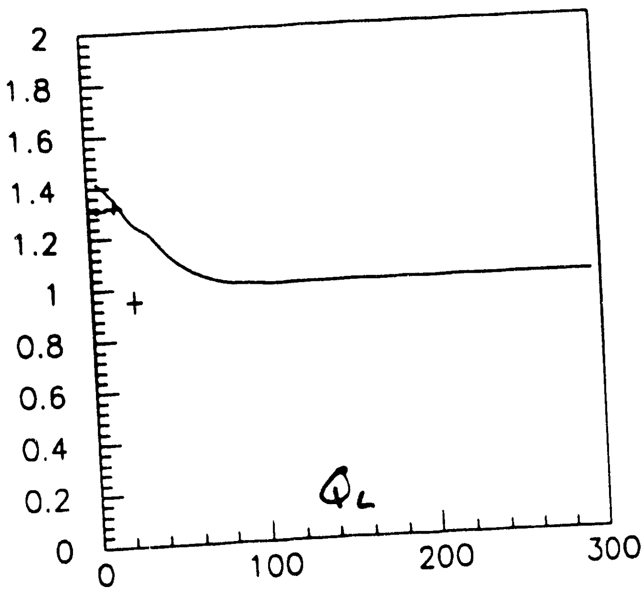

VER C2(QL) AVE. ON QTS, QTO

Preliminary

→ Projections ←

05/03/93 10.0

Two-pion correlation for p-Pb collisions Horizontal

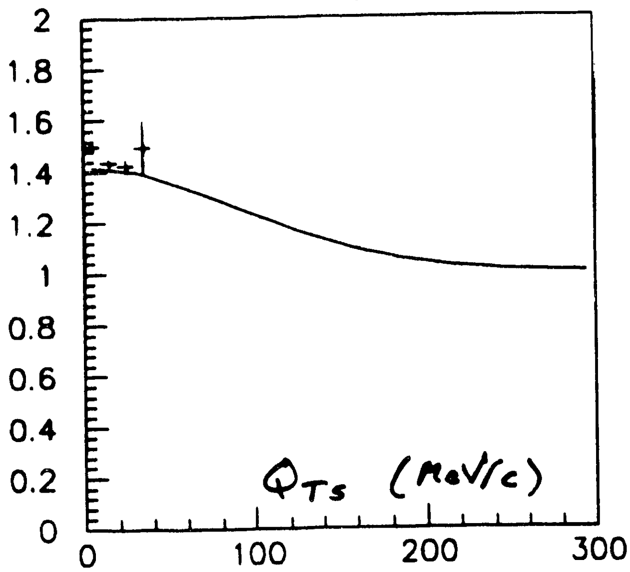

HOR C2(QTS) AVE. ON QTO, QL

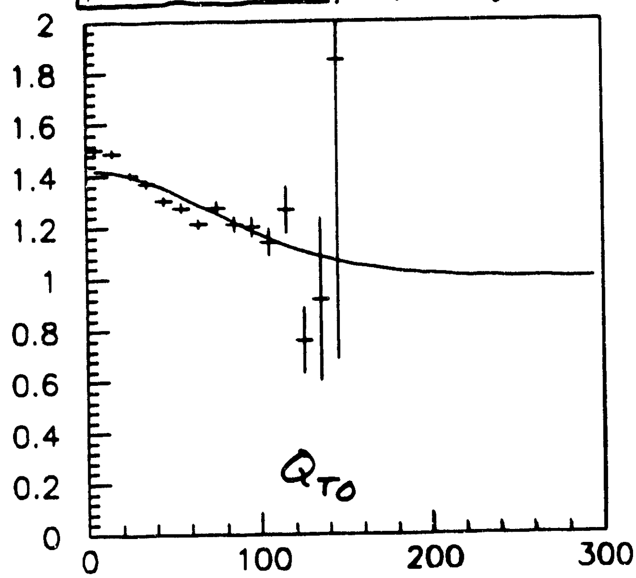

HOR C2(QTO) AVE. ON QTS, QL

C2

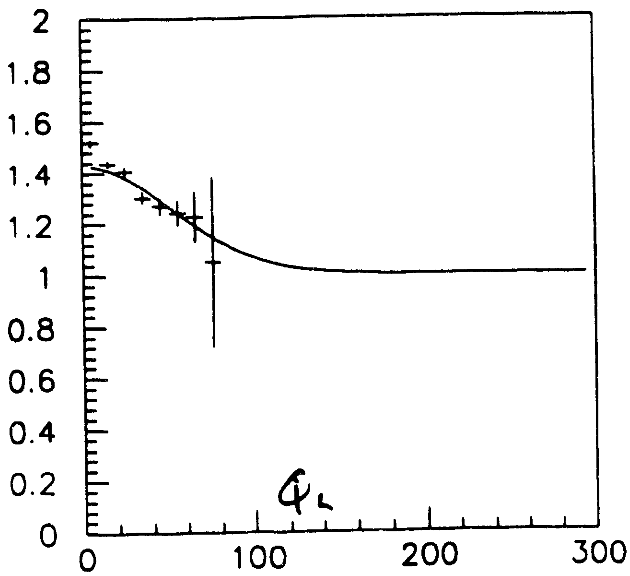

HOR C2(QL) AVE. ON QTS, QTO

Preliminary

→ Projections ←

05/03/93 10.0C

Two-pion correlation for p-Pb collisions Vertical

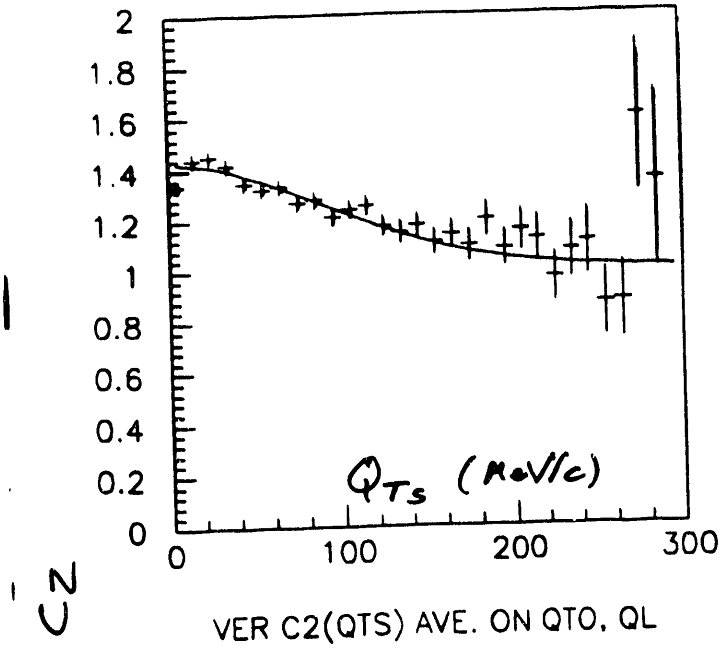

VER C2(QTS) AVE. ON QTO, QL

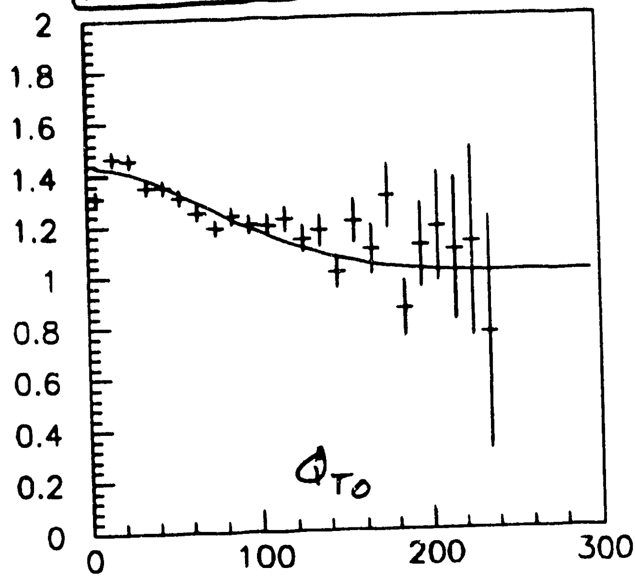

VER C2(QTO) AVE. ON QTS, QL

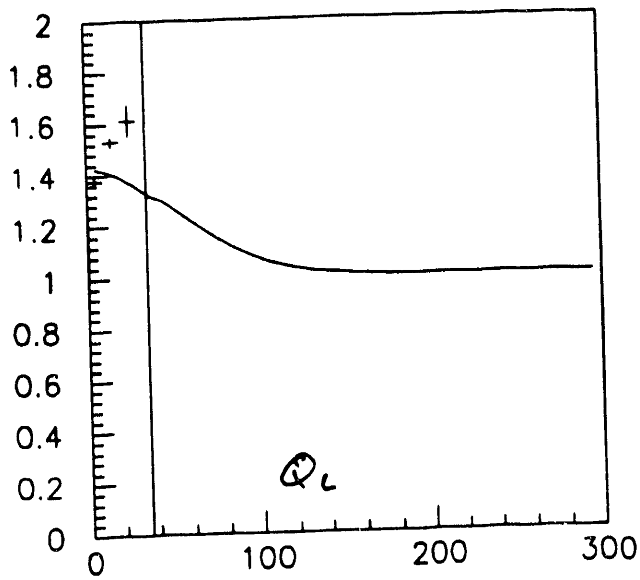

VER C2(QL) AVE. ON QTS, QTO

Preliminary!

$\pi^+\pi^+$ Results of Experiment NA44

The following results are corrected with gamov, acceptance and single pa distortion. Directional analysis are done in the 4 GeV pion rest frame (cent the acceptance).

1. Fit to Q_{inv}

	λ	R_{inv} (fm)	χ^2
S-Pb Peripheral	0.53 ± 0.01	3.86 ± 0.11	2.0
S-Pb Central	0.59 ± 0.02	5.02 ± 0.15	1.7
p-Pb	0.47 ± 0.01	2.54 ± 0.07	2.1

2. Fit to Q_{TS}, Q_{TO}, Q_L

	λ	R_{TS} (fm)	R_{TO} (fm)	R_L (fm)	χ^2
S-Pb Peripheral	0.41 ± 0.02	1.32 ± 0.14	2.17 ± 0.15	2.66 ± 0.20	3.[illegible]
S-Pb Central	0.53 ± 0.04	4.22 ± 0.41	4.19 ± 0.28	2.87 ± 0.36	2.[illegible]
p-Pb	0.40 ± 0.01	1.52 ± 0.08	1.70 ± 0.08	1.06 ± 0.13	2.[illegible]

3. Fit to Q_T, Q_L, Q_O

	λ	R_T (fm)	R_L (fm)	τ (fm)	χ^2
S-Pb Peripheral	0.43 ± 0.02	2.30 ± 0.11	2.54 ± 0.15	0.00 ± 0.44	2.[illegible]
S-Pb Central	0.53 ± 0.03	3.97 ± 0.16	2.84 ± 0.24	0.00 ± 0.54	2.1
p-Pb	0.43 ± 0.01	1.68 ± 0.05	1.11 ± 0.09	0.00 ± 0.15	2.[illegible]

$$\left\{\begin{matrix} K^+ K^+ \\ K^- K^- \end{matrix}\right\}$$

results

Two Kaon Correlation

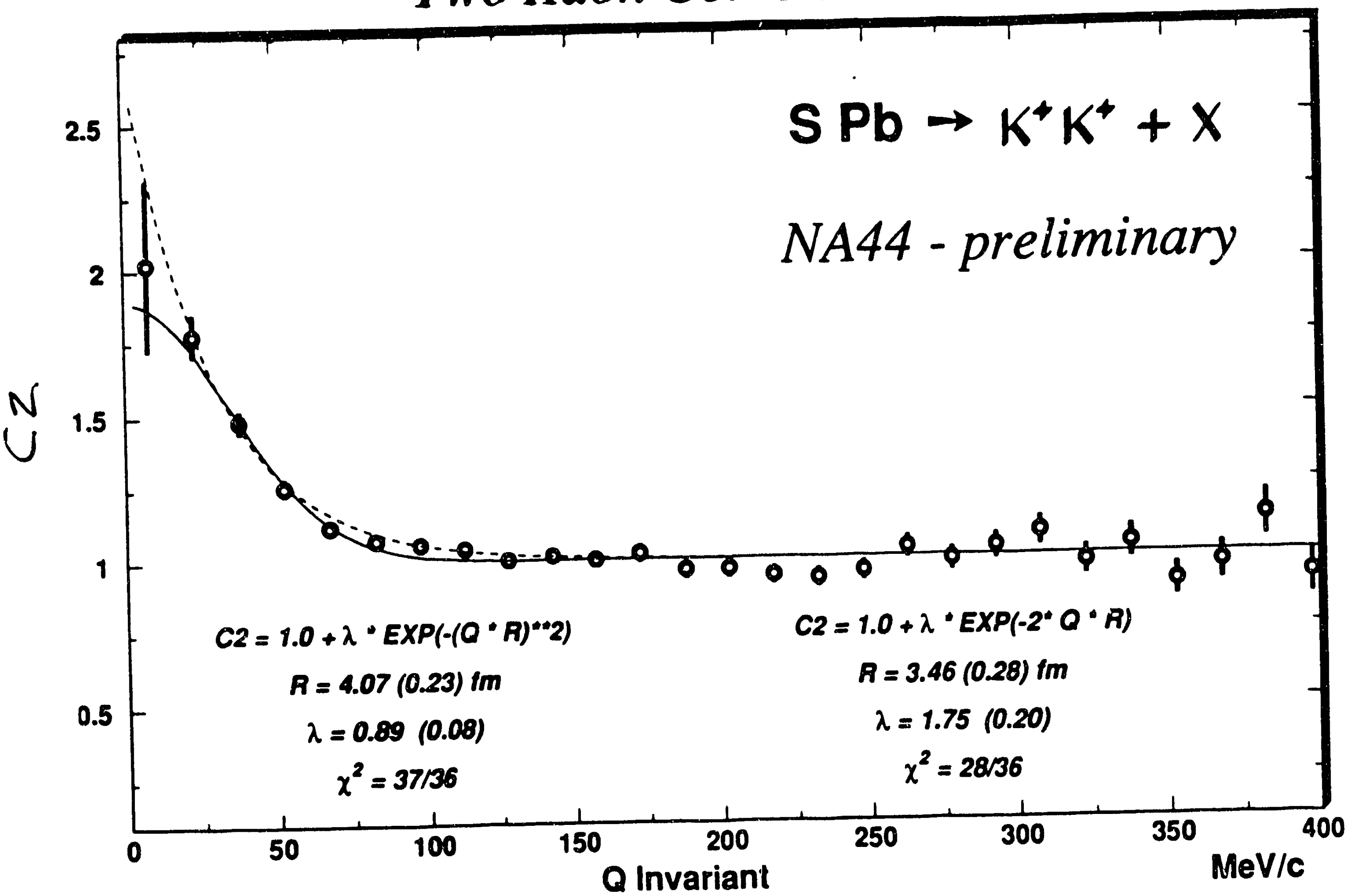

Two Kaon Correlation

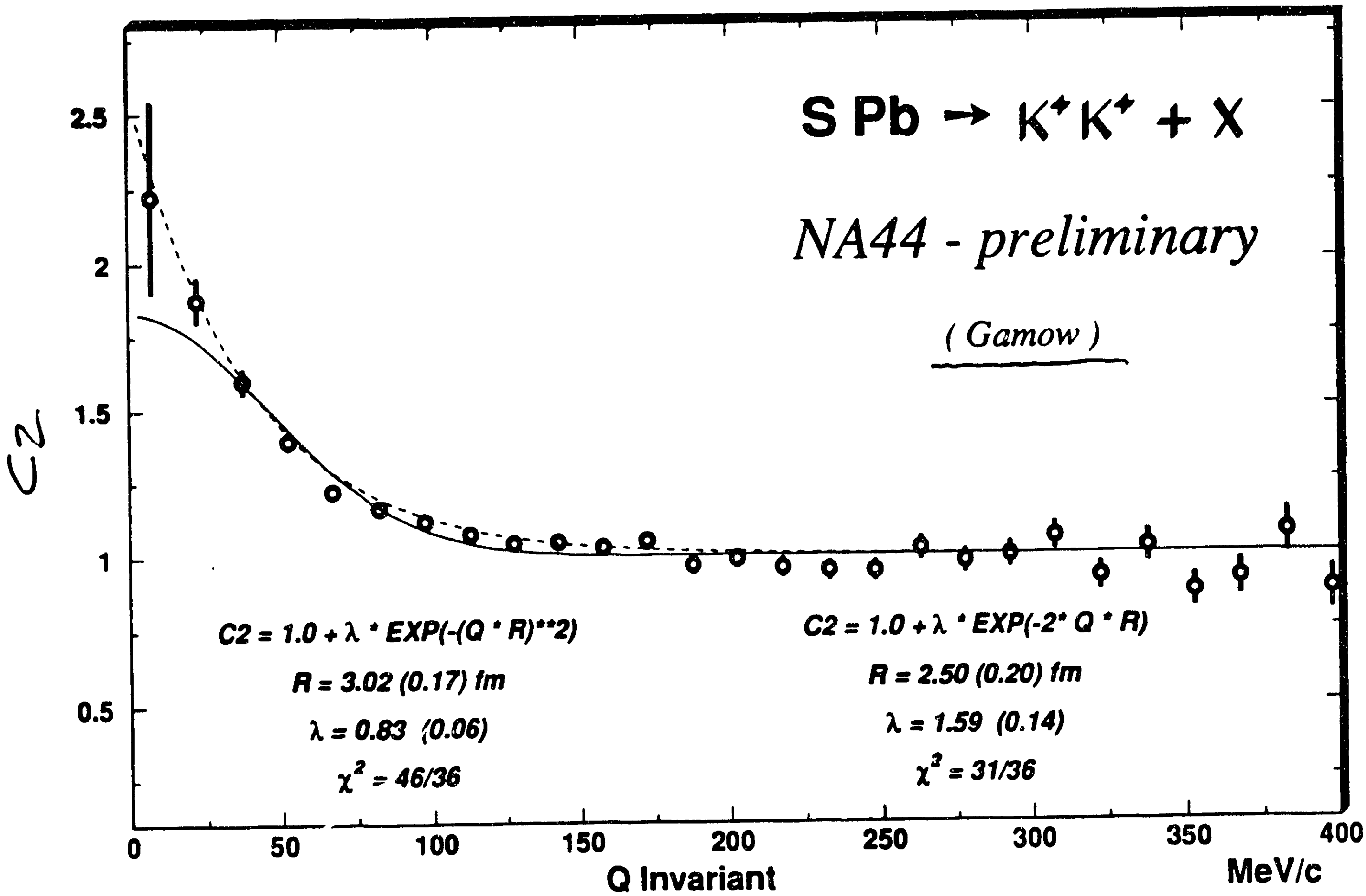

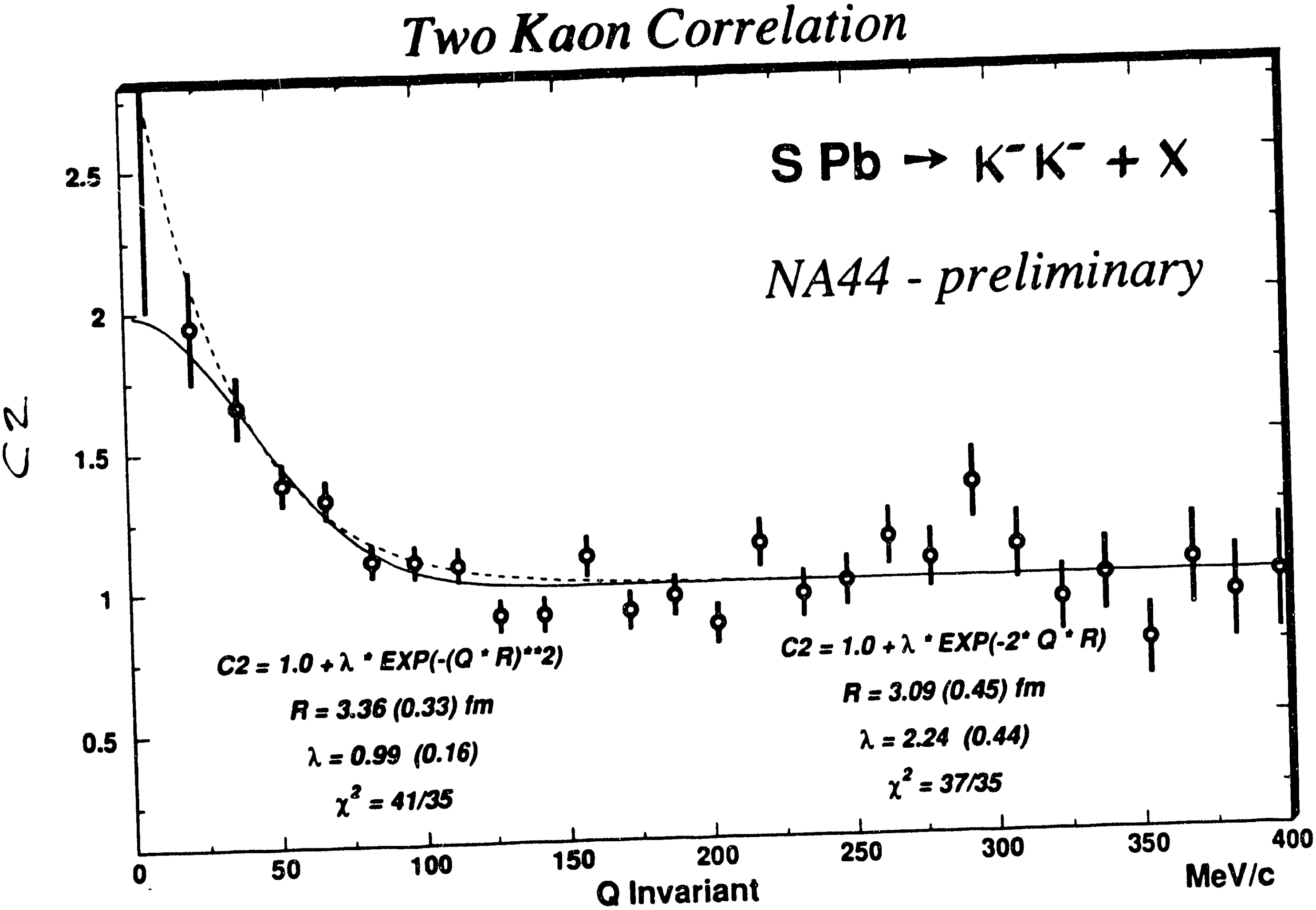
Two Kaon Correlation
S Pb → K⁻K⁻ + X
NA44 - preliminary
C2
2.5
2
1.5
1
0.5
0
50
100
150
200
250
300
350
400
MeV/c
Q Invariant
C2 = 1.0 + λ * EXP(-(Q * R)**2)
R = 3.36 (0.33) fm
λ = 0.99 (0.16)
χ² = 41/35
C2 = 1.0 + λ * EXP(-2* Q * R)
R = 3.09 (0.45) fm
λ = 2.24 (0.44)
χ² = 37/35

Two Kaon Correlation

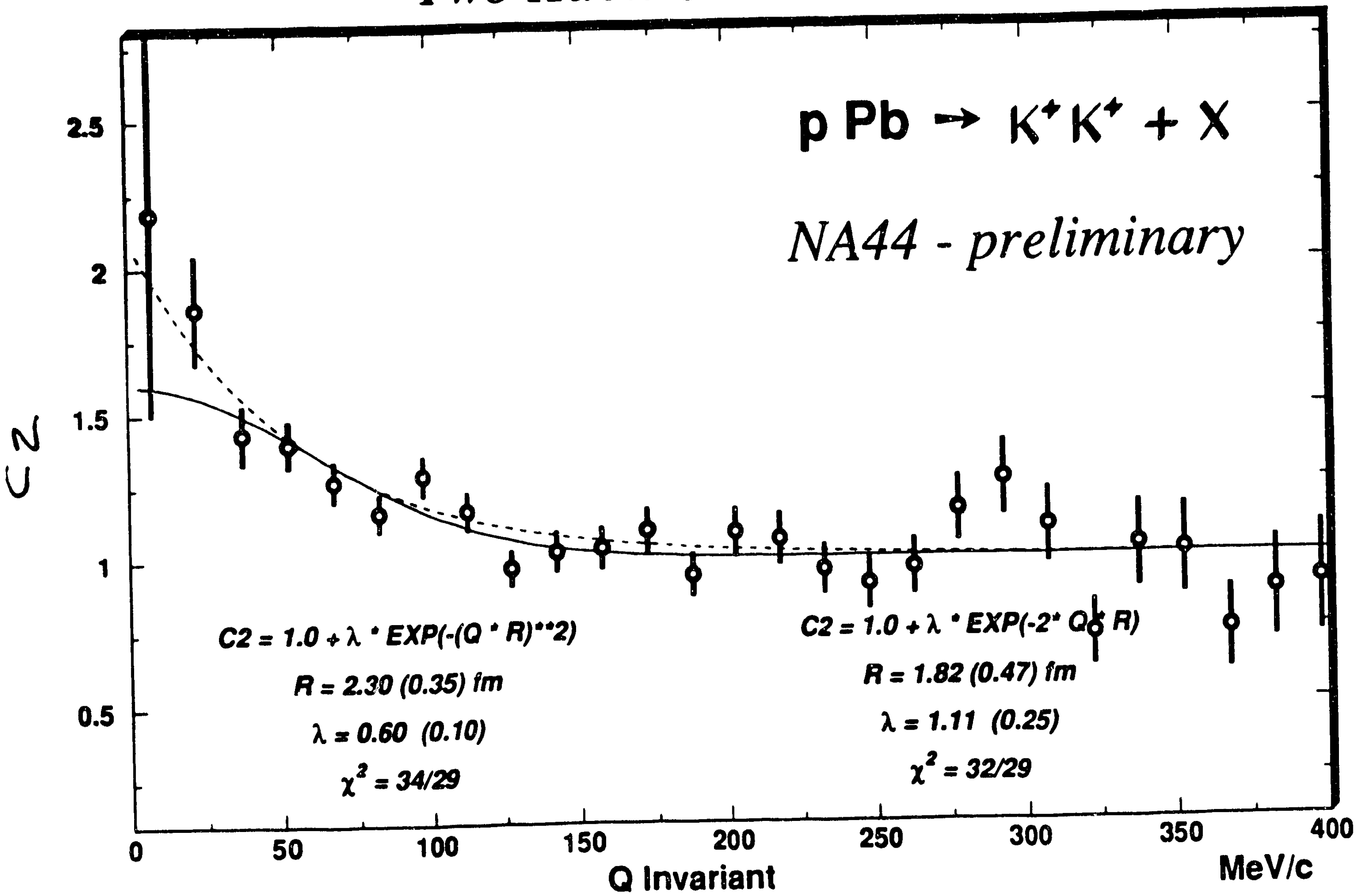

3 D S+ Pb $K^+ K^+$

IN HORIZONTAL
FIX RTS

IN VERTICAL
FIX RTO, RL.

$\lambda = 0.82 \pm .06 \pm 0.3$
$R_{TO} = 2.20 \pm 0.19 \pm 0.3$ fm
$R_{TS} = 2.20 \pm 0.24 \pm 0.1$ FM
$R_L = 2.62 \pm 0.16 \pm 0.4$ FM
$\chi^2 = 257/339$ (IN HORIZONTAL)
(IN VERTICAL ~2.5)

(BY VARYING 1st BIN FIT TOO.)
REALL JUST 1st BIN IN RTD

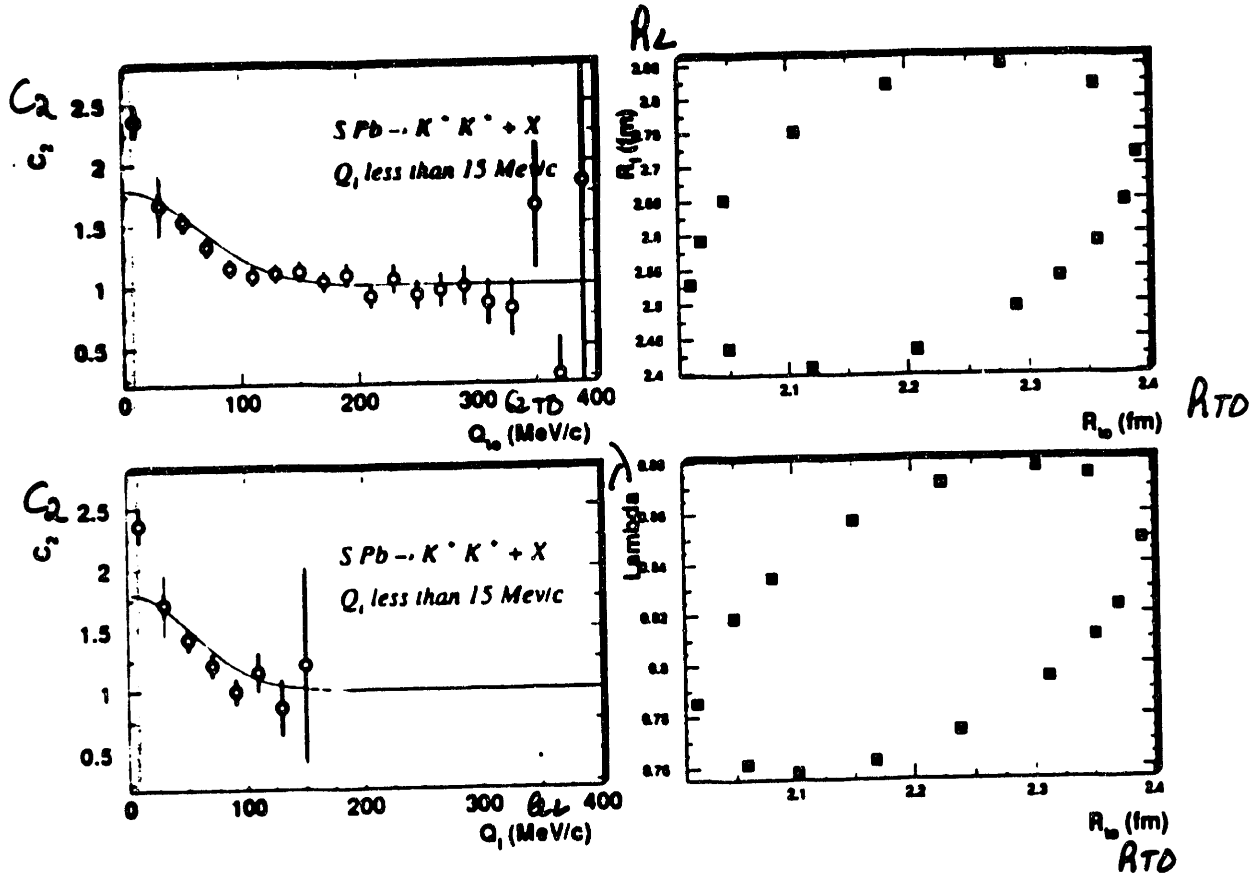

Figure 5: The Q_{to}, Q_l projections and 1σ confidence contours from the horizontal setting. The thick lines are the statistical errors. Systematic and statistical errors have been added in quadrature.

Preliminary

K K Results from NA44

1) Fit to Q_{inv}

	λ	R_{inv} (fm)	χ^2
S-Pb K^+K^+	0.89 ± 0.08	4.07 ± 0.23	37/36
S-Pb K^-K^-	0.99 ± 0.16	3.36 ± 0.33	41/35
p-Pb K^+K^+	0.60 ± 0.10	2.30 ± 0.35	34/29

2) Fit to Q_{TS}, Q_{TO}, Q_L

S-Pb K^+K^+

$$\lambda = 0.82 \pm 0.06$$
$$R_{TO} = 2.20 \pm 0.19 \text{ fm}$$
$$R_{TS} = 2.20 \pm 0.24 \text{ fm}$$
$$R_L = 2.62 \pm 0.16 \text{ fm}$$
$$\chi^2 = 257/339$$

Preliminary!

Coulomb - Corrected unlike - pair Correlation Functions

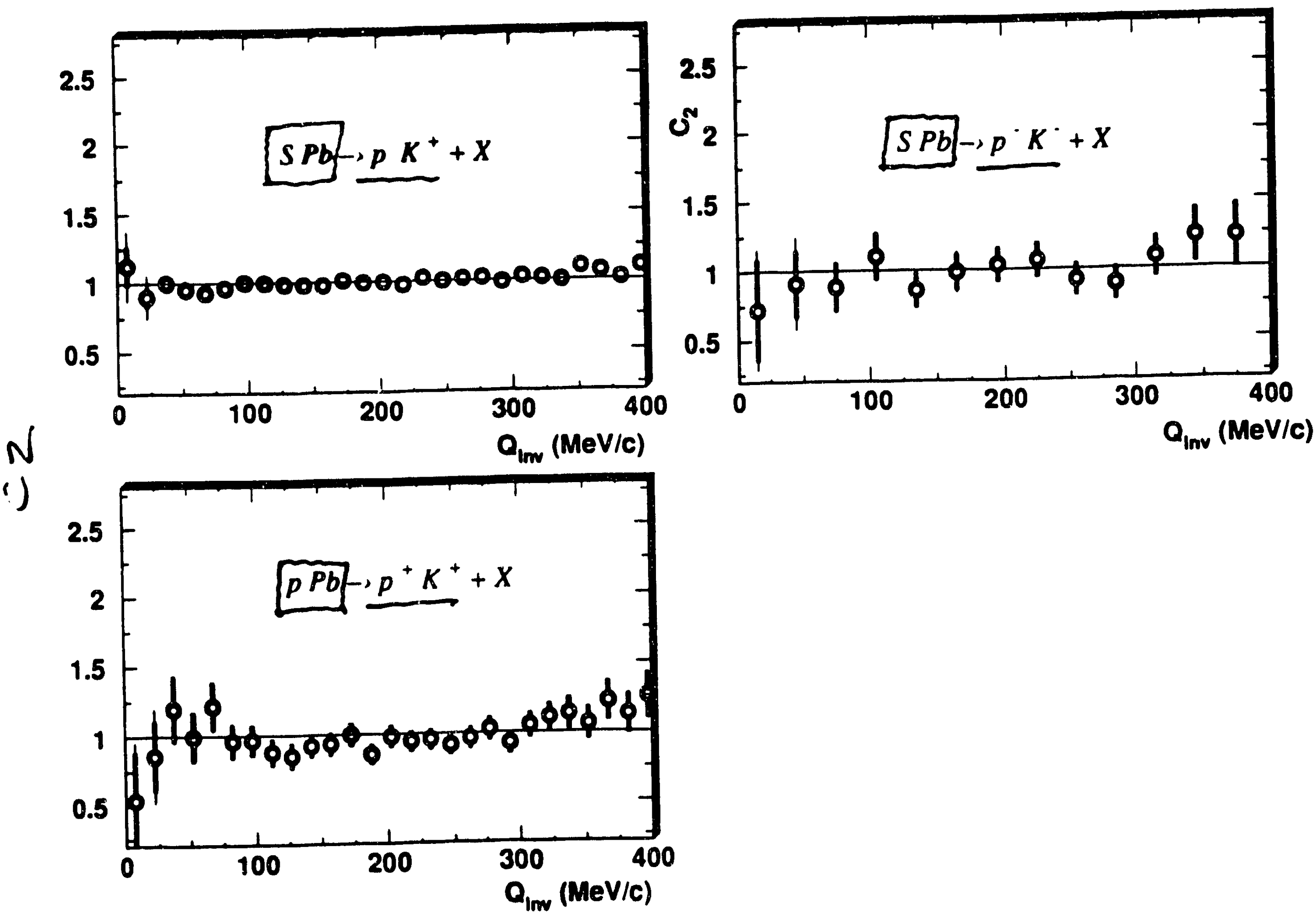

$\pi^+ \; \pi^+$ results

(large angle → 122 MRAD)

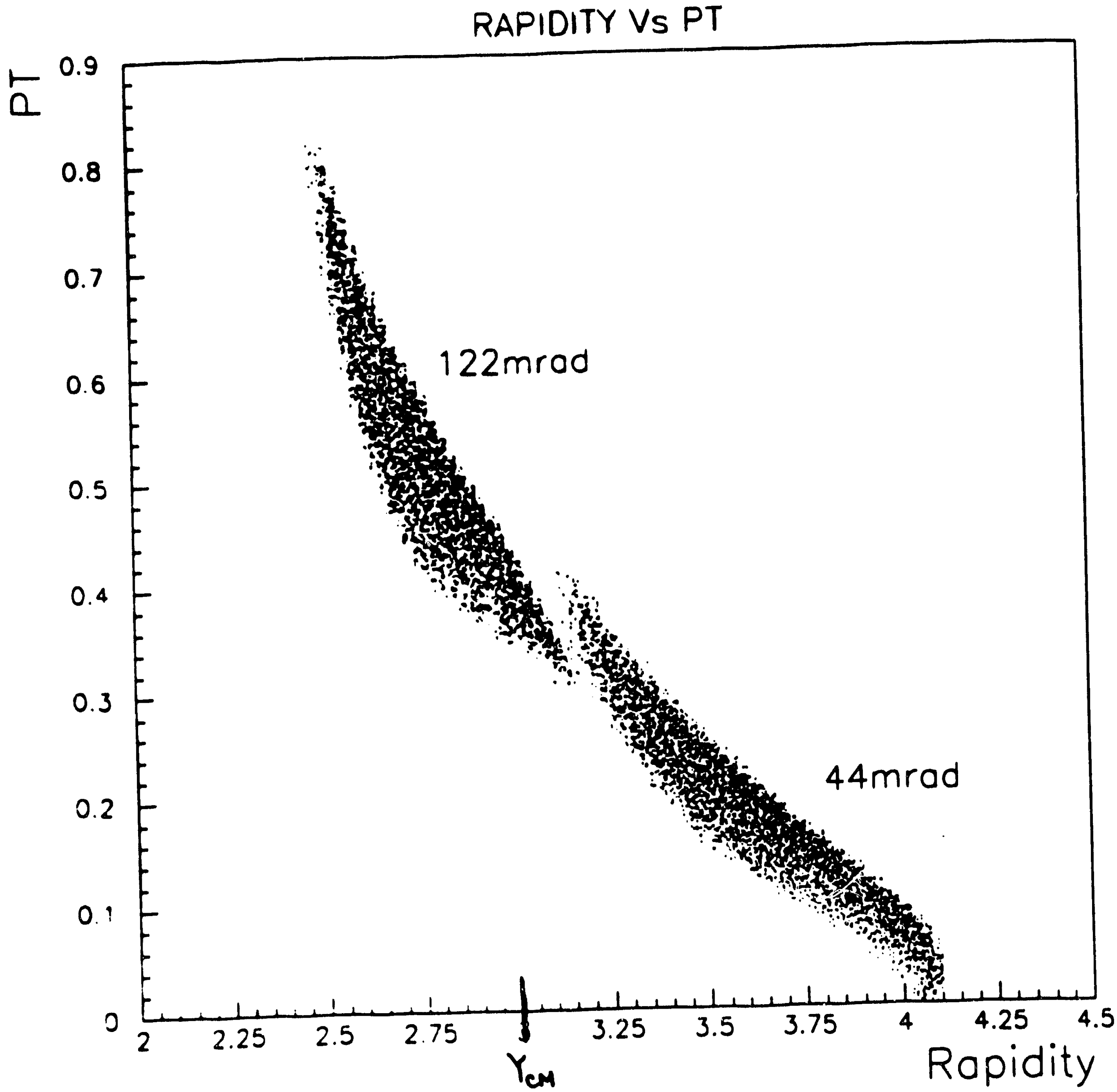

RAPIDITY Vs PT
PT
0.9
0.8
0.7
0.6
0.5
0.4
0.3
0.2
0.1
0
2
2.25
2.5
2.75
3
3.25
3.5
3.75
4
4.25
4.5
Rapidity
Y_{CM}
122mrad
44mrad

$R_{INV} = 4.047 \pm 0.225$ $\lambda = 0.475 \pm 0.02$ $N = 0.112 \pm 0.001$

$\chi^2 = 63.15/3$

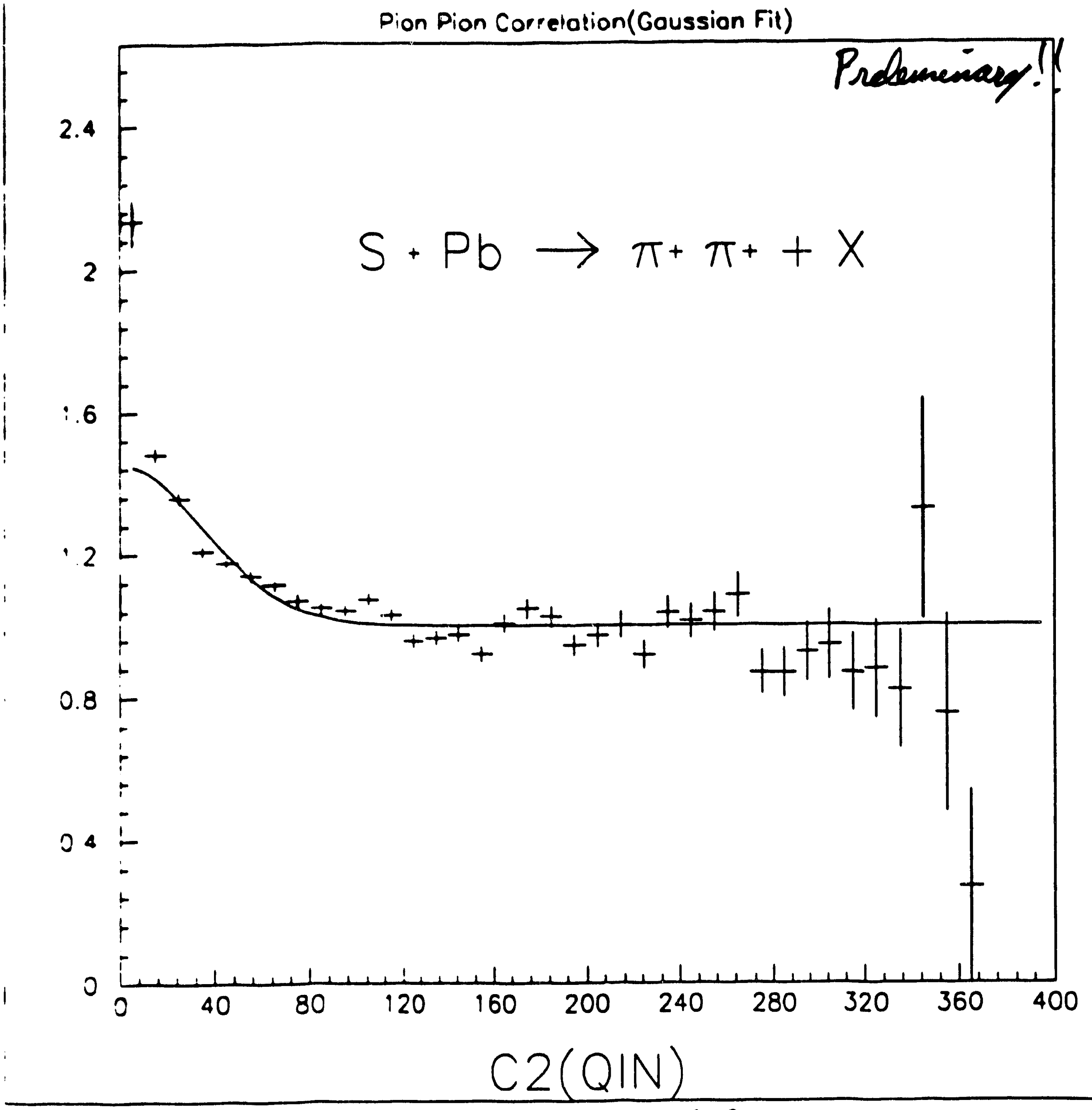

NO OF GOOD PAIRS : 63,778

Large angle (122 MRAD) $\pi^+\pi^+$ Results from NA44

1) Fit to Q_{inv}

	λ	R_{inv} (fm)	χ^2
S-Pb $\pi^+\pi^+$	0.49 ± 0.02	4.05 ± 0.23	63/35

2) Fit to Q_{T_s}, Q_{T_o}, Q_L

S-Pb $\pi^+\pi^+$

$\lambda = 0.62 \pm 0.02$

$R_{T_o} = 2.24 \pm 0.11$ fm

$R_{T_s} = 3.58 \pm 0.34$ fm

$R_L = 2.42 \pm 0.13$ fm

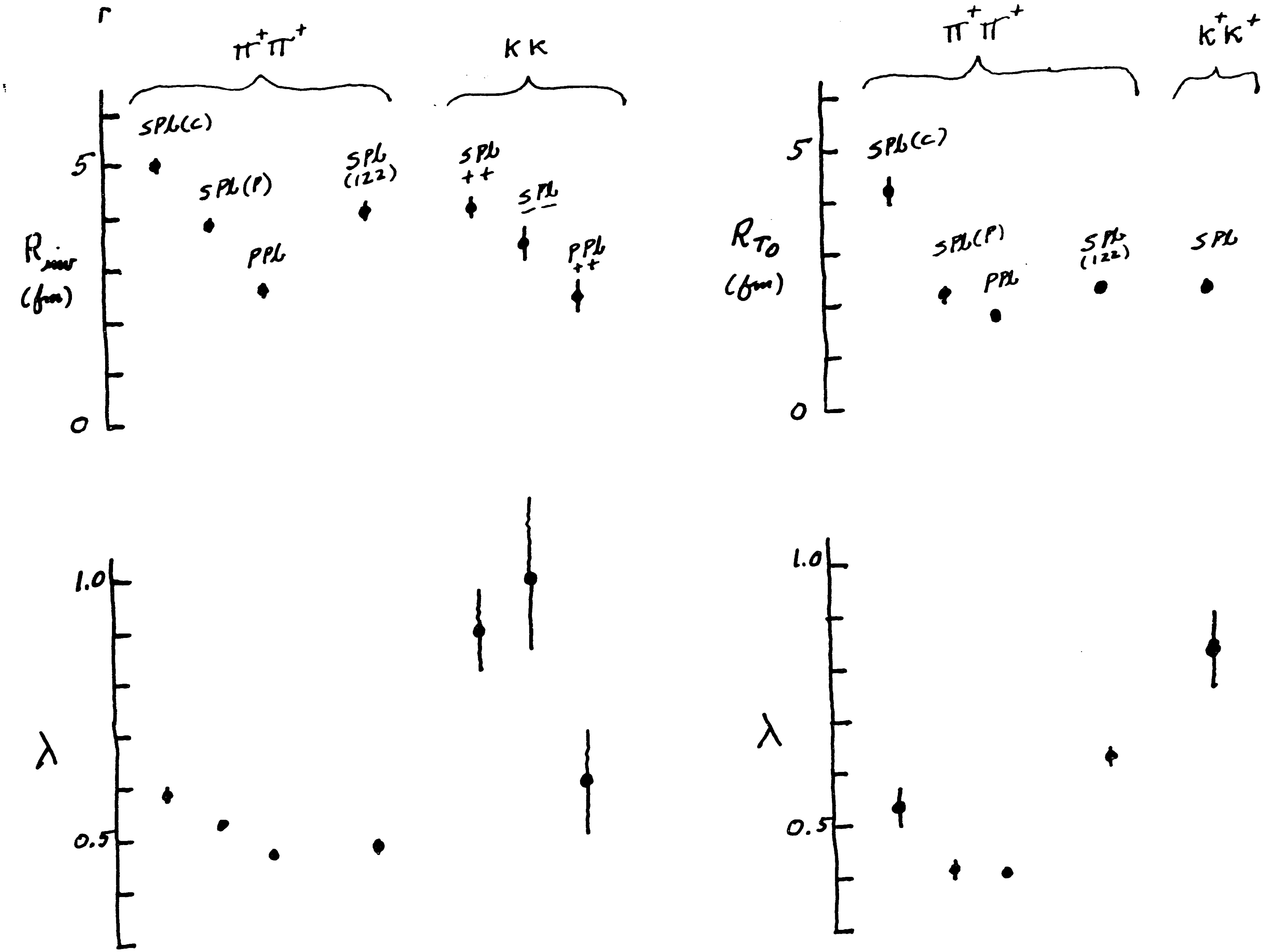

Summary of NA44 HBT results

Preliminary!

Interferometry Results from E802/E859/E866

George Stephans
MIT

Interferometry Results from E802/E859/E866

Includes work of thesis students Richard Morse, Vasilios **Vutsadakis, Ron Soltz**, Vince Cianciolo, Ole Vossnack.

⇒ **Detailed description of the data (Radius, what radius?).**

⇒ **Comments on dynamical correlations between position and momentum** (using ARC).

Physics Goals

- **Protons**
  - **Participant volume.**
  - **Expansion?**
  - **Shadowing?**

- **Pions**
  - **Particle production volume.**
  - **Secondary interactions?**
  - **Shadowing?**

- **Kaons**
  - **Strange particle production volume.**
  - **Reinteractions and shadowing minimal?**

Data Characterization

- All data uses hardware gates on charged particle multiplicity (TMA).
  - Central gate typically 10-15%. No additional offline cuts made.
  - Non-central data use hardware gates on $\overline{\text{TMA}}$.
  - Non-central data gated in software on a range of actual TMA.
  - Some Si + Al central data has been additionally cut using a software trigger on Zero-Degree Calorimeter (ZCAL).

- Most data taken with the spectrometer spanning a laboratory angle of $\sim 14^{o} \rightarrow 26^{o}$ relative to the beam (the so-called 14^{o} setting). Vertical aperture is about $\pm 3^{o}$.
- Integrated field of typically ~0.5 Tm results in a minimum laboratory momentum of ~400 MeV/c.

- Particle identification using Time-of-Flight (TOF). Cutoff is at $\pm 3\sigma$ from expected TOF.
  - Contamination estimated to be a few % or less.
  - Upper momentum cut-off ~1.8 GeV/c for pions and kaons, ~3.5 GeV/c for protons.

- Resolution in relative momentum is $\sigma_q \sim 15$ MeV/c. (protons $p \sim 1$ GeV/c)
- Pair reconstruction inefficiencies relatively small above q~20 MeV/c.

12/01/93 19.00

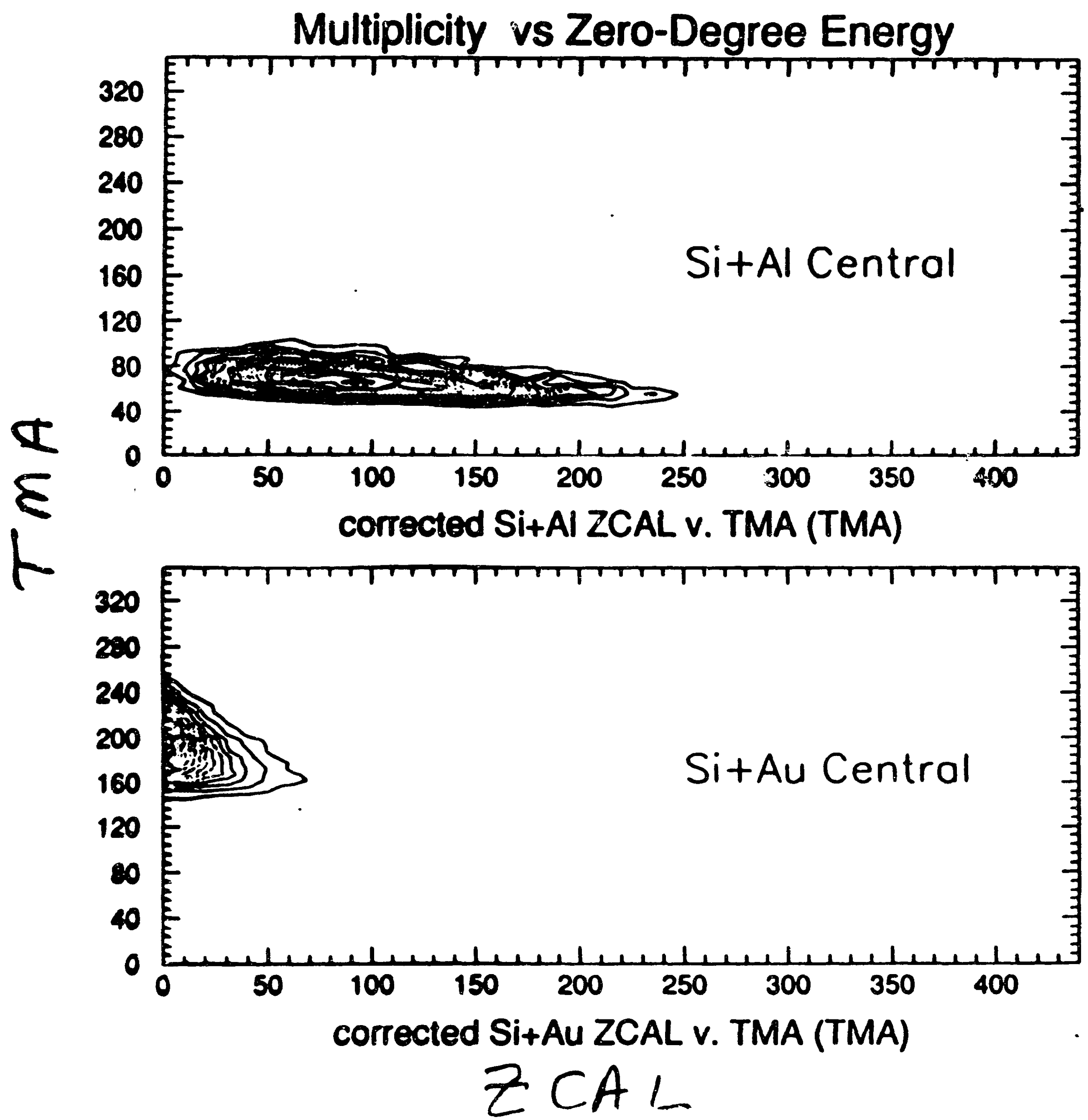

Multiplicity vs Zero-Degree Energy
Si+Al Central
320
280
240
200
160
120
80
40
0
0
50
100
150
200
250
300
350
400
corrected Si+Al ZCAL v. TMA (TMA)
Si+Au Central
corrected Si+Au ZCAL v. TMA (TMA)
TMA
ZCAL

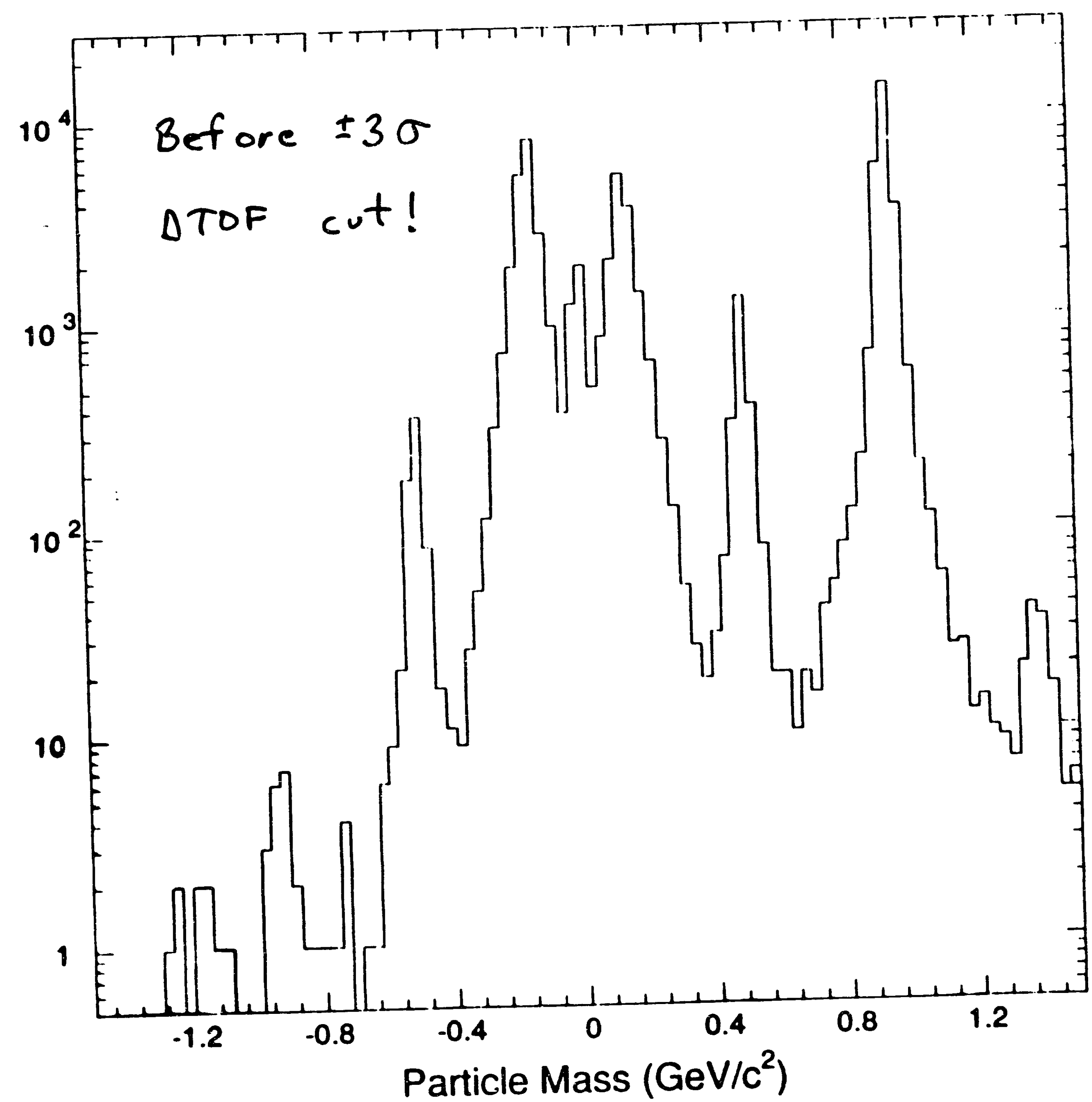

Before ±3σ
ΔTOF cut!
10^4
10^3
10^2
10
1
-1.2
-0.8
-0.4
0
0.4
0.8
1.2
Particle Mass (GeV/c^2)

13/04/93 09.50

Yield Contours in Transverse Momentum and Rapidity

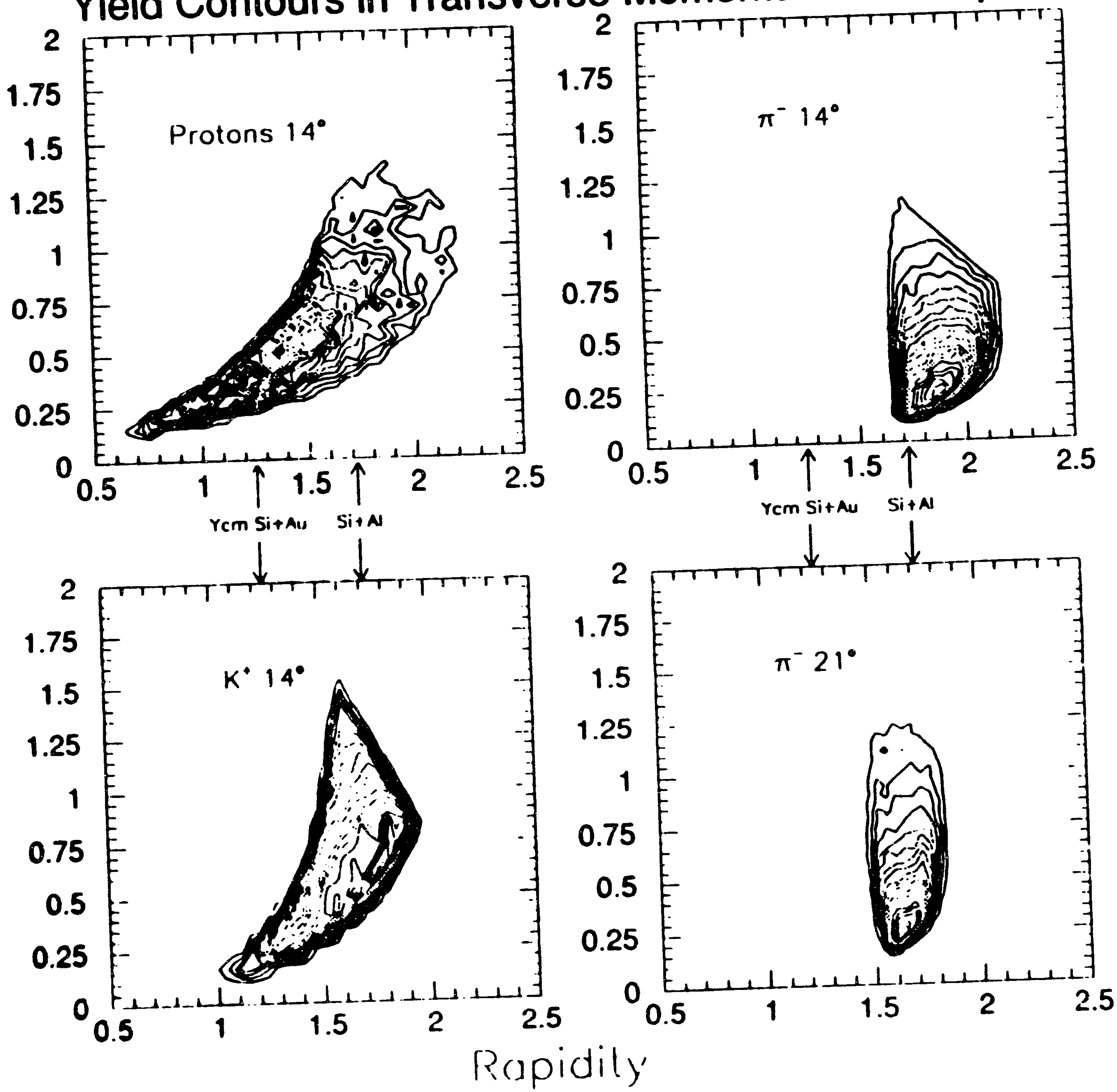

Two-Particle Acceptance Corrections

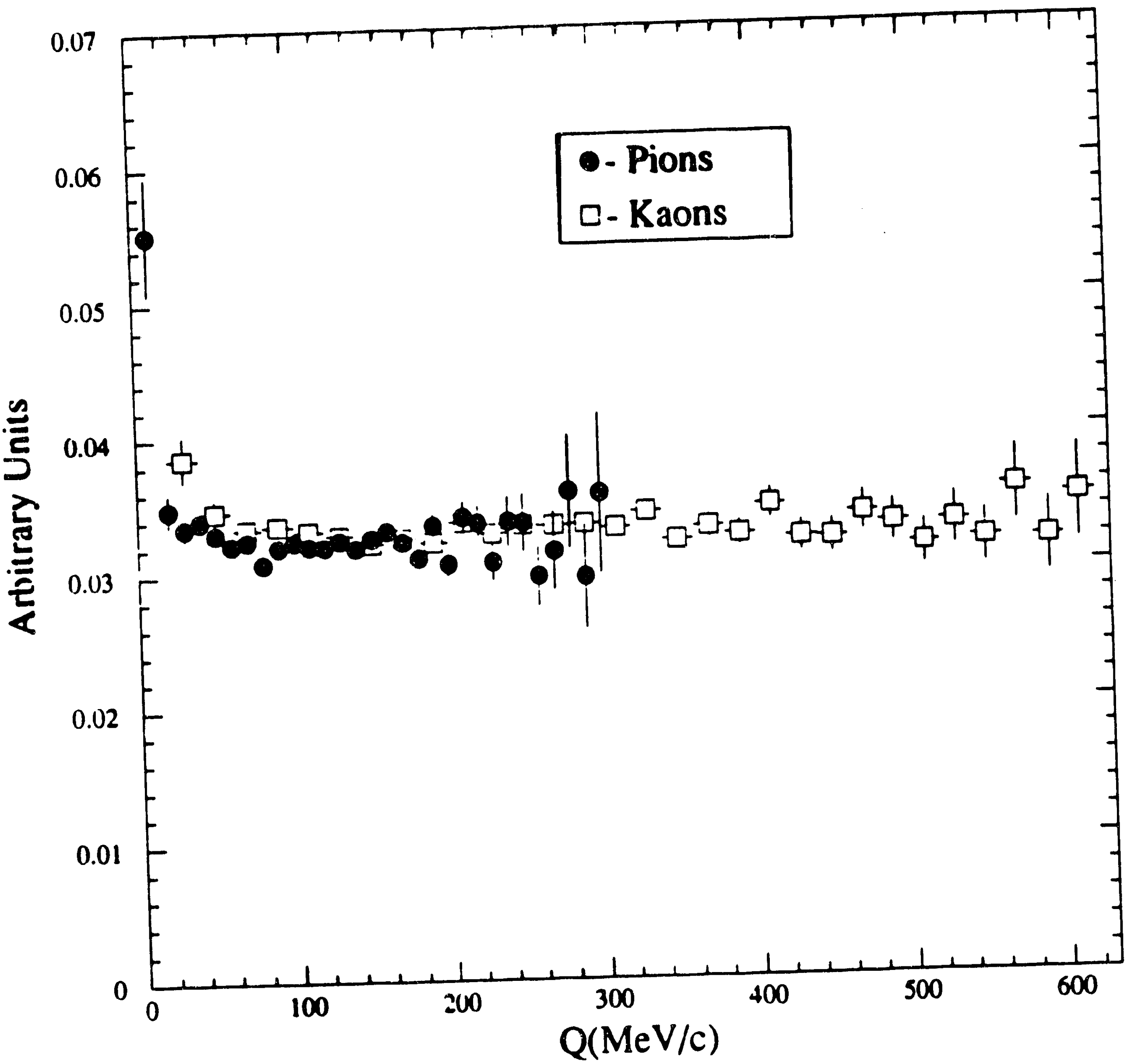

E802/E859/E866 Correlation Data

Number of pairs (in 1000's)

Number in parentheses are unanalyzed

System		π^+	π^-	Proton	K^+
			Detected Particle		
E802					
Si + Au	Central	30	59	82	
Si + Al	Central	8	23		
E859					
Si + Au	Central	(~100)	(~100)		16.5 (16.5 and 3 K^-)
	Peripheral		52		
	Semi-Peripheral		52		
	Central (19°)	86			
	Central (24°)		(~10)		
Si + Al	Central	41		38	
	Peripheral	42			
	Semi-Peripheral	42			
Si + Ag	Central			42	
E866					
Au + Au	Central (21°)		120		

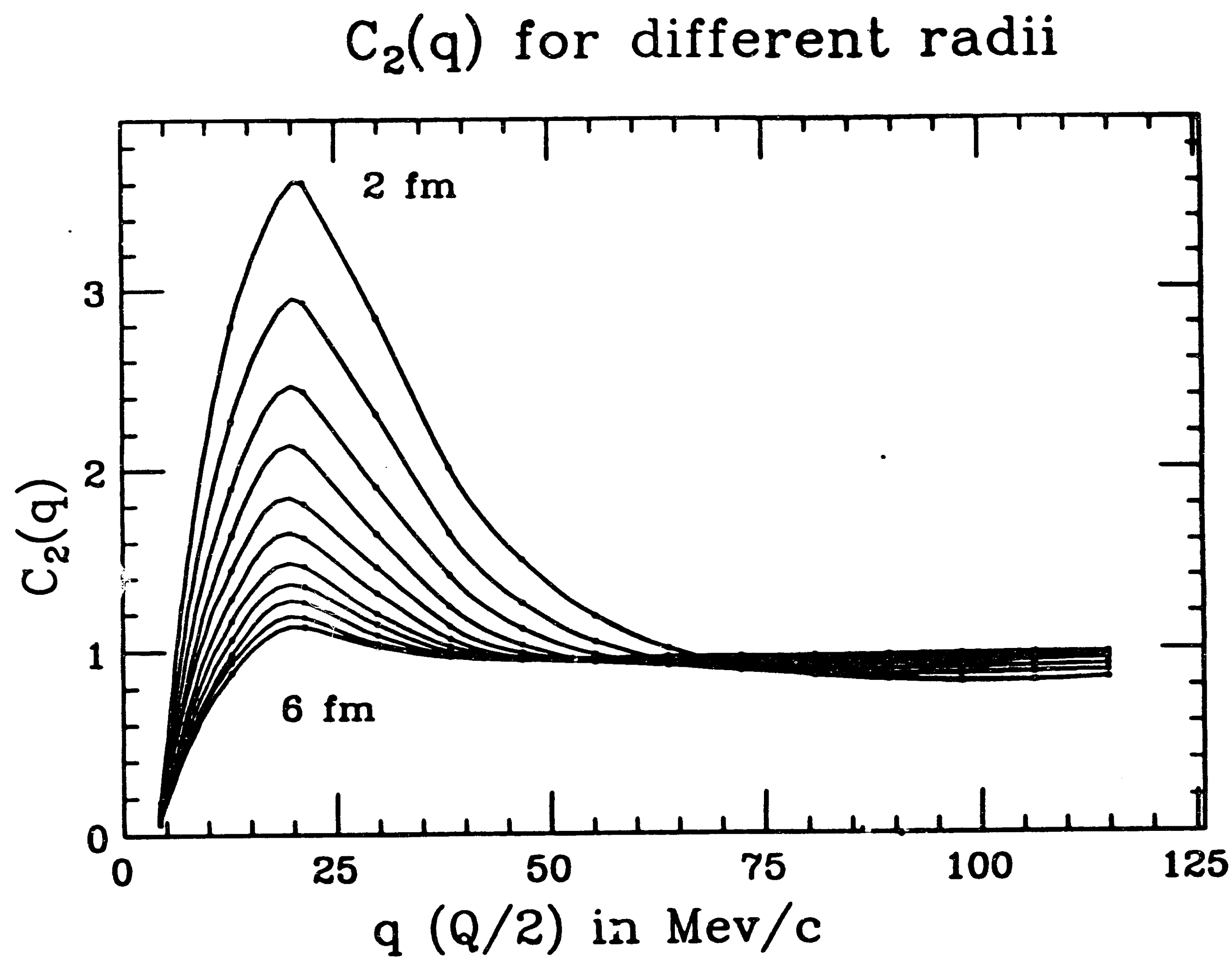

C2(q) for different radii
2 fm
6 fm
C2(q)
0
1
2
3
0
25
50
75
100
125
q (Q/2) in Mev/c

Analysis Procedure

- **Data displayed as** $C_2(q)=Prob(p_1,p_2)/Prob(p_1)Prob(p_2)$ with different **normalization** conventions for plots.
- **Denominator** in C_2 (by convention called "Background"), is formed by mixing particles from different pair events.
    - Guarantees singles distribution is from correct event type.
    - Guarantees presence of residual correlations.

- Protons
    - Correlation only weakly affected by Fermi statistics.
    - Correlation dominated by proton-proton resonance.
    - Source size affects **height** of enhancement in relative momentum.
    - Can only measure source volume, not different components of source size.
    - Coulomb correction typically not divided out in displayed data.
    - Displayed data fit to a calculation of the combined effect of the resonance, the Coulomb repulsion, and the Fermi statistics.
        - Start with radius to calculate theoretical $C_2(q)$.
            - This needs to be parameterized to save time.
        - Add experimental effects to theoretical prediction.
            - Response function generated with full GEANT simulation.
            - Biggest effect is resolution in measuring relative momentum.
        - Compare to data, optimize radius to fit data.
    - Data normalized to theory at large relative momentum.
    - Small Lorentz correction necessary. Effect is larger for Si+Al due to acceptance of spectrometer.

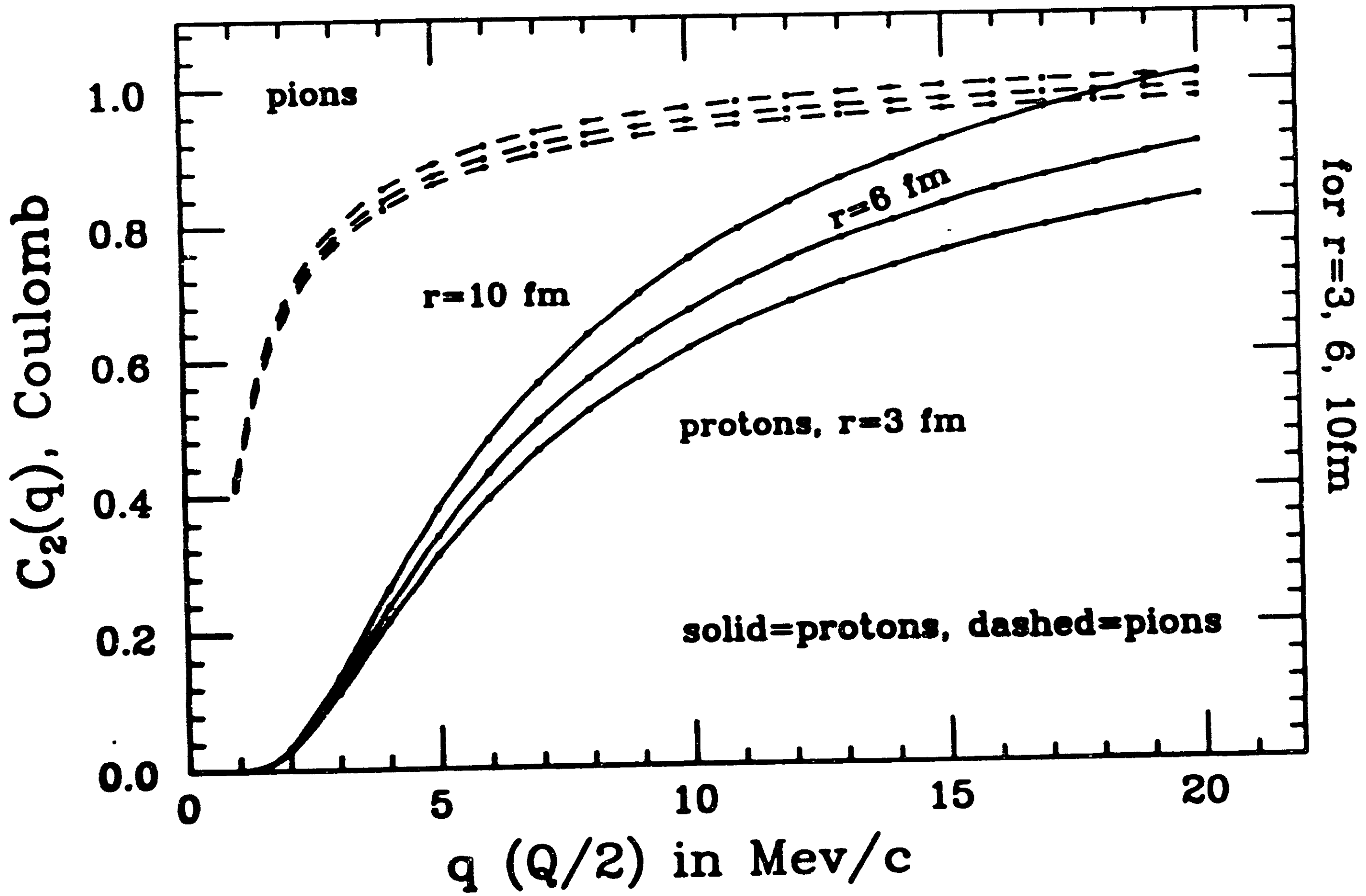

C2(q), Coulomb
1.0
0.8
0.6
0.4
0.2
0.0
0
5
10
15
20
q (Q/2) in Mev/c
pions
r=10 fm
r=6 fm
protons, r=3 fm
solid=protons, dashed=pions
for r=3, 6, 10fm

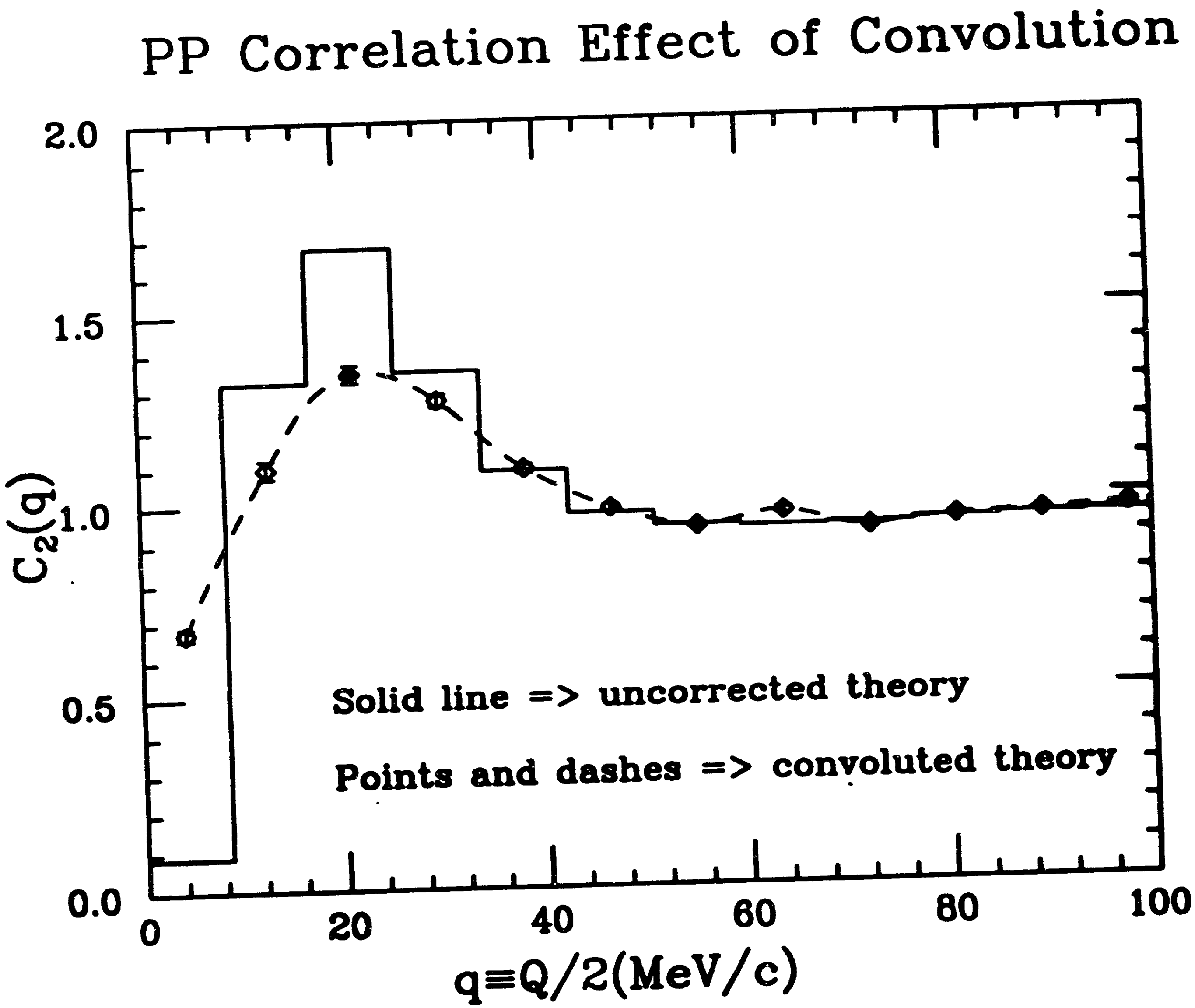
PP Correlation Effect of Convolution
2.0
1.5
1.0
0.5
0.0
$C_2(q)$
0
20
40
60
80
100
$q \equiv Q/2$(MeV/c)
Solid line => uncorrected theory
Points and dashes => convoluted theory

- **Pions and Kaons**
  - Correlation dominated by Bose-Einstein statistics.
  - Non-Coulomb residual interaction negligible.
  - Source size affects **width** of enhancement in relative momentum.
  - Can use different components of relative momentum to measure different components of the source dimension.
  - Coulomb correction typically divided out in displayed data.
  - Displayed data fit to an analytical parameterization.
  - Data normalized to 1.0 at large relative momentum.

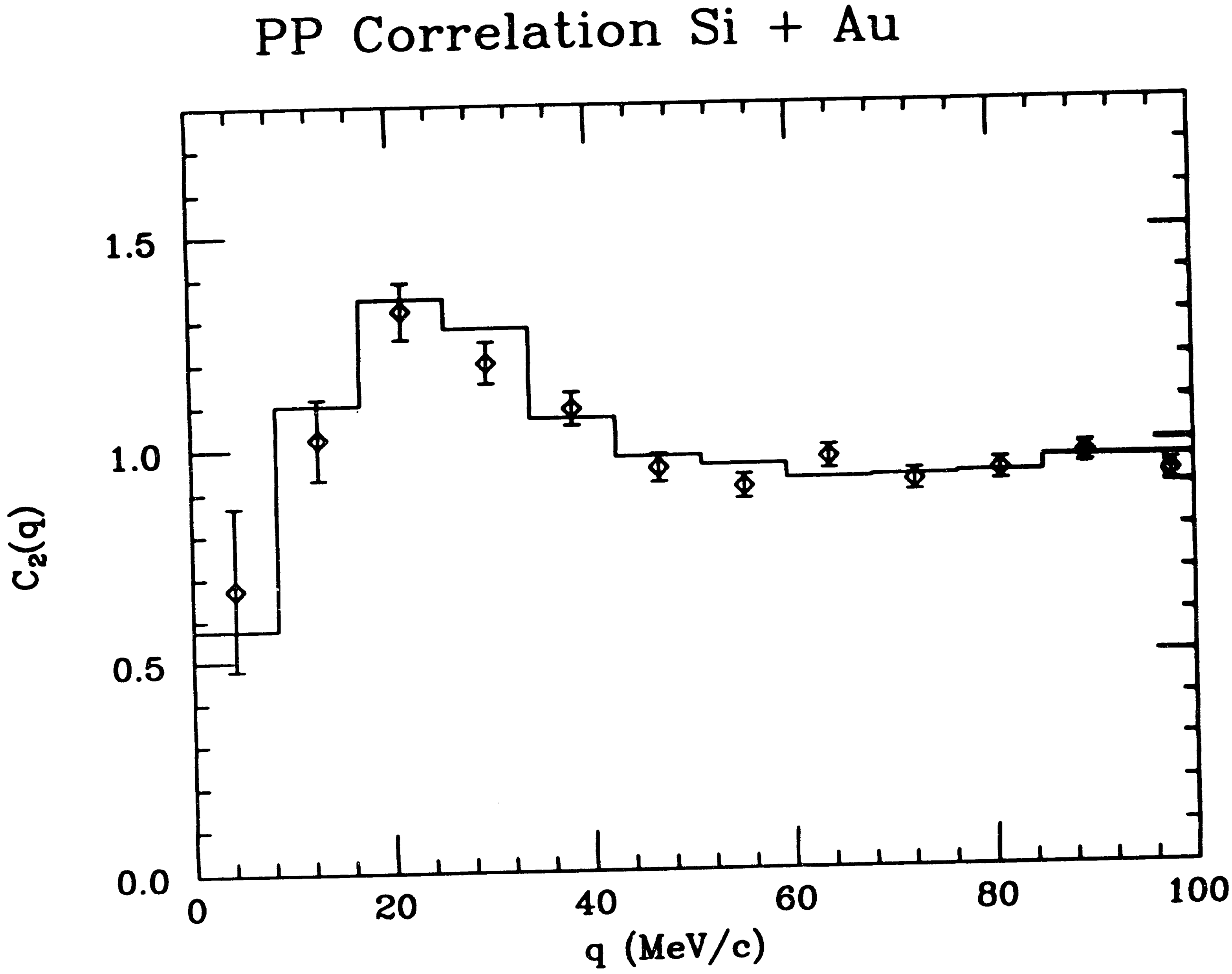
PP Correlation Si + Au
1.5
1.0
0.5
0.0
$C_2(q)$
0
20
40
60
80
100
q (MeV/c)

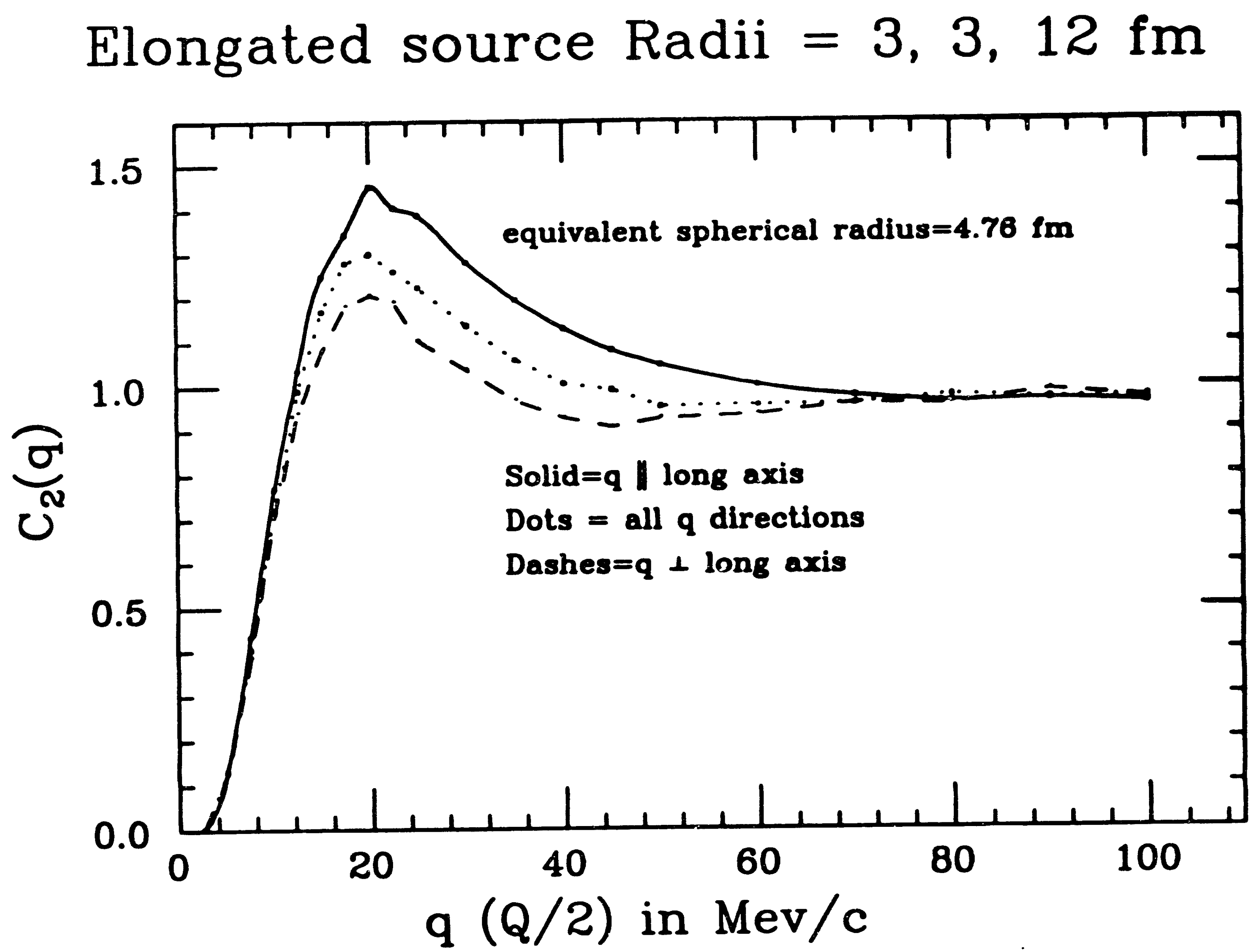

Elongated source Radii = 3, 3, 12 fm
equivalent spherical radius=4.76 fm
Solid=q ∥ long axis
Dots = all q directions
Dashes=q ⊥ long axis
1.5
1.0
0.5
0.0
0
20
40
60
80
100
C2(q)
q (Q/2) in Mev/c

Proton-Proton Correlations Si + A Central

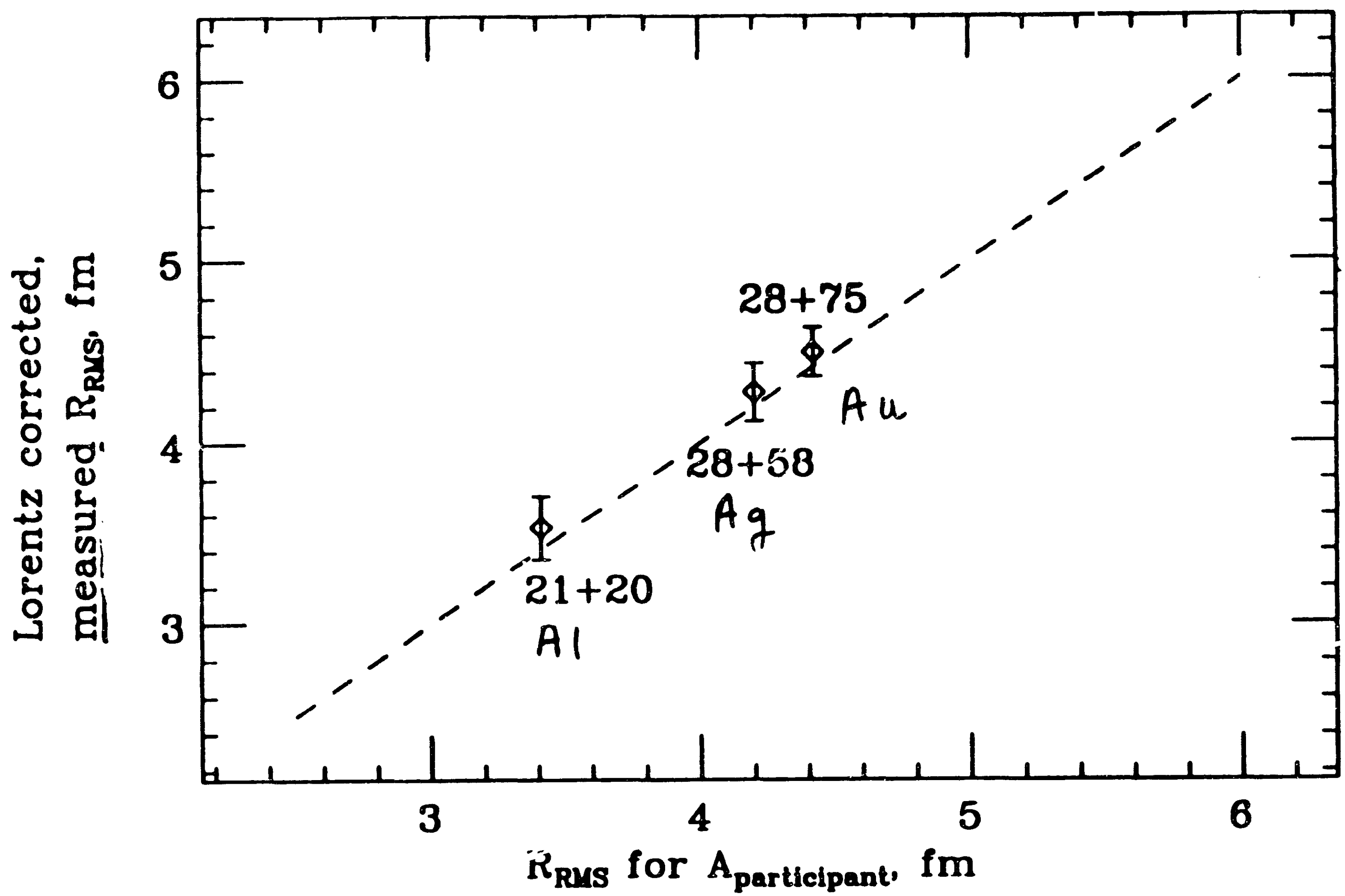

Simple geometrical model

Source Distribution	Correlation Function
$\rho(r_Q) = \exp\left(-\frac{r_Q^2}{2R_Q^2}\right)$	$C_2(Q) = 1 + \lambda\exp\left(-Q^2R_Q^2\right)$
$\rho(\vec{r},t) = \exp\left(-\frac{\vec{r}^2}{2R_Q^2} - \frac{t}{2\tau^2}\right)$	$C_2(\vec{Q},Q_0) = 1 + \lambda\exp\left(-\vec{Q}^2\vec{R}^2 - Q_0^2\tau^2\right)$
$\rho(\vec{r}_L,\vec{r}_T) = \exp\left(-\frac{\vec{r}_L^2}{2R_L^2} - \frac{\vec{r}_T^2}{2R_T^2}\right)$	$C_2(\vec{Q}_L,\vec{Q}_T) = 1 + \lambda\exp\left(-\vec{Q}_L^2\vec{R}_L^2 - \vec{Q}_T^2\vec{R}_T^2\right)$

Q_L, Q_T Distributions for K^+ and π^+ Pairs

K^+K^+	$\pi^+\pi^+$

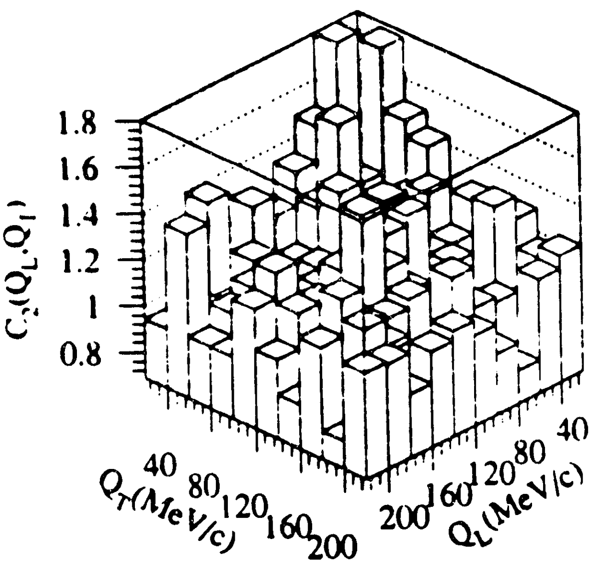

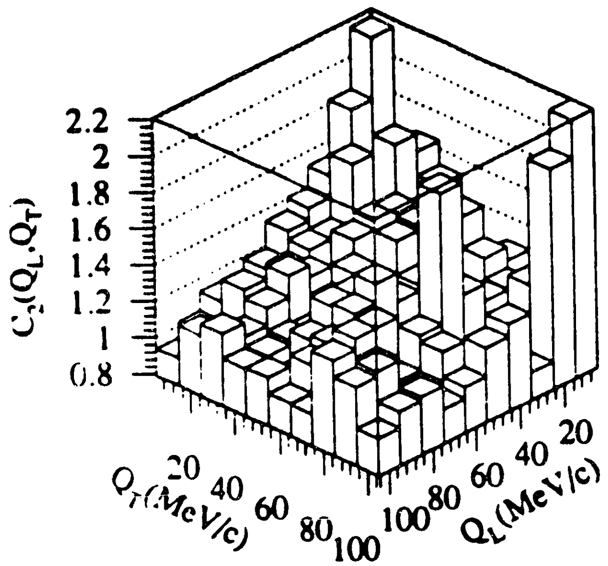

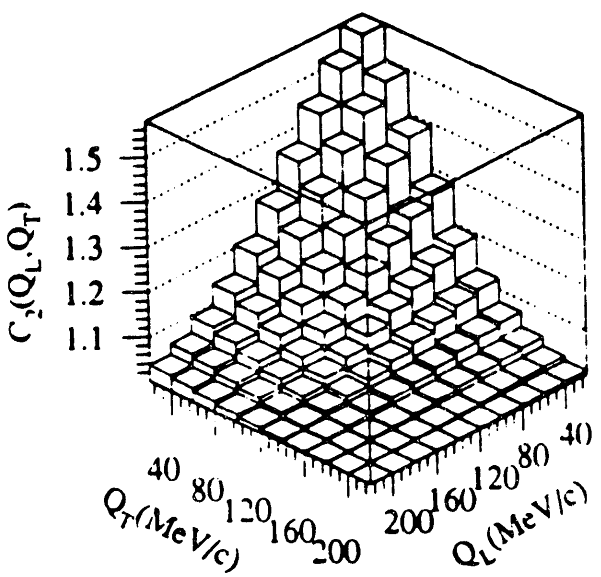

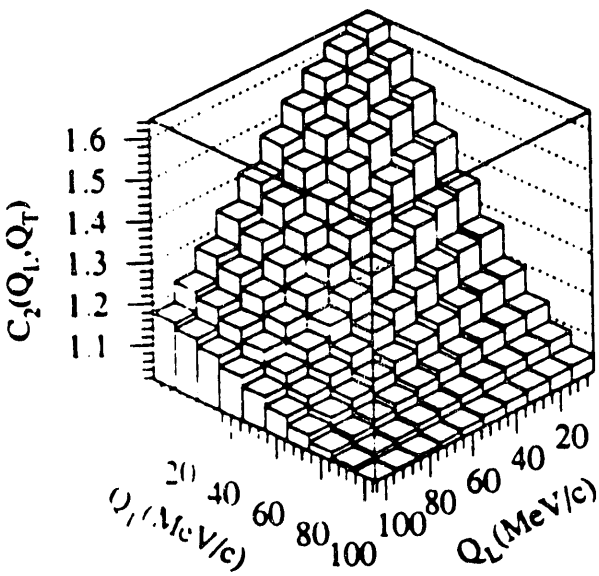

Preliminary

Q_L and Q_T Distributions for K^+ and π^+ Pairs

K^+K^+ Fit Parameters:

$R_L = 1.58 \pm 0.33$ fm
$R_T = 1.94 \pm 0.32$ fm
$\lambda = 0.67 \pm 0.16$
$\chi^2/dof = 405.25/458$

$\pi^+\pi^+$ Fit Parameters:

$R_L = 2.25 \pm 0.32$ fm
$R_T = 3.11 \pm 0.25$ fm
$\lambda = 0.56 \pm 0.06$
$\chi^2/dof = 647.42/676$

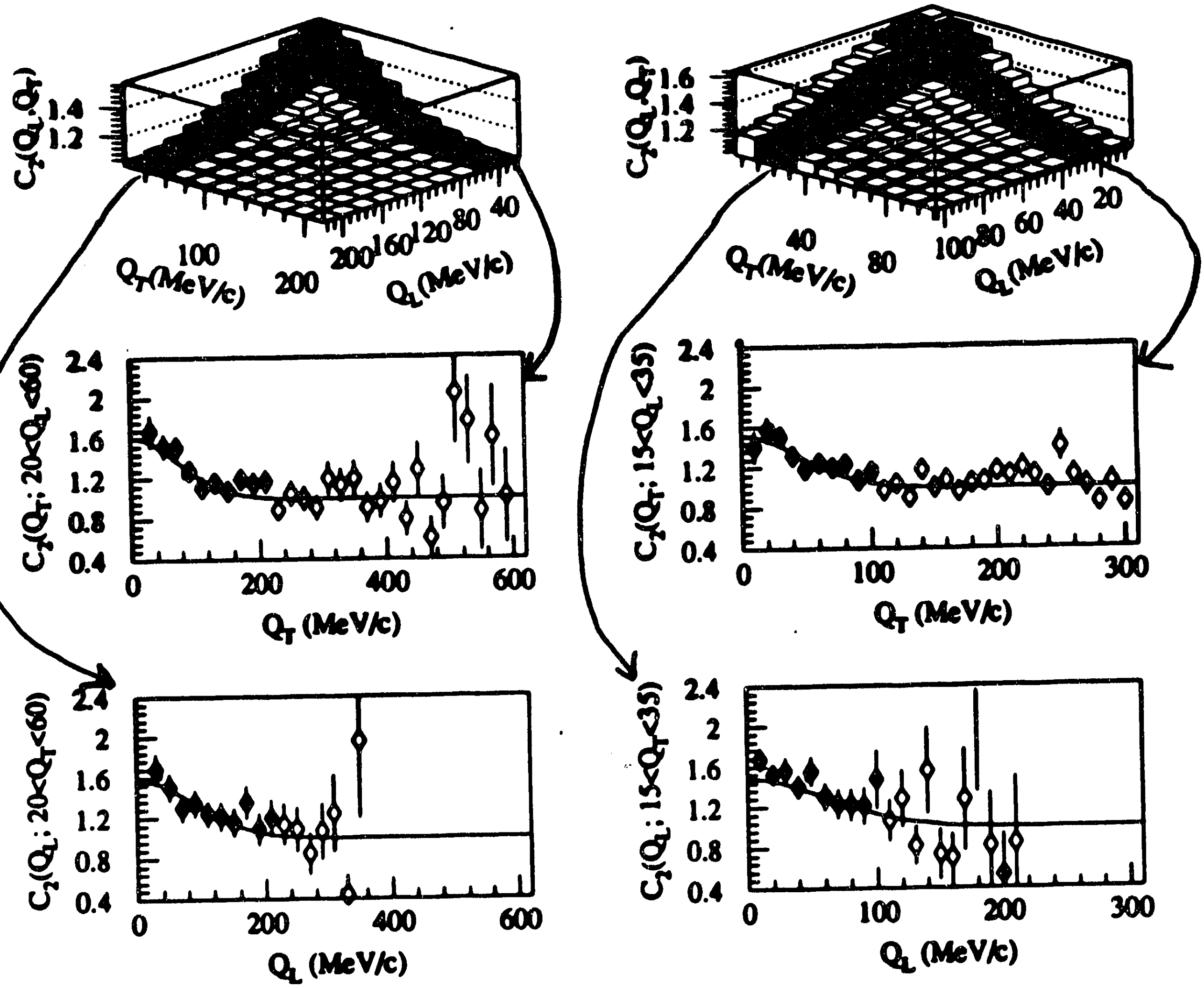

Q, Q_0 Distributions for K^+ and π^+ Pairs

K^+K^+ Fit Parameters:

$R = 1.76 \pm 0.23$ fm
$\tau = 0.00 \pm 1.34$ fm
$\lambda = 0.73 \pm 0.15$
$\chi^2/\text{dof} = 286.81/312$

$\pi^+\pi^+$ Fit Parameters:

$R = 2.66 \pm 0.33$ fm
$\tau = 2.52 \pm 0.56$ fm
$\lambda = 0.55 \pm 0.07$
$\chi^2/\text{dof} = 368.61/369$

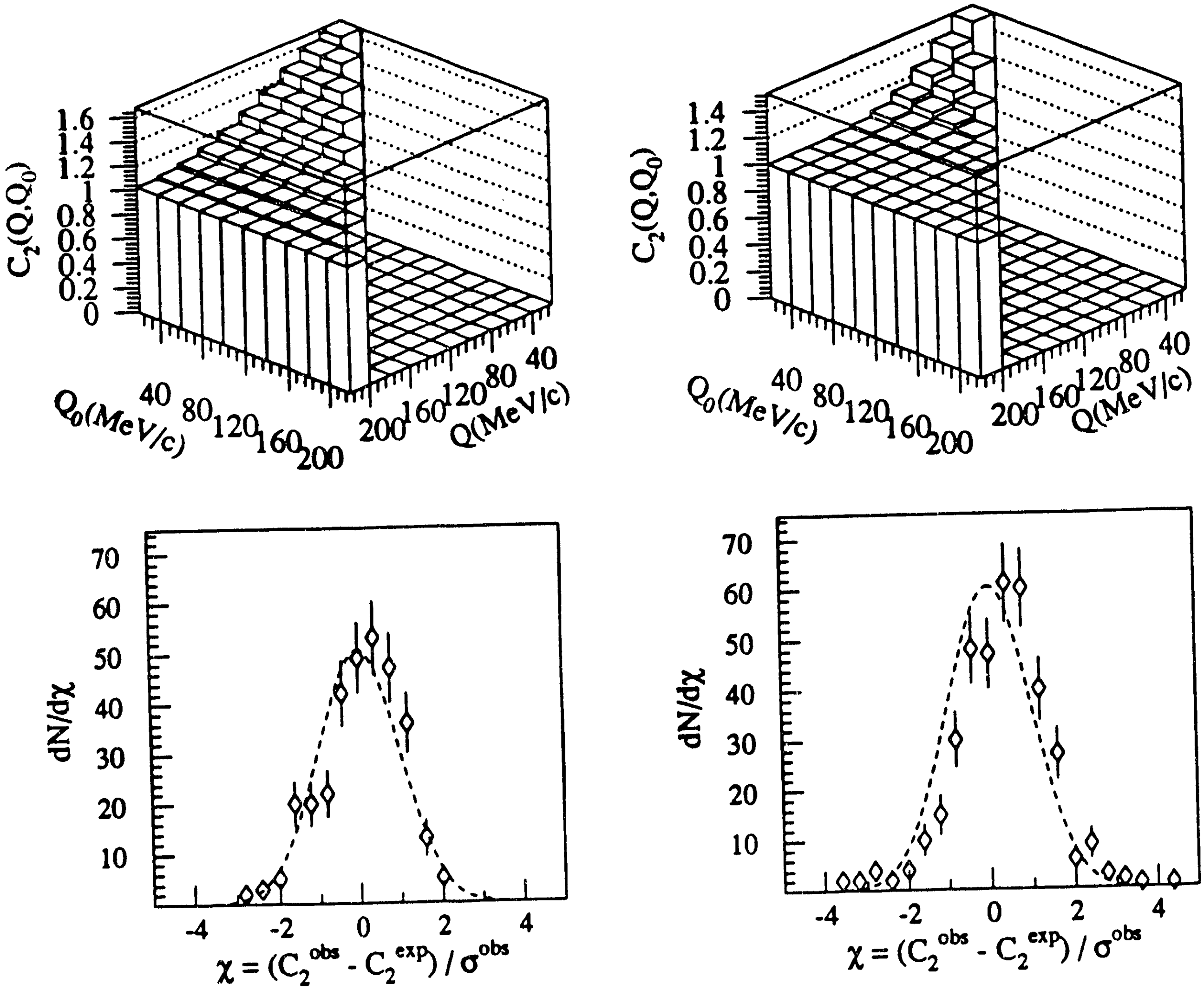

Radii Summary

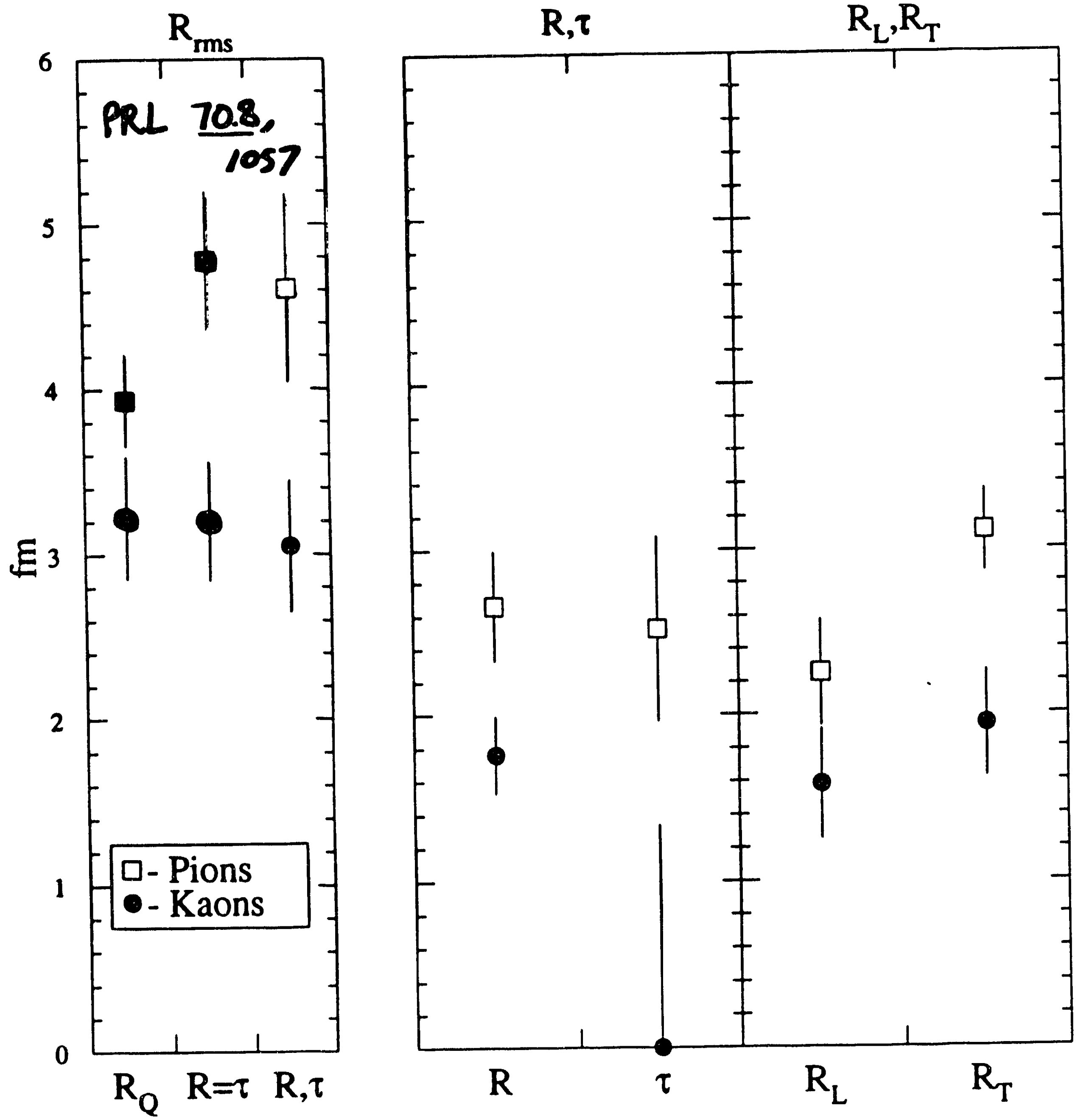

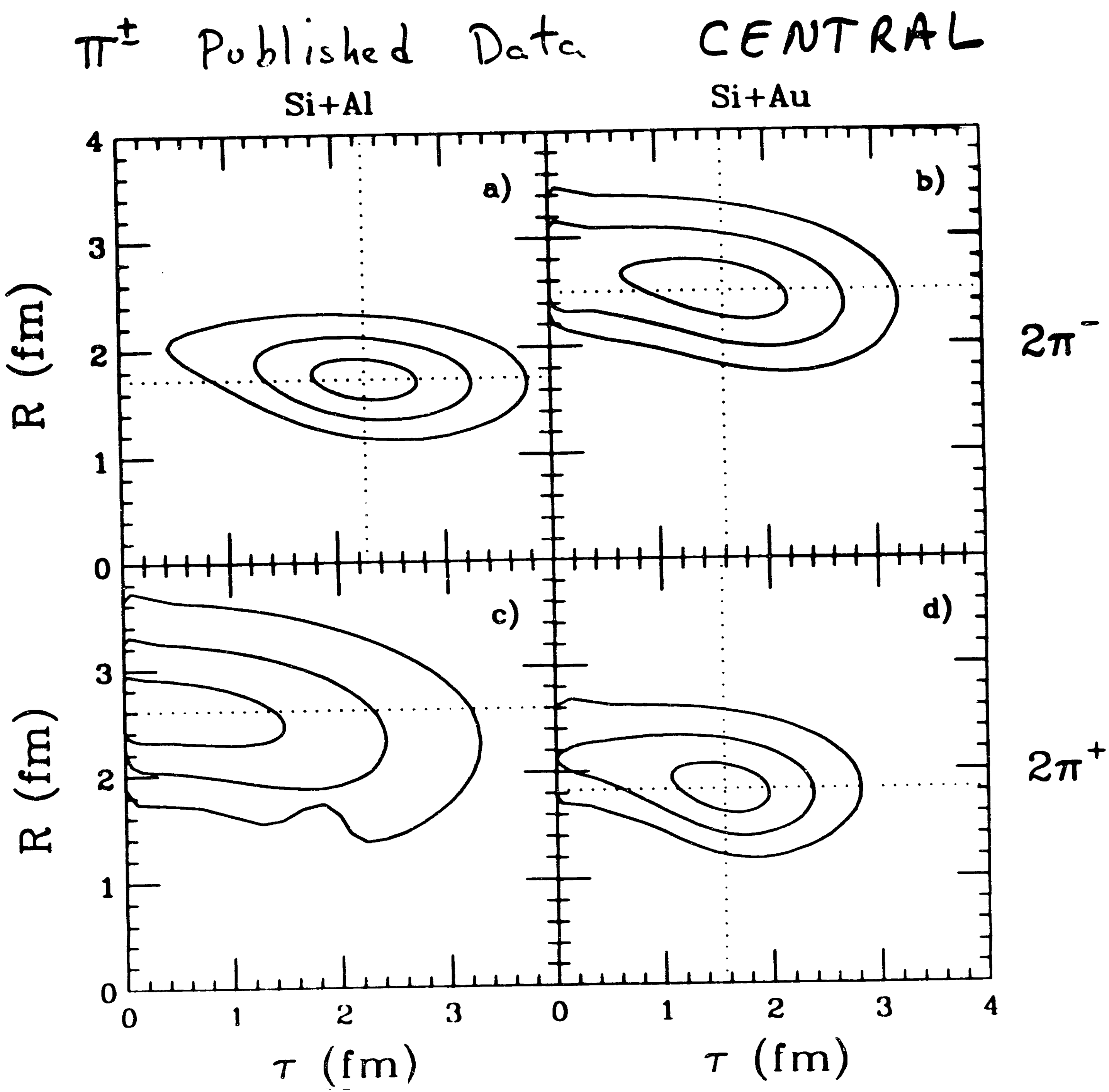

$\pi^{\pm}$ Published Data CENTRAL
Si+Al
Si+Au
a)
b)
c)
d)
$2\pi^-$
$2\pi^+$
R (fm)
R (fm)
τ (fm)
τ (fm)
0
1
2
3
4

Si+Au --> $2\pi^- + X$

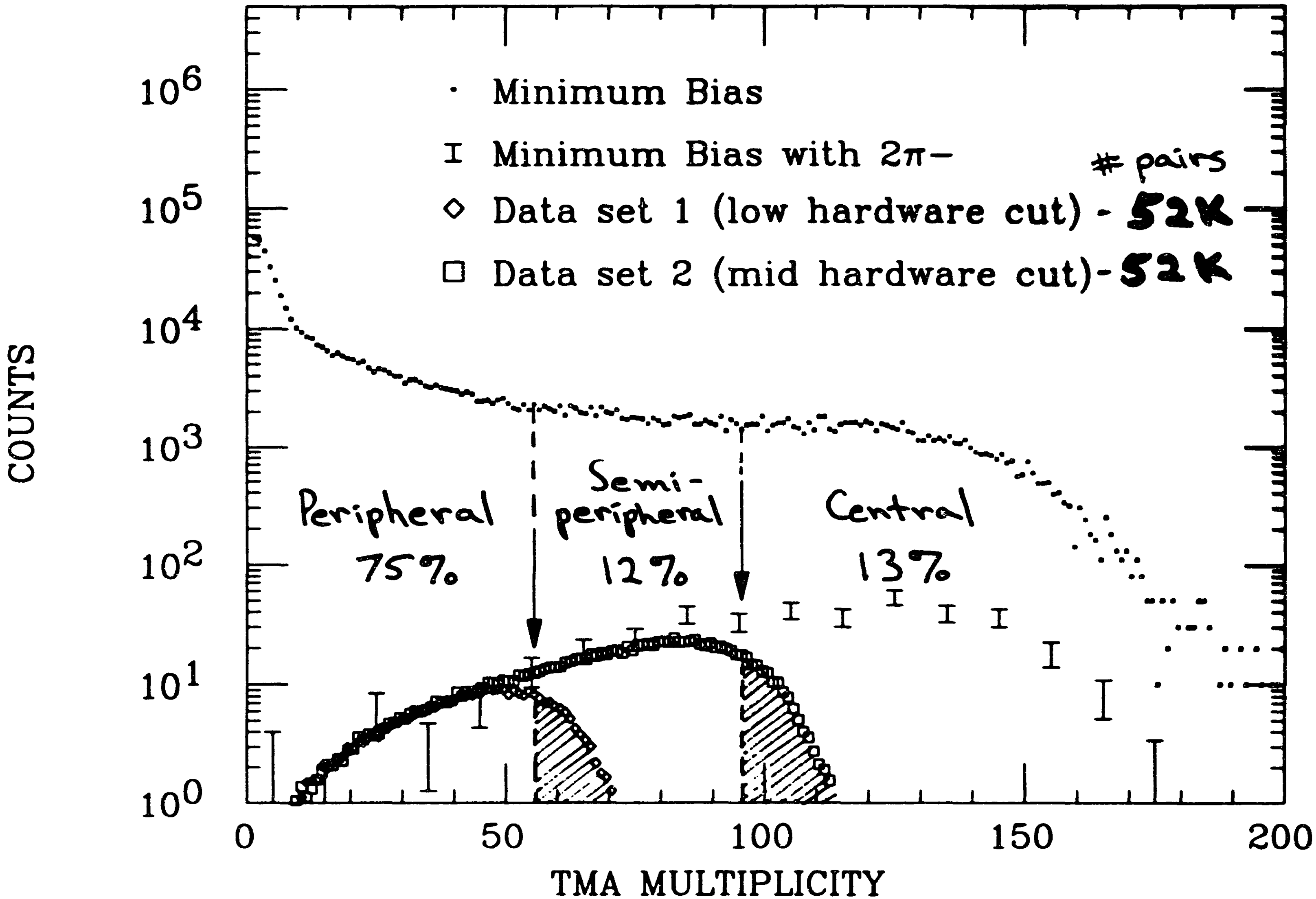

⇨ Taken with world famous E859 trigger!

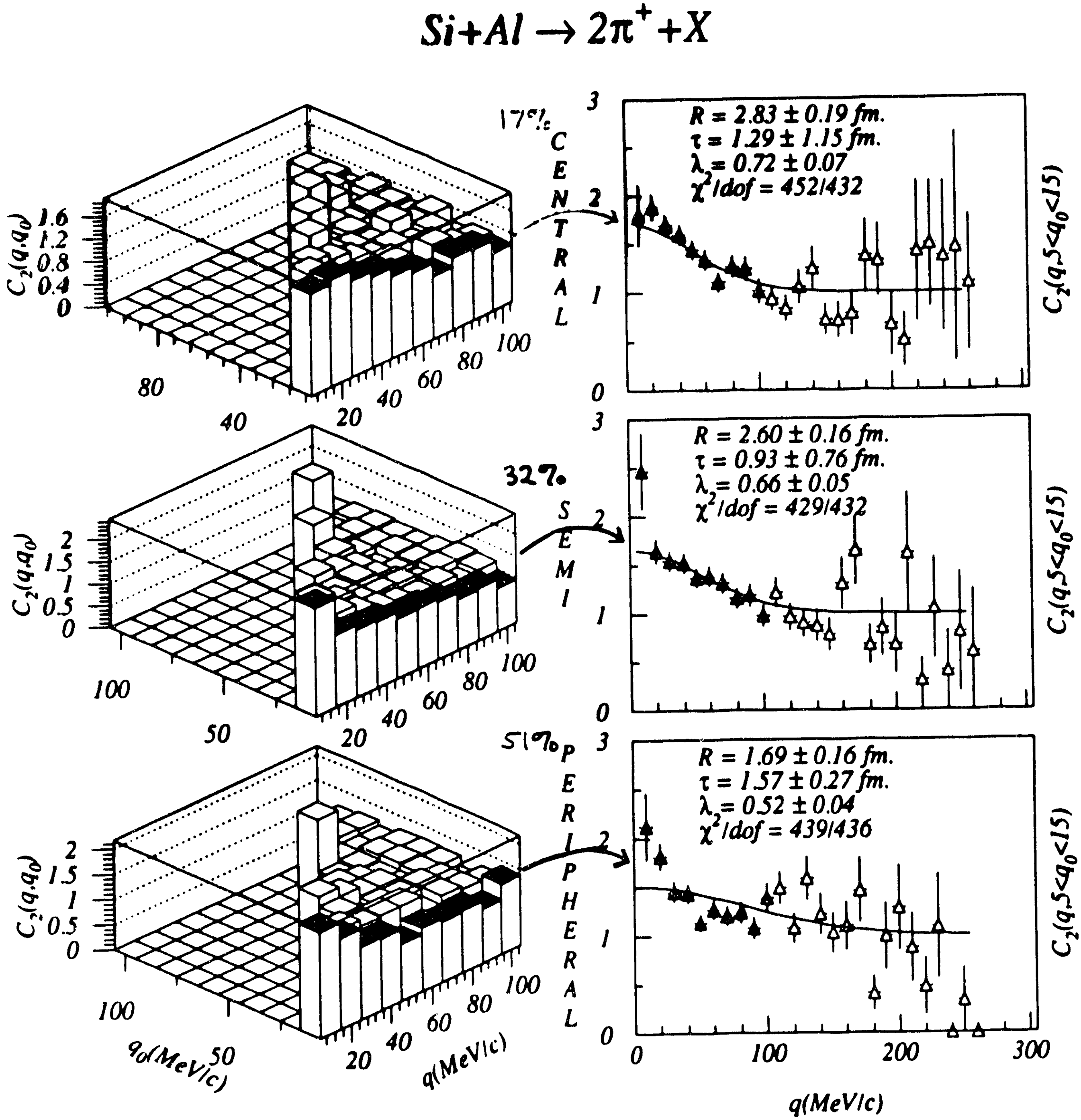
Si+Al → 2π⁺+X
17%
CENTRAL
32%
SEMI
51%
PERIPHERAL
R = 2.83 ± 0.19 fm.
τ = 1.29 ± 1.15 fm.
λ₂ = 0.72 ± 0.07
χ²/dof = 452/432
R = 2.60 ± 0.16 fm.
τ = 0.93 ± 0.76 fm.
λ₂ = 0.66 ± 0.05
χ²/dof = 429/432
R = 1.69 ± 0.16 fm.
τ = 1.57 ± 0.27 fm.
λ₂ = 0.52 ± 0.04
χ²/dof = 439/436
C₂(q,q₀)
C₂(q,5<q₀<15)
q₀(MeV/c)
q(MeV/c)

Si+Au/Al: Radius vs. Multiplicity

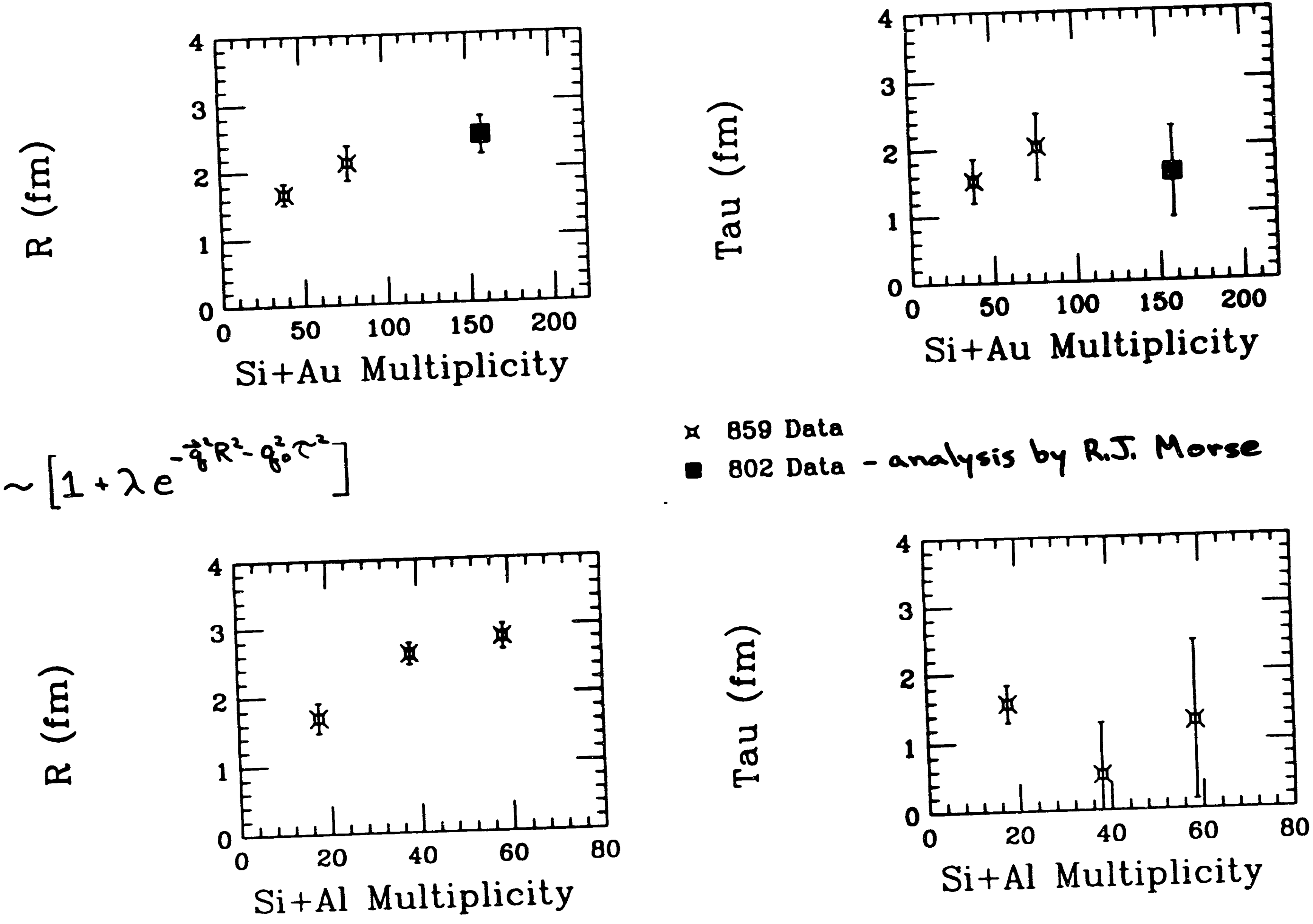

$$C_2 \sim \left[1 + \lambda e^{-\vec{q}^2 R^2 - q_0^2 \tau^2}\right]$$

$Au+Au \rightarrow 2\pi^- + X$ (Central)

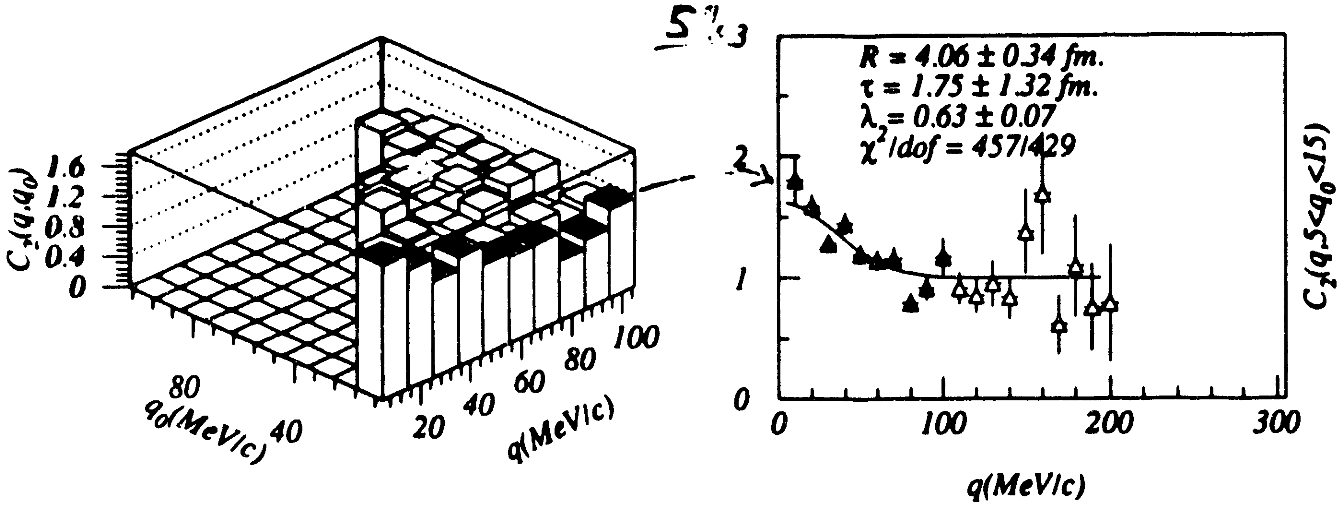

Correlation Fn. Radii vs. Bartke Scaling

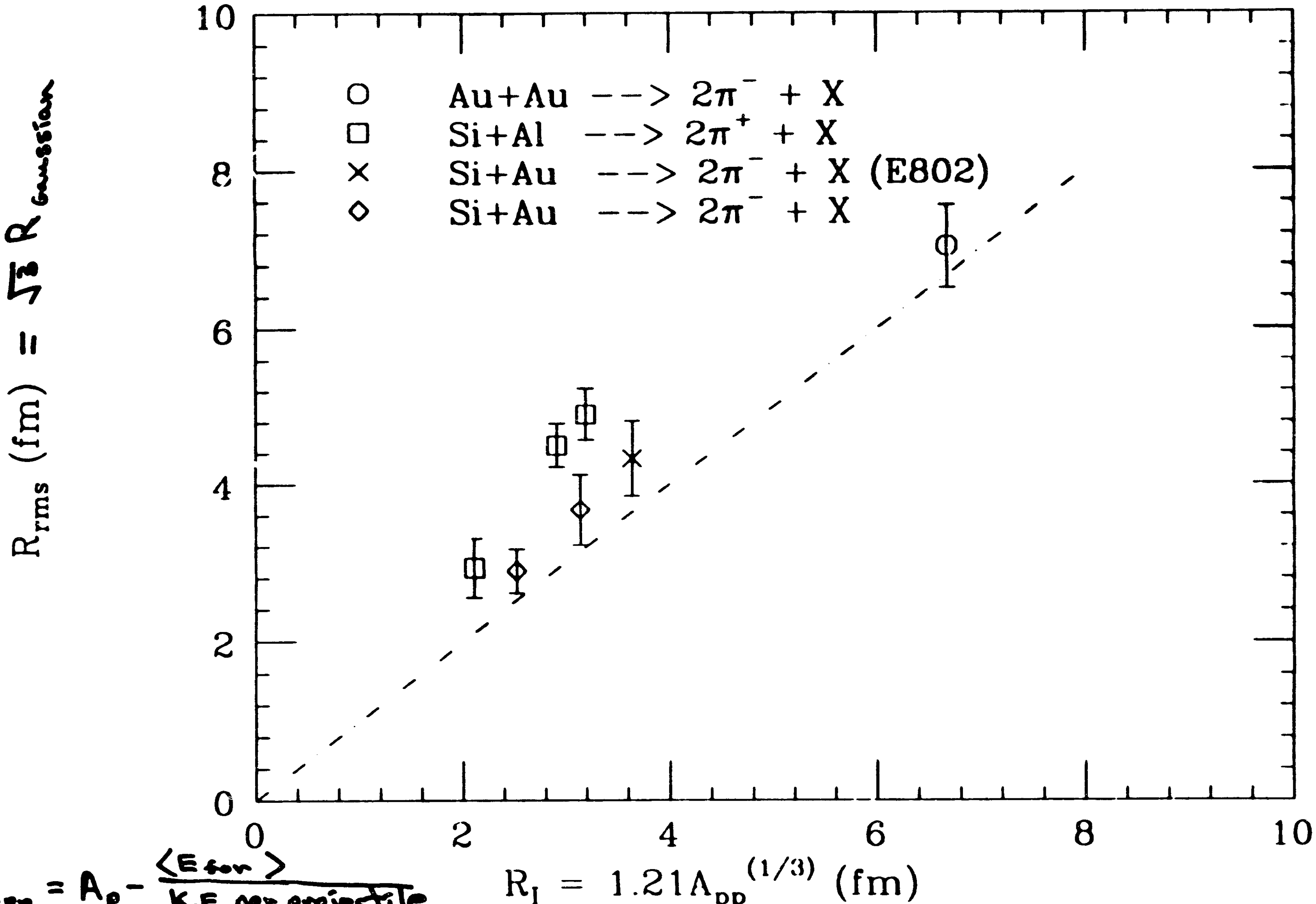

$A_{pp} = A_p - \frac{\langle E_{for} \rangle}{\text{K.E. per projectile}}$

projectile participants

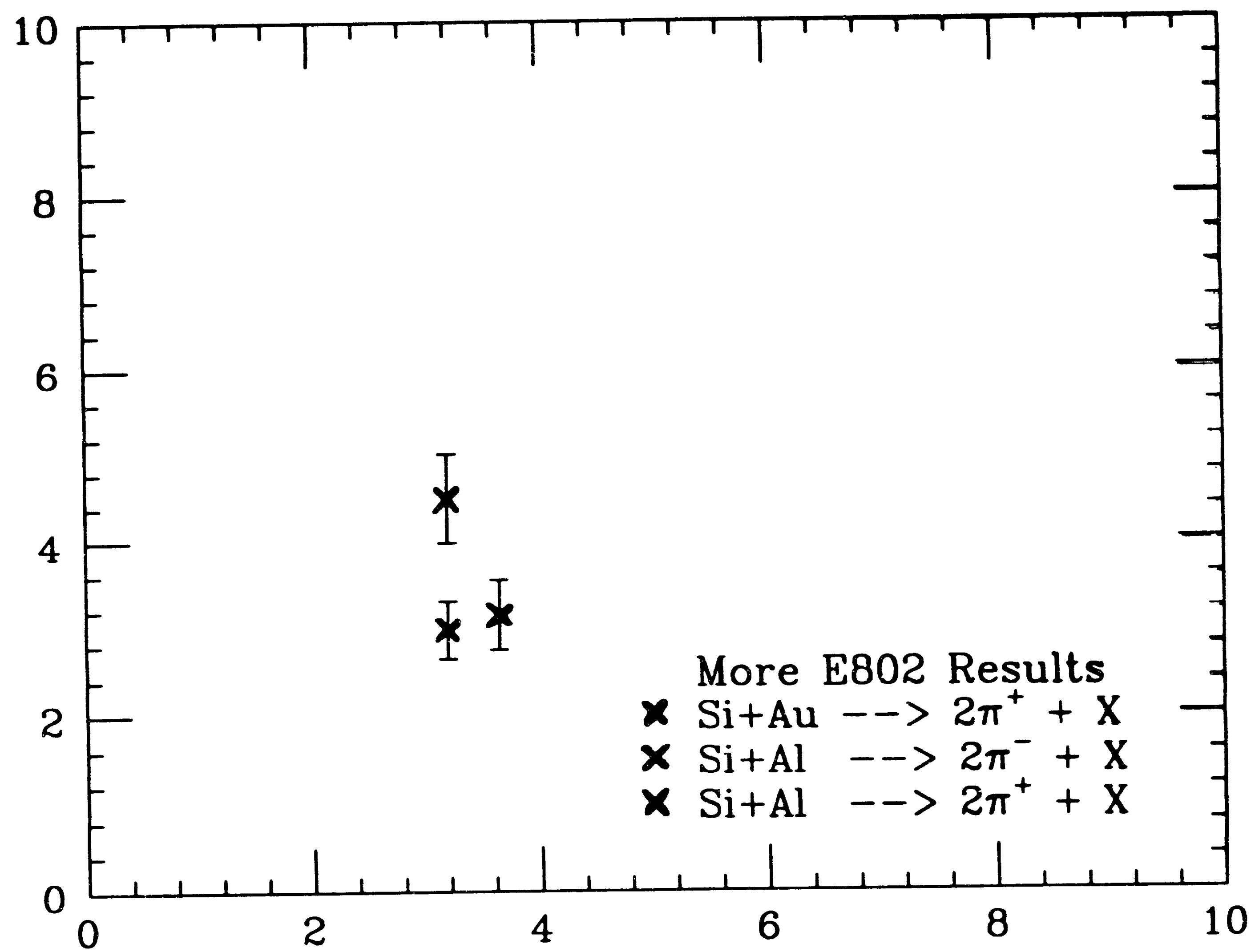
More E802 Results
Si+Au --> 2π⁺ + X
Si+Al --> 2π⁻ + X
Si+Al --> 2π⁺ + X
0
2
4
6
8
10

Summary

- Pion central and non-central data follow a general scaling with the number of projectile participants.
    - Differences between Si + Al and Si + Au, as well as between π^+ and π^-, need to be understood.

- Kaons come from a source that may be slightly smaller than that for pions.

- Protons follow a general scaling with the total number of participants.

- ARC predicts large effects due to dynamical correlations between the direction of the momentum and the location in the source.

- Lots of exciting opportunities to study the dynamics of particle production.

Recent Results on Two Particle Correlations from E814

Nu Xu
Stony Brook

Preliminary Result !

Two-Particle Correlations in ^{28}Si + Pb Collisions at the BNL AGS

Nu Xu — E814 Collaboration: BNL, GSI, McGill Univ., Univ. of Pitt.
SUNY Stony Brook, Univ. of São Paulo, Wayne State Univ., Yale Univ.

- Two-particle correlation functions → Space-Time info.
  0.03 ~ 200 A·GeV/c;
  Apparent source size obtained;
  Resonance effect: Δ, ρ, ω, ... η

- **The reaction:**
  14.6 A·GeV/c ^{28}Si + Pb → 2 particles + X ($\sigma/\sigma_{geom} \leq 10\%$)

- **The correlation functions:**

$$C_2(Q_{inv}) = \frac{N_{tr}(Q_{inv})}{N_{bk}(Q_{inv})} \quad Q_{inv} = 0.5 \cdot \sqrt{-q^{\mu} q_{\mu}}$$

  $N_{tr}(Q_{inv})$–same event, $N_{bk}(Q_{inv})$–mixing events.

- **The results:** ~25% of 1991 run 3 days
  (1) Result of the two-proton correlations
  (2) Result of the two-pion correlations, $\pi^{\pm}$-$\pi^{\pm}$, π^{+}-π^{-}
  (3) Correlation functions from RQMD

- **Conclusions**

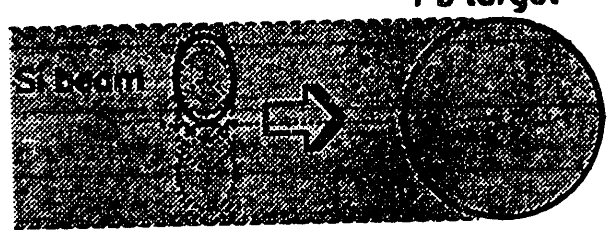

Acc. $-14 < \theta_x < 120$ msr

$-16 < \theta_y < 16$ msr

time: ~ 350 ps

momentum: $\sim 0.5\%$

E814/E877

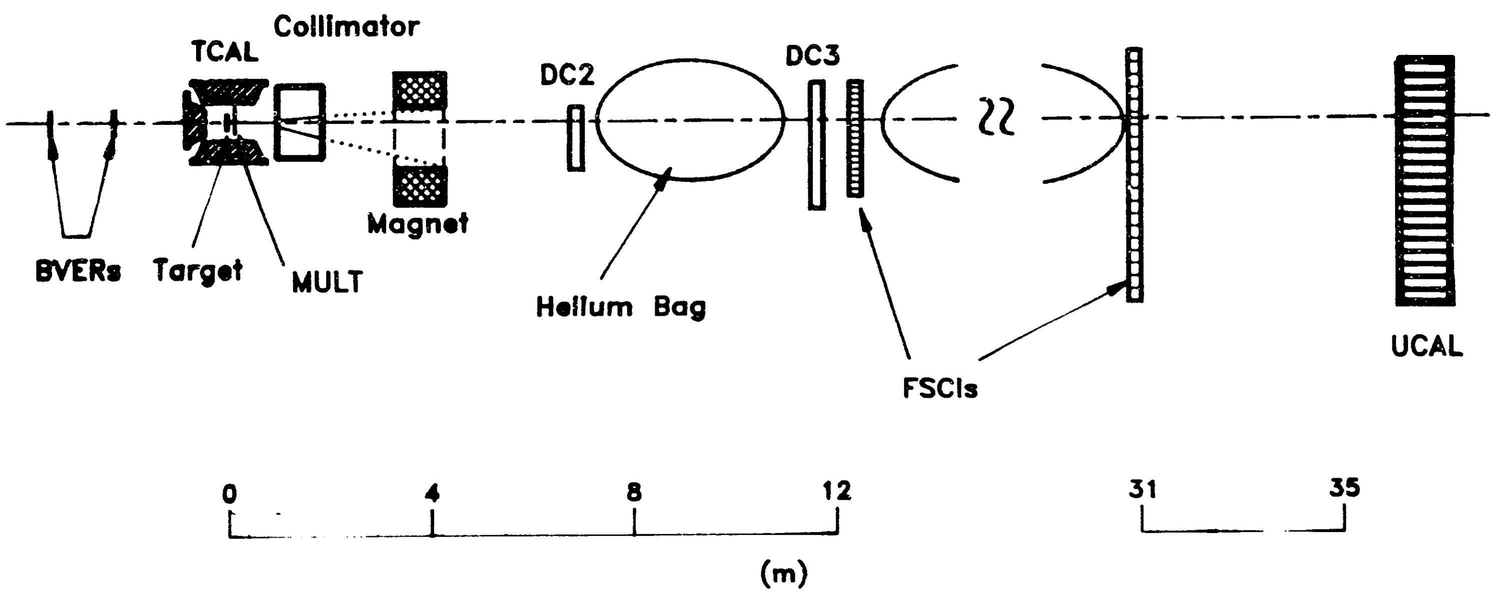

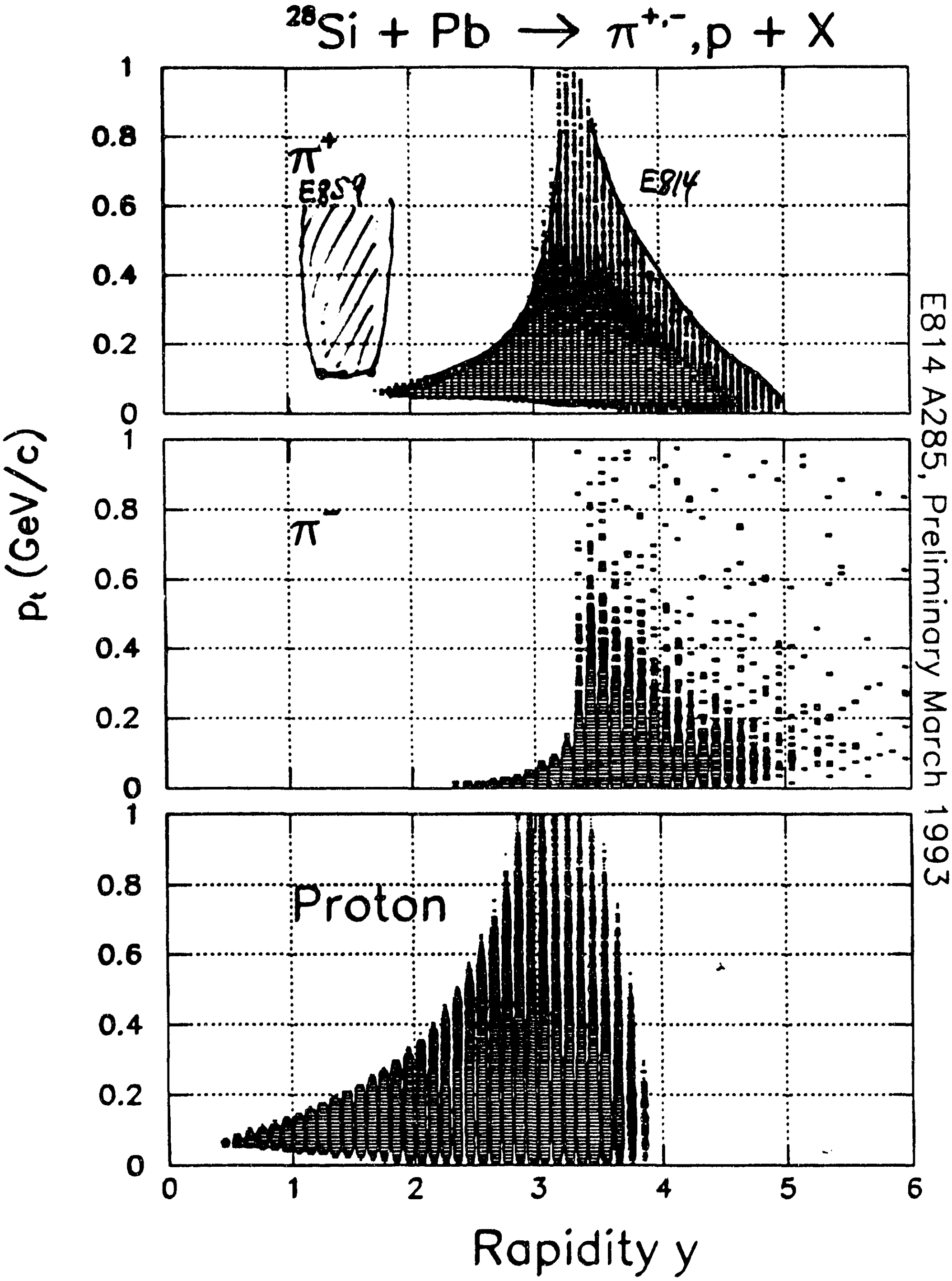

single part. acceptance in E814

Hemmick et al. E814

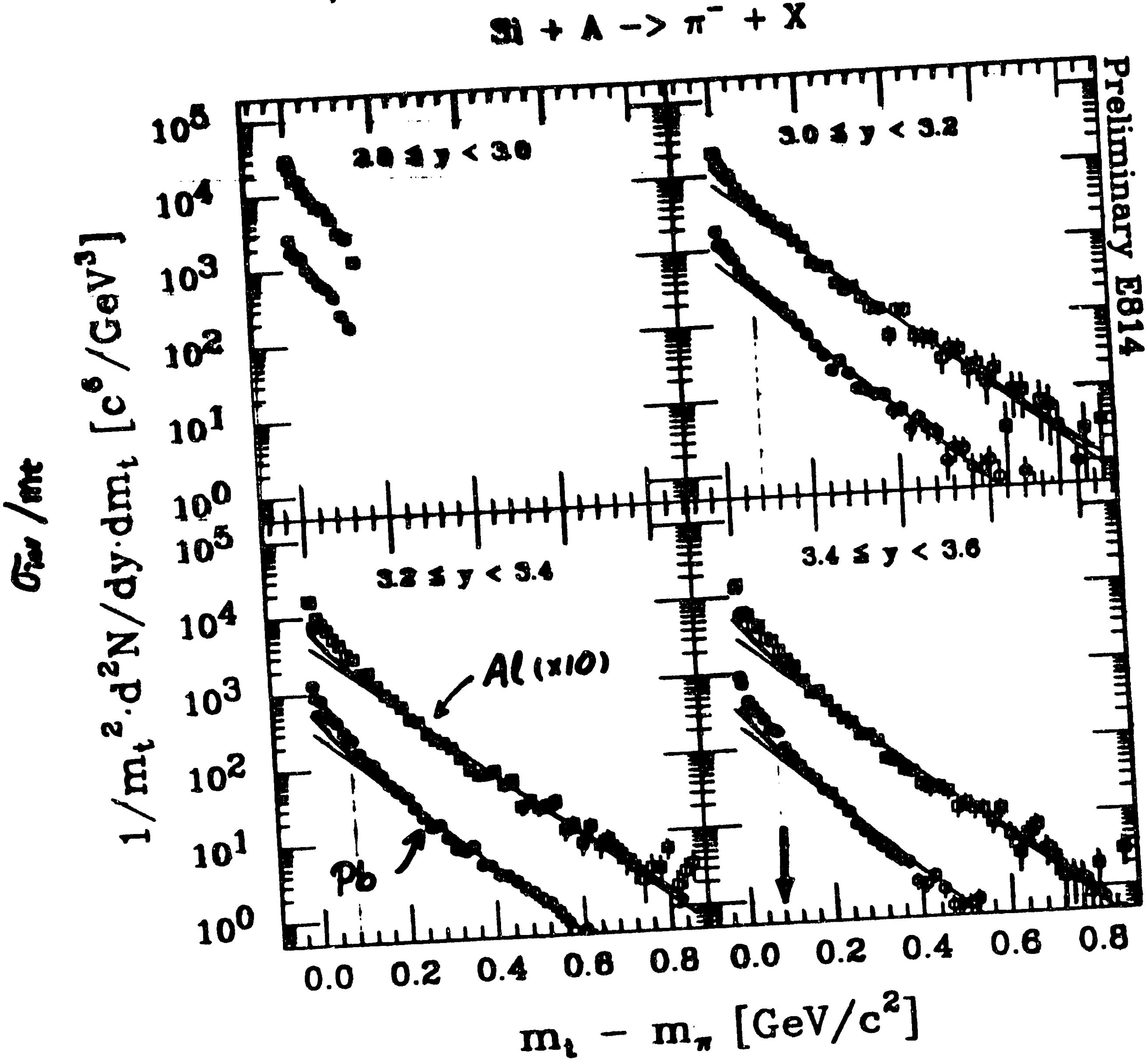

--- Exponential fit

— Boltzman fit

$m_t - m_\pi$	0.06	0.08	0.10
p_t	0.14	0.17	0.20

93/04/01 14.00

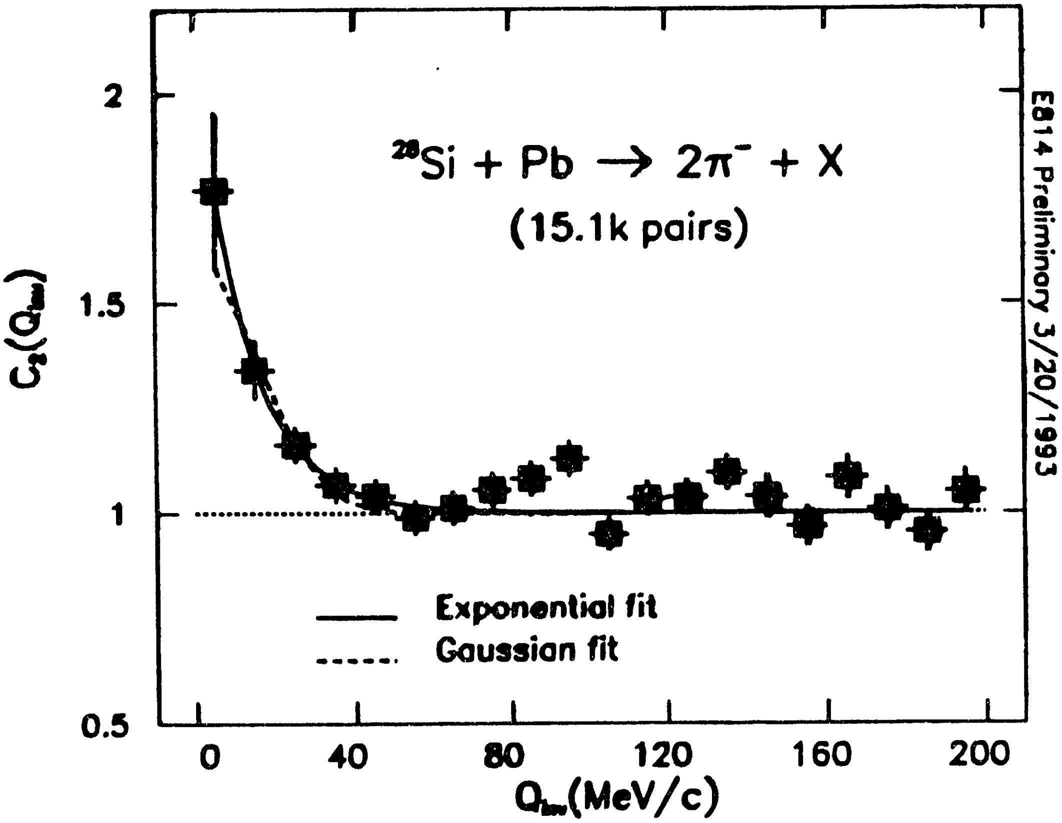

$R^{g}_{inv} = 4.5 (.7)$

$\lambda^{g} = .6 (.2)$

$R^{e}_{inv} = 7.6 (1.1)$

$\lambda^{e} = 1.11 (.3)$

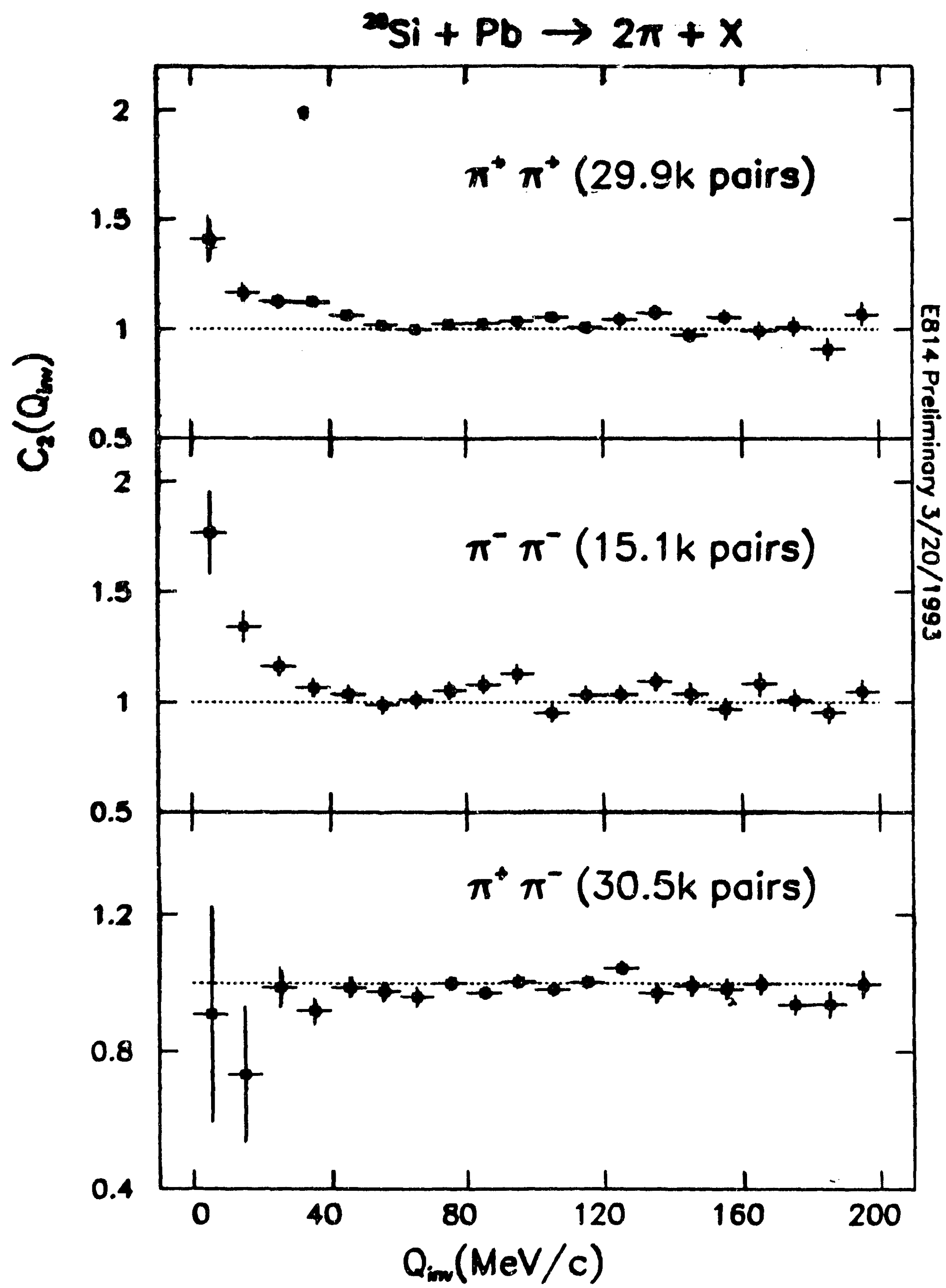

- Coulomb corrected data
- Acc. & eff. ~ 5 - 10%
- All error bars are statistical

93/04/01 23.30

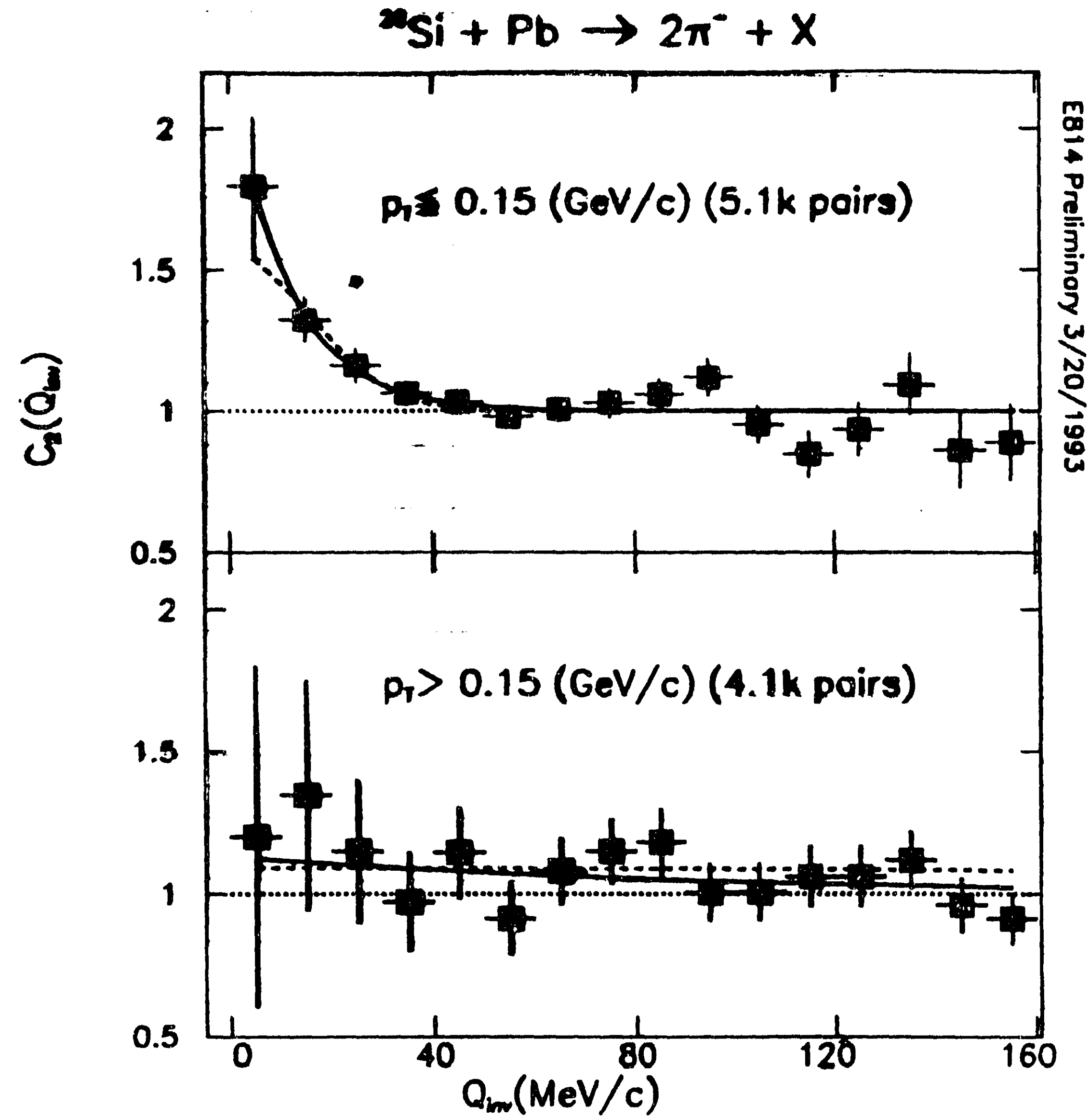

$R^g = 4.4(.8)$
$\lambda^g = .57(.18)$

$R^e = 8.2\ (1.9)$
$\lambda^e = 1.18\ (.42)$

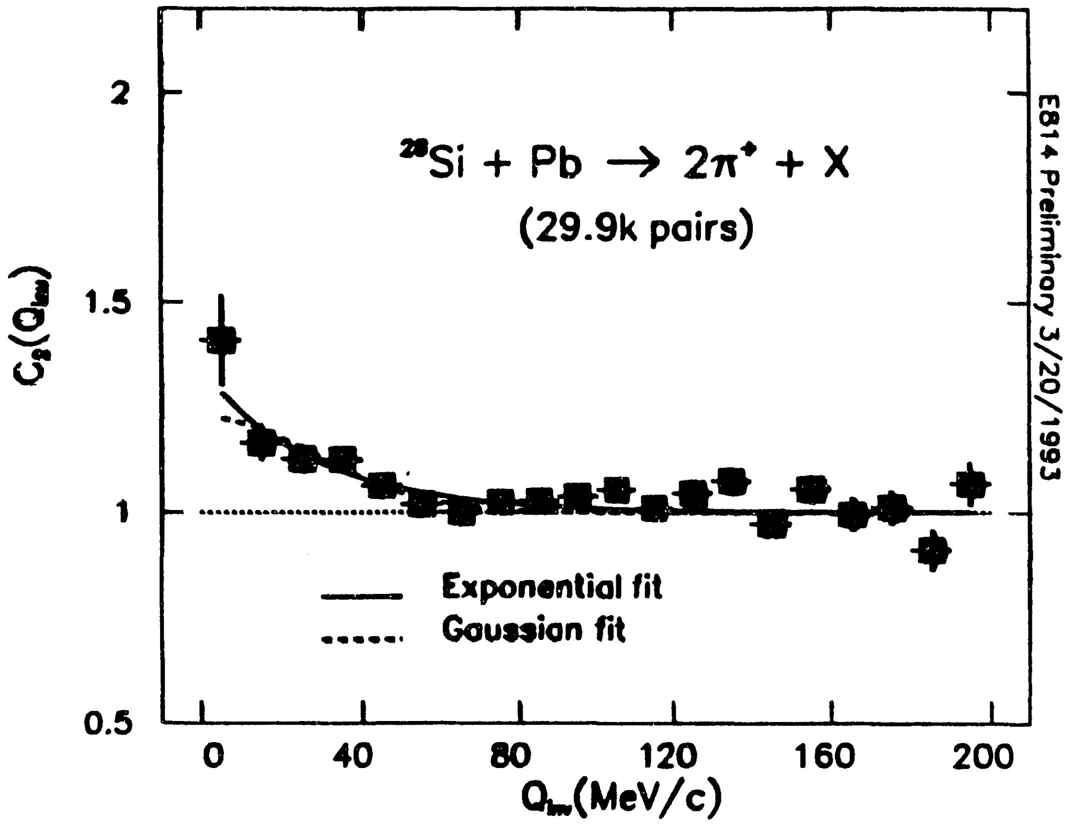

$R^g_{inv} = 2.5(.3)$

$\lambda^g = .23(.04$

$R^e_{inv} = 3.5(.9)$

$\lambda^e = .34(.11$

---- Gaussian Fit

—— Exponential Fit

93/04/01 22.54

$^{28}Si + Pb \rightarrow 2\pi^+ + X$

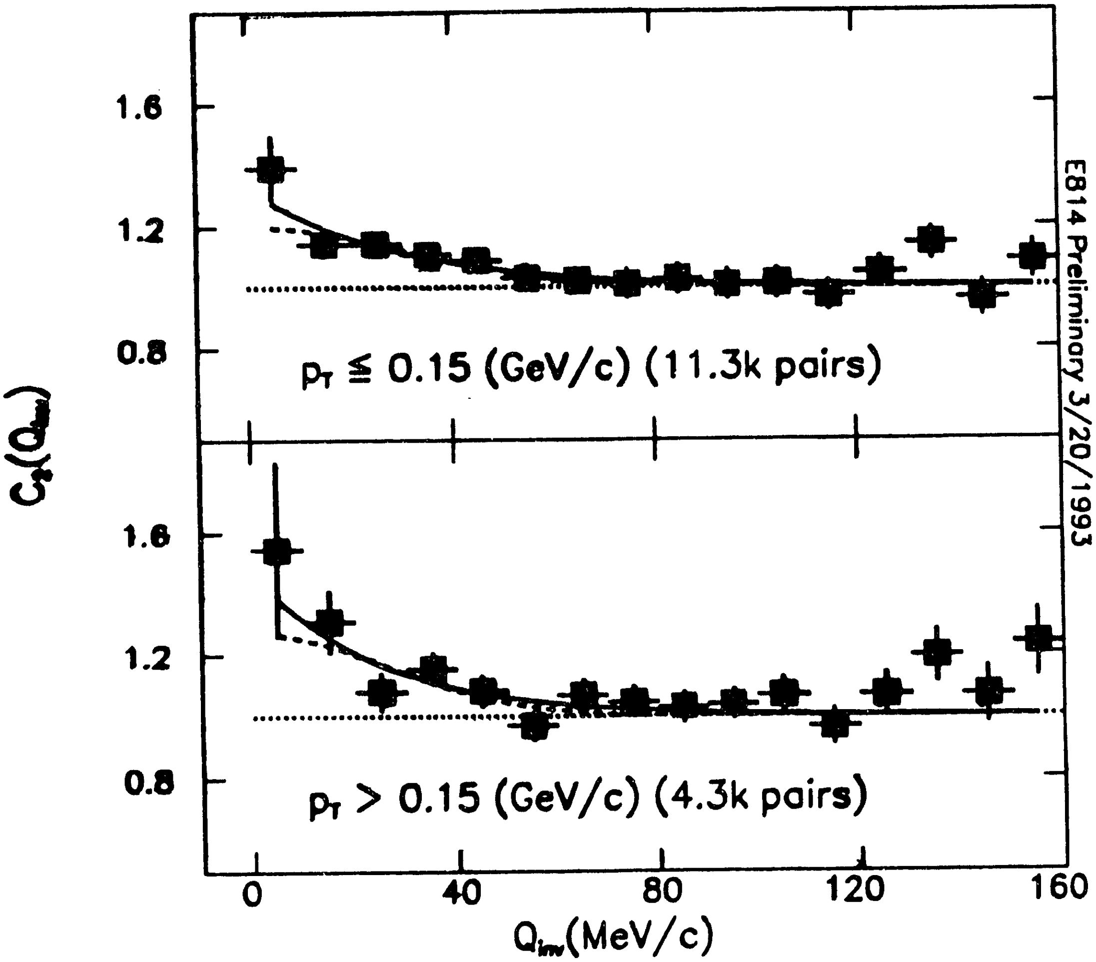

$R^g = 2.3(.4)$

$\lambda^g = .20(.04)$

$R^e = 3.5(1.0)$

$\lambda^e = .33(.1)$

$R^g = 2.7(.9)$

$\lambda^g = .27(.13)$

$R^e = 4.1(2.3)$

$\lambda^e = .47(.32)$

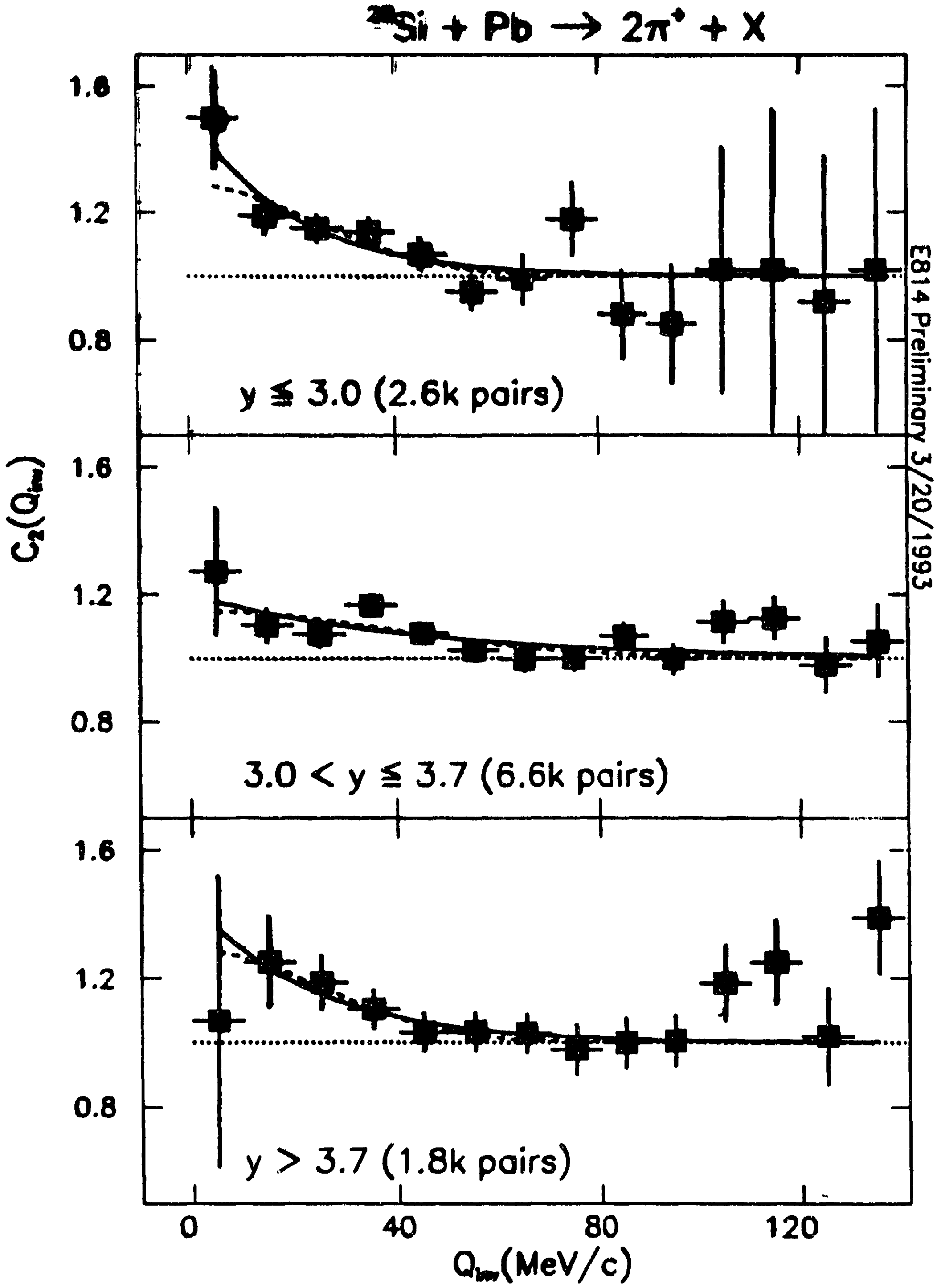

R^g_{inv}	R^e_{inv}
2.9(.1)	5.0(1.9
1.8(.1)	2.3(1.5
2.9(.1)	4.3(3.1

93/01/11 16.05

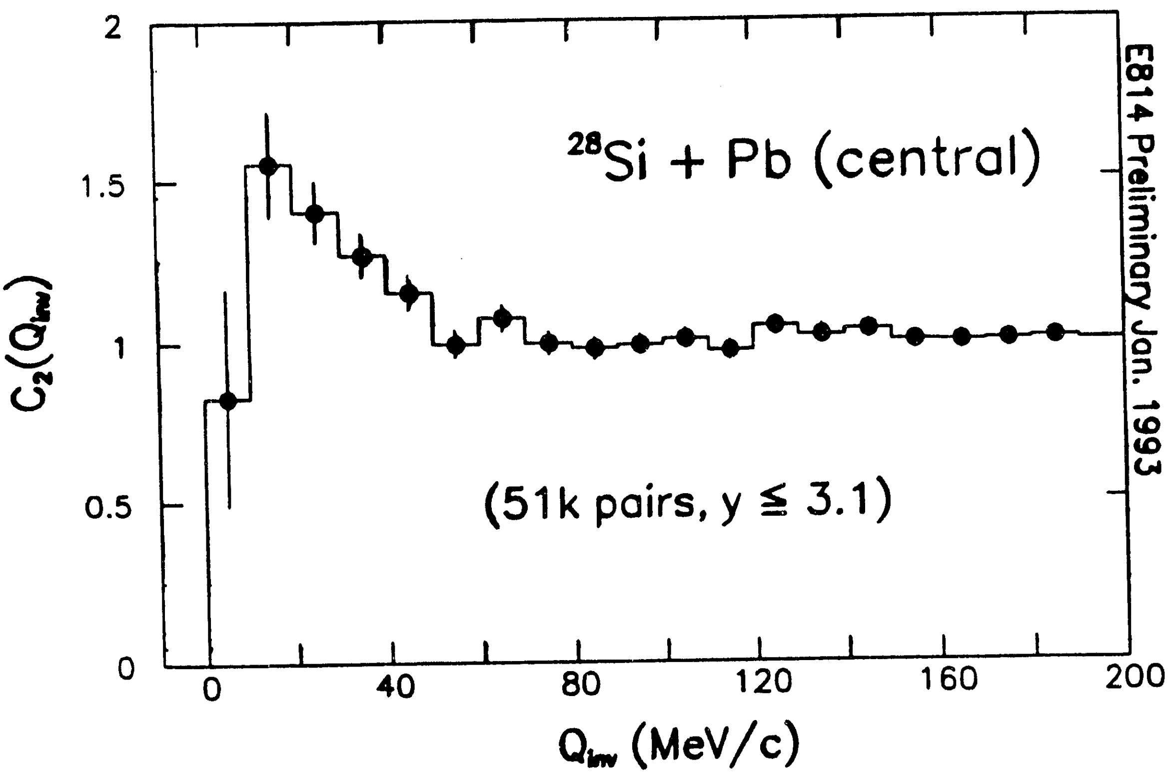

Error bars are statistical

R = 2.3 +/− 0.2 (fm)

$R_{rms} = 3.98 \pm 0.35$ (fm) ~ $R_{proj.}$

N. Xu et. al. HIPAGS '93 E814

93/04/09 15.08

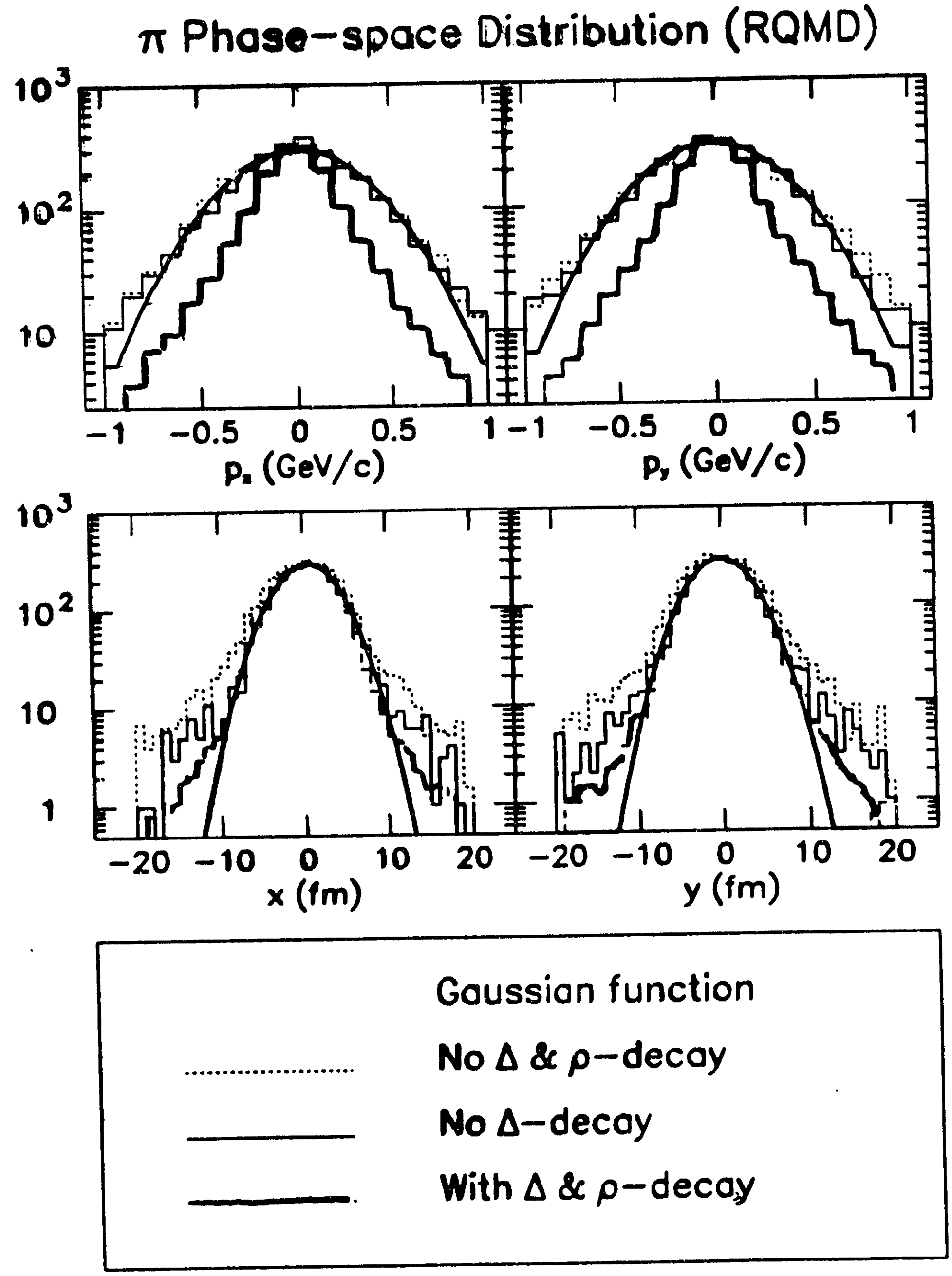

14.6 AGeV/c ^{28}Si + Pb → π + X

93/03/31 12.13

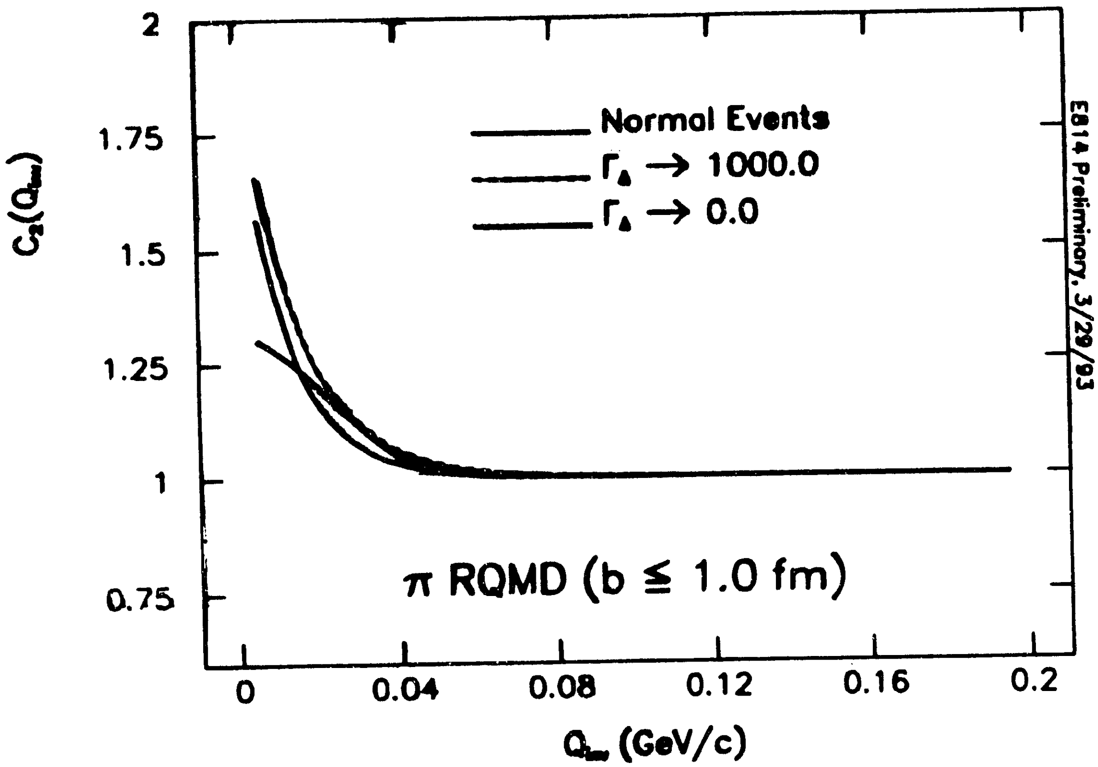

— No Δ-decay

— Δ-decay

Bolz, Ornik, Plümer, Schlei, and Weiner

Volume 300, number 4 PHYSICS LETTERS B 18 February 1

1993

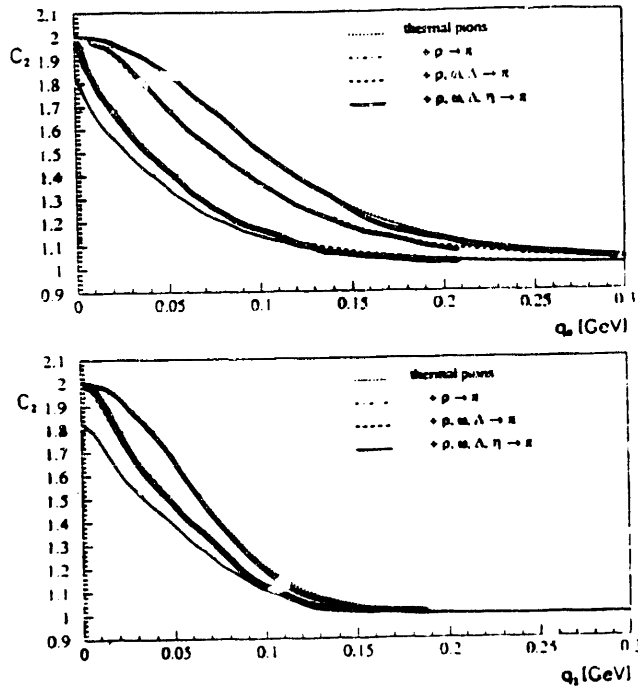

— thermal + ρ

— ρ, ω, Δ

— total (η)

π^-

Fig. 1. Distortion of the Bose–Einstein correlation func of negatively charged pions through resonance decays. contributions from resonance decays are successively a to the correlation function of thermal π^- (dotted line). resultant correlation function of all π^- is given by the line.

The parameter λ takes into account the effective reduction of the intercept due to the contribution from η de ... the effect of coherence. Fig. 2 shows the effective radi

A Hydrodynamic Model

$S + S \to 2\pi^- + X$ 200AGeV/c

Summary

- Proton and pion correlation functions, studied in the E814 forward spectrometer, are reported;
- Non-Gaussian distributions in π^+-π^+ and π^--π^- correlation functions, especially with the low p_t pion pairs, were observed;
- RQMD simulations: Gaussian distribution with excluding Δ, non-Gaussian like distribution in normal event.

The two-pion correlation function is sensitive to resonances, *e.g.* Δ.

Source Sizes from CERN Data

John Sullivan
Los Alamos

Method

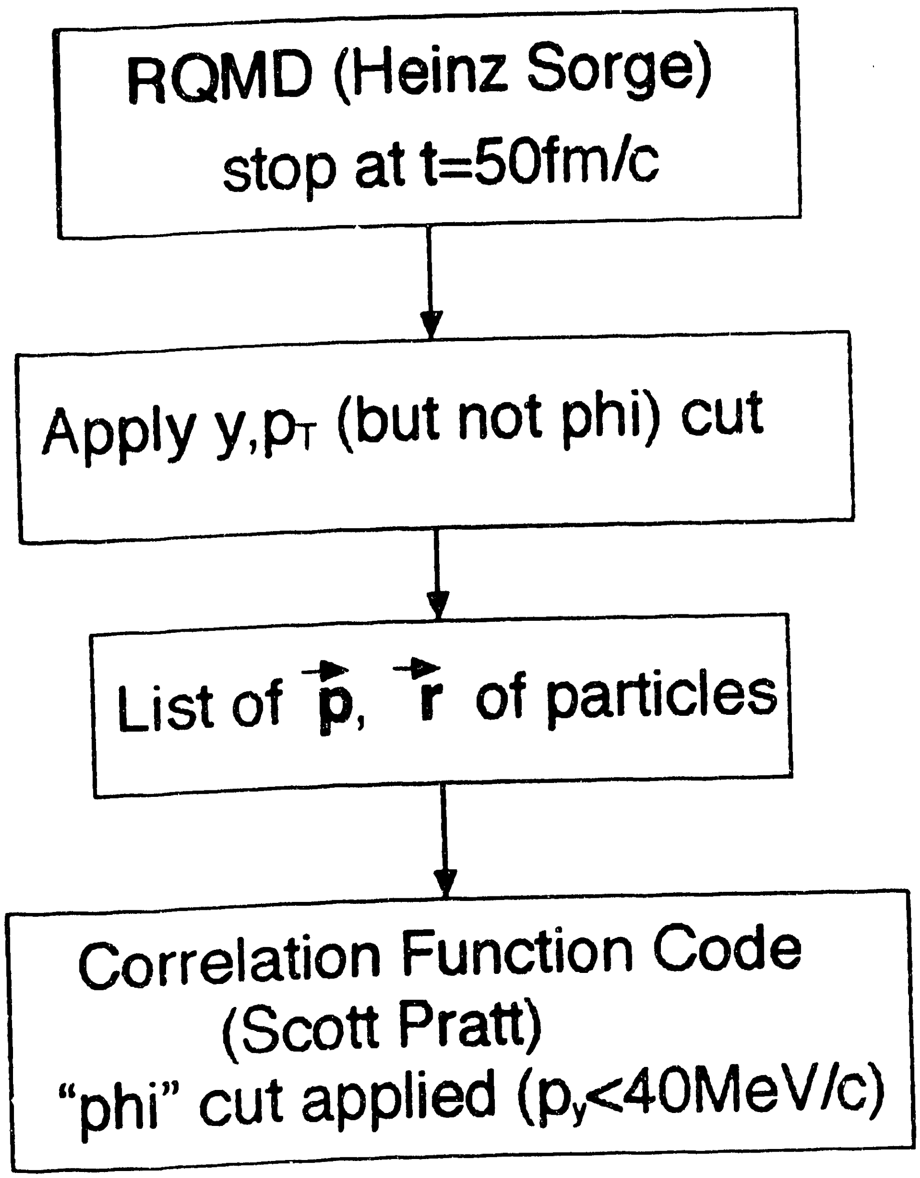
RQMD (Heinz Sorge)
stop at $t=50fm/c$
Apply y, p_T (but not phi) cut
List of $\vec{p}$, $\vec{r}$ of particles
Correlation Function Code
(Scott Pratt)
"phi" cut applied ($p_y<40MeV/c$)

Technique

Given: **r** and **p** of last interaction
Calculate: symmetrized wave-function = $\phi_{12}(\mathbf{r}_1, \mathbf{p}_1, \mathbf{r}_2, \mathbf{p}_2)$
π^{+-} pairs: Coulomb + strong wave-functions
K^+ pairs: Coulomb wave-functions
$|\phi_2|^2$ normalized such that for plane-waves it is
$1 + \cos(q \cdot (r_1 - r_2))$

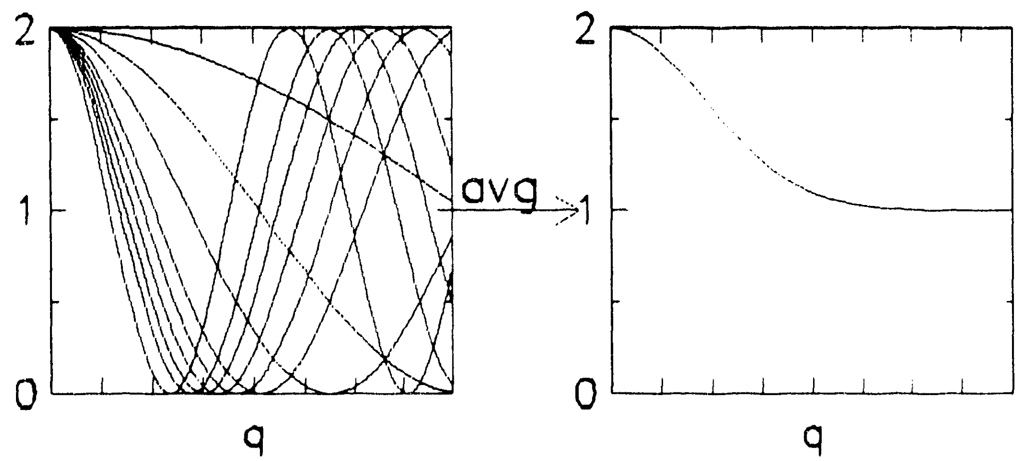

Calculated correlation function (in a given bin of q) is then

$$C_2(q) = \sum_{i=1}^{N(q)} |\phi_2|^2 / N(q), \tag{1}$$

where:

numerator analogous to N in q bin in an experiment,
denominator $N(q)$ = N pairs in bin,
analogous to N pairs in experimental "background" sample

Bose-Einstein Correlations of Pion Pairs and Kaon Pairs from RQMD (LA-UR-92-3191)

J. P. Sullivan, M. Berenguer, B. V. Jacak, M. Sarabura, J. Simon-Gillo, H. Sorge, and H. van Hecke
Los Alamos National Laboratory, Los Alamos, NM 87545

S. Pratt
Michigan State University, East Lansing, MI 48824

Bose-Einstein correlations between charged pion and K^+ pairs are calculated using the space-time and four-momentum distributions from RQMD for 200 GeV/nucleon $^{32}S+Pb$ and compared to pion correlation measurements from two CERN experiments. Good agreement is found. The predicted apparent radii from the K^+ correlation functions are smaller than the corresponding pion radii — reflecting differences in their space-time distributions, the influence of detector acceptance, experimental trigger conditions, and differing contributions from resonances.

200 GeV/u S + Pb

93/04/13 16.20

RQMD

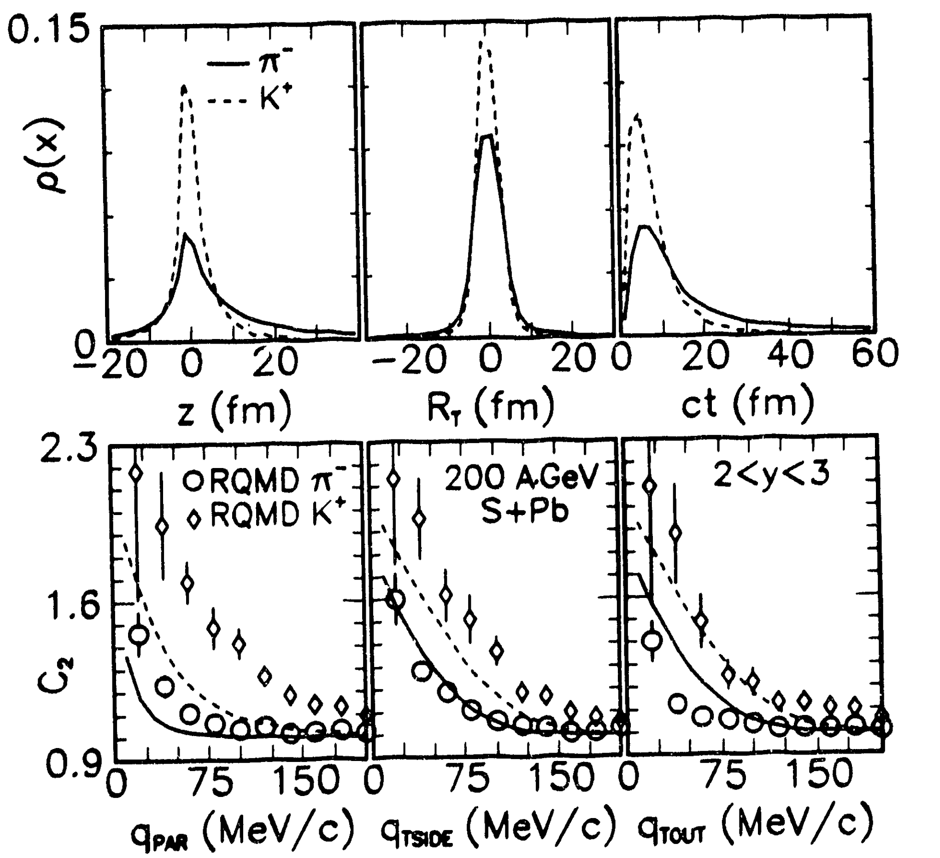

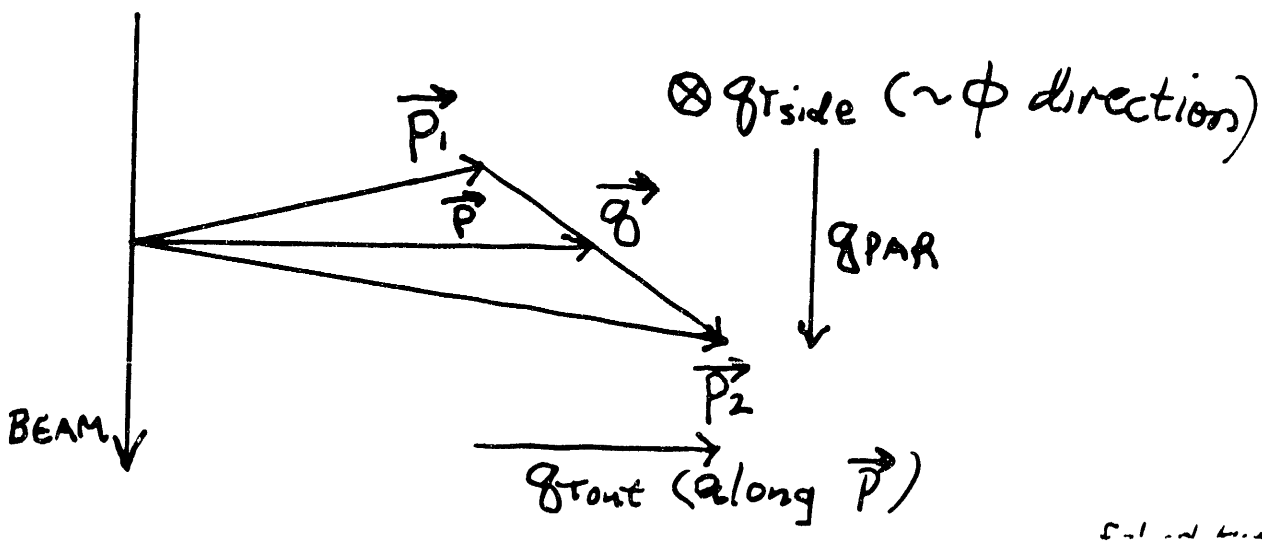

RQMD, rapidity vs z for $\pi+$, K+

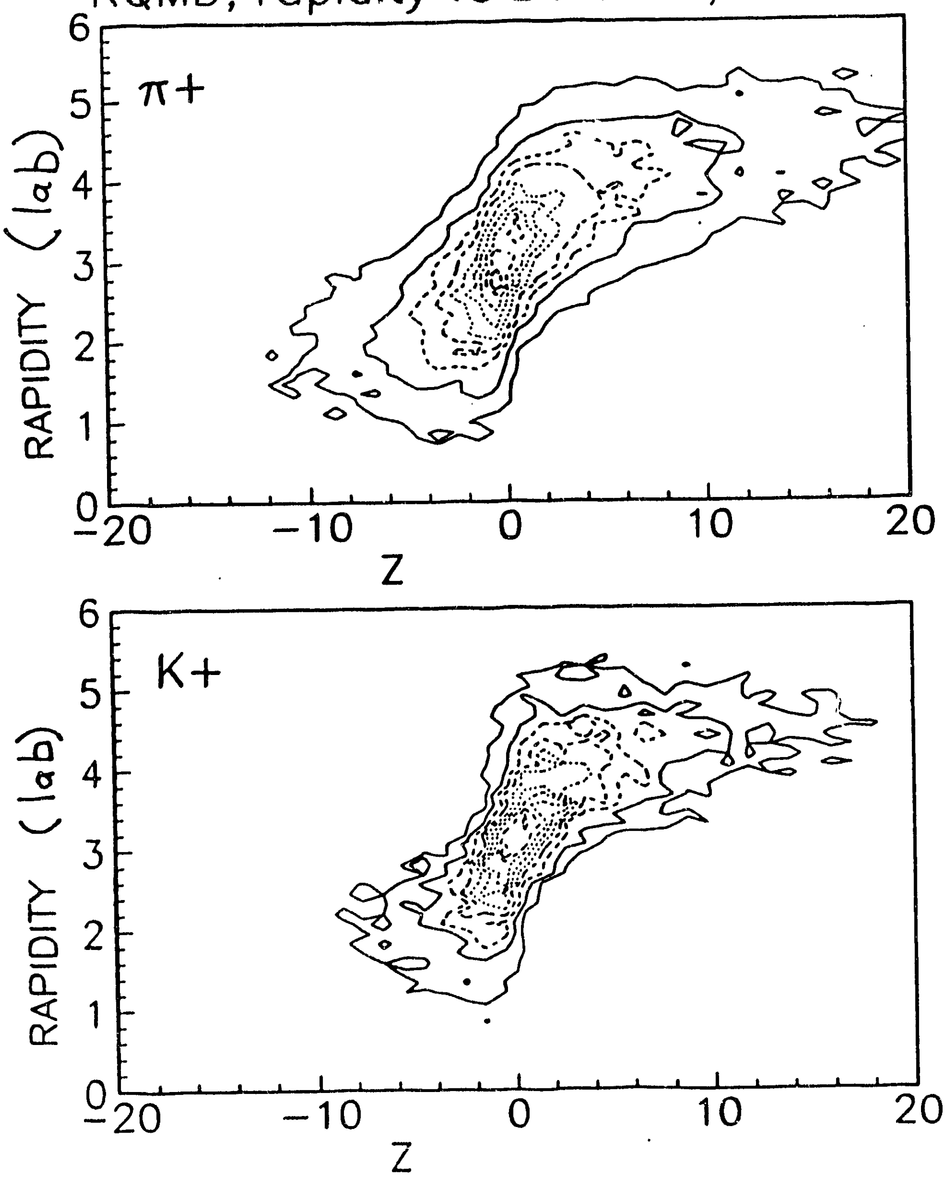

93/02/24 12.03

RQMD

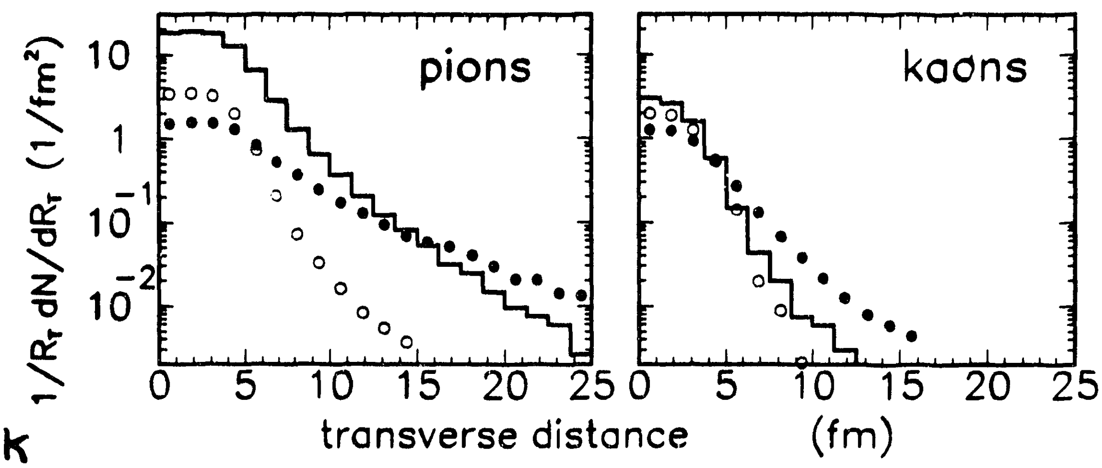

π	K		
0.766	0.393	—	collisions + short−lived resonances ($\Gamma > 100$MeV)
0.126	0.310	●	long−lived resonances ($\Gamma < 100$MeV)
0.108	0.297	○	strings

RQMD vs Data

93/01/08 16.24

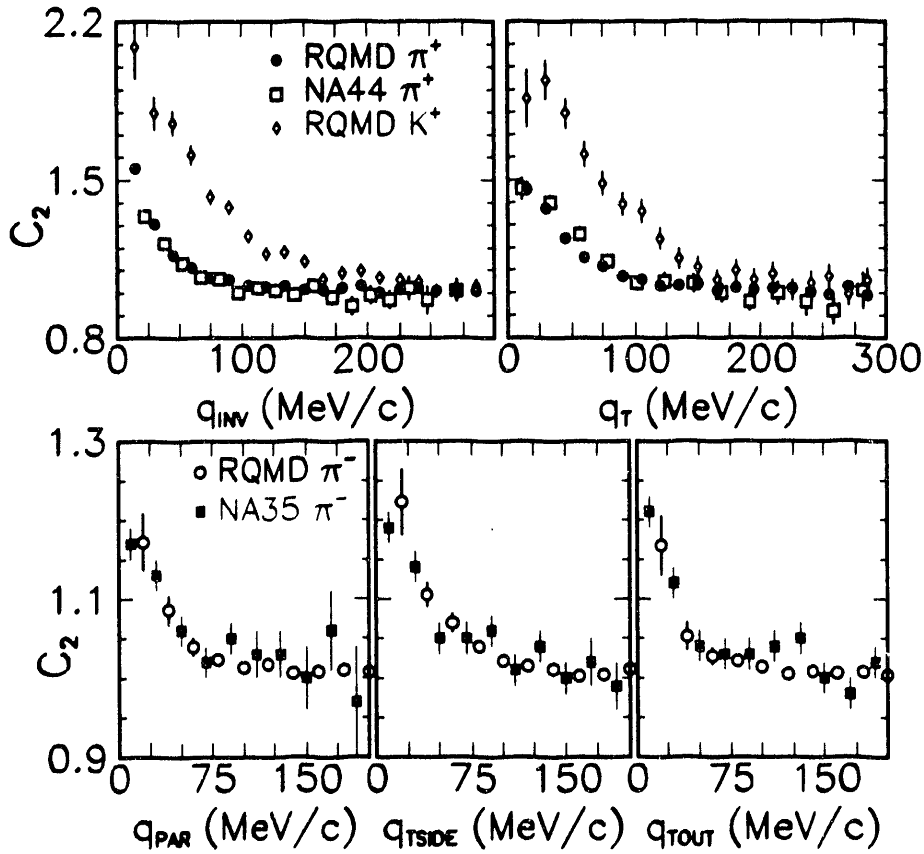

NA44 acceptance

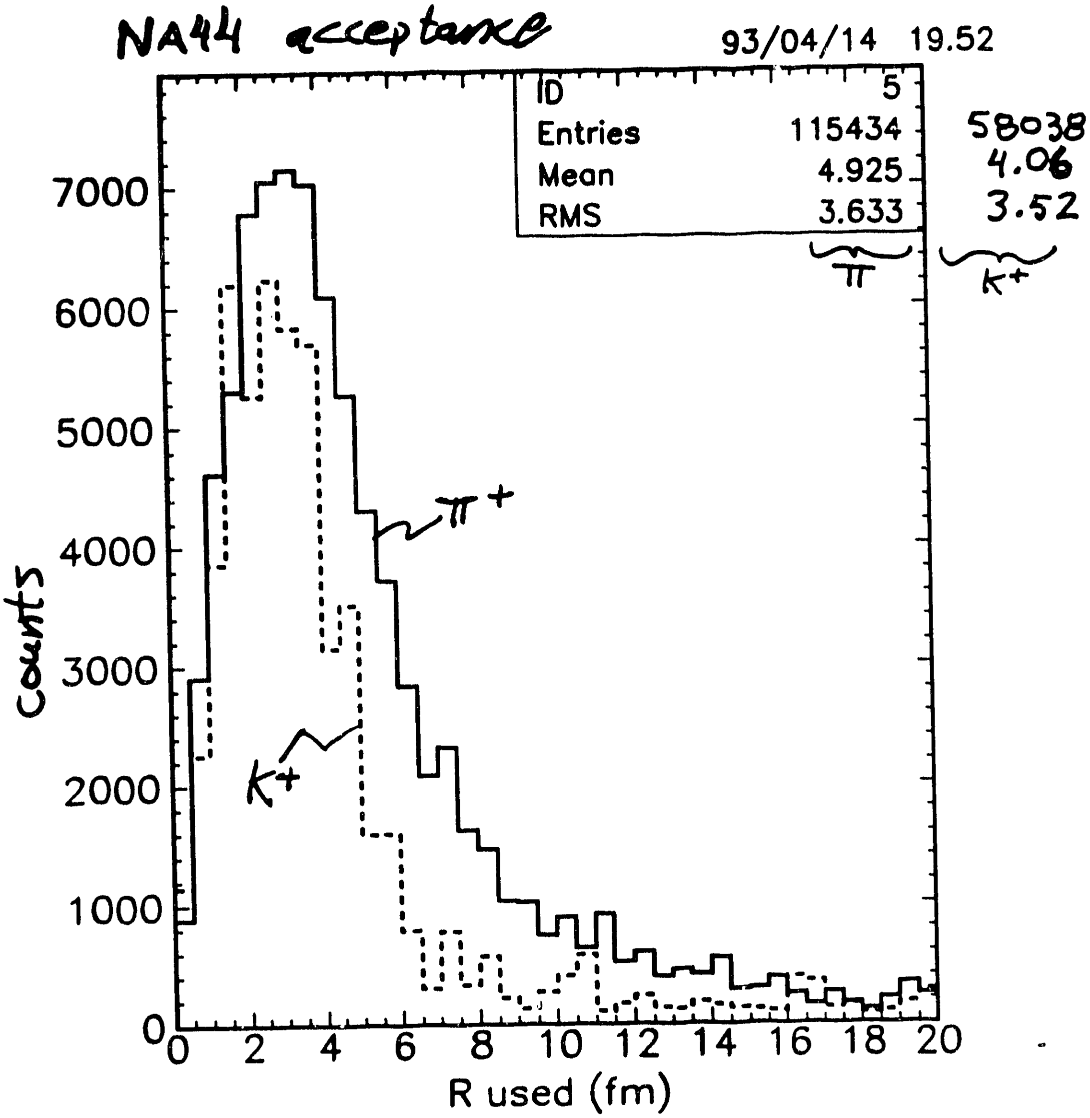

R_T of particles used in NA44 correlation function from RQMD

in $p_\perp$ bins:

$p_\perp$ (MeV/c)	π^+ Fract	$\langle R_\perp \rangle$	K^+ Fract	$\langle R_\perp \rangle$
0 - 200	0.86	5.00 ± .01	0.58	4.00 ± .02
200 - 400	0.14	4.49 ± .03	0.34	4.14 ± .03
400 - 600	2×10^{-4}	6.1 ± 1.2	0.07	4.18 ± .05
600 - 800	—	—	3×10^{-3}	4.9 ± .3

MeV/c

Influence of η^0, η' RQMD 44mr

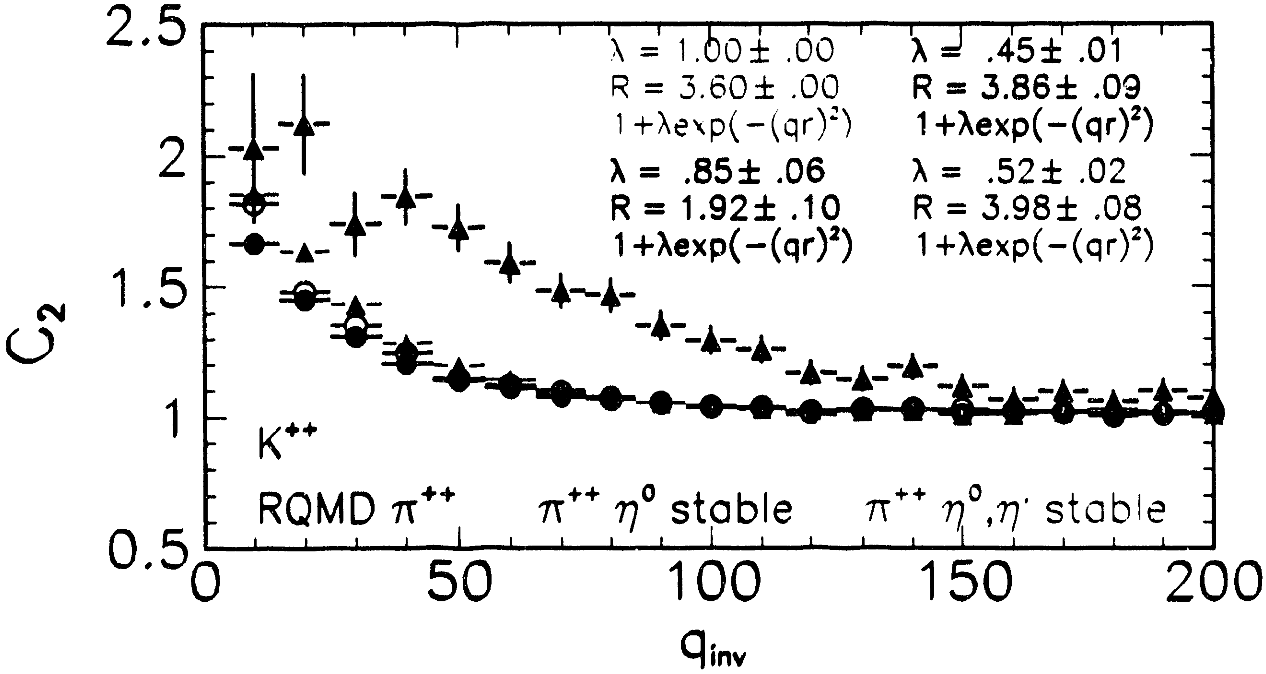

93/03/29 17.46

Contributions of long-lived resonances

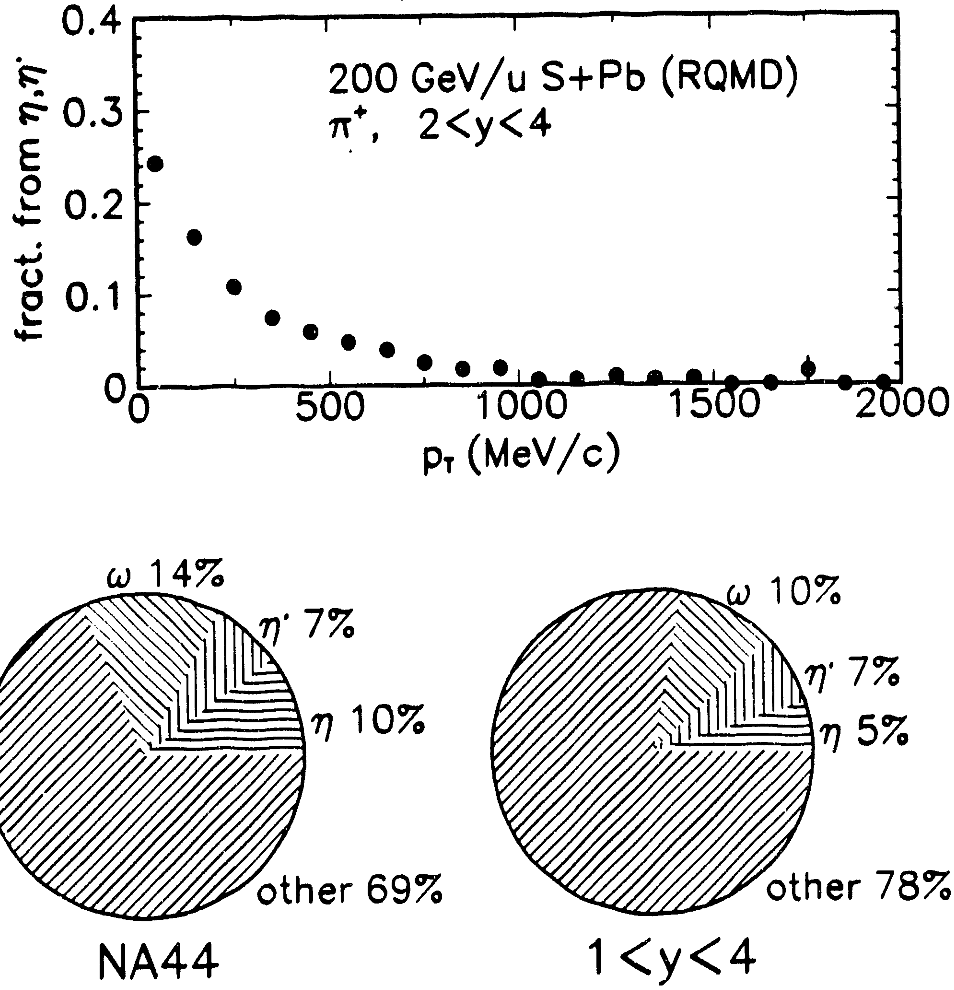

93/03/29 17.46

Contributions of long-lived resonances

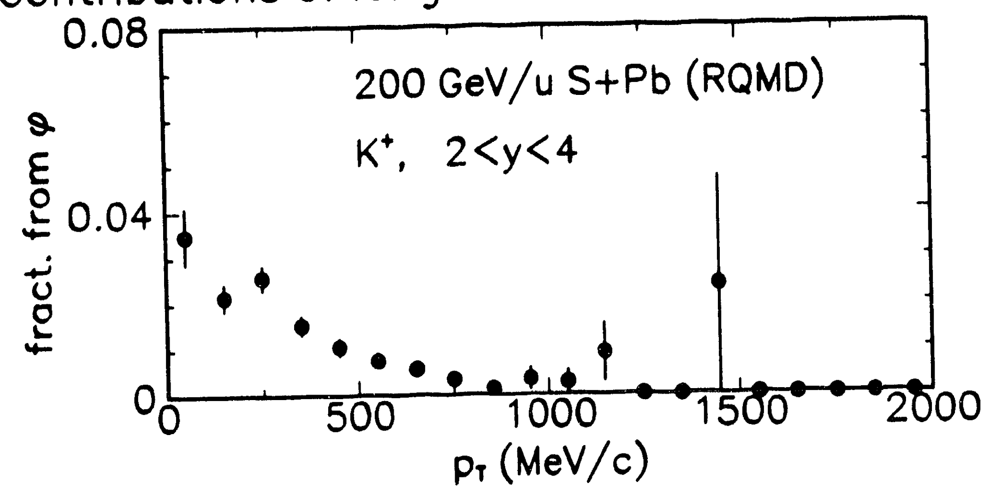

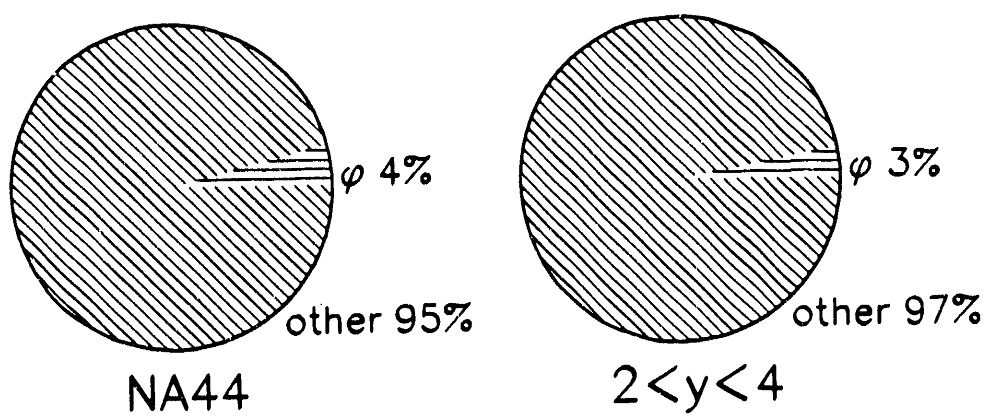

AIIM

Association for Information and Image Management

1100 Wayne Avenue, Suite 1100
Silver Spring, Maryland 20910

301/587-8202

Centimeter

1 2 3 4 5 6 7 8 9 10 11 12 13 14 15 mm

1 2 3 4 5

Inches

MANUFACTURED TO AIIM STANDARDS
BY APPLIED IMAGE, INC.

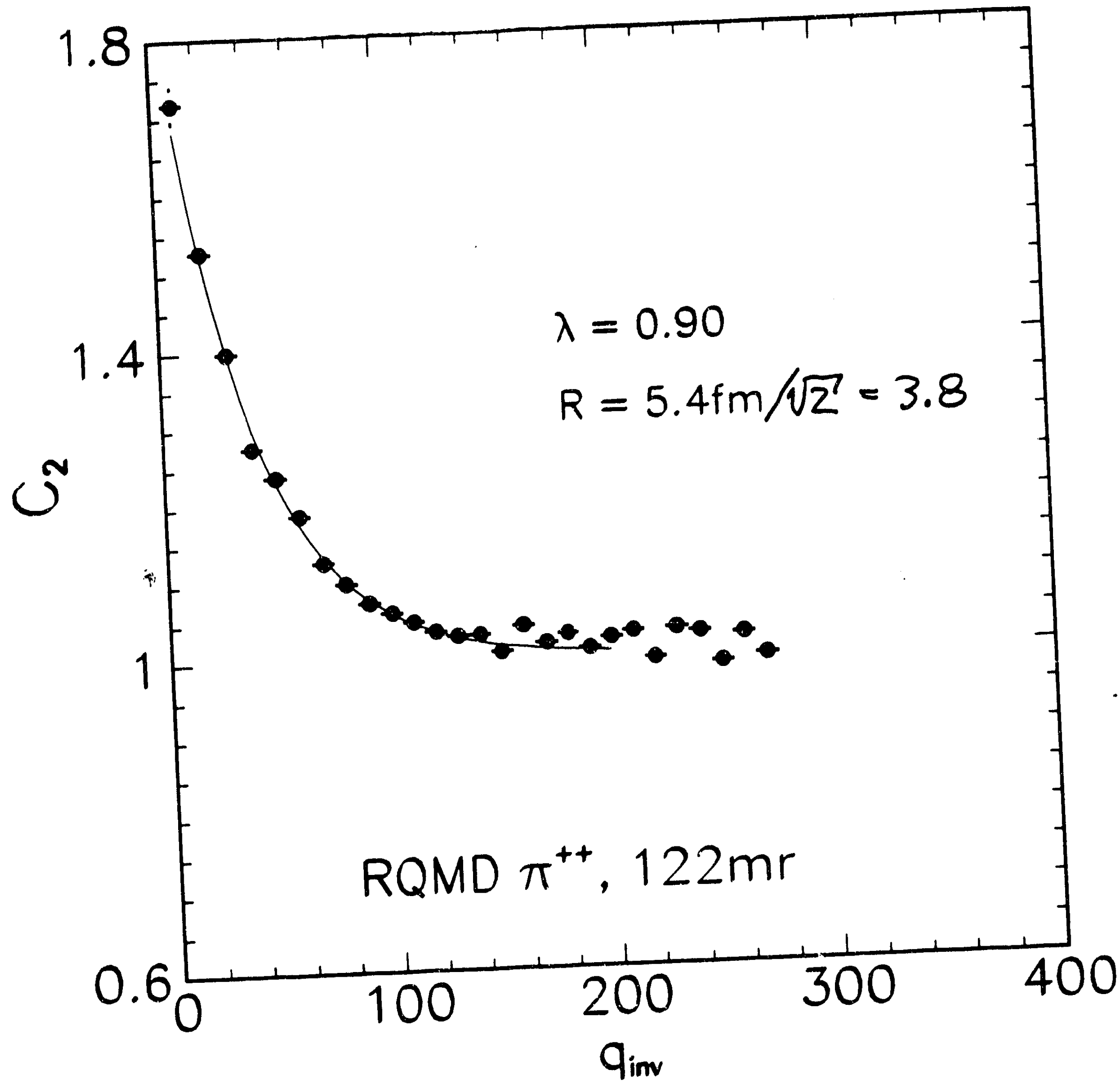

csmdo: 5.ximac

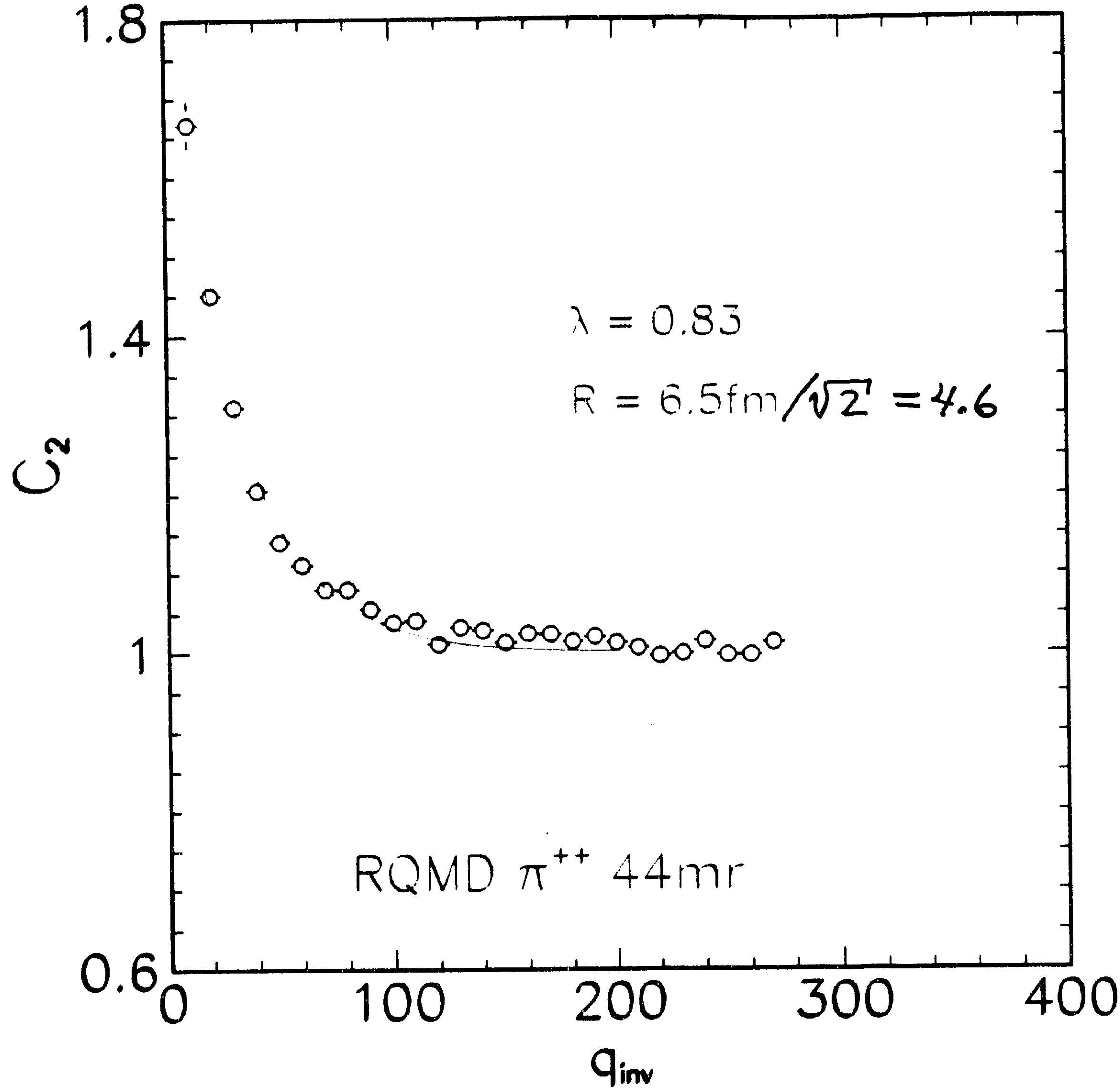

1.8
1.4
1
0.6
C2
λ = 0.83
R = 6.5fm/√2 = 4.6
RQMD π++ 44mr
0
100
200
300
400
qinv

93/02/01 17.58

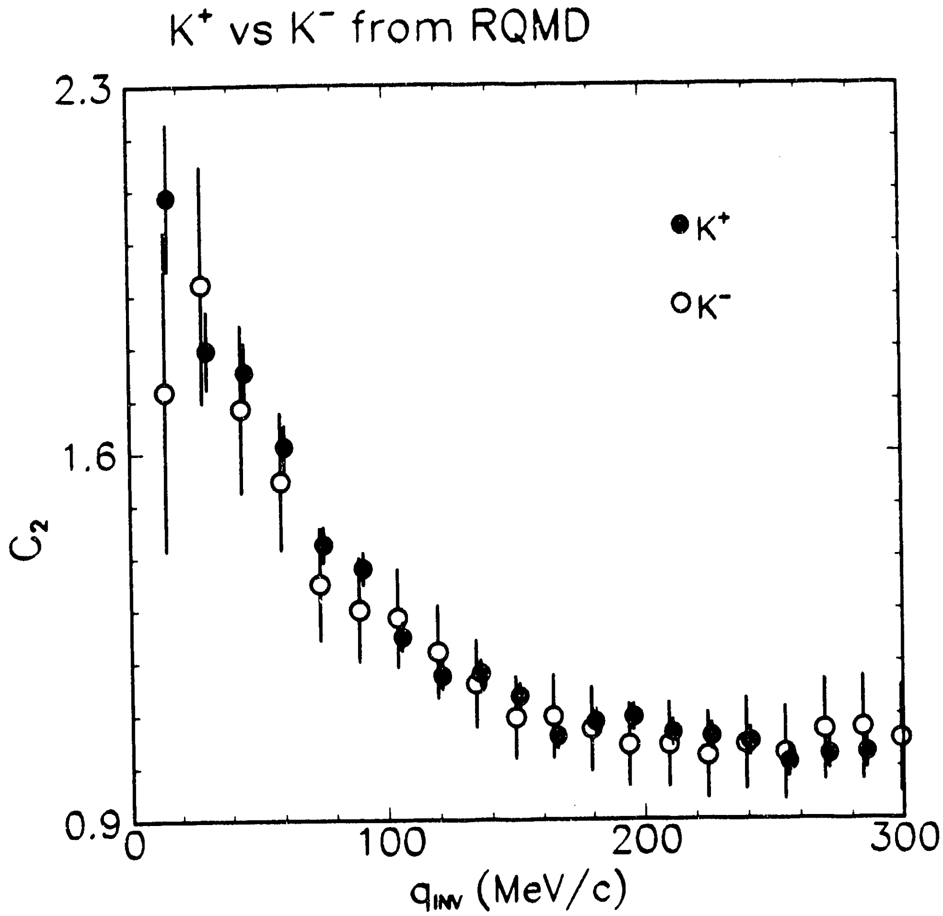

93/04/01 17.20

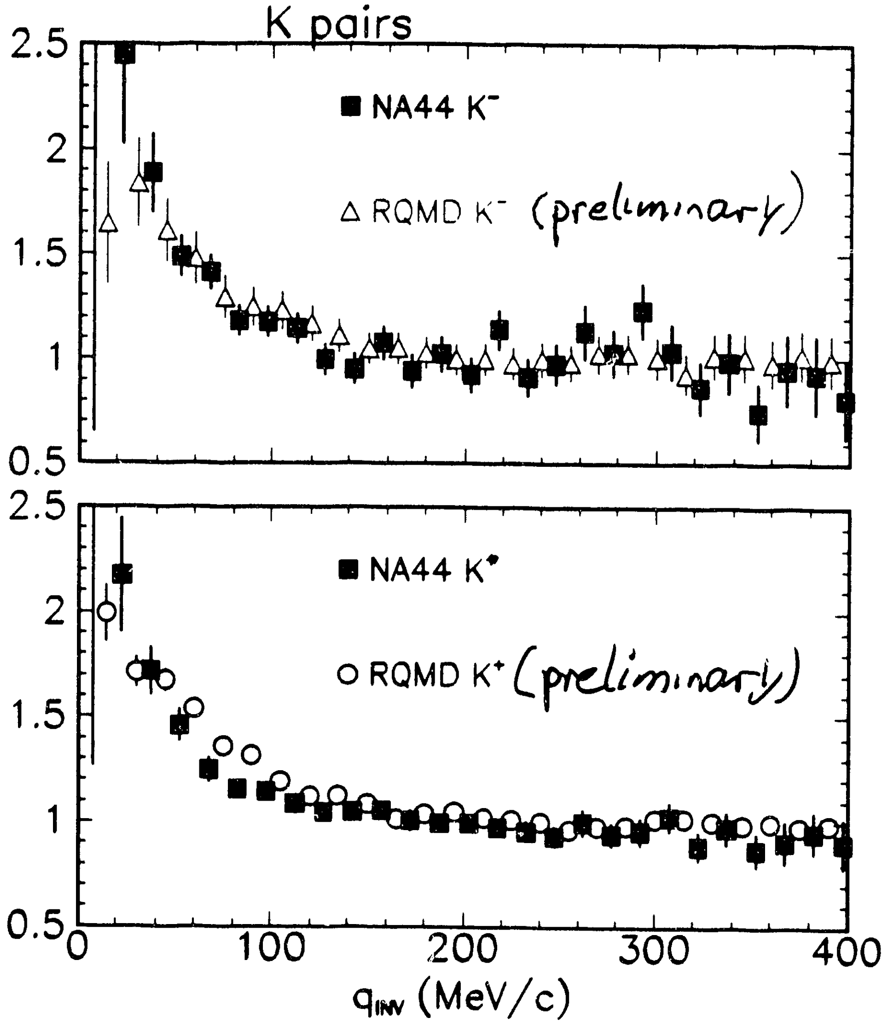
K pairs
2.5
2
1.5
1
0.5
NA44 K⁻
RQMD K⁻ (preliminary)
2.5
2
1.5
1
0.5
NA44 K⁺
RQMD K⁺ (preliminary)
0
100
200
300
400
q_INV (MeV/c)

Intermittency and Interferometry?

Michael Tannenbaum
BNL

Results from AGS E802

Negative Binomial Distribution Fits to Multiplicity Distributions in Restricted $\delta\eta$ Intervals from Central O+Cu Collisions at 14.6A GeV/c and their Implication for "Intermittency"

M. J. Tannenbaum, BNL

Acknowledgement—

How results really happen in large collaborations

- The target multiplicity array TMA was designed and built by:

  Lou Remsberg and Steve Gushue, BNL

- The original TMA analysis was done by:

  Tony Abbott and Ju Kang, U.C. Riverside

- The multiplicity **distributions** in bins of $\delta\eta$ were made for me by:

  Ju Kang, U.C. Riverside

- Fits to the distributions and further analysis was done by:

  M.J.T, BNL

- Many useful critical comments and discussions with:

  Chellis Chasman—BNL, George Stephans—MIT, Ingvar Otterlund—Lund(PHENIX)

How is this related to Intermittency?

**There is a phenomenology, dubbed "Intermittency"
which attempts to explain
the large single event (JACEE) bin-by-bin multiplicity fluctuations
as the result of large local fluctuations on many scales
which exhibit self-similarity and power-law scaling.
According to this phenomenology,
intermittency would be indicated by a
power-law increase of Normalized Factorial Moments of multiplicity
in rapidity bins $\delta\eta$ as the bin size is reduced:**

$$F_q(\delta\eta) \propto (\delta\eta)^{-\phi_q} \quad . \tag{1}$$

The Factorial Moment with the clearest interpretation is

$$F_2 = \frac{< n(n-1) >}{< n >^2} = 1 + \frac{\sigma^2}{\mu^2} - \frac{1}{\mu} \tag{2}$$

**Since we start from the Negative Binomial Distribution
we know ALL the moments**

$$\sigma = \sqrt{\mu(1 + \frac{\mu}{k})} \qquad \frac{\sigma^2}{\mu^2} = \frac{1}{\mu} + \frac{1}{k} \qquad F_2 = 1 + \frac{1}{k} \tag{3}$$

The Normalized Factorial Moments of the NBD are particularly simple.

$$F_q = \frac{< n(n-1)\ldots(n-q+1) >}{< n >^q} \tag{4}$$

$$\begin{aligned}
F_2 &= 1 + \frac{1}{k} \\
F_3 &= (1 + \frac{1}{k})(1 + \frac{2}{k}) \\
F_4 &= (1 + \frac{1}{k})(1 + \frac{2}{k})(1 + \frac{3}{k}) \\
F_q &= F_{(q-1)}(1 + \frac{q-1}{k})
\end{aligned} \tag{5}$$

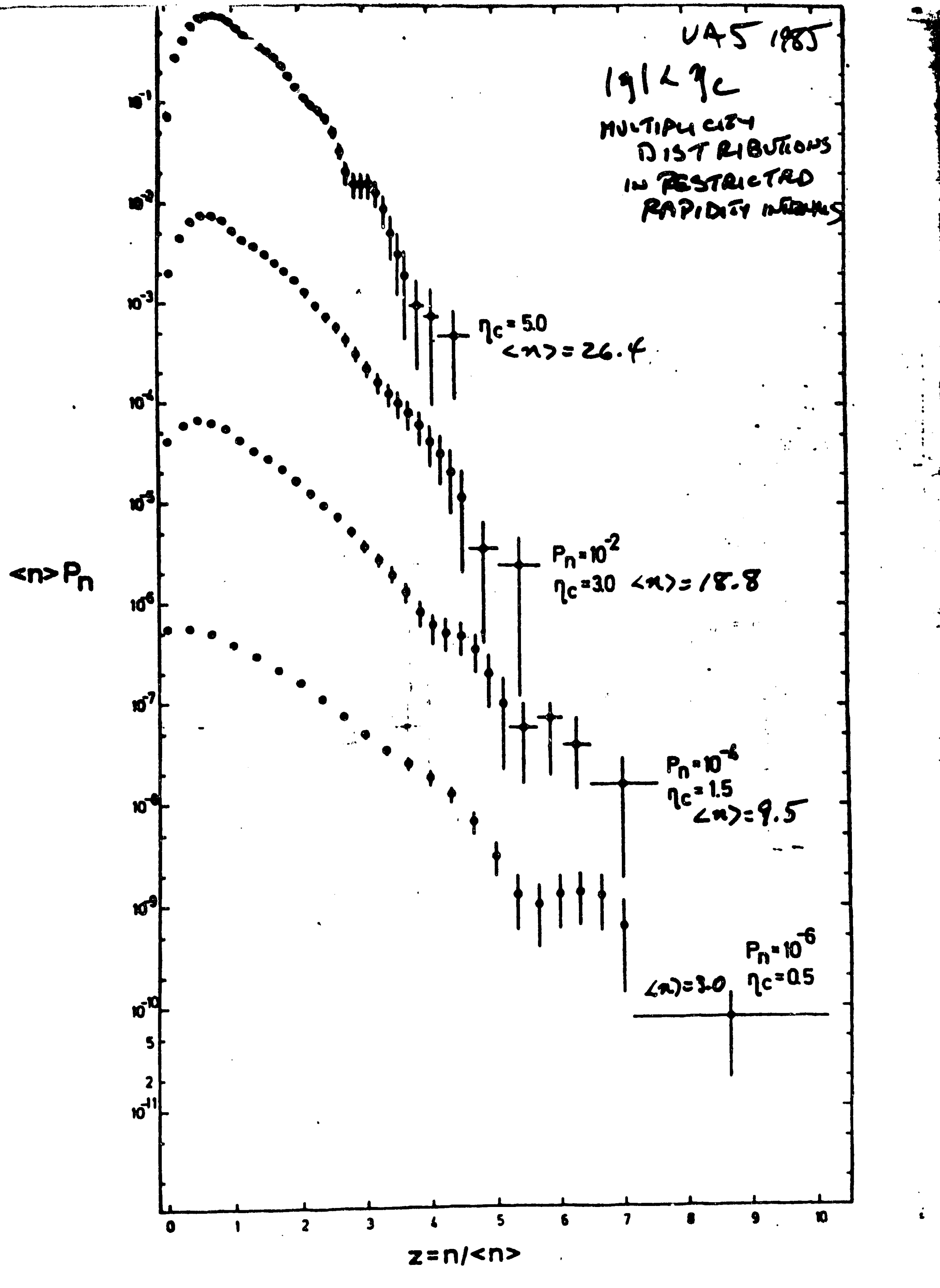

PLOTTED IN UNITS OF $\langle n \rangle$ IN EACH INTERVAL $= \mu$

Fig. 1b

BINOMIAL DISTRIBUTION:

PROBABILITY OF m SUCCESSES ON n INDEPENDENT TRIALS, EACH WITH PROBABILITY p OF SUCCESS & $q = 1 - p$ OF FAILURE

$$\boxed{P(m)\Big|_n = \frac{n!}{m!(n-m)!}\, p^m q^{n-m}}$$

$$\langle m \rangle = np \qquad \sigma_m^2 = \langle m^2 \rangle - \langle m \rangle^2 = npq$$
$$= np - np^2$$
$$= \langle m \rangle - \frac{\langle m \rangle^2}{n}$$

NEGATIVE BINOMIAL

$$p < 0 \quad n < 0 \quad k \equiv -n$$

$$p = \frac{\langle m \rangle}{n} = -\frac{\langle m \rangle}{k} \qquad \sigma_m^2 = \langle m \rangle + \frac{\langle m \rangle^2}{k}$$

$$\boxed{P(m)\Big|_k = \frac{-k!}{m!(-k-m)!}\left(-\frac{\langle m \rangle}{k}\right)^m \left(1 + \frac{\langle m \rangle}{k}\right)^{-(k+}}$$

FOR $k \to \infty \to$ POISSON, $k = 1$ BOSE EINSTEIN,

FOR $\langle m \rangle \to \infty$ BECOMES Γ DIST, FOR $k = -$INTEGER IS BINOMIAL!

Negative Binomial

Instead of the probability of m successes on n independent trials, each with probability p of success & $q = 1 - p$ of failure, one can fix the required number of successes k and ask the distribution of n for fixed k.

This is negative binomial. Let $l = n - k$

$$P(n)|_k = P(l)|_k = \frac{(l+k-1)!}{l!(k-1)!}\, p^k\, q^l \tag{1}$$

and $P(l)$ is normalized for $0 \leq l \leq \infty$.

$$<n>= \frac{k}{p} \quad <l>=<n> - k = k\,\frac{q}{p} \tag{2}$$

$$\sigma_n^2 = \sigma_l^2 = k\,\frac{q}{p^2} \tag{3}$$

This goes to the standard form with the substitution

$$<l>= \mu \quad p = \frac{1}{1+\frac{\mu}{k}} \quad q = 1 - p = \frac{\frac{\mu}{k}}{1+\frac{\mu}{k}} \tag{4}$$

Poisson

The Poisson Distribution is the limit of the Binomial Distribution for large number of trials n with very small probability of success p such that the expectation value $\mu = np$ is fixed

$$P(m)|_\mu = \frac{\mu^m e^{-\mu}}{m!} \tag{5}$$

$$<m>= \mu \quad \sigma_m^2 = \mu \tag{6}$$

$$\frac{\sigma^2}{\mu^2} = \frac{1}{\mu} \tag{7}$$

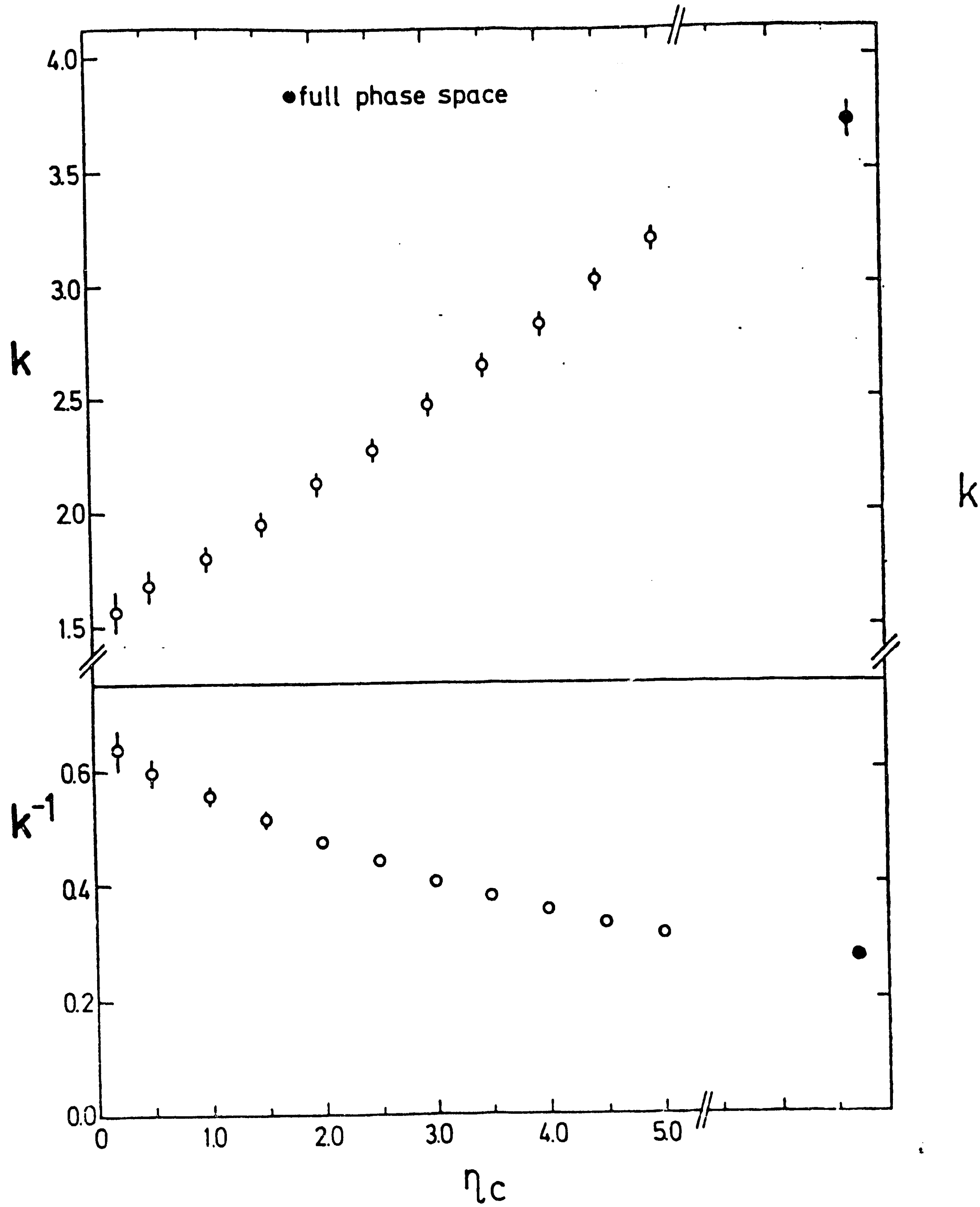

full phase space
k
k^{-1}
k
4.0
3.5
3.0
2.5
2.0
1.5
0.6
0.4
0.2
0.0
0
1.0
2.0
3.0
4.0
5.0
η_c

Fig. ~~3~~ 1

E802 November, 1986

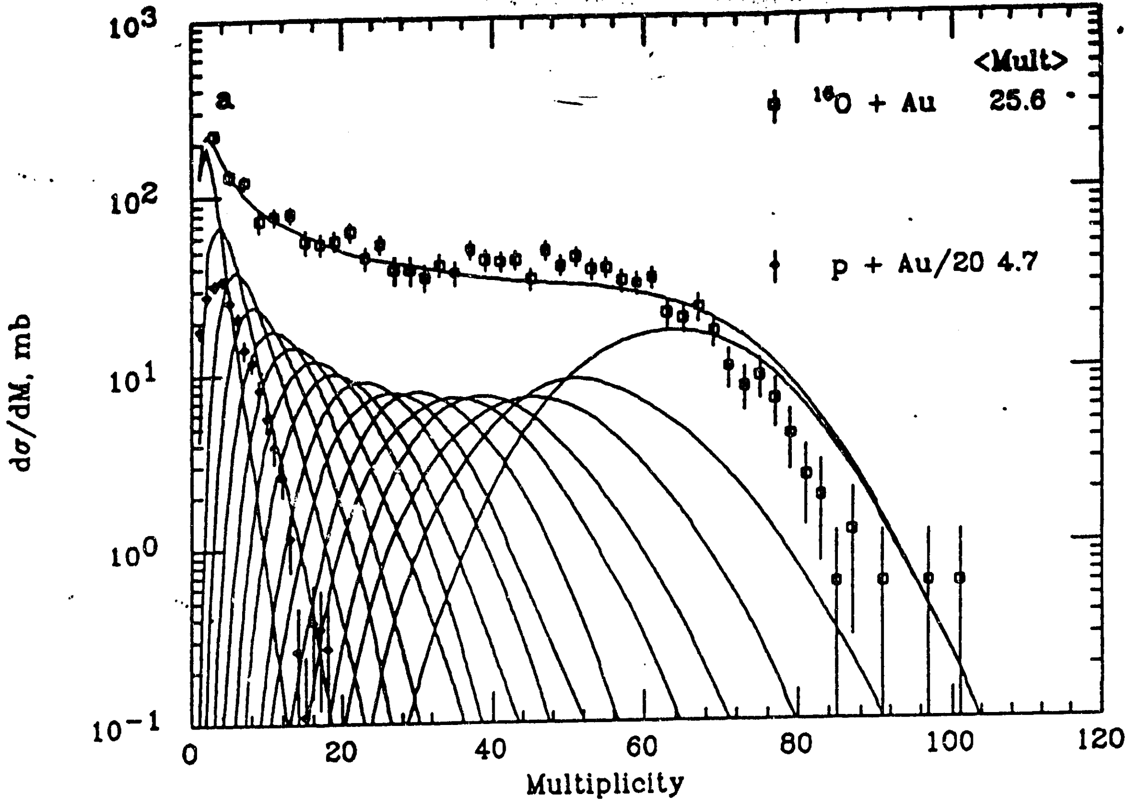

E802 November, 1986

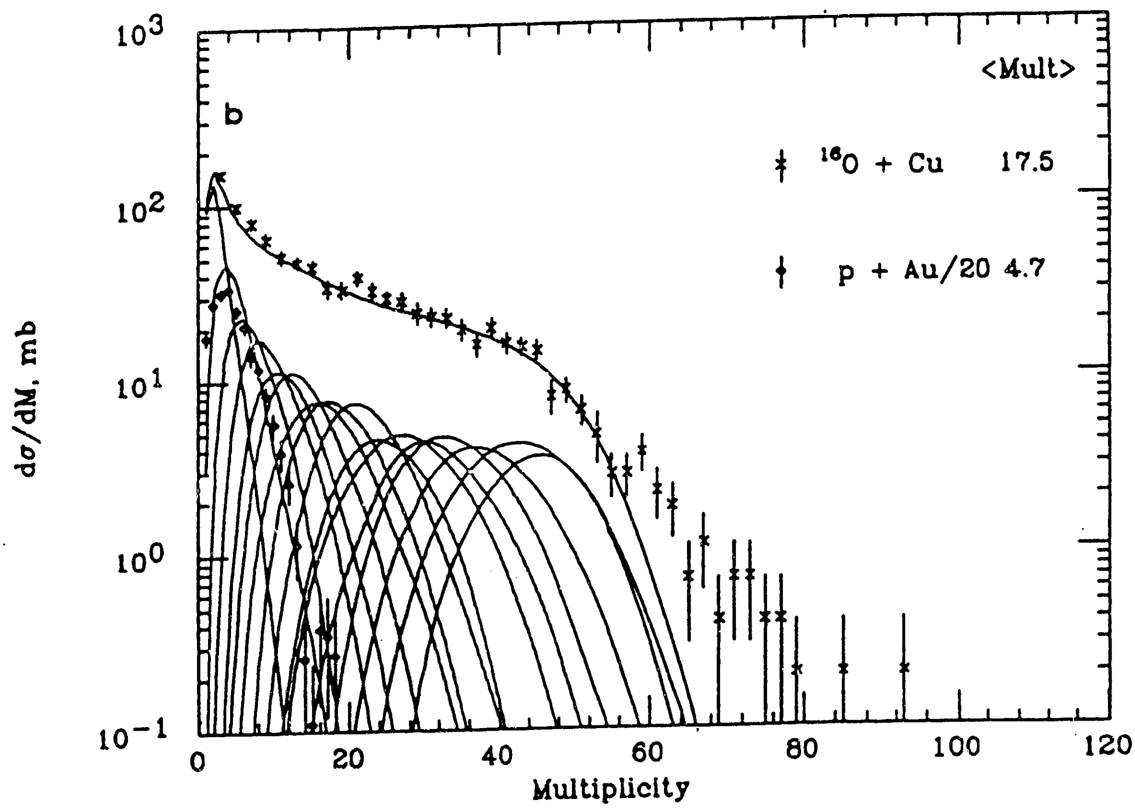

Fig. 12

O+Cu Central Multiplicity data in eta bins

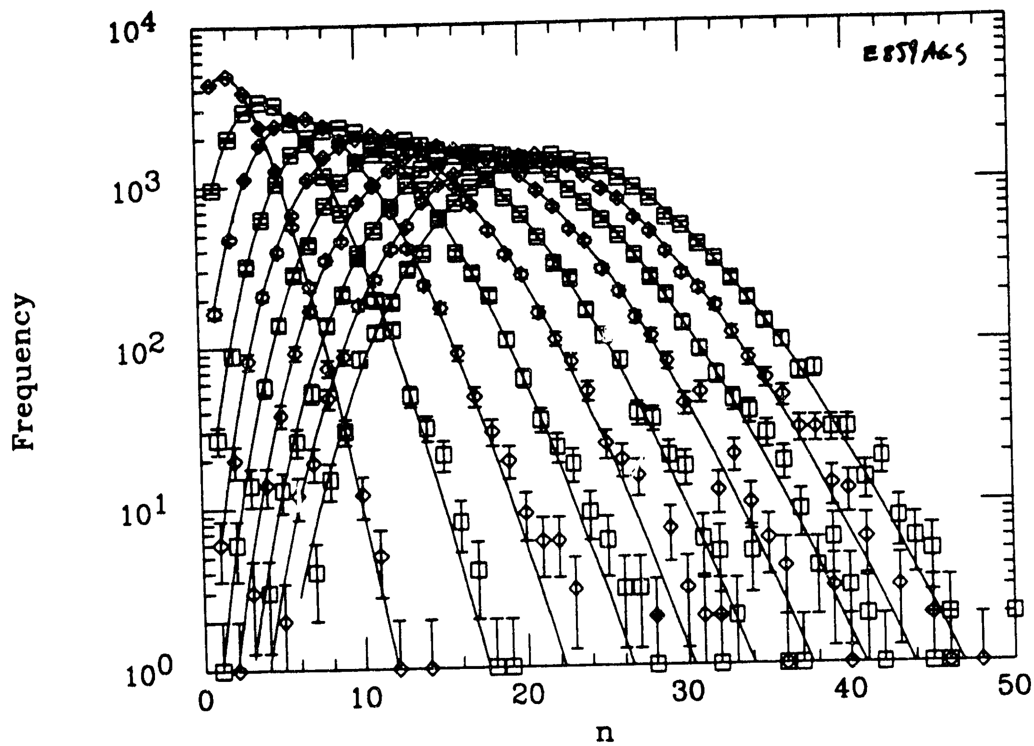

FIG 2a

O+Cu Central Multiplicity data in eta bins

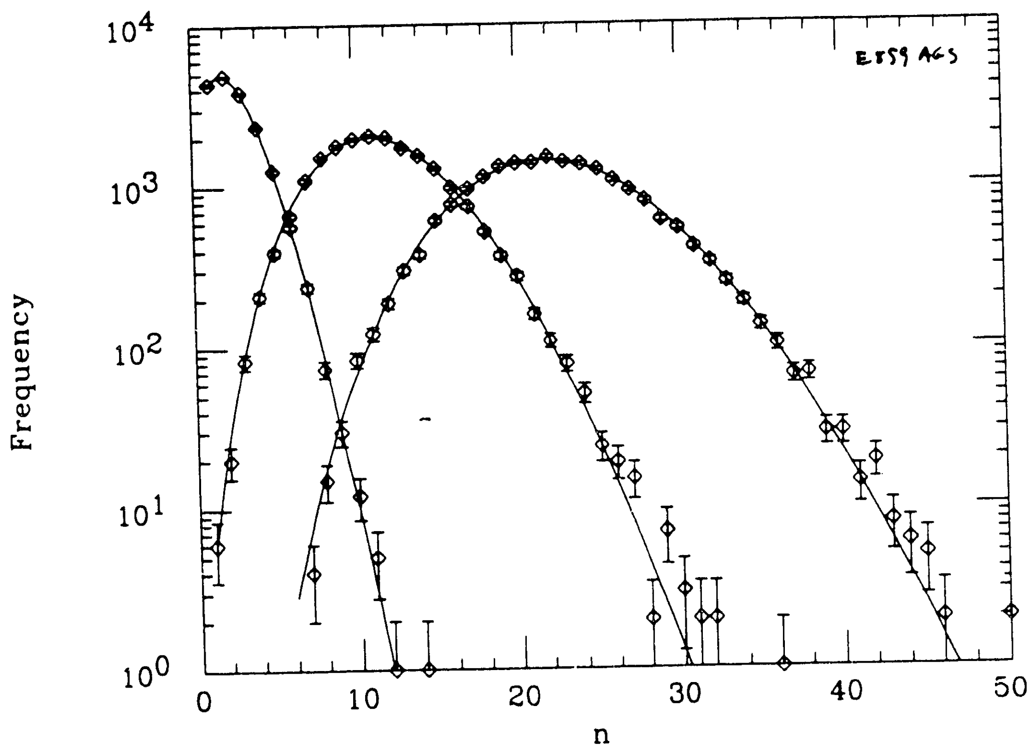

FIG 2b

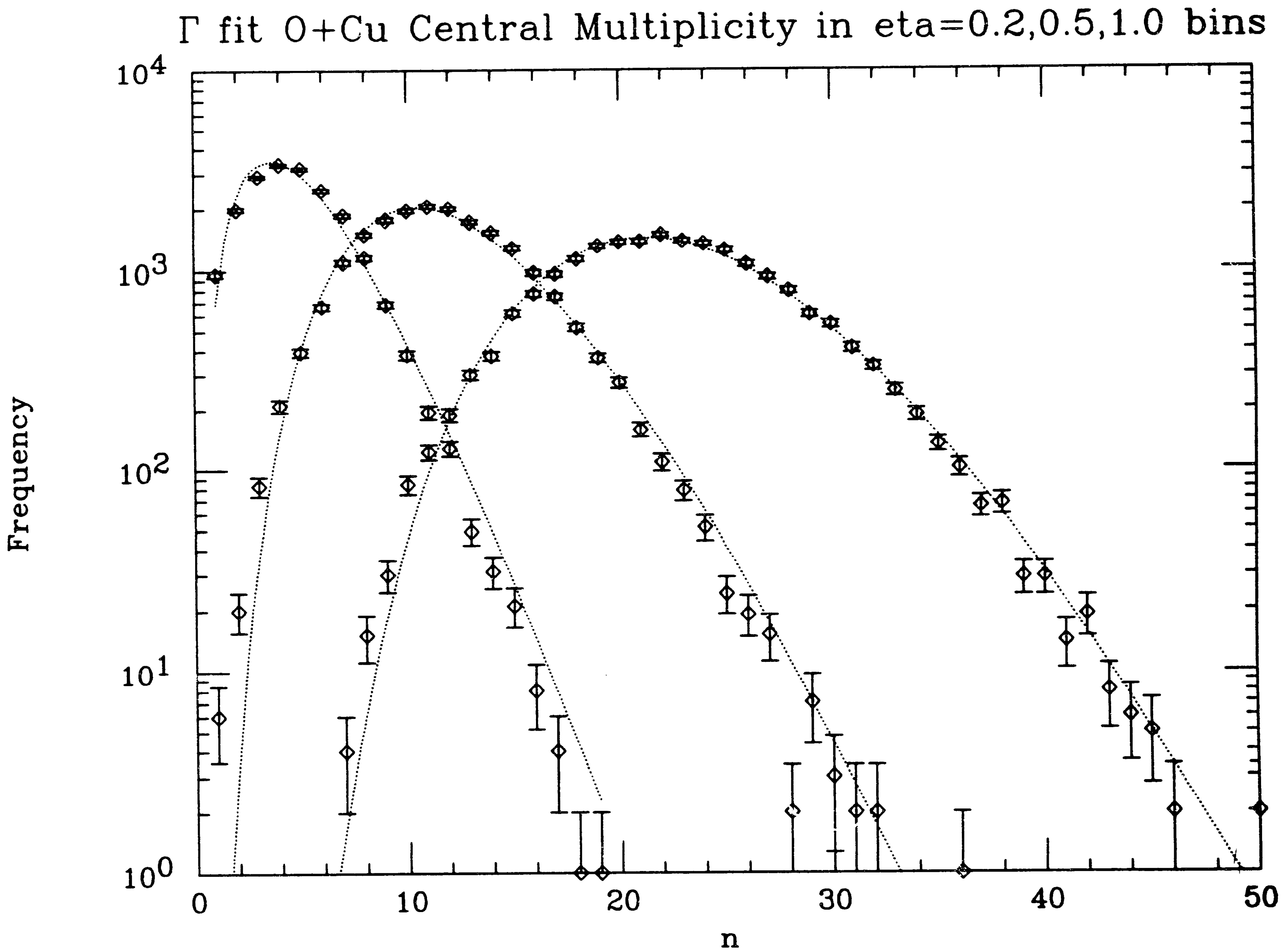
Γ fit O+Cu Central Multiplicity in eta=0.2,0.5,1.0 bins
Frequency
10^4
10^3
10^2
10^1
10^0
0
10
20
30
40
50
n

NBD O+Cu Central Multiplicity in eta=0.2,0.5,1.0 bins

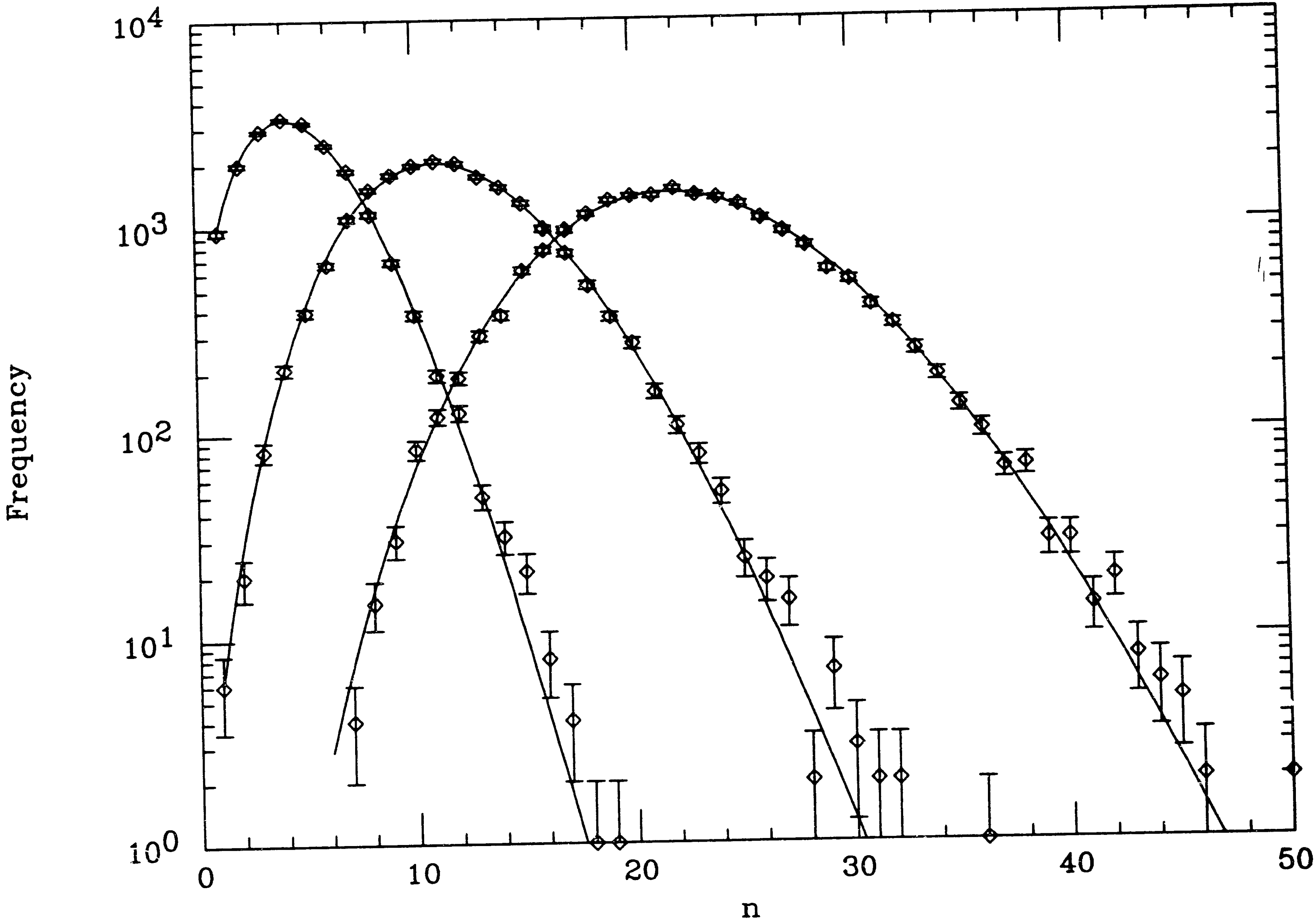

Results of NBD Fits to J.Kang data MJT

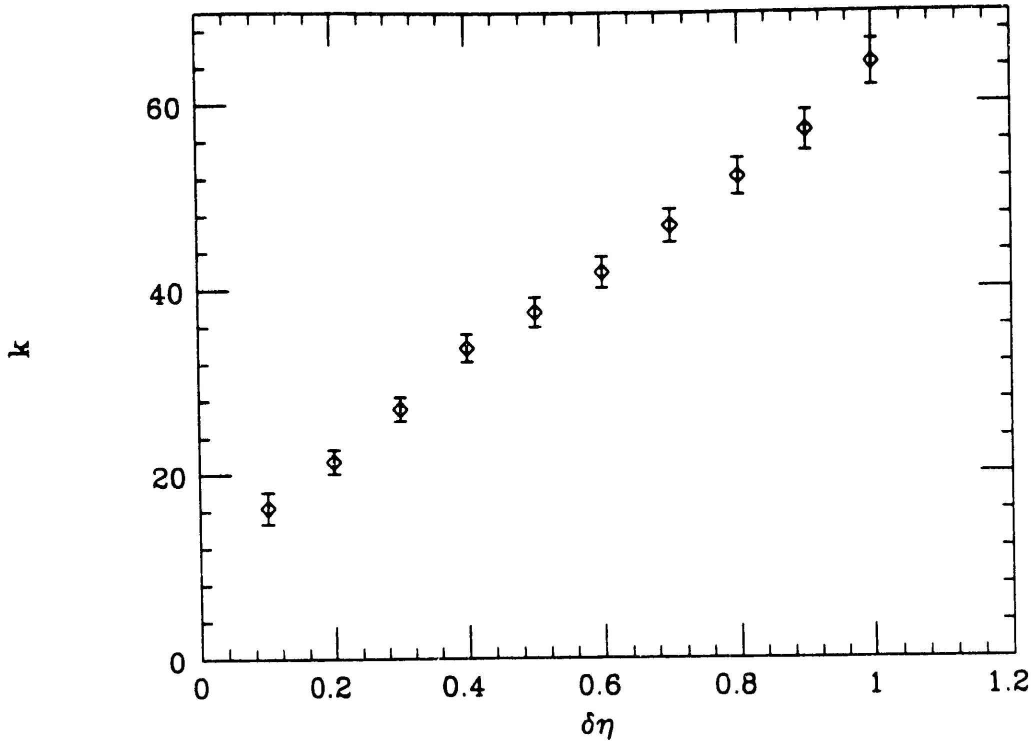

Fig 3a

Results of NBD Fits to J.Kang data MJT

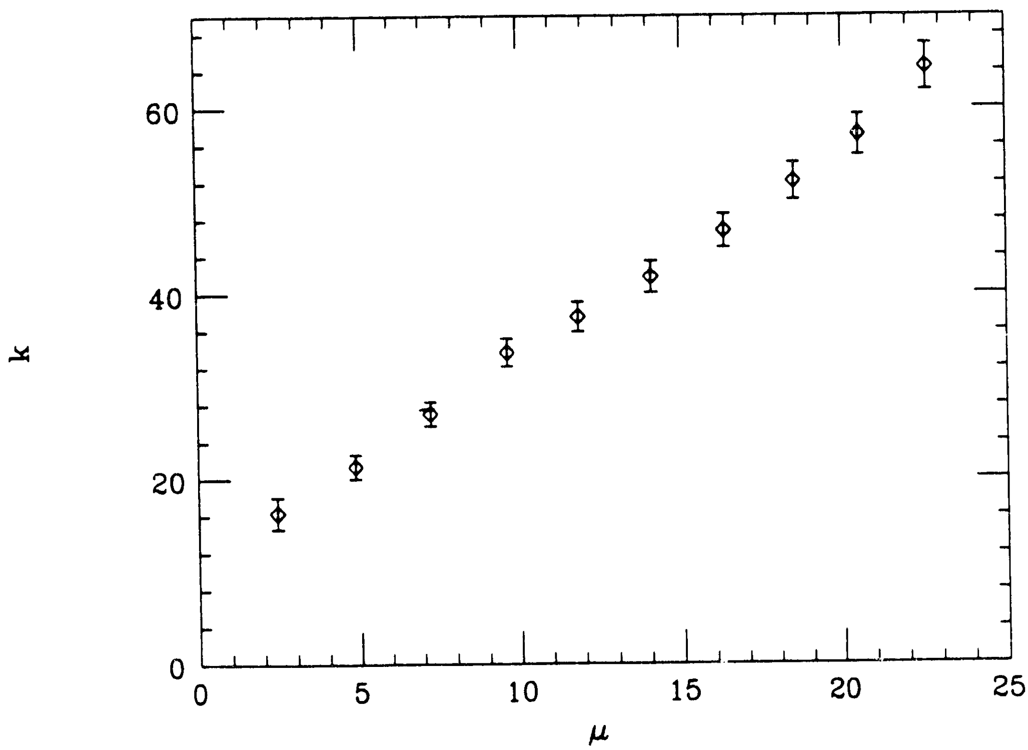

Fig 3b

Correlations and Multiplicity Distributions
The Mueller Moments
"Physics Highlights of 1972"

Al Mueller pointed out that Multiplicity Distributions would be POISSON

Only if the particles were emitted INDEPENDENTLY, WITH NO CORRELATION

The "inclusive" probability of observing a particle at rapidity y is:

$$\rho_1(y) = \frac{1}{\sigma}\frac{d\sigma}{dy} = \frac{dn}{dy} \tag{1}$$

The Joint probabibility of a particle at y_1 and another at y_2 is:

$$\rho_2(y_1, y_2) = \frac{1}{\sigma}\frac{d^2\sigma}{dy_1 dy_2} \tag{2}$$

and for q particles at $y_1, y_2 \cdots y_q$

$$\rho_q(y_1, \cdots y_q) = \frac{1}{\sigma}\frac{d^q\sigma}{dy_1 \cdots dy_q} \tag{3}$$

If there is no correlation,
then the emission of the particles is statistically independent, and

$$\rho_2(y_1, y_2) = \rho_1(y_1)\rho_1(y_2) \tag{4}$$
$$\rho_q(y_1, \cdots y_q) = \rho_1(y_1)\rho_1(y_2)\cdots\rho_1(y_q) \tag{5}$$

Factorial Moments Appear

The integrals of the q-particle densities $\rho_q(y_1, \cdots, y_q)$ on any interval are the **unnormalized** Factorial Moments on that interval:

$$\int dy_1 \int dy_2\ \rho_2(y_1, y_2) = < n(n-1) > \quad = < n >^2 F_2 \tag{6}$$

$$\int dy_1 \cdots dy_q\ \rho_q(y_1, \cdots y_q) = < n(n-1)\ldots(n-q+1) > \quad = < n >^q F_q \tag{7}$$

The Mueller Moments and Correlation Functions

Mueller Introduced a series of
Moments and Correlation Functions
"Mueller Moments"

The Mueller moments are just the unnormalized Factorial Moments, ***with all combinations of lower order q-particle correlations subtracted:***

$$
\begin{aligned}
f_2 &= <n>^2\, F_2 - f_1^2 \\
f_3 &= <n>^3\, F_3 - (f_1^3 + 3f_1 f_2) \\
f_4 &= <n>^4\, F_4 - (f_1^4 + 6f_1^2 f_2 + 3f_2^2 + 4f_1 f_3) \\
&\dots
\end{aligned} \tag{1}
$$

where $f_1 = <n>$.

The Mueller Moments are the integrals of the Mueller Correlation functions

$$f_2 = \int dy_1 \int dy_2\, C_2(y_1, y_2) \tag{2}$$

where C_q are the q-particle rapidity densities ρ_q
with all combinations of lower order correlations subtracted out.
The most famous being:

$$C_2(y_1, y_2) = \rho_2(y_1, y_2) - \rho_1(y_1)\rho_1(y_2) \tag{3}$$

The 2-particle correlation is also expressed
in the Reduced or normalized form

$$R(y_1, y_2) = \frac{C_2(y_1, y_2)}{\rho_1(y_1)\rho_1(y_2)} = \frac{\rho_2(y_1, y_2)}{\rho_1(y_1)\rho_1(y_2)} - 1 \tag{4}$$

Note that the 2-particle correlation function used for the study of Quantum Statistical (Hanbury-Brown Twiss) Correlations is

$$r_2(y_1, y_2) = \frac{\rho_2(y_1, y_2)}{\rho_1(y_1)\rho_1(y_2)} = R(y_1, y_2) + 1 \tag{5}$$

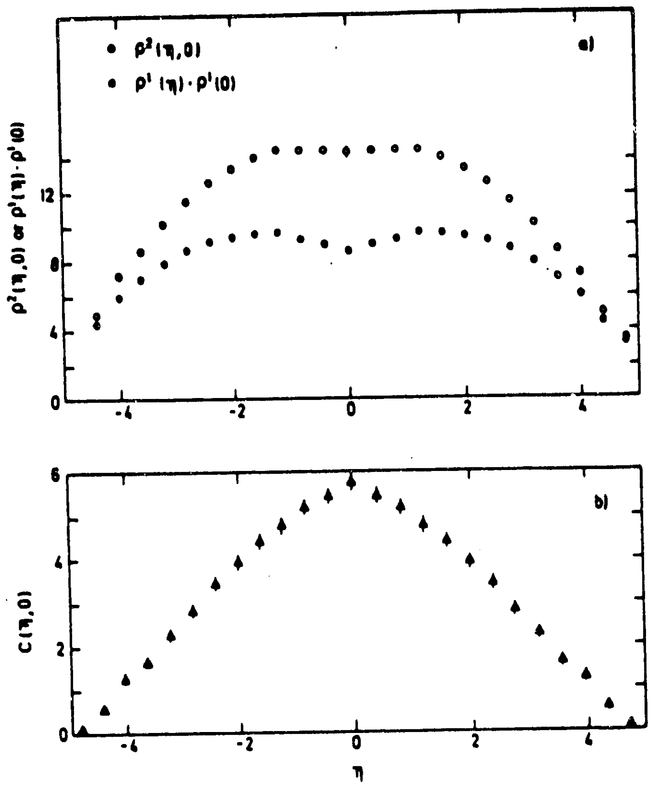

Fig. 4.37. (a) Two-particle pseudorapidity density $\rho^2(\eta, 0)$ compared with the product of the one-particle densities $\rho^1(\eta)\cdot\rho^1(0)$. (b) Correlation function $C(\eta, 0) = \rho^2(\eta, 0) - \rho^1(\eta)\cdot\rho^1(0)$.

Two Particle Correlations, Intermittency and NBD

The importance of Two-Particle correlations
to completely determine the multiplicity distribution
was pointed out by Fowler and Weiner Phys Rev **D17**, 3118 (1978)

More recently, Carruthers and Sarcevic PRL **63**, 1562 (1989)
contended that "the increase of bin-averaged factorial moments
with decreasing size of the rapidity bin δy can be understood on the basis
of conventional short range correlations... ."

**The Reduced 2-particle Correlation is parameterized
in an exponential form**

$$R(y_1, y_2) = \frac{C_2(y_1, y_2)}{\rho_1(y_1)\rho_1(y_2)} = \gamma_2\, e^{-|y_1 - y_2|/\xi} \tag{1}$$

Then

$$\frac{f_2}{<n>^2} = F_2 - 1 = \frac{\int^{\delta\eta} dy_1 dy_2\, C_2(y_1, y_2)}{<n>^2} = \frac{\gamma_2\,(1 - e^{-\delta\eta/2\xi})}{\delta\eta/2\xi} \tag{2}$$

where ξ is the correlation length.

My Neat Formula
but Van Hove did it first!

Since I knew the distribution to be NBD, with $F_2 - 1 = 1/k$

$$k(\delta\eta) = k_o \frac{\delta\eta/2\xi}{(1 - e^{-\delta\eta/2\xi})} \tag{3}$$

where

$$k_o \equiv \frac{1}{\gamma_2} = \frac{1}{R(0,0)} \quad . \tag{4}$$

Note that this formula represents a mathematical expression of my conjecture that the observed linear increase of k with $\delta\eta$ is an indication of the randomness of the multiplicity in adacent $\delta\eta$ bins, while the constancy of k with increasing $\delta\eta$ would be an indication of 100% correlation. In the limit $\delta\eta \ll \xi$, when the $\delta\eta$ interval is well inside the correlation length, $k(\delta\eta)=k_o$, a constant. In the limit $\delta\eta \gg \xi$, k increases linearly with $\delta\eta$, $k(\delta\eta) \simeq \delta\eta/2\xi$, as expected from convolutions of independent bins.

FROM CARRUTHERS + SARCEVIC PRL 63, 1562 (1989)
RELATED TO NBD BY HST

$$\boxed{k(\delta\eta) = k_0 \frac{\delta\eta/2\xi}{(1-e^{-\delta\eta/2\xi})}}$$

$k_0 = \frac{1}{\nu_2}$

O+Cu fit to correlation length $\xi=0.12 \pm 0.01$

$R(0,0) = 0.0$(± 0.0(

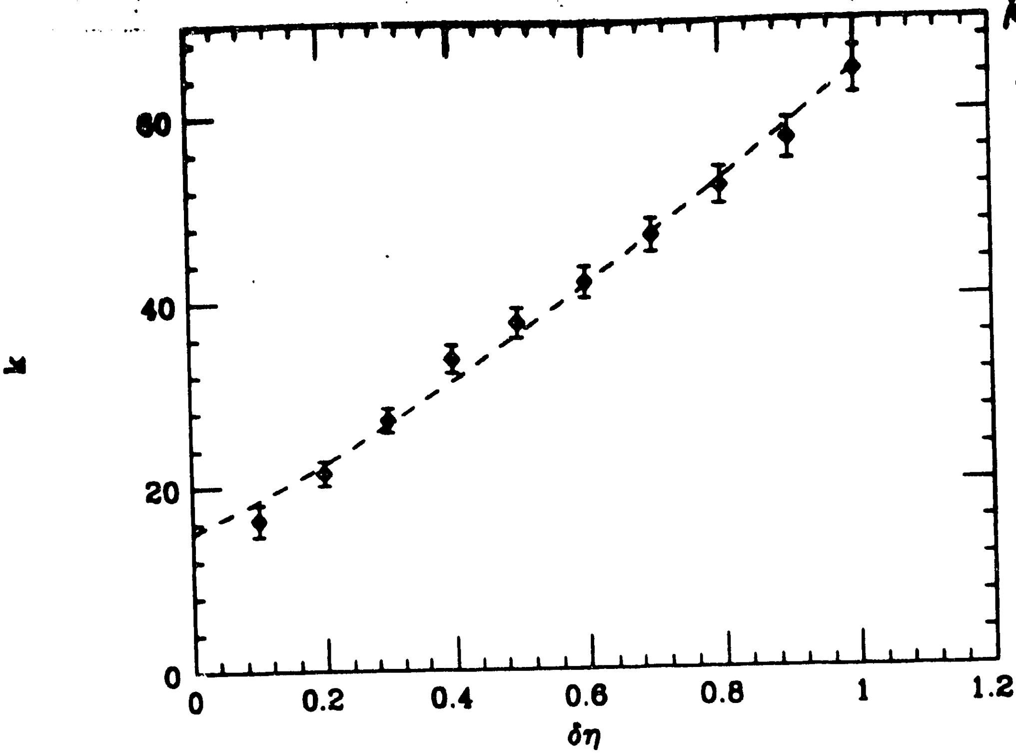

UA5 fit to correlation length $\xi=2.9 \pm 0.1$

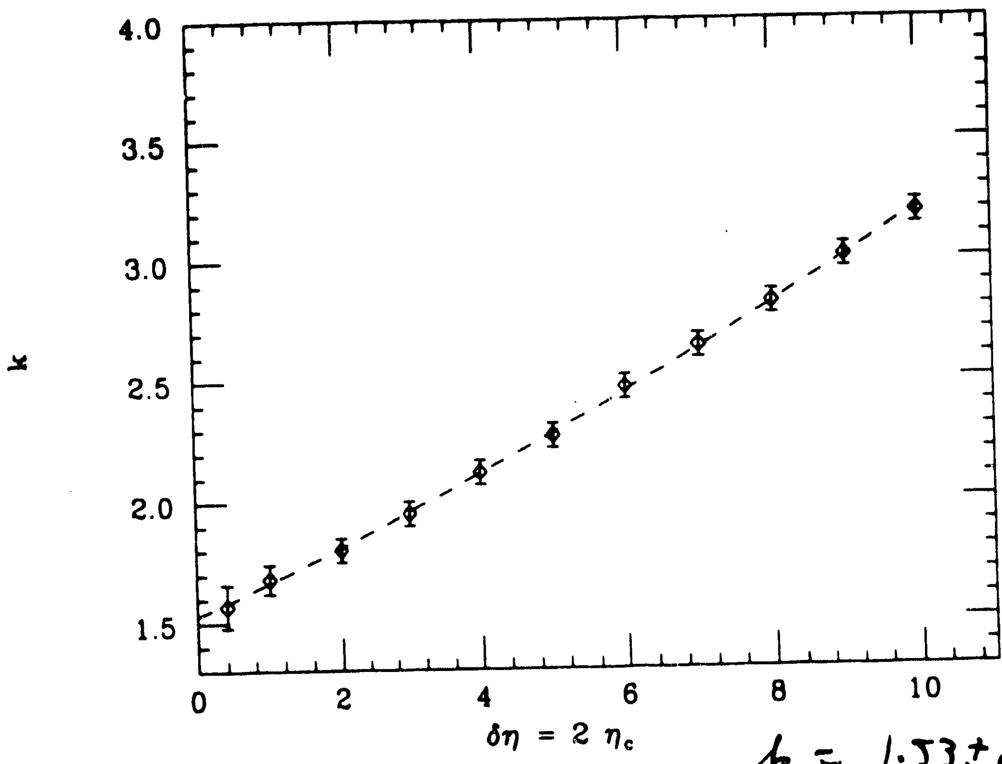

$k_0 = 1.53 \pm 0.03$

$R(0,0) = \frac{1}{k_0} = 0.65 \pm 0.01$

2.0, 32 and 65 respectively. This indicates a collective effect as the source of fluctuations and Bose-Einstein correlations are an obvious candidate. Simulated events from the Fritiof model [33] which does not produce nonstatistical fluctuations, were used to verify that background and detector effect do not reproduce the observed moments.

To further investigate the source of the fluctuations Bose-Einstein correlations as well as Coloumb interactions of pions were introduced in an approximate manner into the Fritiof model [34]. The parameters were chosen to reproduce the experimental correlation function $C_2(Q_{INV})$. The resulting moments which include the contributions from the detector background are shown in Fig. 11d for OAu central collisions. One finds that the data in Fig. 11b can be reproduced to a large extent.

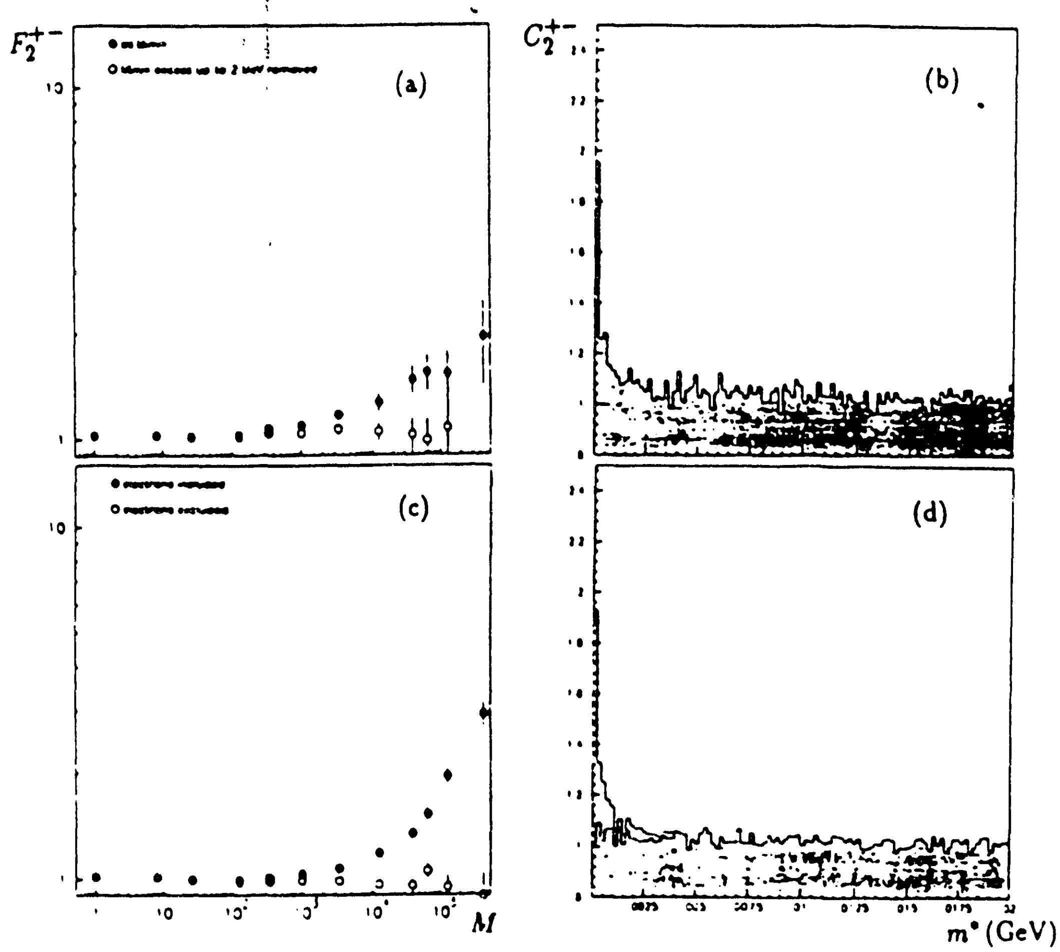

Fig. 12: Central OAu collisions: normalized factorial moment F_2^{+-} versus the number of phase-space cells M and correlation function C_2^{+-} versus $m^* = m_{inv} - 2m_\pi$ for data (a,b) and the modified Fritiof model with detector simulation (c,d). Full and open symbols in (a,c) show results before and after removing electrons (preliminary).

The number of pion pairs of opposite charge is not enhanced by Bose-Einstein correlations. However pairs of oppositely charged particles are contaminated by electron-positron pairs from photon conversion. Figure 12 displays the normalized moment $F_2^{+-}(M)$ and

Conclusions

- E802 ^{16}O+Cu Central(ZCAL) Multiplicity distributions in bins of pseudorapidity $\delta\eta = 0.1, 0.2, 0.3 \ldots 1.0$ exhibit excellent fits to Negative Binomial Distributions.

- The k paramater of the NBD fit increases linearly with the $\delta\eta$ interval which is an **unexpected** and **particularly striking result.**

- Due to the well known property of the NBD under convolution, the linear evolution of the NBD parameter $k(\delta\eta)$ with $\delta\eta$ for Central ^{16}O+Cu collisions indicates that the multiplicity distributions in adjacent bins of pseudorapidity $\delta\eta \sim 0.1$ are **largely statistically independent.**

- This explains the large single event bin-by-bin multiplicity fluctuations observed ty the JACEE collaboration from a Cosmic Ray Si+AgBr event.

- The evolution of $k(\delta\eta)$ can be neatly related to the 2-particle short-range correlation strength and correlation length.

$$k(\delta\eta) = \frac{1}{F_2 - 1} = \frac{<n(\delta\eta)>^2}{\int^{\delta\eta} dy_1 dy_2\, C_2(y_1, y_2)} = \frac{1}{R(0,0)} \frac{\delta\eta/2\xi}{(1 - e^{-\delta\eta/2\xi})} \qquad (1)$$

- The derived parameters from the E802 $k(\delta\eta)$ indicate a weak correlation strength $R(0,0) = 0.066 \pm 0.004$ and a very short rapidity correlation length $\xi = 0.12 \pm 0.01$, e.g. compared to $p - \bar{p}$ collisions where UA5 measured $R(0,0) \sim 2/3$ and $\xi \sim 3$.

- The weak short-range correlation in nucleus-nucleus collisions had been predicted—since the conventional nucleon-nucleon short-range correlations should be washed out by the random superposition of correlated sources so that eventually only Quantum Statistical (Bose-Einstein) Correlations should remain.

- Direct measurements of this B-E correlation in the variable $\delta\eta$ (instead of the usual variable ($Q = p_1 - p_2$) are being attempted—to verify the derived parameters.

Bose–Einstein Correlations in 200A GeV S+Au Collisions

Richard Morse
LBL

Bose-Einstein Correlations in 200 A GeV S+Au Collisions

NA35 Collaboration

J.Baechler[9], J.Bartke[5], H.Bialkowska[13], M.Bloomer[3], R.Bock[6], R.Brockmann[6], P.Bunčić[14], S.I.Chase[3], J.Cramer[11], I.Derado[10], V.Eckardt[10], J.Eschke[7], C.Favuzzi[2], D.Ferenc[14], B.Fleischmann[6,7], P.Foka[6], M.Fuchs[6,7], M.Gazdzicki[12], E.Gladysz[5], J.W.Harris[3], W.Heck[7], M.Hoffmann[8], P.Jacobs[3], K.Kadija[4,14], S.Kabana[7], A.Karabarbounis[1], R.Keidel[9], J.Kosiec[12], M.Kowalski[5,10], A.Kuhmichel[7], M.Lahanas[7], Y.Lee[7], M.LeVine[7,15], A.Ljubičić Jr.[14], S.Margetis[7], R.Morse[3], E.Nappi[2], G.Odyniec[3], G.Paić[4,14], A.D.Panagiotou[1], A.Petridis[1], A.Piper[9], F.Posa[2], A.Poskanzer[3], H.Pugh[3], F.Puhlhofer[9], G.Rai[3], W.Rauch[10], R.Renfordt[7], W.Retyk[12], G.Roland[7], D.Rohrich[7], H.Rothard[7], K.Runge[8], A.Sandoval[6], J.Schambach[3], E.Schmidt[7], N.Schmitz[10], E.Schmoetten[8], I.Schneider[7], P.Seyboth[10], J.Seyerlein[10], E.Skrypczak[12], P.Spinelli[2], P.Stefanski[5], R.Stock[7], H.Stroebele[7], L.Teitelbaum[3], S.Tonse[3], T.Trainor[11], G.Vassileiadis[1], M.Vassiliou[1], G.Vesztergombi[10], D.Vranić[14], S.Wenig[7], D. Brinkmann, J.T. Mitchell

1)Phys. Dept. Univ. of Athens 2)Dipartmento di Fisica, Univers. di Bari 3)Lawrence Berkeley Lab. 4)CERN, 5)Inst. of nucl. phys. Cracow 6)GSI Darmstadt 7)Fachbereich Physik, Univ. Frankfurt/M 8)Fakultaet fuer Physik Univ. Freiburg 9)Univ. Marburg 10)Max-Planck Inst. fuer Physik, Munchen 11)Univ. of Washington Seattle 12)Inst. of Experim. Phys. Univ. Warsaw 13)Inst. of Nucl. Studies, Warsaw 14)Rudjer Bošković Inst. Zagreb 15)BNL, N.Y.

I. Motivation
   Technique
   Variables

II. NA35 — Hardware
   Phase Space Region

III. Data

IV. Results / Conclusion

R. Morse
LBL

Two Pion Interferometry

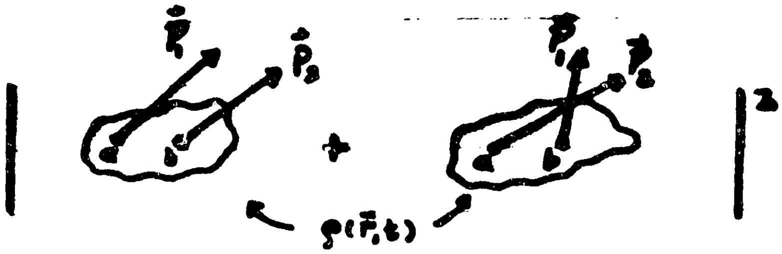

$$N(\vec{p}_1,\vec{p}_2) = \int d\vec{r}_a\, dt_a\, d\vec{r}_b\, dt_b\; \rho(\vec{r}_a,t_a)\,\rho(\vec{r}_b,t_b)\; |\Psi(\vec{p}_1,\vec{p}_2)|^2$$

$$= \left[1 + |\tilde{\rho}(\vec{p}_1-\vec{p}_2)|^2 \right] N(\vec{p}_1)\, N(\vec{p}_2)$$

Assumptions : plane wave approx.
source density $\longrightarrow g(x,p) = \rho(x)\, f(p)$
uncorrelated emission amplitudes (chaotic lim.)

Experimental Approach

make a transformation from variables appropriate to sp phase space to those appropriate to tp phase space...

$$C2 \equiv \frac{N(\vec{p}_1,\vec{p}_2)}{N(\vec{p}_1)\, N(\vec{p}_2)} = \frac{N \frac{d^2n}{dp_1 dp_2}}{\frac{dn}{dp_1}\,\frac{dn}{dp_2}} \longrightarrow \frac{\text{Actual}(q)}{\text{Background}(q)}$$

isolates "interesting term"

Actual(q) : Observed tp phase space
Background(q) : " " in absence of Bose-symm
Distortions : two particle Coulomb. track-finding biases. etc...

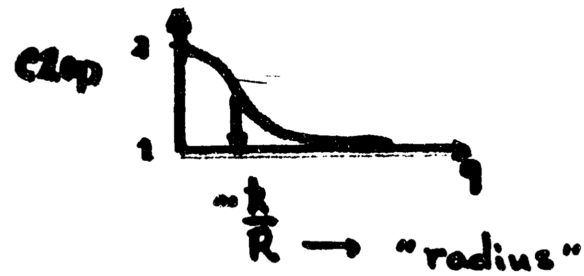

Two Particle Phase Space Variables

$Q_{inv} = \sqrt{(P_1 - P_2)^2}$

boost-invariant particle prdn ↔ longitudinal phase space

$$\begin{cases} Q_L & \parallel \text{ beam axis} \\ Q_{T_{out}} & \perp \text{ beam} ;\ \parallel \vec{K}_T \qquad (\vec{K} = \vec{P}_1 + \vec{P}_2) \\ Q_{T_{side}} & \perp \text{ beam} ;\ \perp \vec{K}_T \end{cases}$$

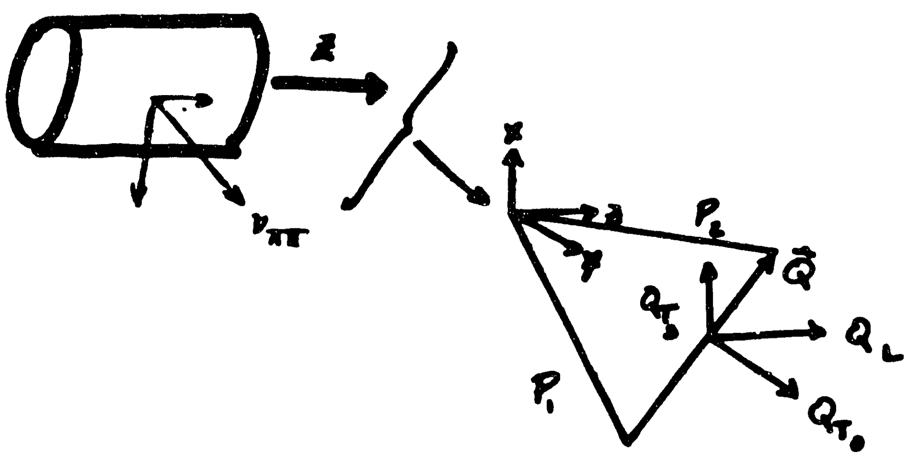

$$\left.\begin{matrix} R_L \\ R_{T_{out}} \\ R_{T_{side}} \end{matrix}\right\} \begin{matrix} R_L \sim \tau_f \\ R_{T_{out}} - R_{T_{side}} \sim \Delta\tau \\ R_{T_{side}} \sim R_{geom} \end{matrix}$$

Physics Motivations

$C2(Q) \rightarrow R$	reaction volume		(ϵ)
$C2(Q) \rightarrow \tau$, $\Delta\tau$	reaction time scales		(direct r, ℓ)
$C2(Q,y) \rightarrow y_0$ (?)		$g(x,p) \stackrel{?}{=} g(x) f(p)$	$\left(\frac{dv}{dz}\right)$
$C2_\pi(Q)$ vs $C2_K(Q)$		$g_\pi(x,p) \stackrel{?}{=} g_K(x,p)$	(quark species relative abund $\frac{K}{\pi}$)
$\boxed{C2(Q,p_T)}$		$\boxed{g(x,p) \stackrel{?}{=} g(x) f(p)}$	$\boxed{\frac{dv}{dz} \quad \frac{dv}{dr_\perp}}$

CERN NA35

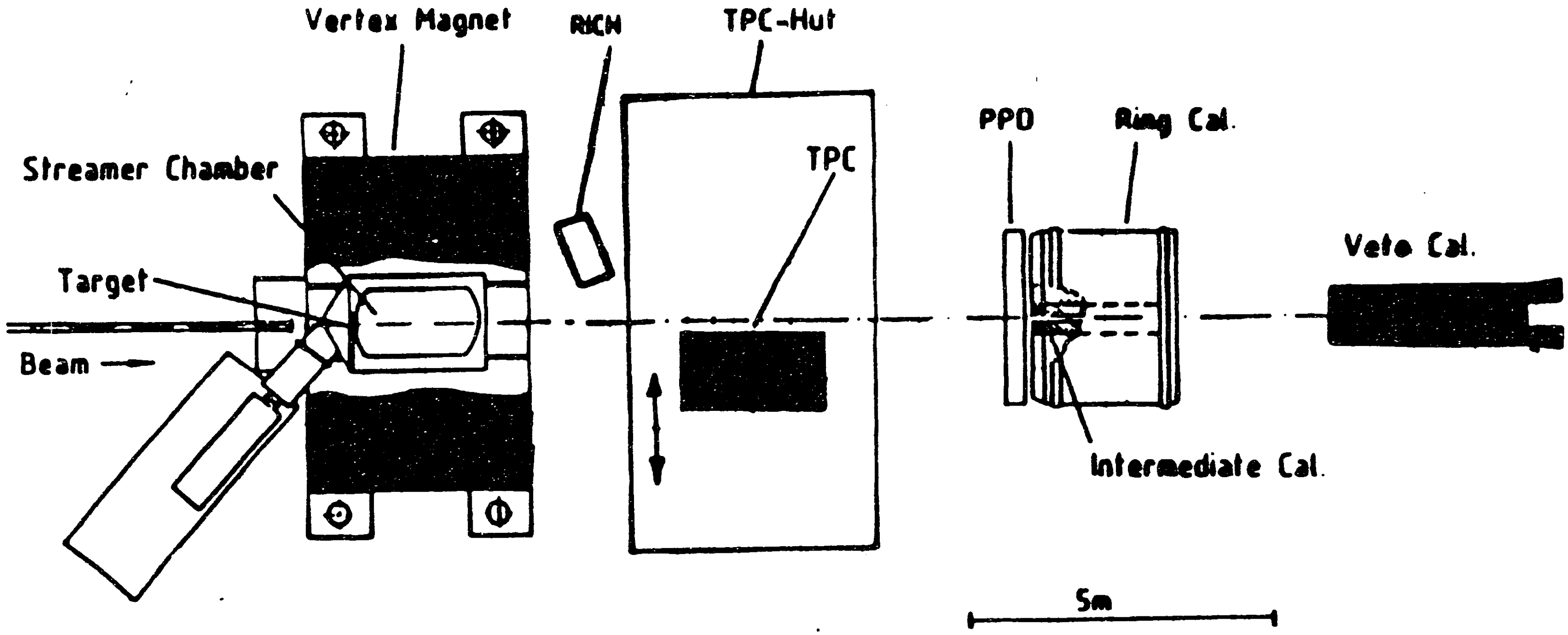

Fig. 1

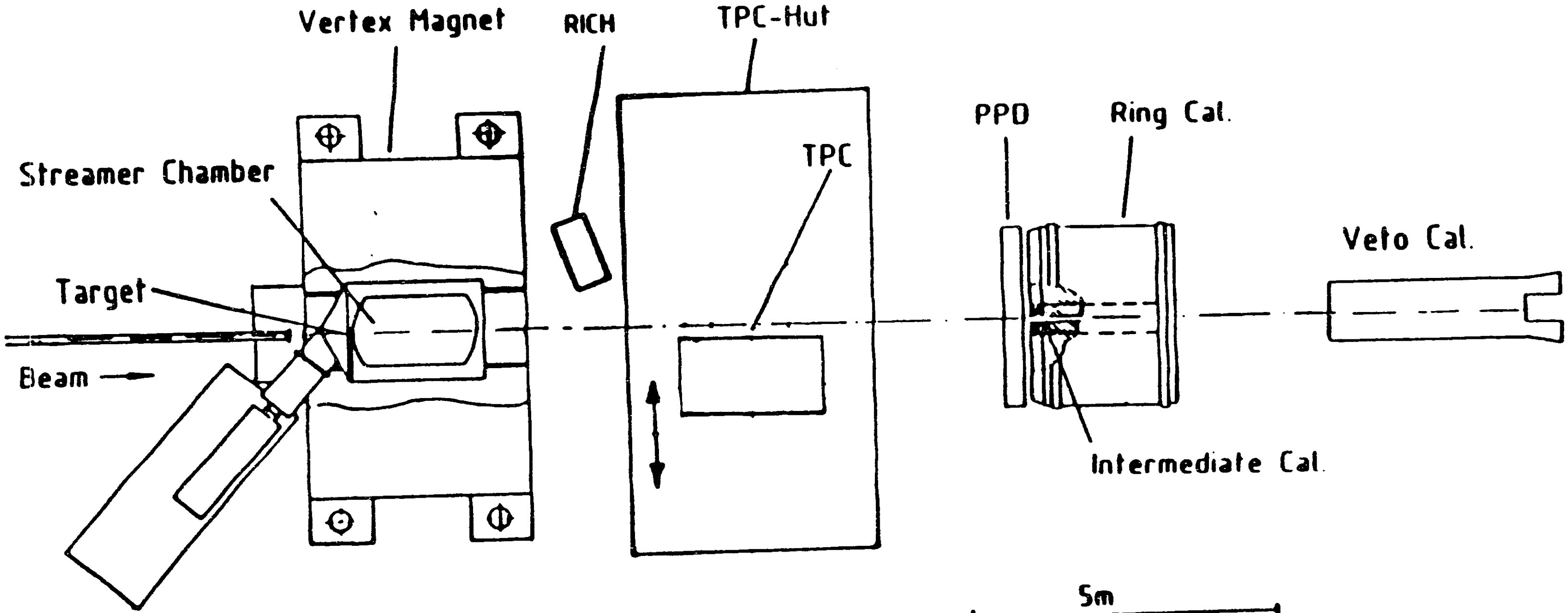
Vertex Magnet
RICH
TPC-Hut
PPD
Ring Cal.
Streamer Chamber
TPC
Veto Cal.
Target
Beam
Intermediate Cal.
5m

Fig. 1

2. Exp. Layout

i) a large volume streamer chamber ($2 \times 1.2 \times 0.72\ m^3$) in a 1.5 T magnet

ii) a TPC of ($2.4 \times 1.2 \times 1.08\ m^3$) downstream of the magnet

iii) trigger & event characterisation detectors ...

Physics history:

- forward & transverse energy dist.
- h^- spectra (y, p_T)
- two particle correlations
- $K^\pm$
- V_0 (Λ, K^0_s)
- "baryon" spectra (+)-(-)

Table 2 - TPC Parameters.

Drift Volume	approx. 2500x1000x1400 mm^3
Readout Area	2370x1260 mm^3
Sampled Track Length	1200 mm
Drift Length	1000 mm
Drift Field Ne(Ar)/10%CH_4	200(115) V/cm
Max. Drift Time Ne(Ar)	30(20) μs
No. of Readout Modules	6
Module Dimensions	790x630 mm^2
Pad Size	39.5x5.5 mm^2
No. of Pad Rows/Module (Total)	15(30)
No. of Pads/Row	128
No. of Pads equipped with Electronics	5376
Gap Sense Wire-Pad (Grid cathode)	3(4) mm
Sense Wire Diameter	20 μm
Field Wire Diameter	125 μm
Sense Wire Voltage [19]	approx. 1200 V

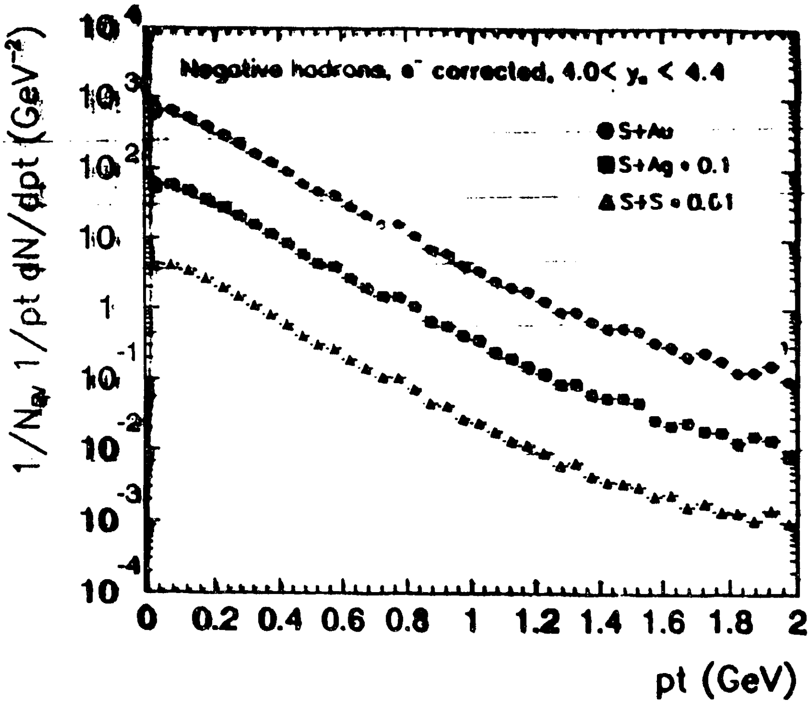

Single Particle Inclus: Spectra

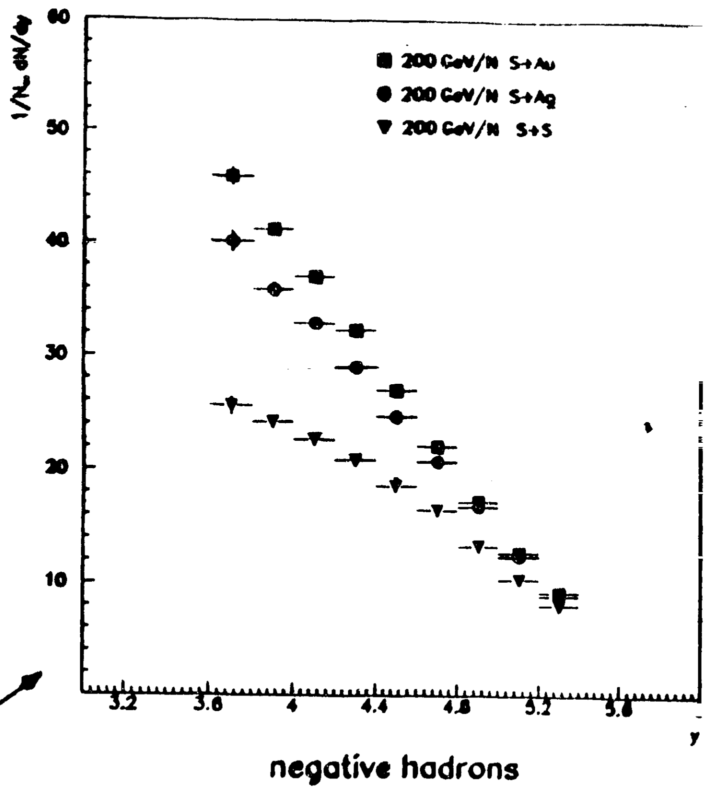

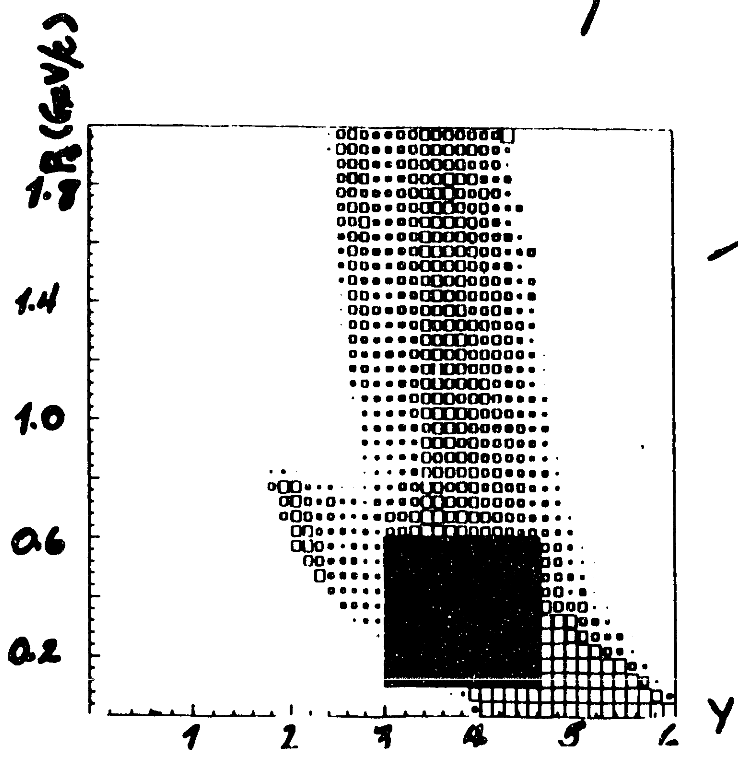

$Y_{nn} \approx 3.0$

dN/dy, p_T agree w/ S.C.

slopes (p_t) = identical

$y = 4.2$

Data

$S+Au \rightarrow 2h^-$ $(2\pi^-)$

- ~ 26k events
- $\langle n \rangle \sim 48$
- $\sigma_{trig} \sim 6\% \; \sigma_{mol}$

VETO
↳ "dive-in"

Analysis

0) source parameterisation : Gaussian in $\begin{cases} R_{inv} \\ R_{T_{side}} \; R_{T_{out}} \; R_L \end{cases}$

i.e. $\rho(x) \sim e^{-x^2/R_{inv}^2}$

$\rho(x,y,z) \sim e^{-x^2/R_{Ts}^2} \, e^{-y^2/R_{To}^2} \, e^{-z^2/R_L^2}$

$$\Rightarrow \boxed{\begin{aligned} C2 &= 1+\lambda e^{-q_{inv}^2 R_{inv}^2/2} \\ C2 &= 1+\lambda e^{-Q_{Ts}^2 R_{Ts}^2/2} \, e^{-Q_{To}^2 R_{To}^2/2} \, e^{-Q_L^2 R_L^2/2} \end{aligned}}$$

1) event-mixed background
2) Gamow-penetration factor
Two-track resolution "cut"

3) $y_{obs} = y_{NN}$

Resolutions ↔ Sensitivity

$\left.\begin{array}{l} \delta q_{inv} \\ \delta q_{Ts} \; \delta q_{To} \; \delta q_L \end{array}\right\} \leq 17 \text{ MeV}/c \Rightarrow r_{max} \leq 10 \text{ fm}$

↳ 20 MeV/c binning

200AGeV S+Au (Spring 92)

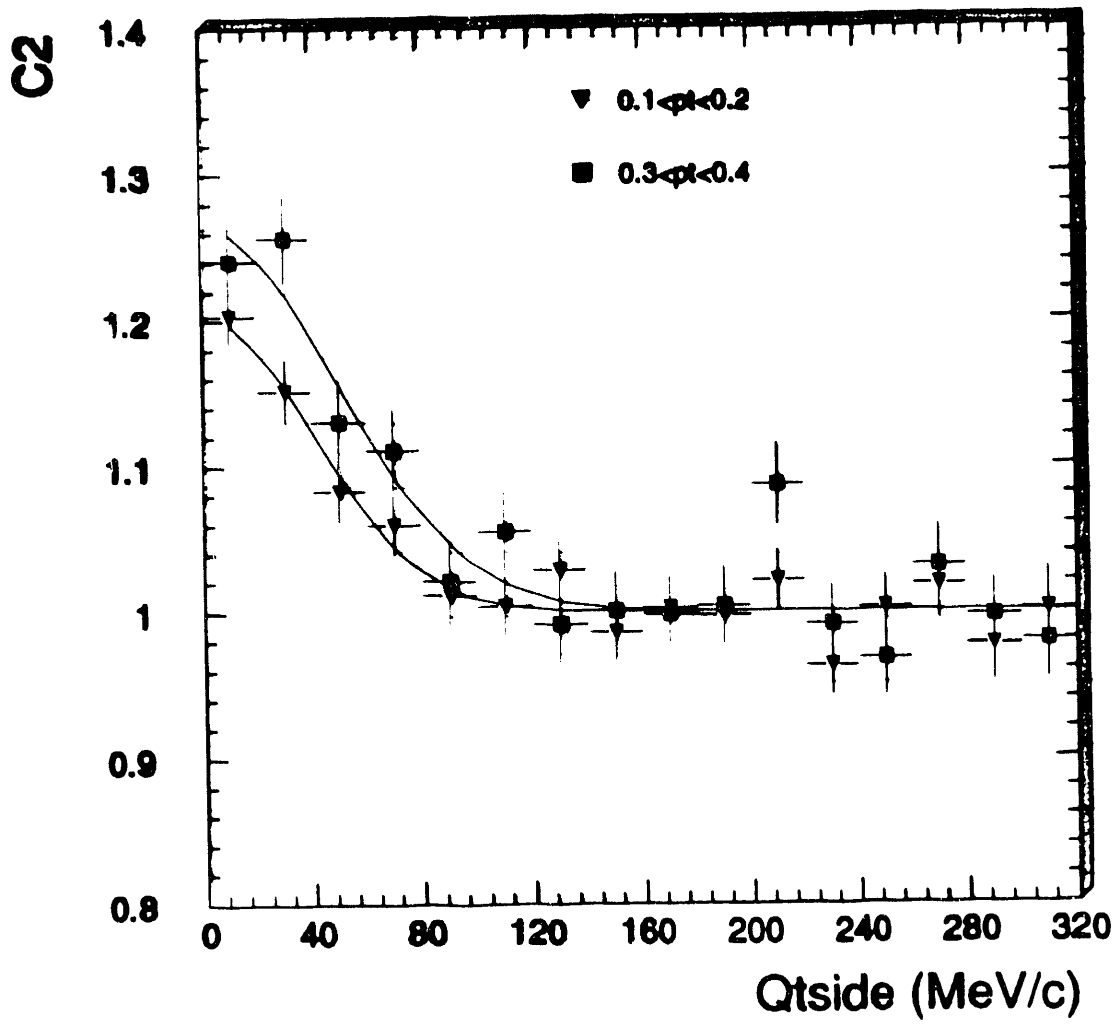

R_{Tside}

$4.7 \pm .3$

$3.8 \pm .3$

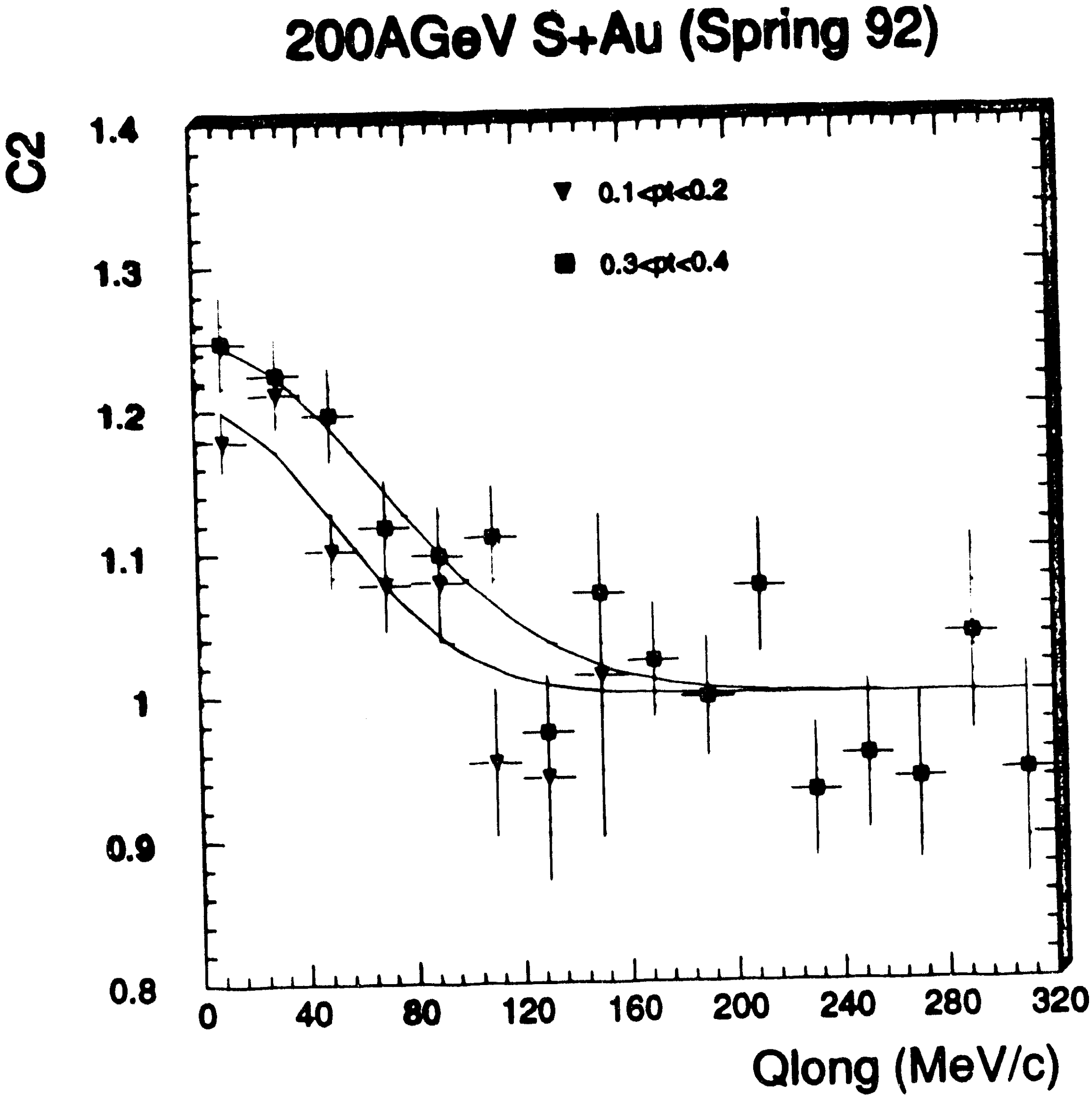
200AGeV S+Au (Spring 92)
C2
1.4
1.3
1.2
1.1
1
0.9
0.8
0.1<pt<0.2
0.3<pt<0.4
0
40
80
120
160
200
240
280
320
Qlong (MeV/c)

R_L

3.9±.5

3.0±.4

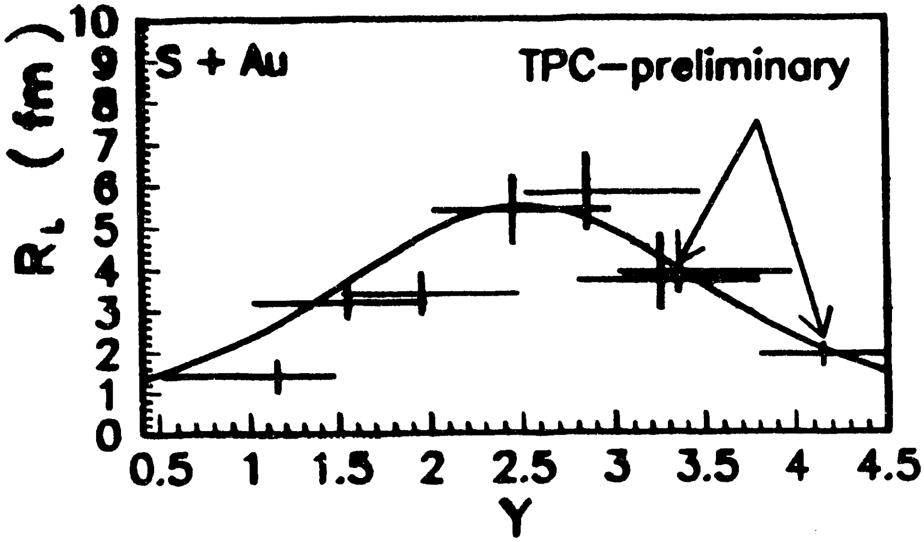

→ $1/\cosh(y-y_0)$ behaviour

↳ 'longitudinally' expanding source

↳ dynamics

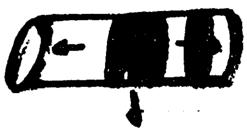

longitudinal expansion : $v = z/t$

$(v = z/\gamma\tau)$

$$f(p,z) = \exp -\frac{1}{T}\left\{E_p + \frac{m z^2}{2\tau^2}\right\}$$

$\tau^2 \to \gamma^2\tau^2$

$\gamma^2 = 1/1-\beta^2 = \frac{1}{\cosh\Delta y}$

$$R_{eff} = \sqrt{2\tau^2 T/m}$$

$R_{eff} \Rightarrow \frac{R_{eff}}{\cosh\Delta y}$

C2(y)

$_0 = 3.0$?

$\frac{\text{osh}(1.1)}{\text{osh}(0.5)} = 1.5$

$C2(p_T)$??

"mass effect"

higher p_t particles look "heavier"

$\Rightarrow R_L(p_{t_1}) > R_L(p_{t_2}) \quad p_{t_1} < p_{t_2}$

(or again, separation in "pair frame"...)

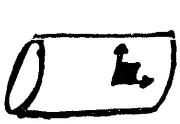 vs 

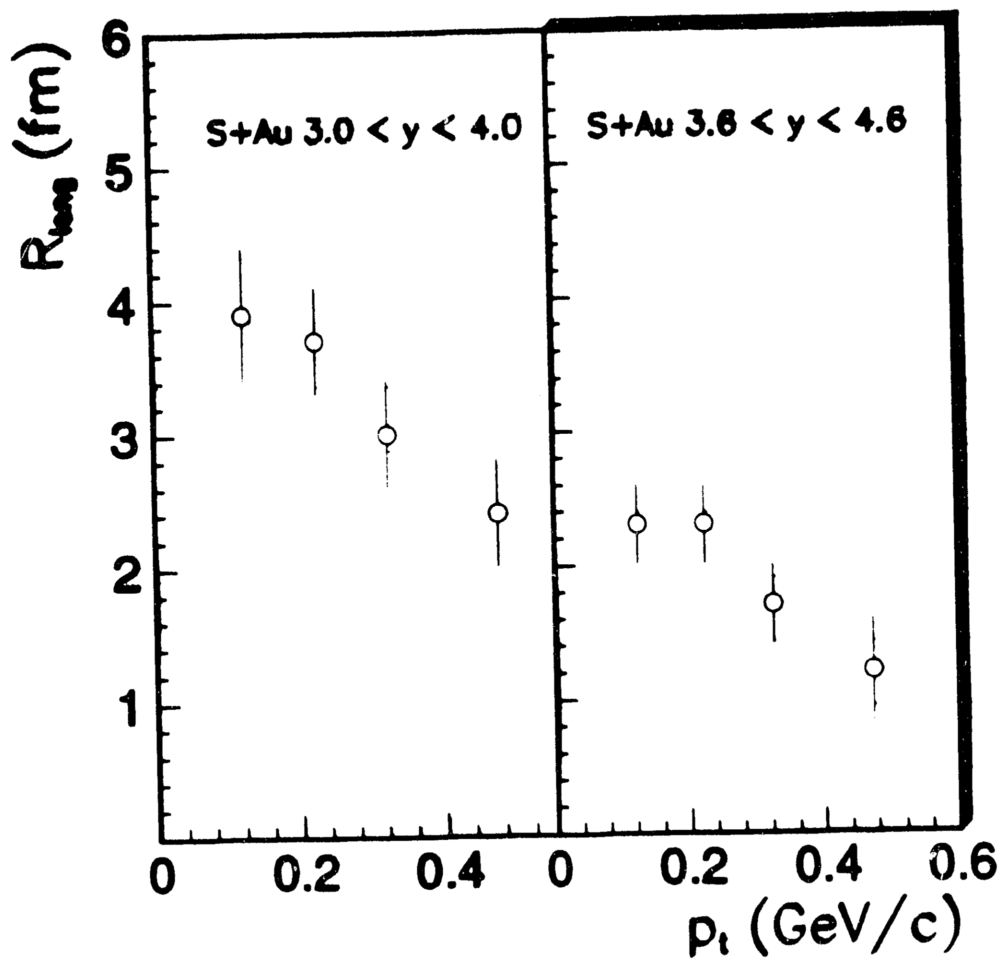

R_{long} (fm)
S+Au 3.0 < y < 4.0
S+Au 3.6 < y < 4.6
p_t (GeV/c)

Resolutions → Sensitivity

single track : $\langle \delta y \rangle \sim 650\mu$ (pad)
$\langle \delta z \rangle \sim 450\mu$ (drift)

$\left\{ \begin{array}{l} \delta p/p^2 \sim 0.8 \times 10^{-3} \, (\mathrm{GeV}/c)^{-1} \\ \langle \delta p_t \rangle \sim 6.1 \, \mathrm{MeV}/c \end{array} \right.$

two track :

spatial	mult. scatt.
$\delta q_{inv} \sim 12.5$ MeV/c	14.3 MeV/c
$\delta q_L \sim 6.1$	13.1
$\delta q_{t\,side} \sim 8.7$	6.4
$\delta q_{t\,out} \sim 8.2$	6.7

in quadrature → $\delta q_{inv} \sim 17$ MeV/c
$r_{max} \lesssim 10$ fm

$C(q) \sim 1 + \lambda \exp(-\tfrac{1}{2} r^2 q^2)$

$\tfrac{1}{2} \sim \exp(-r_{max}^2 \delta q^2)$; $r_{max} \sim \sqrt{\frac{\ln 2}{\delta q^2}}$ (0.196 GeV/c)

two track resln : δ 1.5-2cm in "pad-drift" plane

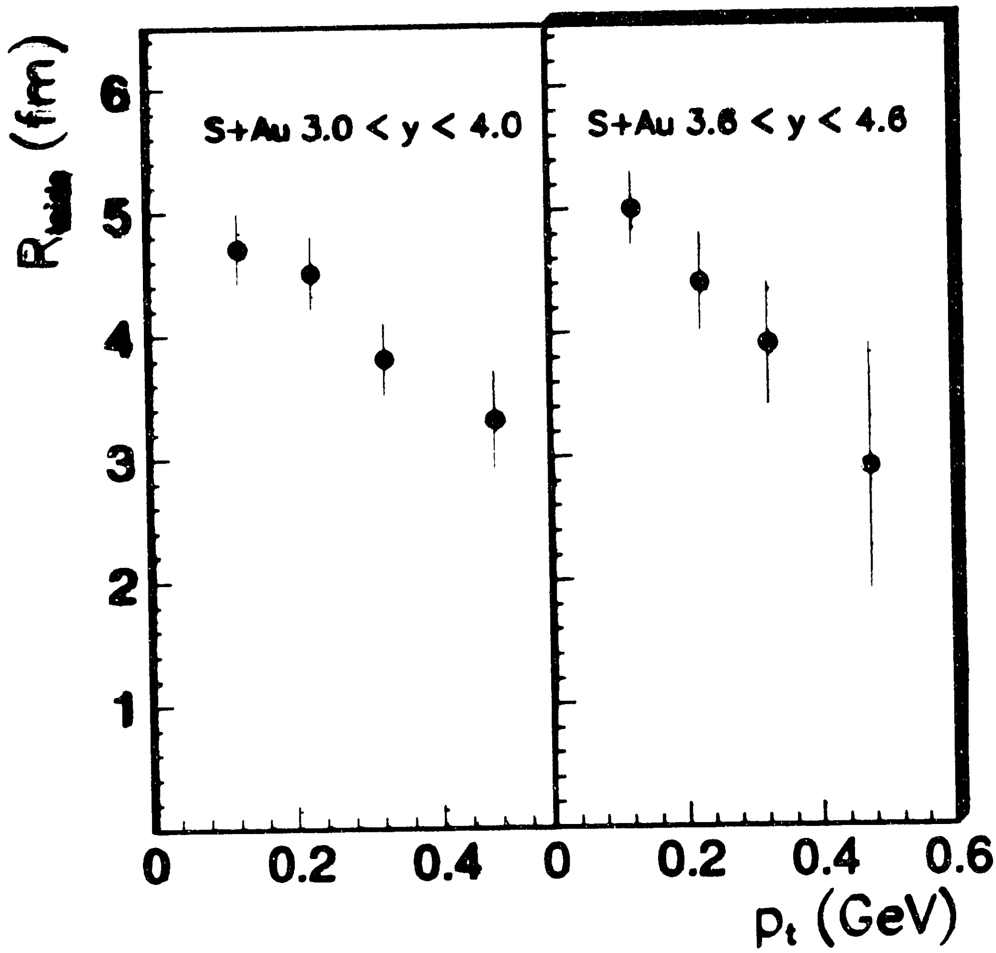

S+Au 3.0 < y < 4.0
S+Au 3.6 < y < 4.6
R_{side} (fm)
p_t (GeV)

200AGeV S+Au (Spring 92)

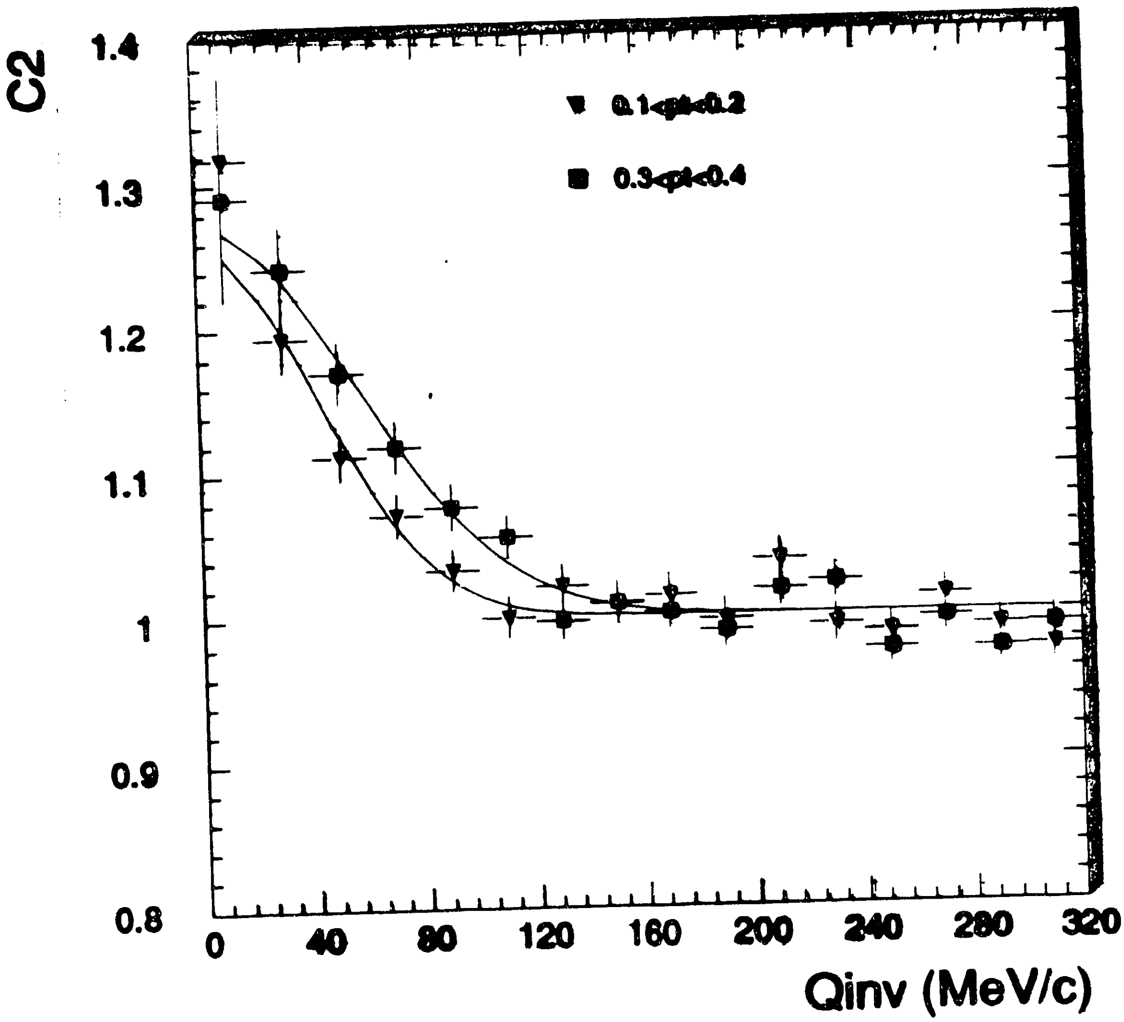

R_{inv}	λ	χ^2/dof
4.72 ± .41	0.26 ± .03	1.1
3.58 ± .24	0.27 ± .026	0.95

Similarly, recast E_p with an "outward" (transverse) velocity gradient $\Rightarrow$ expansion + cooling
$\Rightarrow$ decreasing radius with p_t ...

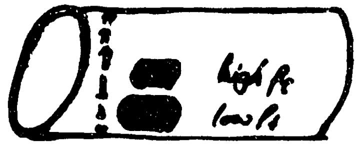

What about more "serious" emission functions ??
ie. microscopic phase space approach with a full space-time picture
eg. RQMD (cf. Sorge's talk)

Summary / Conclusions

a) In p_t-dependent study of the two-particle correlation function we observe significant effects in R_L & $R_{T\,side}$

b) former "expected" latter not !?

Future

a) study of systematics / biases (enhanced low p_t coverage for 3cy+4)

b) RQMD model calculation → is the observed trend predicted?

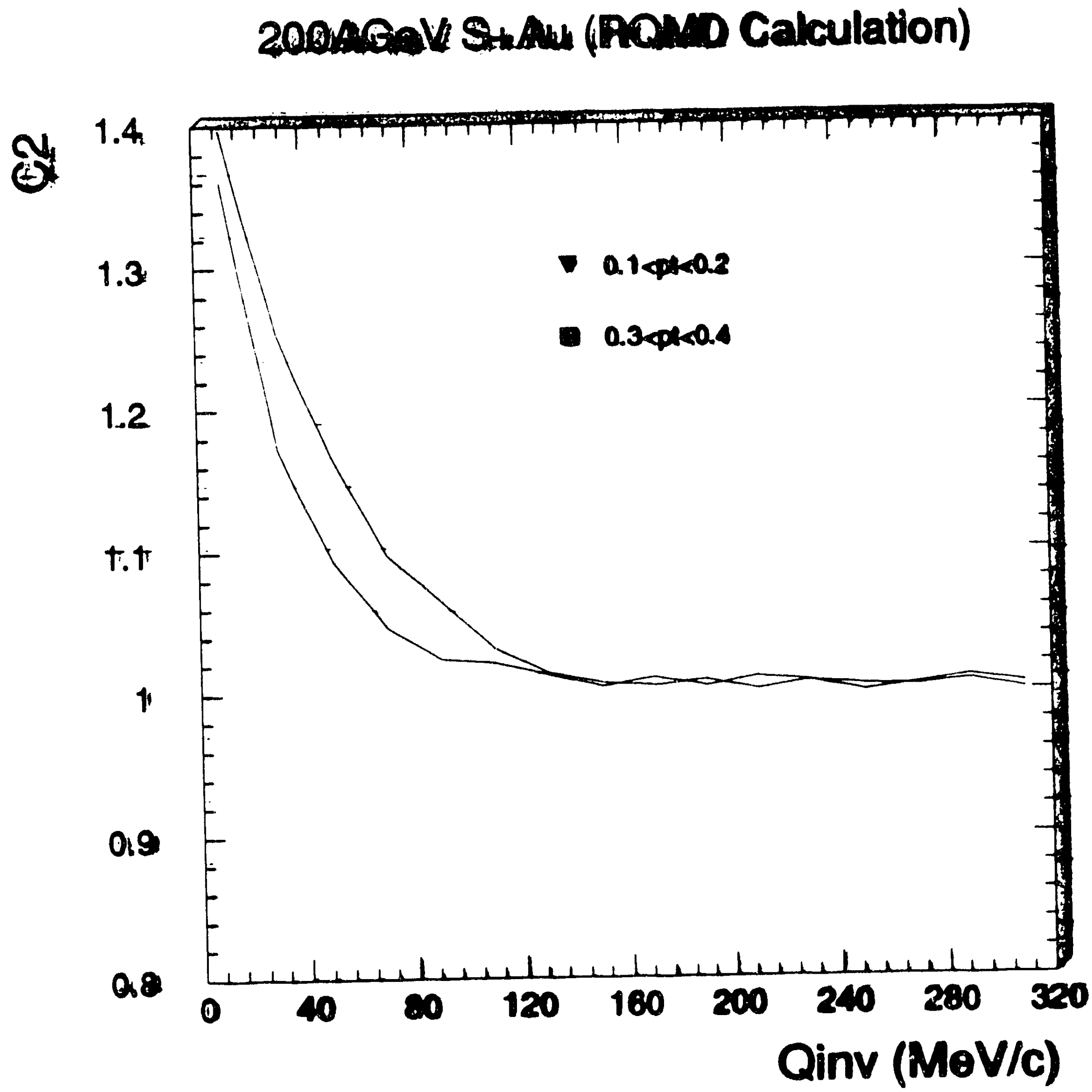

microscopic phase space RQMD (H. Sorge)

=> symmetrisation + fsi => C2 (Scott Pratt)

HBT Correlations at STAR

John Cramer
University of Washington

HBT at STAR

John G. Cramer
University of Washington
Seattle, Washington

Talk presented at
Informal HBT Workshop
Brookhaven National Laboratory
April 16 and 17, 1993

Report on work by:
J.G.C.
Richard Morse
Dean Chacon
Declan Keane
and the STAR Collaboration

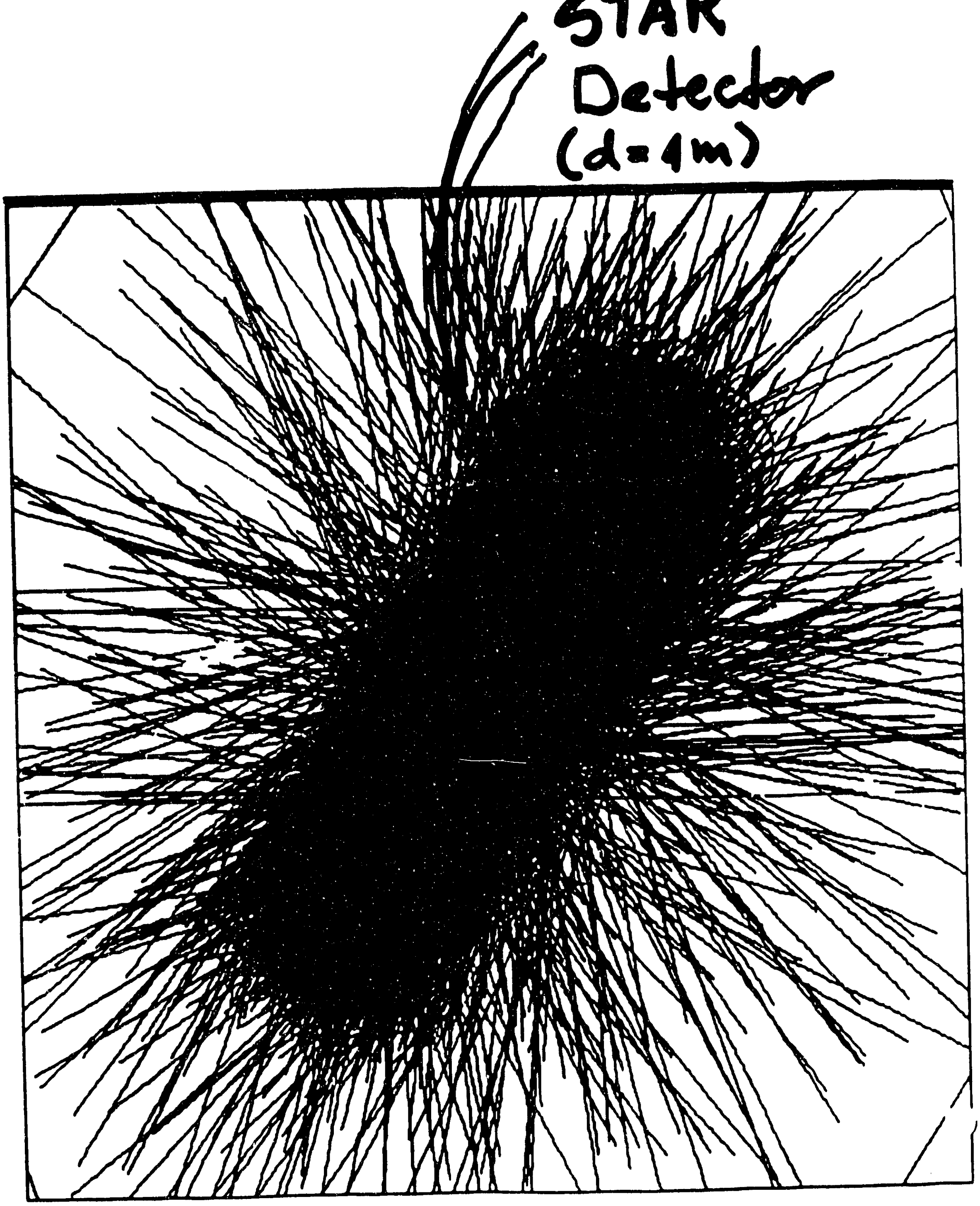

A RHIC Au+Au Central Collision at 200 GeV/nucleon.

2,500 π^+ 260 K^+ Per Event!
2,500 π^- 260 K^-

GEANT PART.ID	PART. NAME	# DIRECT		# FROM DECAYS	
1	GAMMA	2193		0	
2	POSITRON	10		0	
3	ELECTRON	10		0	
7	PION 0	511		2015	
8	PION +	573	+	1854	= 2,427 π^+
9	PION -	599	+	1871	= 2,470 π^-
10	KAON 0 LONG	66		199	
11	KAON +	103	+	161	= 264 K^+
12	KAON -	97	+	142	= 239 K^-
13	NEUTRON	183		131	
14	PROTON	162		124	
15	ANTIPROTON	74		56	
16	KAON 0 SHORT	184		397	

FRITIOF Event W. Christie, LBL Workshop, [illegible]

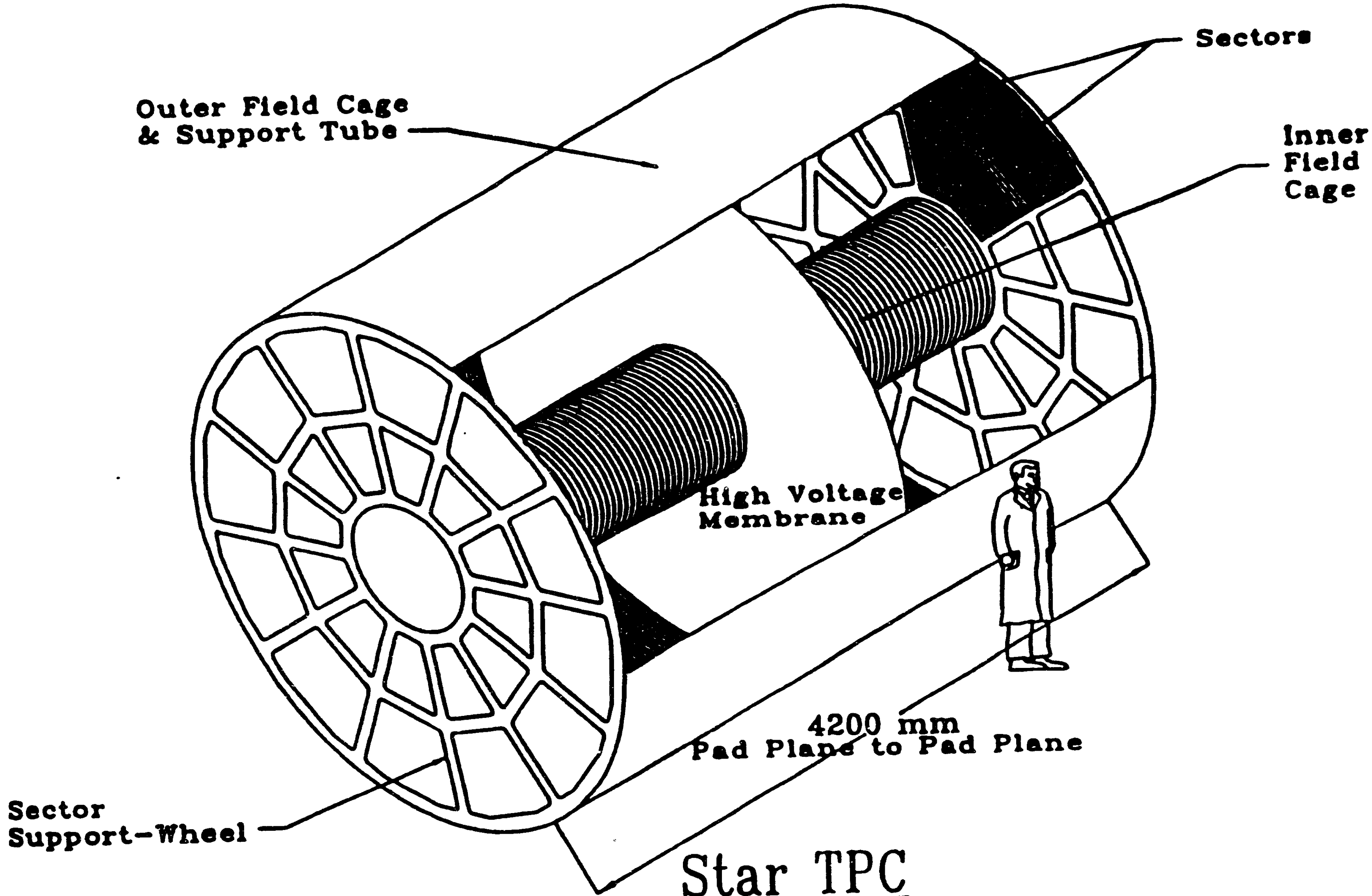

Outer Field Cage
& Support Tube
Sectors
Inner
Field
Cage
High Voltage
Membrane
4200 mm
Pad Plane to Pad Plane
Sector
Support-Wheel

Star TPC

Drift Volume Inner Radius Outer Radius Length	Coaxial Cylinder - 0.5 m 2.0 m 4.2 m
PID acceptance	$\lvert\eta\rvert < 1$ ~ Identified
Tracking acceptance	$\lvert\eta\rvert < 2$ Tracked
Drift Gas	Ar + 10% CH4
Pressure	Atmospheric
Sampling Rate	12.3 MHz
Time Samples	512
# of pad rows	50
Pad Sectors Type, Number of rows Pad Size Type, Number of rows Pad Size	Two types Inner, 18 2.85 mm x 11.5 mm Outer, 32 6.2 mm x 19.5 mm
Total number of pads	140,000
Total # pixels	77,000,000
Dynamic range for dE/dx	10 bits
Position resolution ($p_t > 1$ GeV/c)	460 μm in x,y and 700 μm in z
Drift time	40 μs

STAR

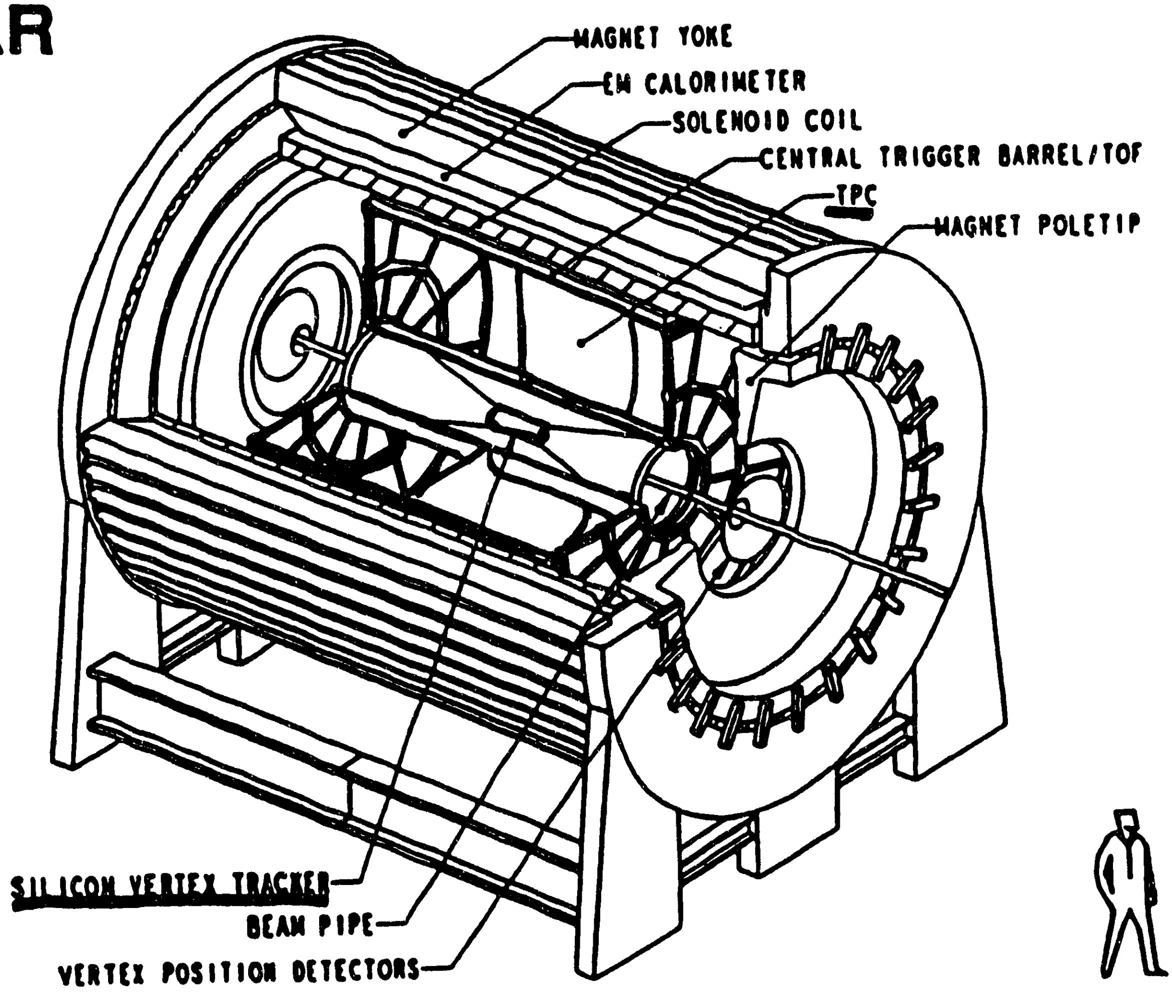
MAGNET YOKE
EM CALORIMETER
SOLENOID COIL
CENTRAL TRIGGER BARREL/TOF
TPC
MAGNET POLETIP
SILICON VERTEX TRACKER
BEAM PIPE
VERTEX POSITION DETECTORS

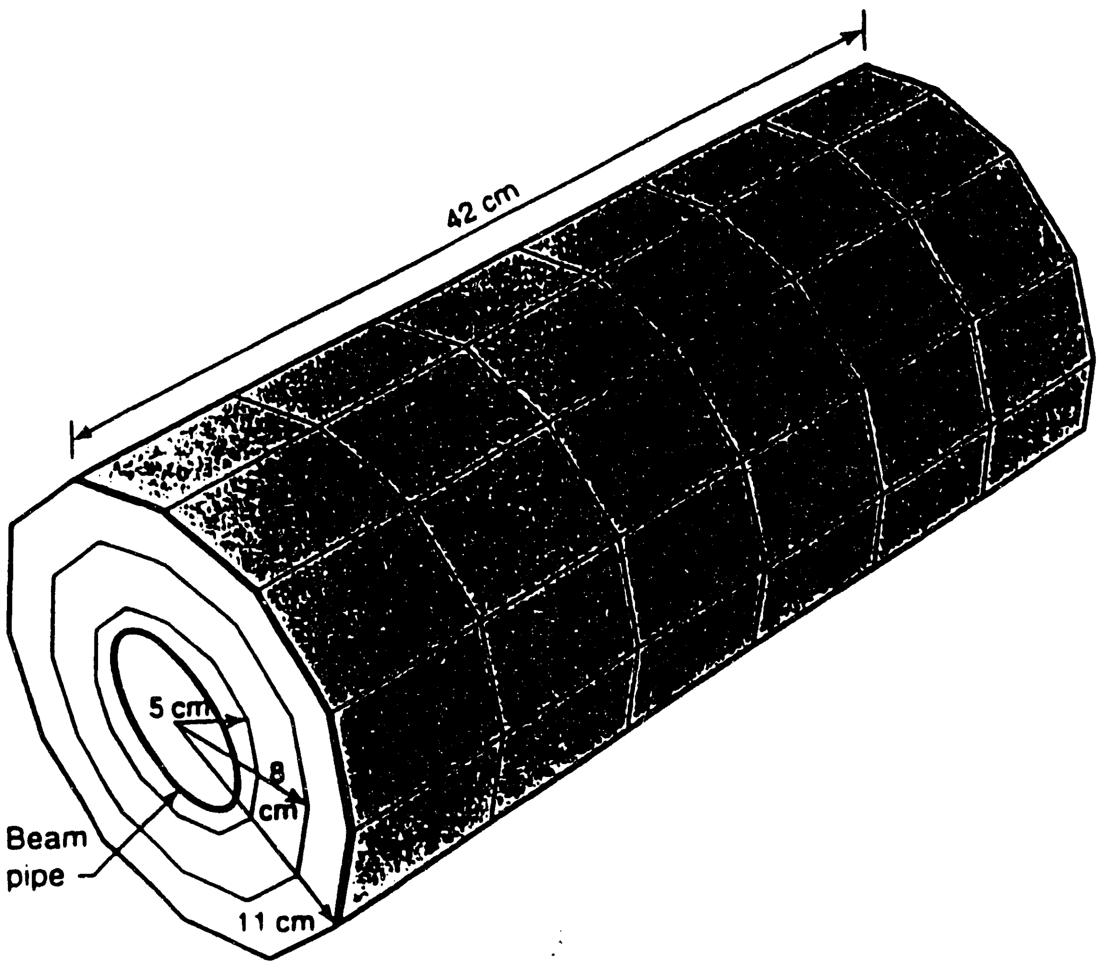

Silicon Vertex Tracker (SVT)

Length	42 cm
Inner Barrel (radial distance)	5 cm
Middle Barrel (radial distance)	8 cm
Outer Barrel (radial distance)	11 cm
Thickness of detectors (SDD)	300 μm
Total thickness	900 μm ~ 0.9% X_o
Number of detectors	162
Inner Barrel	36
Middle Barrel	54
Outer Barrel	72
Diameter of Si wafer	10.00 cm
Length of detector (SDD)	7.05 cm
Width of detector (SDD)	5.68 cm
Drift length of detector	3.50 cm
Average drift time	~3.5 μs
Time samples	256
Sampling Rate	40 MHz
Anode pitch	250 μm
Number of channels	72576
Position resolution	25 μm

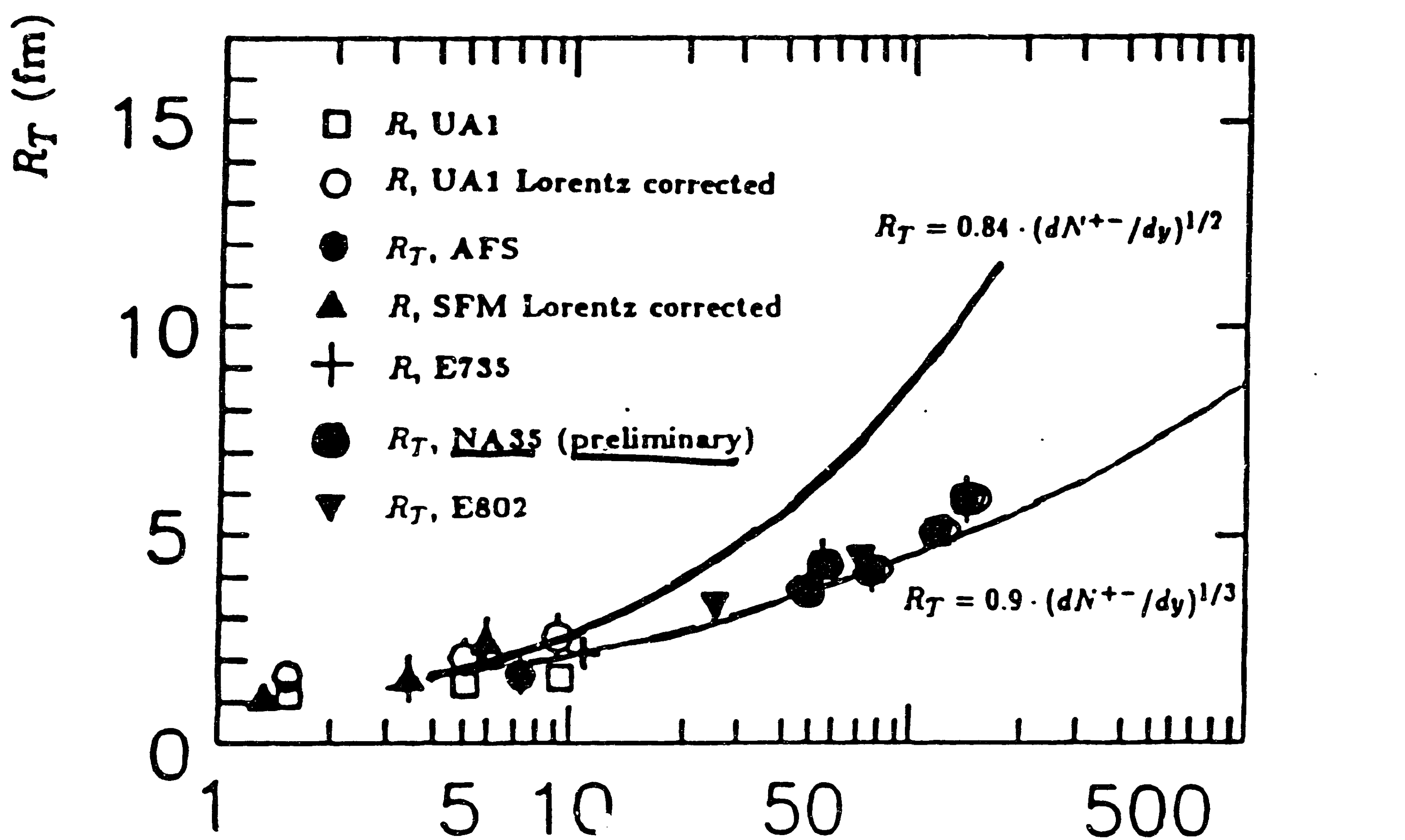

—— Freezout at $R_T = \lambda_{\pi\pi}$ ($\sigma_{\pi\pi} \sim 20$ mb)

—— Freezout at $n_\pi = 0.5\ fm^{-3}$

STAR Detector

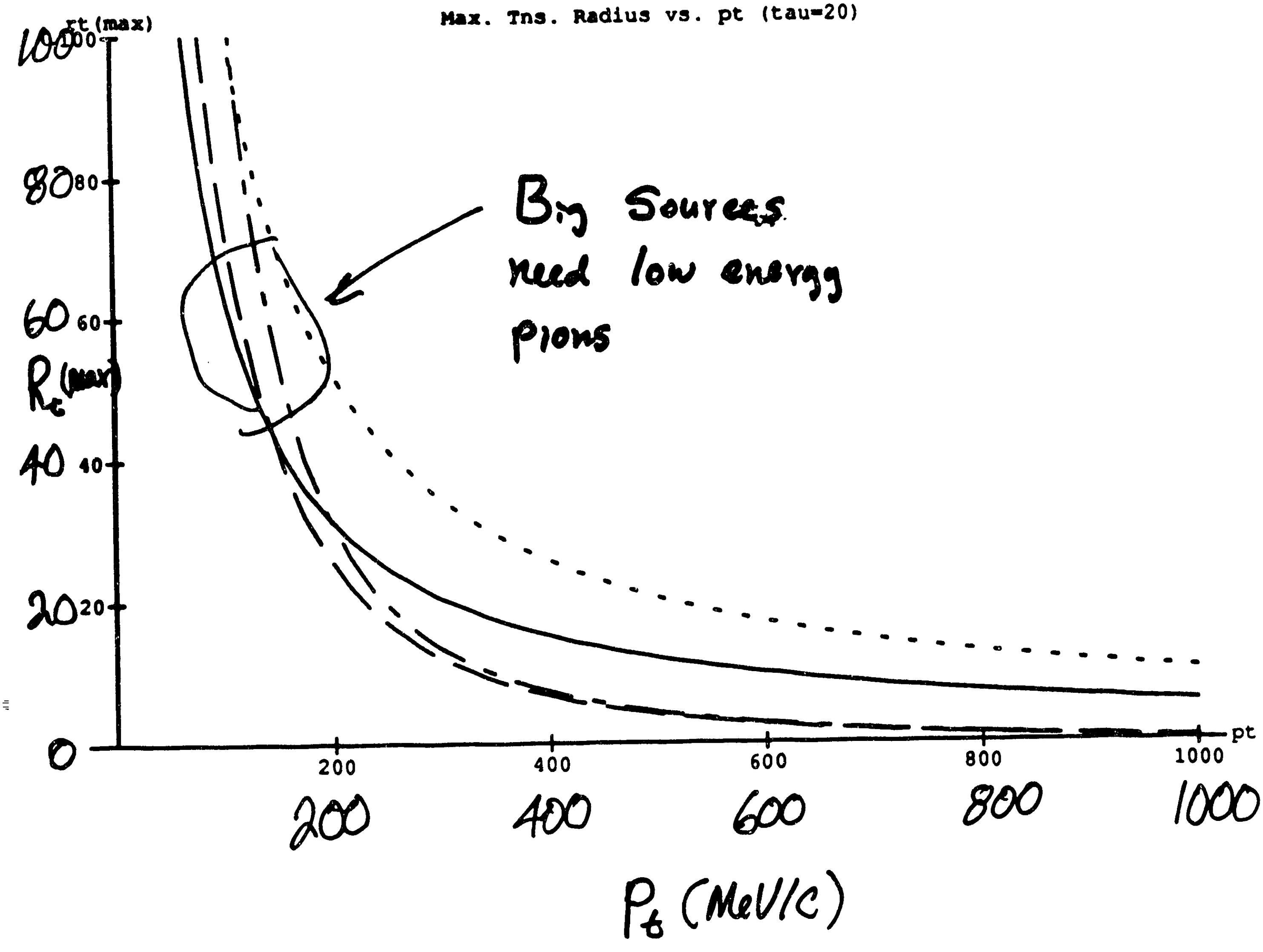

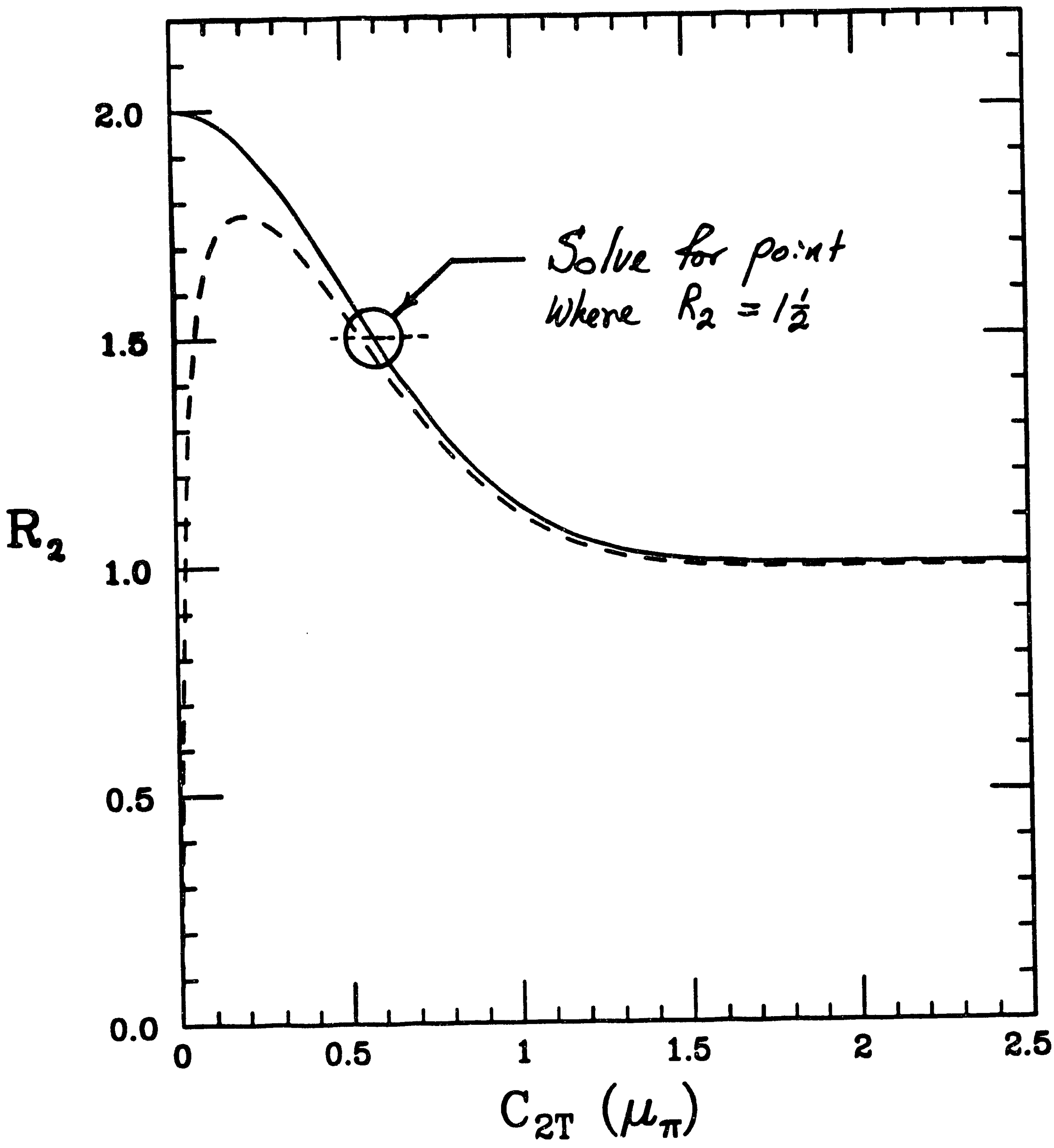

2.0
1.5
1.0
0.5
0.0
R_2
0
0.5
1
1.5
2
2.5
C_{2T} (μ_π)
Solve for point where $R_2 = 1\frac{1}{2}$

Maximum Measurable Radius

$$r_t(q_r, q_t, q_l; p_t) = \frac{\hbar}{\sqrt{q_r{}^2 + q_t{}^2}} \times$$

$$\sqrt{\frac{1}{2}\log\left(2\frac{|K_0(\sqrt{u_{12}+v_{12}})|^2}{K_0(\frac{m_1}{T})K_0(\frac{m_2}{T})}\right)}$$

Transverse masses:

$$m_1 = \sqrt{(p_t + q_r)^2 + \mu^2}$$

$$m_2 = \sqrt{(p_t - q_r)^2 + \mu^2}$$

Functions:

$$u_{12} = [\frac{1}{2T}(m_1 + m_2) + i\frac{\tau_0}{\hbar}(m_1 - m_2)]^2$$

$$v_{12} = 2[(\frac{1}{2T})^2 + (\frac{\tau_0}{\hbar})^2] m_1 m_2 \sinh^2[\frac{1}{2}(y_1 - y_2)]$$

K_0 = Irregular Modified Bessel Function.

Source Parameter Sensitivity

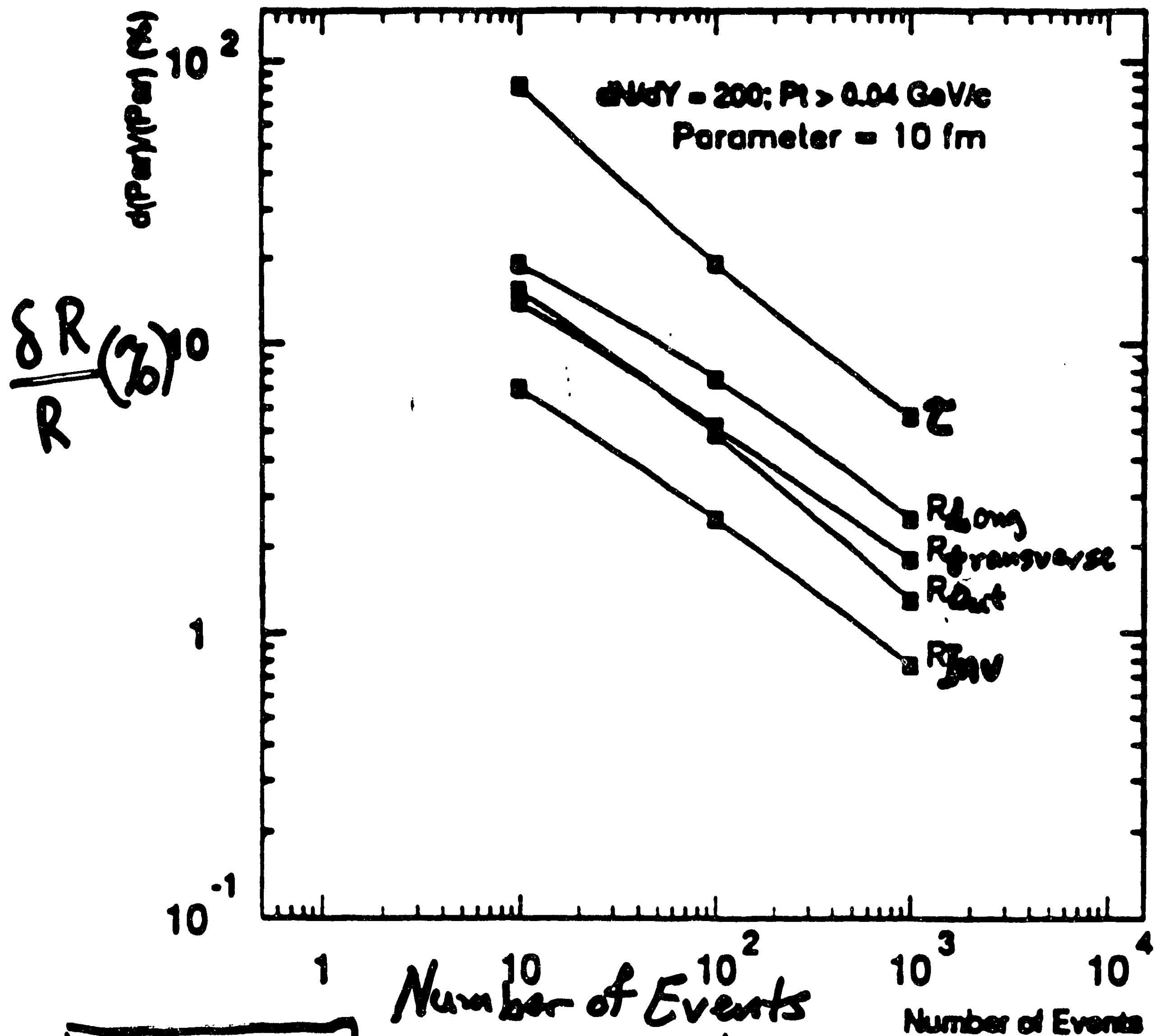

$\boxed{\frac{dN}{dy} = 200}$ $\boxed{p_t > 40 \text{ MeV/c}}$ $\boxed{R_{param} = 10 \text{ fm}}$

(need SVT)

R_{Inv}

Source Parameter Sensitivity

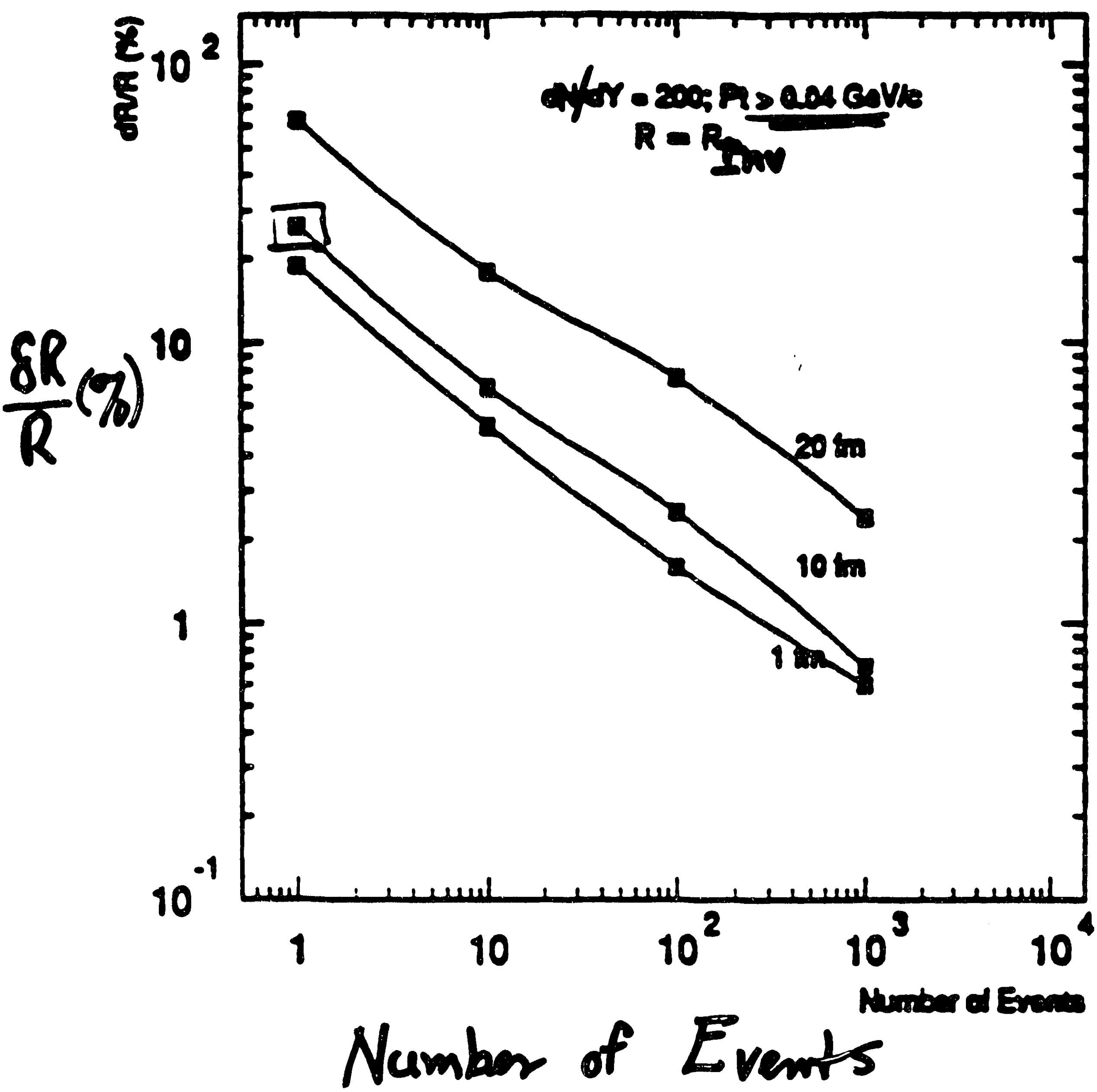

Single-Event Q_{inv} HBT

with $\boxed{R_{inv} = 20\,fm}$ $\boxed{\frac{dN}{dy} = 500}$

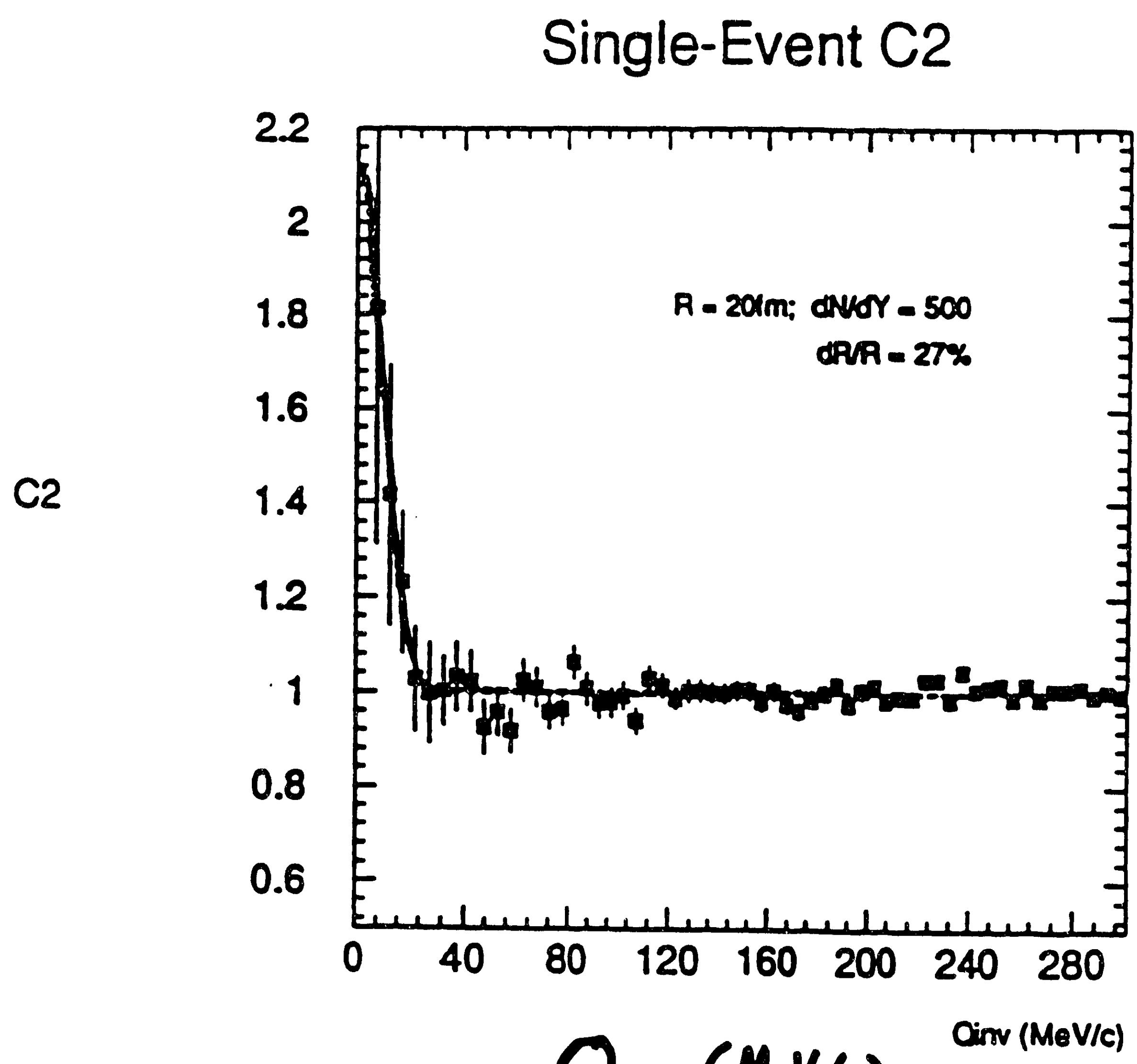

Q_{inv} (MeV/c)

HBT with K^0_S

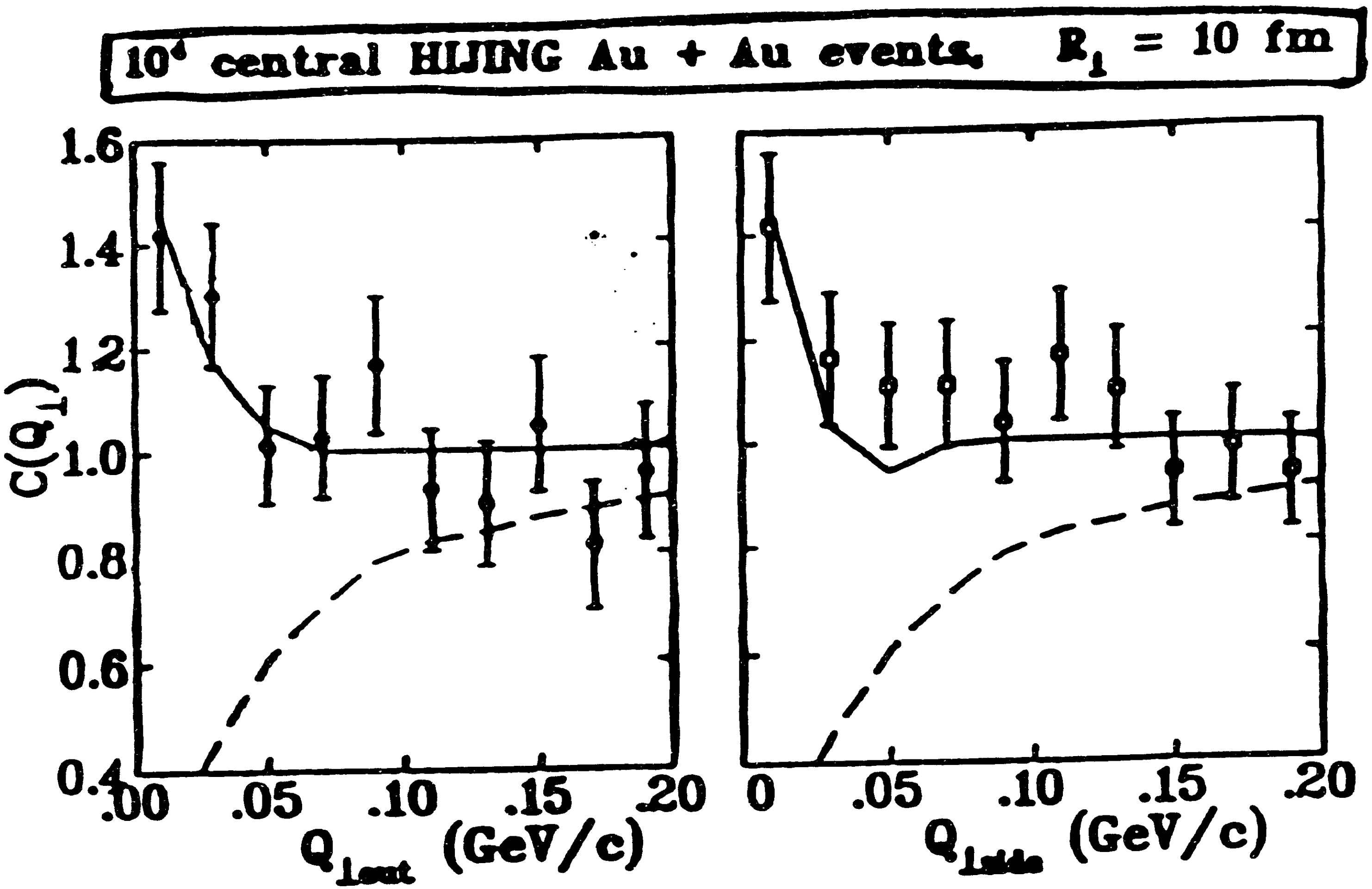

10^4 central HIJING Au + Au events. $R_\perp$ = 10 fm
$C(Q_\perp)$
1.6
1.4
1.2
1.0
0.8
0.6
0.4
.00
.05
.10
.15
.20
$Q_{\perp out}$ (GeV/c)
0
$Q_{\perp side}$ (GeV/c)

Multiplicity Effects:

2-Particle HBT in an n-Particle Envi

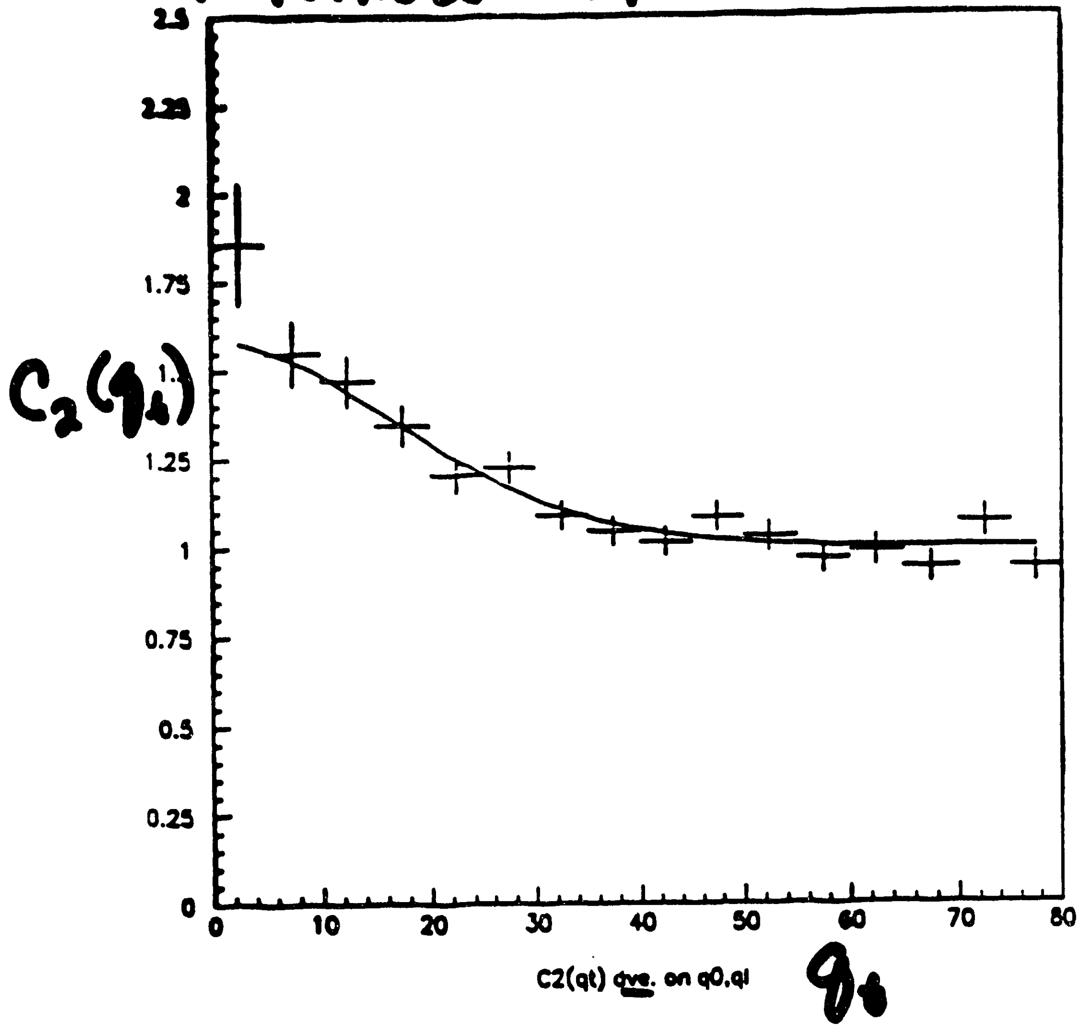

	Input	Extracted
λ	1.0	1.0 ± 0.12
r_T	10.0	9.9 ± 0.8
r_L	12.0	12.8 ± 1.4
τ	9.0	12.7 ± 2.4

$\chi^2/ndof = 2513/2441$

An Experimentalist's Wish List

- An event generator that includes Bose-Einstein correlations *to all orders*.
- A "T.C." multi-particle Coulomb correction for HBT correlations.
- A *tractable* formalism for analyzing multi-particle HBT correlation data.
- Better ways of including experimental error in all aspects of HBT data analysis.
- More consideration of high-multiplicity effects: (super-radiance, stimulated emission, coherence, coalesence, ...)
- More consideration of "information theory" aspects of HBT: (source imaging, extraction of higher moments, ...)

Stellar Imaging with Bose Einstein Interferometry

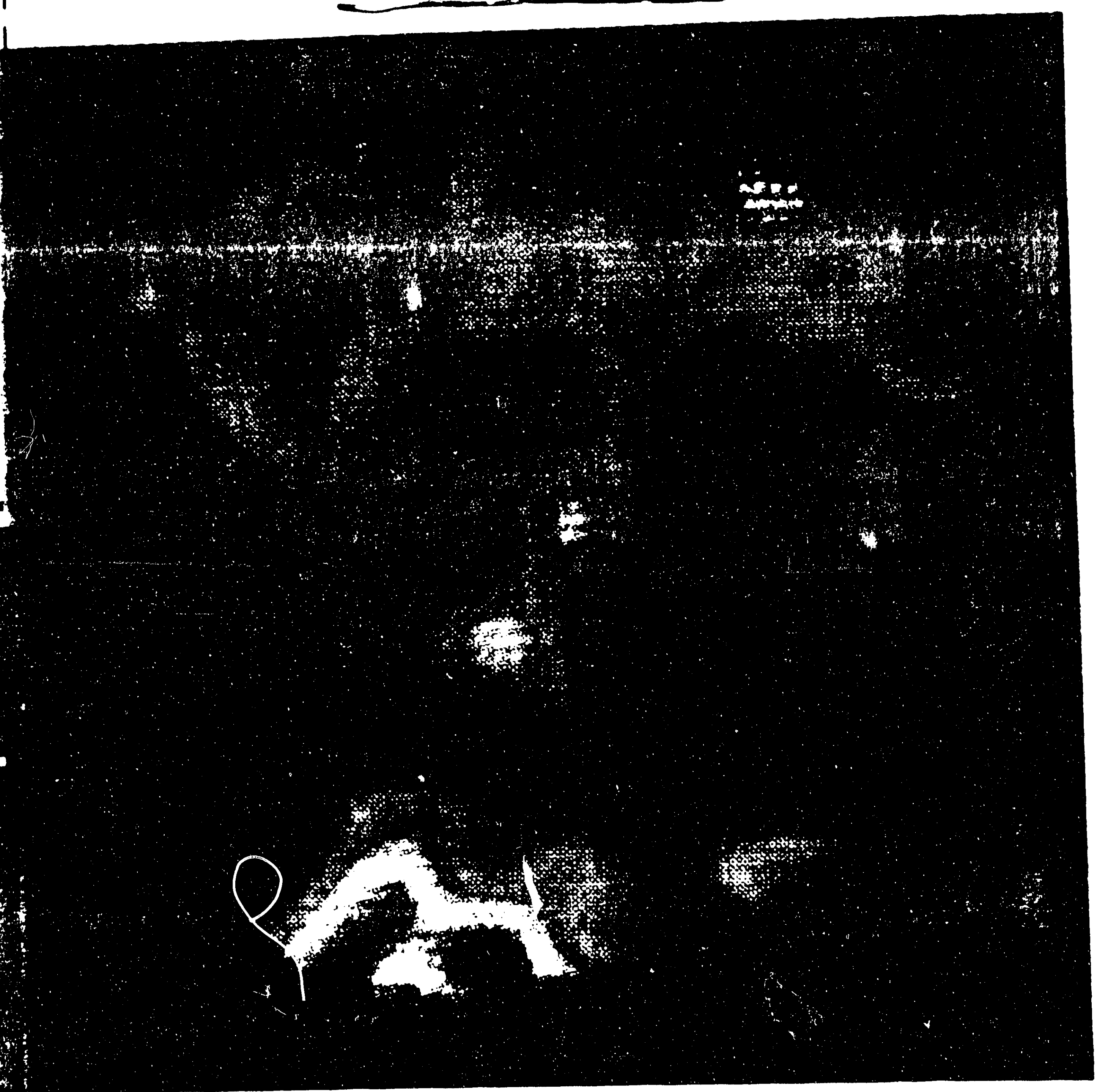

Temperature Profile of Surface of Betelgeuse Constructed with Speckle interferometry

Distance = 470 Light years

HBT Interferometry with PHENIX

Bill Zajc
Columbia

PHYSICS

WITH

PHENIX

W. A. ZAJC
Columbia University
BNL HBT Workshop
17-APR-93

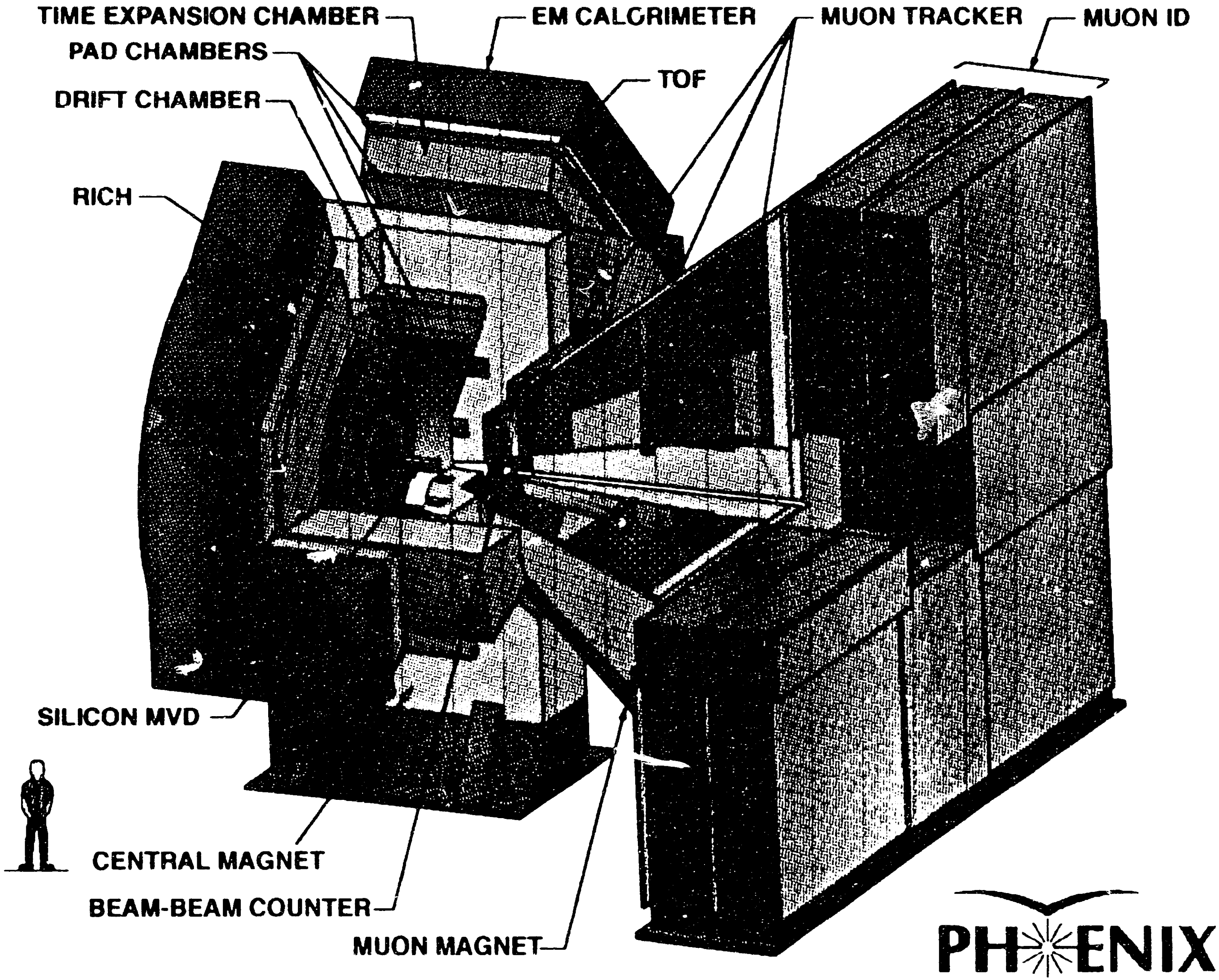
TIME EXPANSION CHAMBER
EM CALCRIMETER
MUON TRACKER
MUON ID
PAD CHAMBERS
TOF
DRIFT CHAMBER
RICH
SILICON MVD
CENTRAL MAGNET
BEAM-BEAM COUNTER
MUON MAGNET
PHENIX

Table 3.1: Physics Variables to be Measured by the PHENIX Experiment

Quantity to be Measured	Category*	Physics Objective
<u>e^+e^-, $\mu^+\mu^-$</u>		
• $\rho \to \mu^+\mu^- / \rho \to \pi\pi$, $d\sigma/dp_\perp$	BCD	Basic dynamics (T, τ, etc.,) for a hot gas,
$\omega \to e^+e^- / \omega \to \pi\pi$, $d\sigma/dp_\perp$		transverse flow, etc.
• ϕ-meson's width and $m_{\phi \to e^+e^-}$	QGP	Mass shift due to chiral transition (C.T.) [2]
$\phi \to e^+e^- / \phi \to K^+K^-$	QGP	Branching ratio change due to C.T. [3]
ϕ-meson yield (e^+e^-)	ES	Strangeness production ($gg \to s\bar{s}$)
• $J/\psi \to e^+e^-, \mu^+\mu^-$	QGP, QCD	Yield suppression and the distortion
$\psi' \to \mu^+\mu^-$		of p_T spectra due to Debye screening
$\Upsilon, \to \mu^+\mu^-$		in deconfinement transition (D.T.) [4]
• $1 < m_T(l^+l^-) < 3$ GeV	ES, QGP	Thermal radiation of hot gas, and
(rate and shape)		effects of QGP [5, 6, ?]
• $m_{l^+l^-} > 3$ GeV $\to \mu^+\mu^-$	QCD	A-dependence of Drell-Yan, and
	QGP	thermal $\mu^+\mu^-$ [5, 6, 7, 8]
• $\sigma \to \pi\pi, e^+e^-, \gamma\gamma$	QGP	Mass shift, narrow width due to C.T. [2]
<u>$e\mu$ coincidence</u>		
• $e\mu$, $e(p_T > 1$ GeV/c)	QCD, QGP	$c\bar{c}$ background, charm cross section [9]
<u>Photons</u>		
• $0.5 < p_T < 3$ GeV/c γ	ES, QGP	Thermal radiation of hot gas, and
(rate and shape)		effect of QGP [6, 7]
• $p_T > 3$ GeV/c γ	QCD	A-dependence of QCD γ
• π^0, η spectroscopy	BCD	Basic dynamics of hot gas, strangeness in η
• $N(\pi^0)/N(\pi^+ + \pi^-)$ fluctuations	QGP	Isospin correlations and fluctuations [10, 11]
• High p_T π^0, η from jet	QGP	Reduced dE/dx of quarks in QGP [12]
<u>Charged Hadrons</u>		
• p_T spectra for $\pi^\pm$, $K^\pm$, p, $\bar{p}$	BCD	Basic dynamics, flow, T, baryon density,
		stopping power, etc.
	QGP	Possible second rise of $< p_T >$ [13]
• $\phi \to K^+K^-$	ES, QGP	Branching ratio, mass width [3, 14]
• K/π ratios	ES	Strangeness production
• $\pi\pi$ + KK HBT	BCD	Evolution of the collision, $R_\perp$
	QGP	Long hadronization time ($R_{out} \gg R_{side}$) [15]
• Antinuclei	QGP	High baryon susceptibility due to C.T.? [16]
• high p_T hadrons from jet	QGP	Reduced dE/dx of quarks in QGP [12]
<u>Global</u>		
• N_{tot} (total multiplicity)	BCD	Centrality of the collision
• $dN/d\eta, d^2N/d\eta d\phi, dE_T/d\eta$	BCD	Local energy density, entropy
	QGP	Fluctuations, droplet sizes [17]

* BCD = Basic collisions dynamics. ES = Thermodynamics at early stages.
QGP = Effect of QGP phase transition. QCD = Study of basic QCD processes.

HOW TO SIMULATE

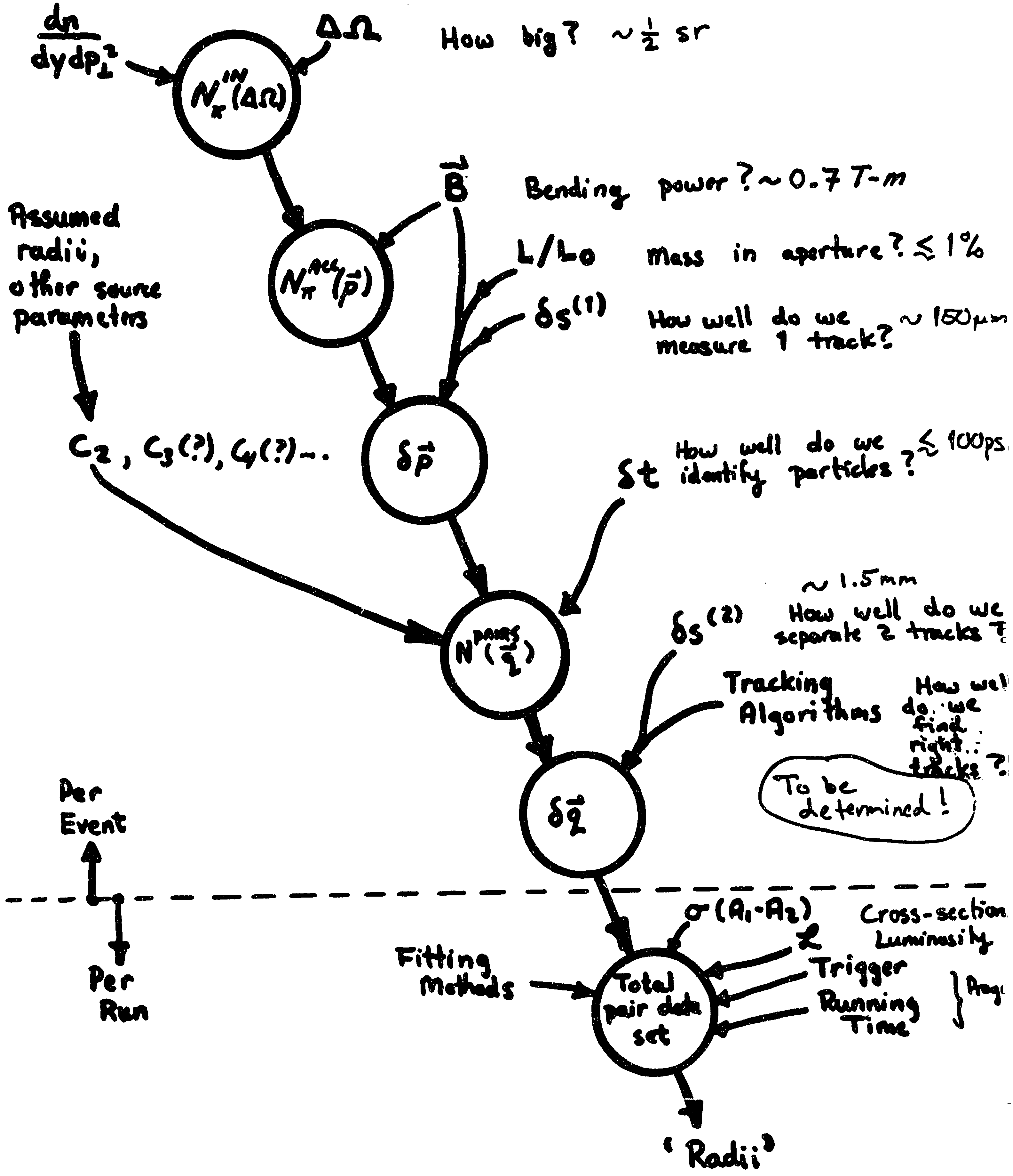

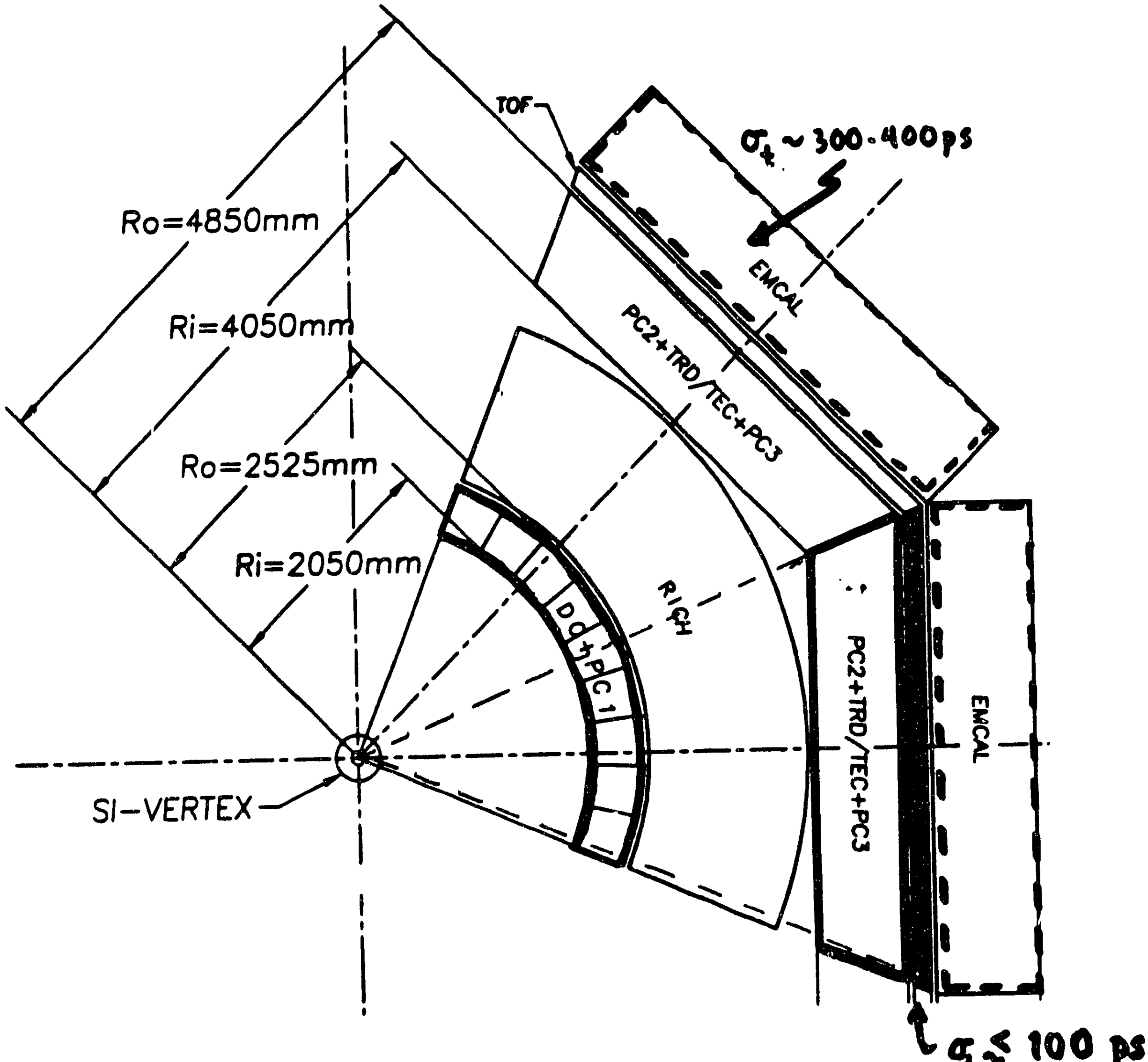

Figure 6.1: Schematic of PHENIX detector including the tracking subystem.

⇒ π-K separati
to ~ 2 GeV

loss (dE/dx) information.

The momentum measurement is accomplished by placing the low mass drift chambers as close to the vertex as track densities allow. Location at small radii allows an easier measurement of the bend angle from the axial field magnet and better identification of tracks not originating from the vertex. The TEC is located behind the RICH so that photon conversions generated by its material (about 0.8% X_o) do not degrade the performance of the Cherenkov counter. Pad detector locations are determined by their need to be positioned close to both the detectors providing track vectors (DC and TEC) and those with which they interact on the trigger level (RICH and EMCal).

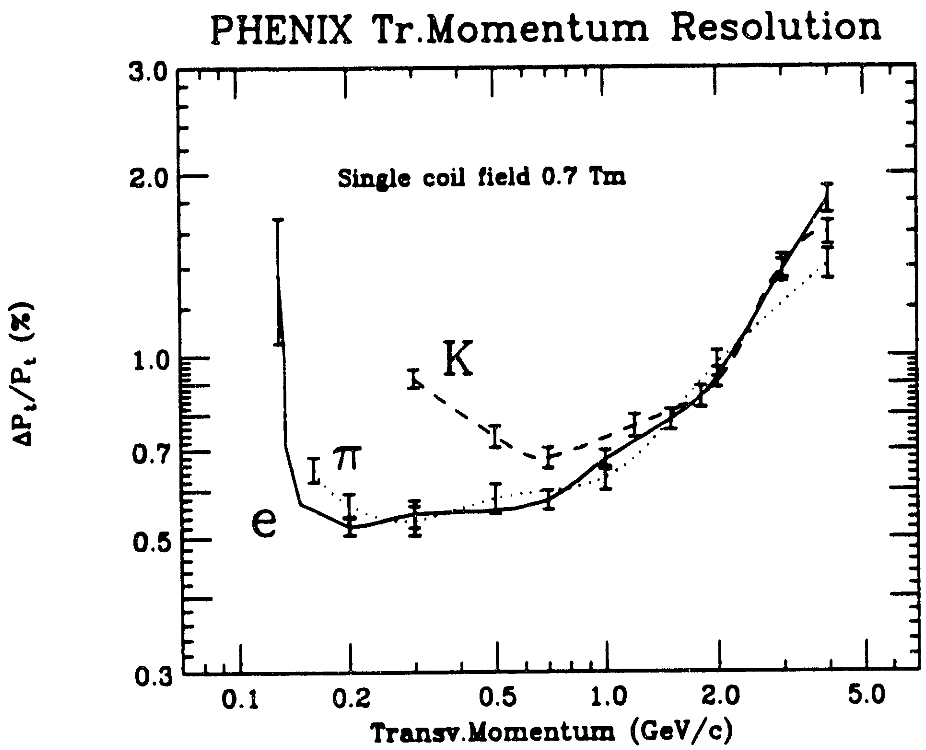

Figure 6.34: Transverse momentum resolution of PHENIX tracking detector.

the p_T of the track. The calculation uses only the information provided by DC1, DC2, and PC1. The resolution is dominated at low p_T by multiple scattering and at high p_T by the intrinsic position resolution of the detectors. The moment arm of the momentum measurement affects the resolution to a lesser degree. The dependence of multiple scattering on the momentum and velocity $1/p\beta$, accounts for the poorer resolution for the kaon as compared to the electron. At high p_T, both kaon and electron momenta, are measured equally well.

To calculate the particle momenta, a thorough investigation was conducted of the trajectories of charged particles in the focussing field of the Phenix spectrometer. This information was used to generate a table in which α, ζ, z_1, and ϕ were determined as functions of p_T, z_v, $\theta(p_z/p_T)$, and ϕ_0. The parameter α is the angle of incidence of a track relative to the local normal of DC1. The z position of a track at PC1 is z_1. The DC1 hit location in cylindrical coordinates in the plane normal to the beam direction is ϕ. The parameter ζ is the angle the track makes to the normal of PC1 in a plane containing the beam, and the intersection of the track with PC1. The vertex position is z_v, and ϕ_0 is the initial direction of travel of a particle trajectory in a plane perpendicular to the beam direction. The first four variables are those measured by the detectors. The tables were inverted to obtain related tables that could be used to calculate the three momenta of the tracks from the information measured

HBT MEASUREMENTS

1. SIMPLE FREEZEOUT ARGUMENTS (+ DATA?) IMPLY

$$R_\perp \text{ (in fm)} \approx \sqrt{\frac{dn_{ch}}{dy}}$$

$\Rightarrow$ 20–30 fm at RHIC (!)

2. REQUIREMENT FROM LARGE $R_\perp$ $\Rightarrow$ NEED SMALL Δ

Resolution $= \frac{\delta p}{p} \sim \frac{\text{constant}}{\beta}$ (at fixed $\int B\,dl$)

$\Rightarrow$ small p gives small δp (until β kicks in

NUMERICALLY: $\delta p = E \cdot \frac{16 \text{ MeV/c}}{P_\perp^K} \sqrt{\frac{L}{L_o}}$,

$$\delta p = |\vec{p}| \cdot \underline{\Delta\theta} \nearrow \frac{1\text{cm}}{200\text{ cm}}$$

$$P_\perp^K \equiv \frac{e}{c} \int B \cdot dl$$

3. ASSUME WE NEED 4 GOOD POINTS IN ENHANCEMENT REGION:

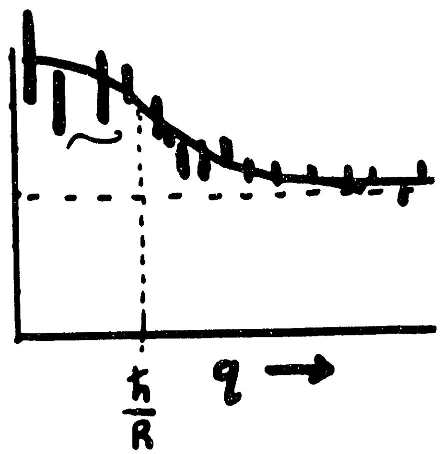

$\delta q = \delta|\vec{p}_1 - \vec{p}_2| \sim \sqrt{2}\,\delta p$

$\Rightarrow \delta p \lesssim \frac{1}{4\sqrt{2}} \frac{\hbar}{R_{max}}$

or R_{max} (in fm) $\lesssim 2 \frac{P_\perp^K}{E} \sqrt{\frac{L_o}{L}}$ — 210 MeV/c

$\Rightarrow$

R_{max}	π	K
(LOW FIELD)	~25 fm	~6 fm
(HIGH FIELD)	" "	~10 fm

ASSUMING $\frac{L}{L_o} = 1\%$

RESONANCES VS. P_T

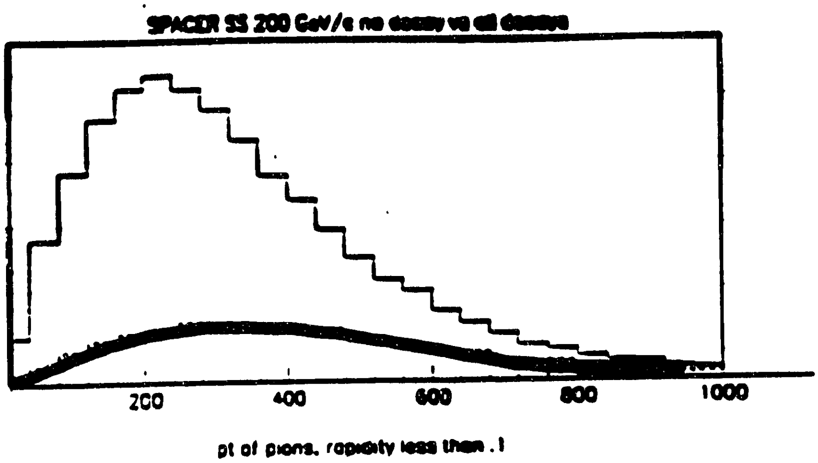

- Central region for 200 A·GeV/c S+S
- SPACER
  (⇒ FRITIOF abundences)
- Courtesy of B. Lorstad

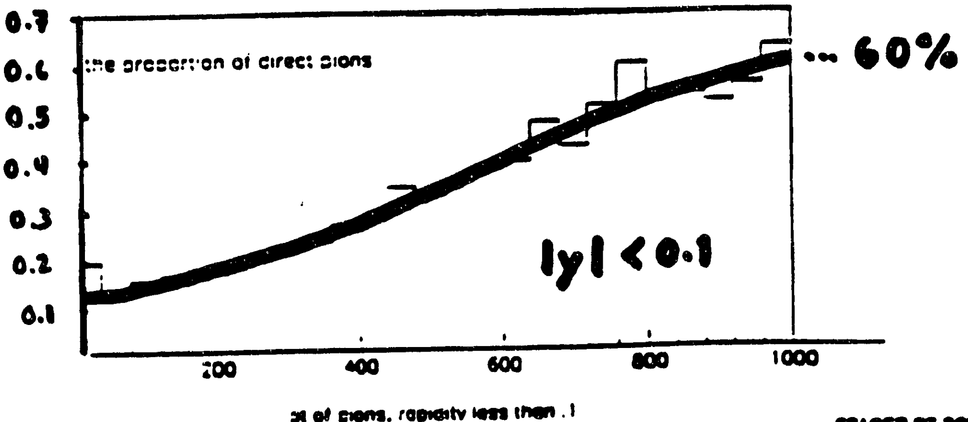

$p_\perp \longrightarrow$

- Qualitative result should persist (increase?) at RHIC
- ⇒ Need good PID out to high P_T
- ⇒ Rates of 'useful' pairs may be much lower than naive estimates

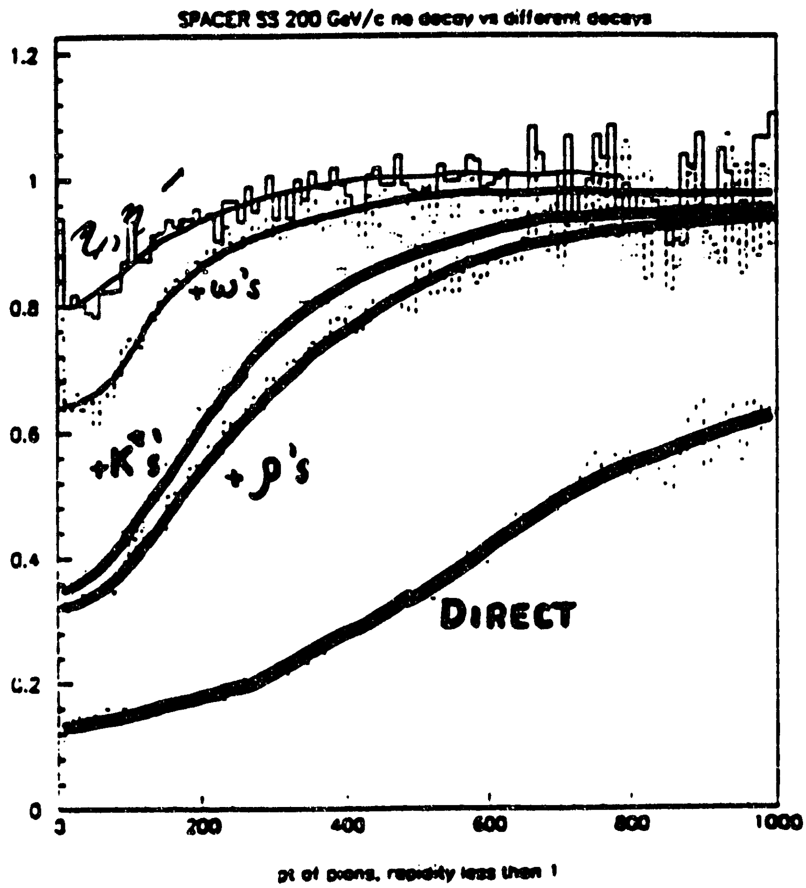

PAIR RATES IN PHENIX HIGH-RES SECTOR

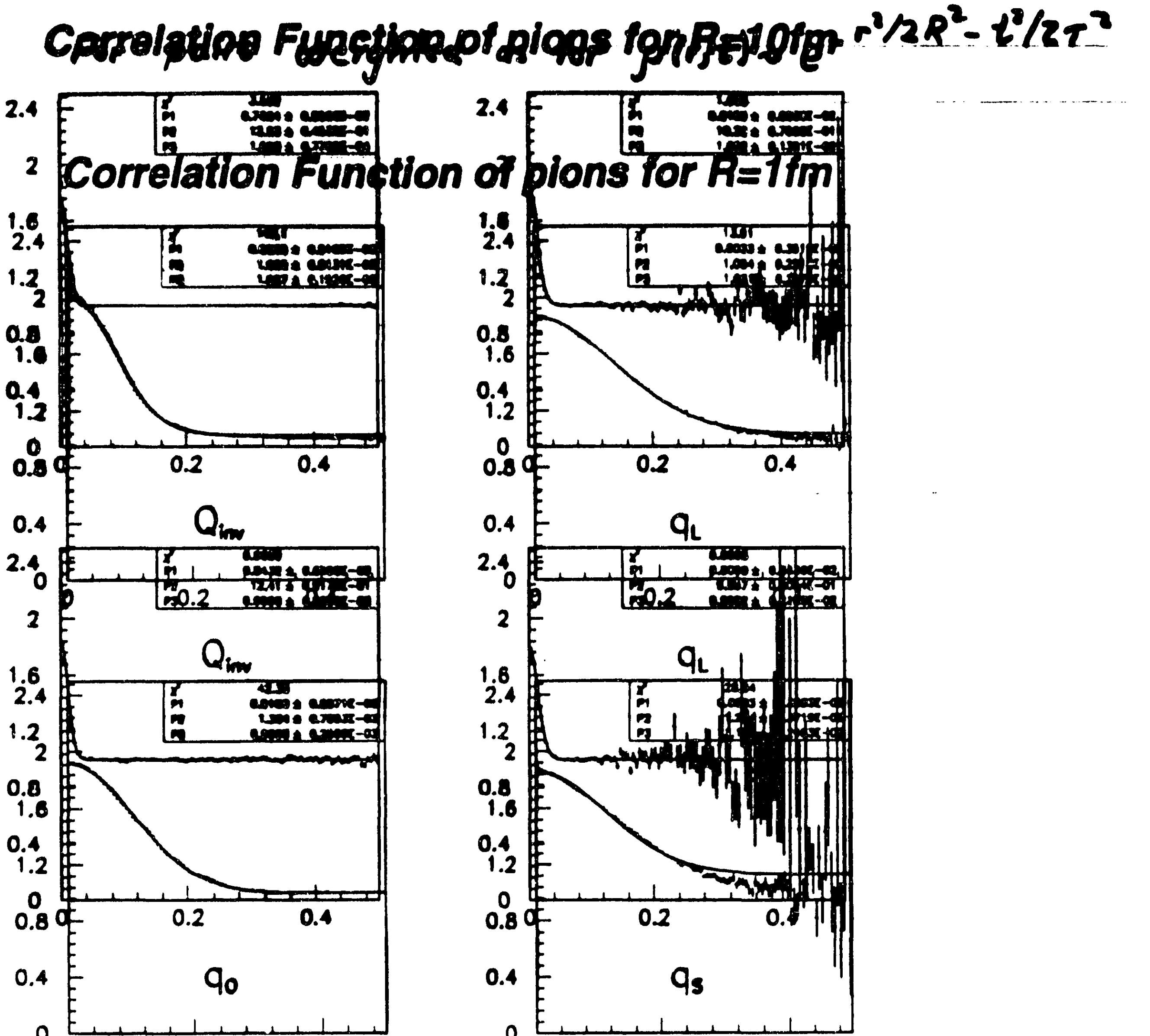

Figure 0.2: The correlation function of pions for a $R = \tau = 10$ fm source as seen in an aperture of $|\eta| < 0.7$, $\Delta\Phi = 30°$ for 1 million Au + Au events.

Figure 0.1: The correlation function of pions for a $R = \tau = 1$ fm source as seen in an aperture of $|\eta| < 0.7$, $\Delta\Phi = 30°$ for 1 million Au + Au events.

ESTIMATE OF SYSTEMATIC ERROR

'Things are difficult to predict, especially the future'

- *Calibrate using E859 Proposal vs. Reality*

  - K^+K^+ measurement:

    Proposed : 30K pairs in 400 hours

    Actual : 30K pairs in ~200 hours

  - Trigger Commisioning:

    Proposed : 250 hours Si + 400 hours secondari

    Actual : ~300 hours Si

- *Warning:*

  1. *This was <u>small</u> extrapolation, starting from known rates in known detector*

  2. *Very little dependence on theory*

PHENIX DAQ CAPABILITIES

- Assumes full (not Day 1) machine $\mathcal{L}$ ←
- Assumes recording at 20 Mb/s

Combination	Accepted Events (per sec)	2pi pairs (per day)	2K pairs (per day)	Vector res. (per day)
p-p(MB)	7177	276390	30	413
O-O(MB)	3867	3822898	413	1127
Si-Si(MB)	2597	8794569	950	1401
Cu-Cu(MB)	1280	25810850	2787	1685
I-I(MB)	641	60380222	6519	1823
Au-Au(MB)	406	100578350	10859	1873
p-p(Cn)	2479	9548222	1031	1426
O-O(Cn)	1371	23537099	2541	1665
Si-Si(Cn)	796	46806000	5053	1789
Cu-Cu(Cn)	344	120433972	13003	1887
I-I(Cn)	162	265818035	28699	1926
Au-Au(Cn)	101	433805798	46836	1939
p-O	6699	462640	50	516
p-Si	6480	569789	62	563
p-Cu	6116	783988	85	642
p-I	5756	1046486	113	719
p-Au	5511	1259515	136	772
Si-Cu(MB)	1161	29339385	3168	1711
Si-I(MB)	1003	35320618	3813	1745
Si-Au(MB)	925	39048793	4216	1761

HBT (GGLP) DOESN'T MEASURE SHAPE

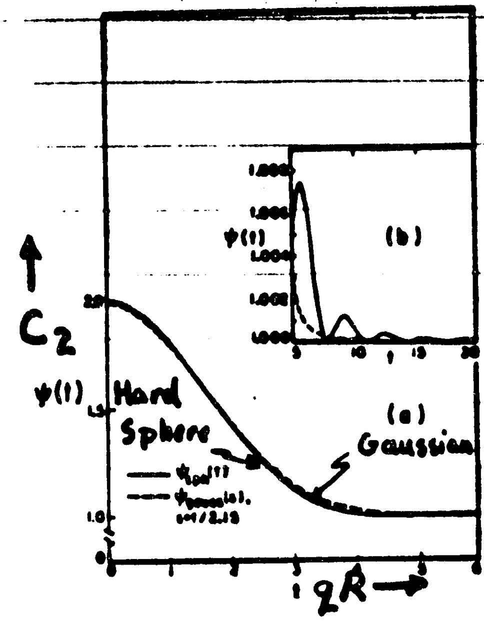

Explicitly noted in very first application of HBT to particle physics:

GGLP, Phys. Rev. 120, 300, (1960)

volume Ω but also on its shape. It is premature to discuss this shape dependence in any detail, but one point is of some computational interest, namely that ψ(12) for a spherical model, given by Eq. (11), differs very little from ψ(12) for a Gaussian-shaped volume:

$$\psi(12)=\int\int|\phi^s(1,2)|^2\exp[-(r_1^2+r_2^2)/2\lambda]dr_1dr_2$$

$$=1+\exp(-s^2),\quad s=|p_1-p_2|\lambda^{\frac{1}{2}},\quad \text{(Gaussian)},\qquad (12)$$

where we integrate twice over all space. This well-known property of the Fourier transform of a sphere relative to that of a Gaussian is shown in Fig. 1 where the two curves refer to a ratio of ρ to $\lambda^{\frac{1}{2}}$ given by

$$\rho=2.15\lambda^{\frac{1}{2}}.\qquad (13)$$

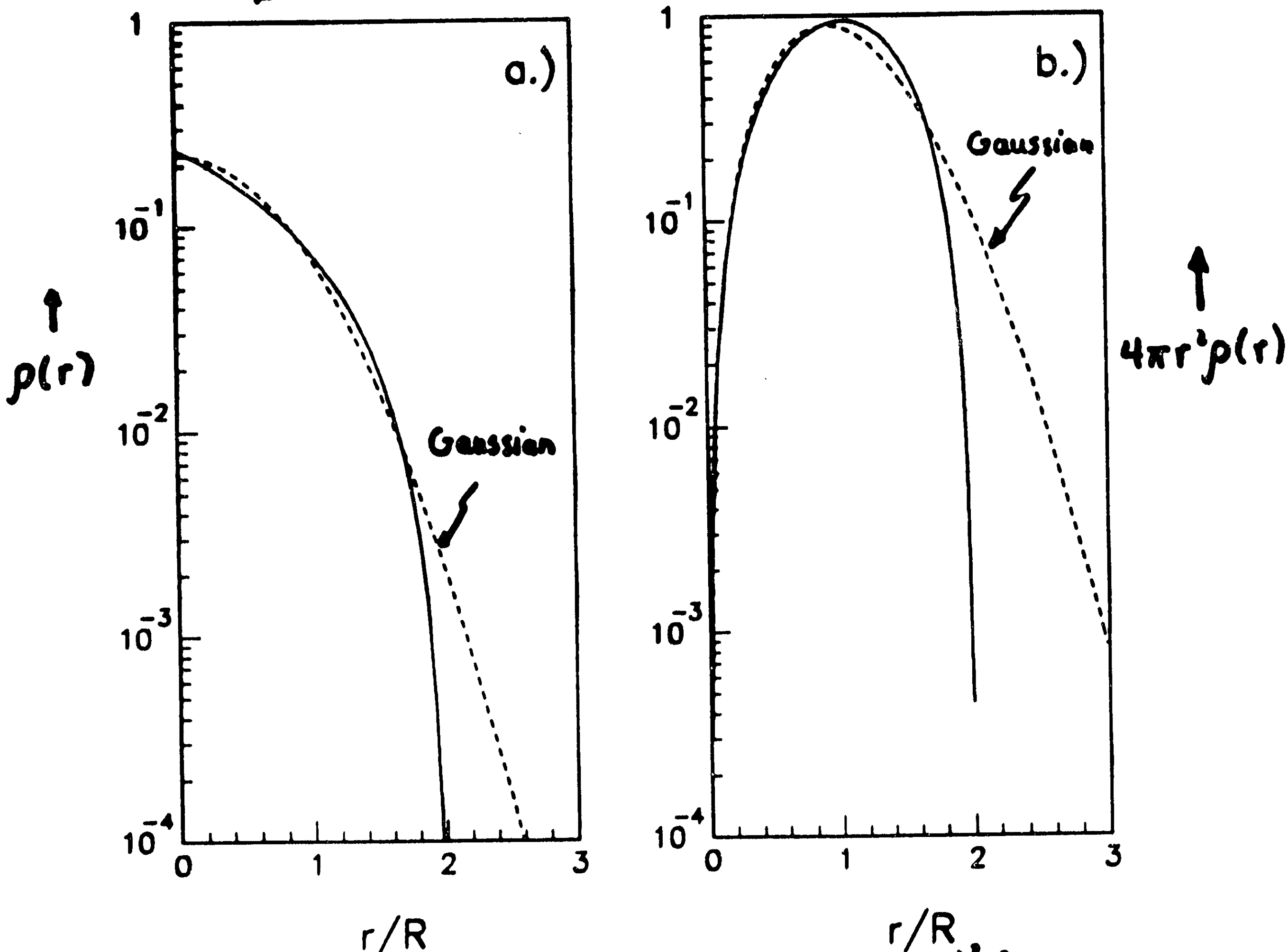

Uniform sphere: $\rho(r)=\left\{1-\frac{3}{2}\left(\frac{r}{2R}\right)+\frac{1}{2}\left(\frac{r}{2R}\right)^2\right\}$, $r\equiv|\vec{r}_1-\vec{r}_2|$

$(r<2R)$

BUT SHAPES ARE INTERESTING

ARC Events for b=0 (pions)

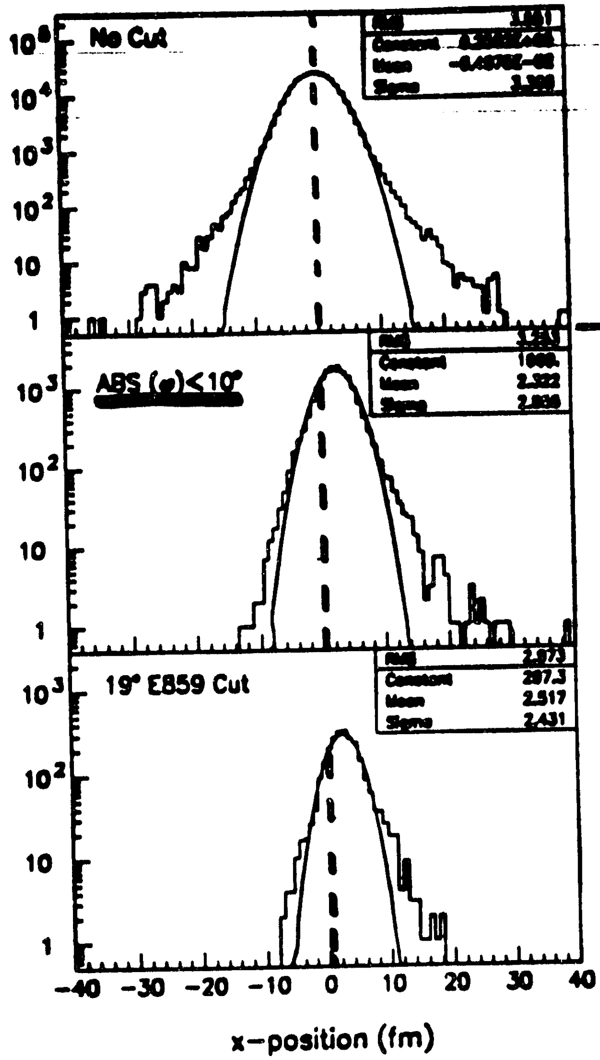

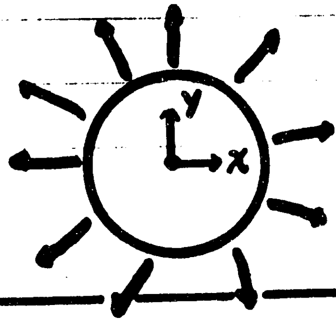

$\langle x \rangle = 0.0$

$\langle x^2 \rangle - \langle x \rangle^2 = 3.4$ fm

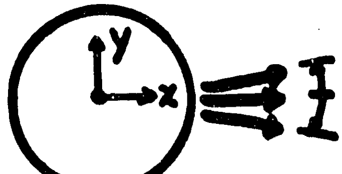

$|\varphi| < 10°$ ⇒ See only one 'side' of source

⇒ $\langle x \rangle = 2.3$ fm

$\langle x^2 \rangle - \langle x \rangle^2 = 2.8$ fm

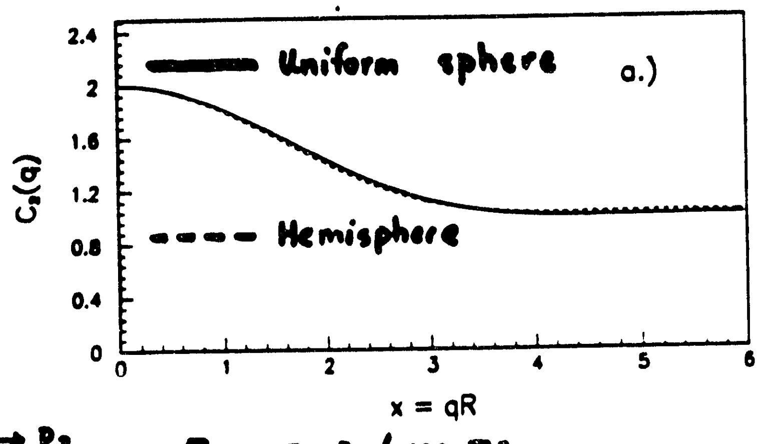

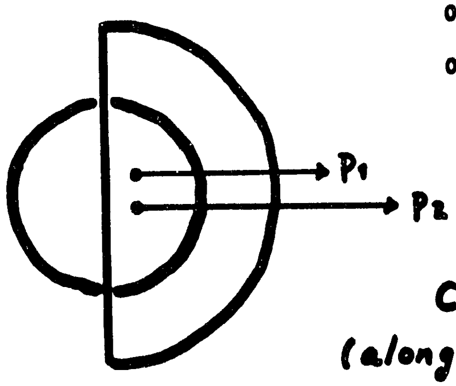

EXTREME LIMIT:

$C_2(qR)$ virtually identical (along symmetry axis) for

uniform sphere of radius R_0

vs. uniform hemisphere of radius $R_D = 1.9 R_0$

TWO VS. THREE PARTICLE INTERFEROMETR

$$C_2(q^{12}) = 1 + |\rho(q^{12})|^2$$

$$C_3(q^{12}, q^{23}, q^{31}) = 1 + |\rho(q^{12})|^2 + |\rho(q^{23})|^2 + |\rho(q^{31})|^2 + 2\cdot \mathrm{Re}\{\rho(q^{12})\rho(q^{23})\rho(q^{31})\}$$

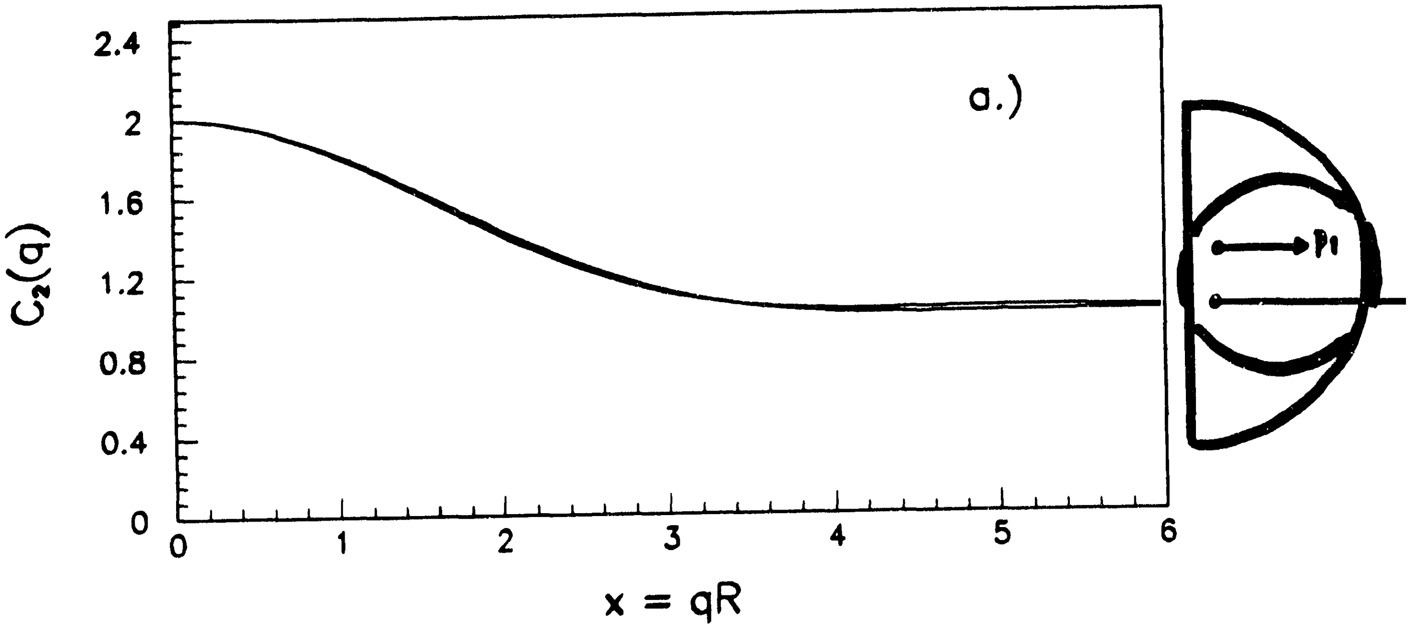

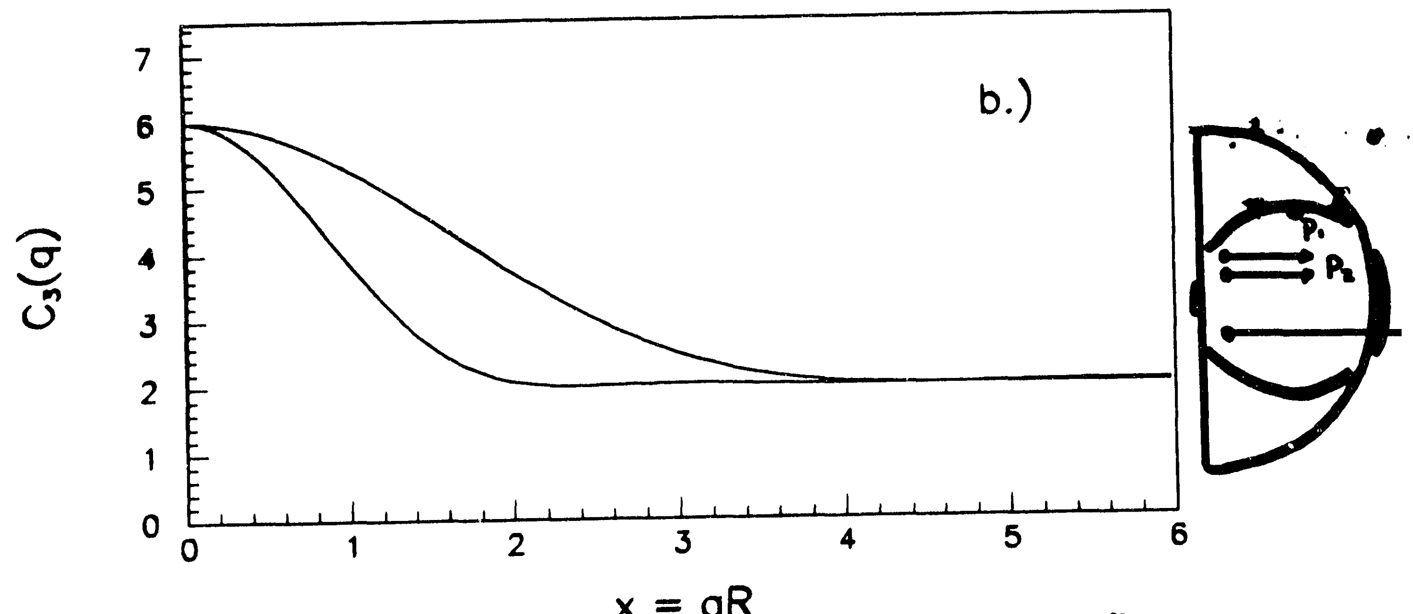

$$\rho(\vec{r}) \neq \rho(-\vec{r}) \quad \Rightarrow \quad \rho(q) \neq \rho^*(q)$$

E.g., hemisphere $\Rightarrow \rho = \frac{3}{x^3}\left\{[\sin x - x\cos x] + i\left[1 + \frac{x^2}{2} - \cos x - x\sin x\right]\right\}$
$(x = qR)$

3-PION RATES IN PHENIX

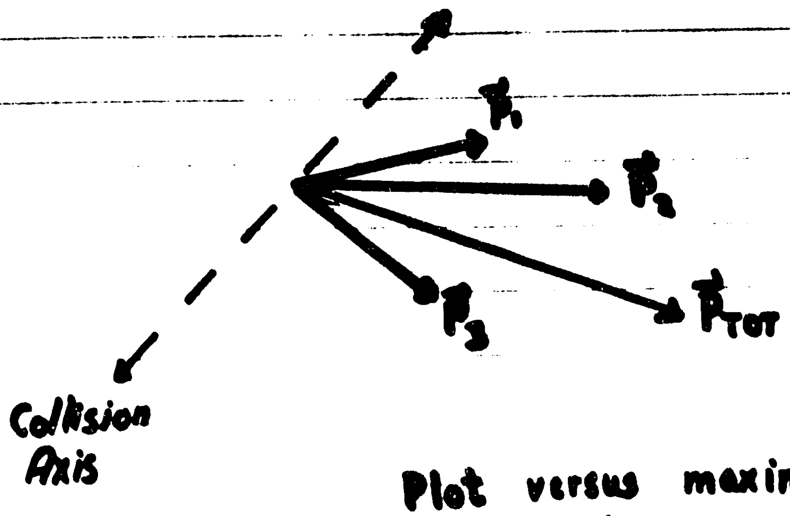

Require:

All q_L's $< \hbar / R_L$

All q_S's $< \hbar / R_S$

One $q_{OUT}^{ij} < \hbar / R_O$

Plot versus maximum remaining $q_{OUT}^{jk} \equiv q_{OUT}^{(3)}$:

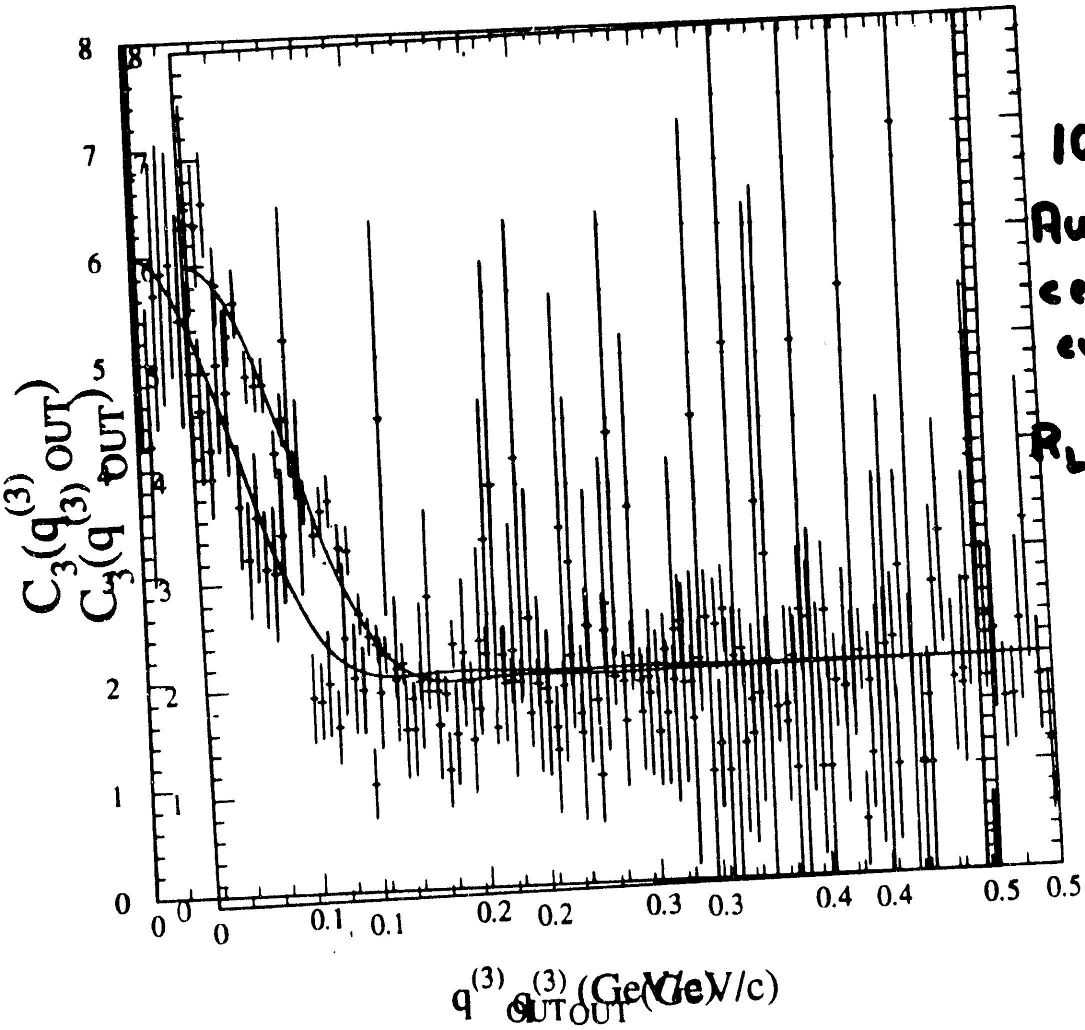

10^4 Au-Au central events

$R_L = R_S = R_O = 6$ fm

HOW DO TRIPLETS SCALE WITH A ?

$$n^{(3)} = \frac{n(n-1)(n-2)}{3!} \sim n^3 \sim (A^{1.1})^3 \sim A^{3.3} \Big\}$$ Gain w.↑ f

Cut on $q_L^{12}, q_L^{23}, q_L^{31} \lesssim \frac{1}{R} \sim \left(\frac{1}{A^{1/3}}\right)^3 \sim A^{-1}$

Cut on $q_S^{12}, q_S^{23}, q_S^{31} \lesssim \frac{1}{R} \sim \left(\frac{1}{A^{1/3}}\right)^3 \sim A^{-1}$

Require one of $q_{OUT}^{ij} \lesssim \frac{1}{R} \sim \frac{1}{A^{1/3}} \sim A^{-1/3}$

Lose w.↑

$\Rightarrow$ per event lose (gain) as $\dfrac{A^{3.3}}{A \cdot A \cdot A^{1/3}} \sim A$

But: Relevant factor is

$$\left\{\begin{matrix}\text{Yield per} \\ \text{event}\end{matrix}\right\} \times \left\{\begin{matrix}\text{Events to tape} \\ \text{per second}\end{matrix}\right\}$$

$$\approx \quad A \quad \times \quad \frac{1}{A}$$ $\sim$ species independent !
(excluding p-p)

Rates at RHIC

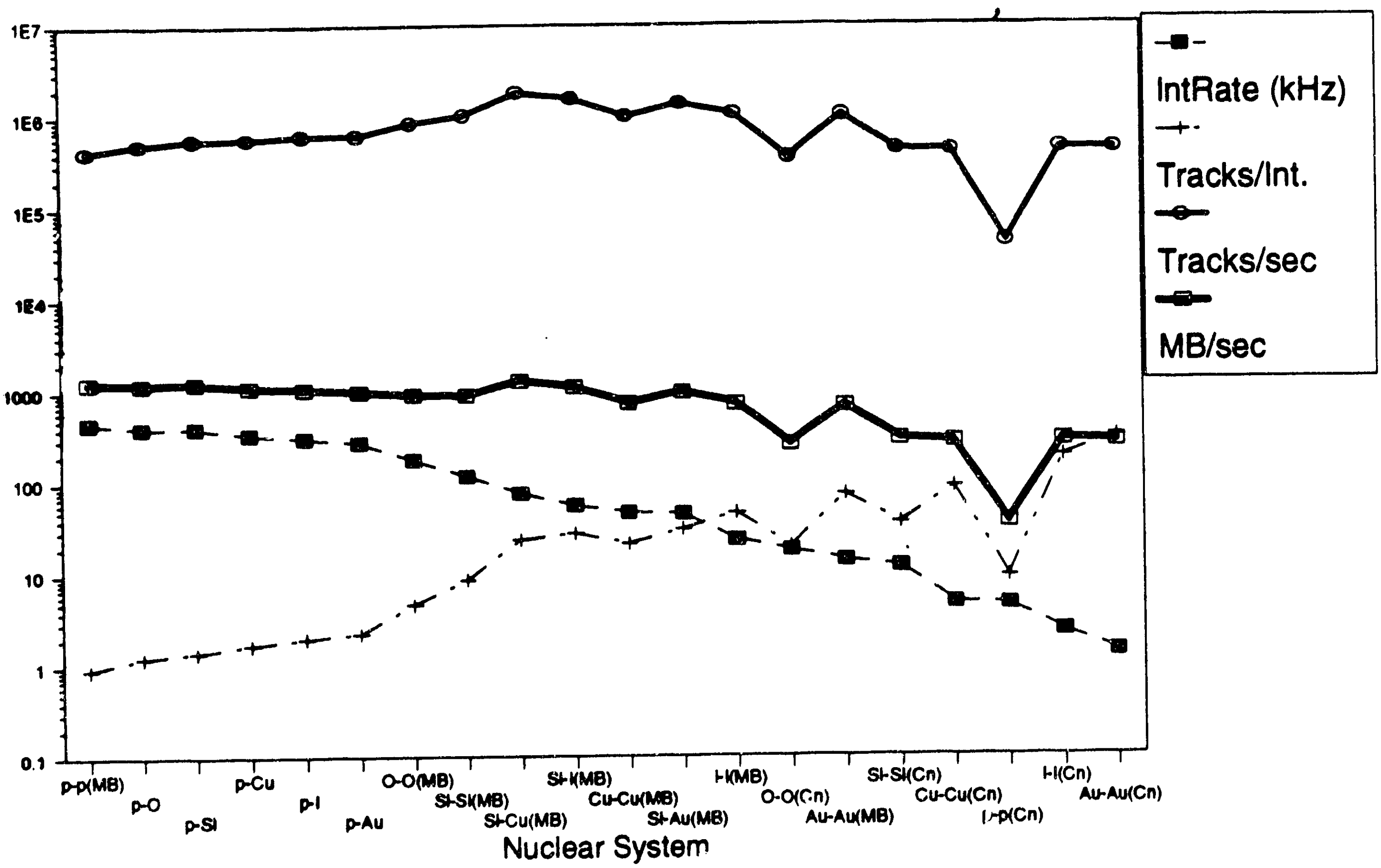

SUGGESTED PROGRAM

I. EXPERIMENTAL

A. STATISTICS, STATISTICS, STATISTICS ...

$\Rightarrow$ DEDICATED EXPERIMENTS
(E.g., NA44, E859)

B. DIFFERENT PROBES

1. BOSONS
   $2\pi^-$ vs. $2\pi^+$, $\pi^-\pi^+$ calibration, $2\pi^0$
   $2K$
   2γ (?)

2. FERMIONS
   pp, nn, $\Lambda\Lambda$, pn ... $p\bar{n}$ ...

C. STUDY RESONANCES IN PP

A-dependent production?
Coherence in PP

D. STUDY ASYMMETRIC SYSTEMS IN p-A

E. LEARN HOW TO DO $n_\pi > 2$

(But don't forget multiplicity distributions!)

II. THEORETICAL

A. MODEL, MODEL, MODEL

$\Rightarrow$ STATISTICS, STATISTICS, STATISTICS

B. UNDERSTAND HIGH n_π LIMIT

(Both statistical + dynamical correlations)

C. STUDY FINAL STATE INTERACTIONS

(+ resonances)

HBT Calculations from ARC

Yang Pang
BNL

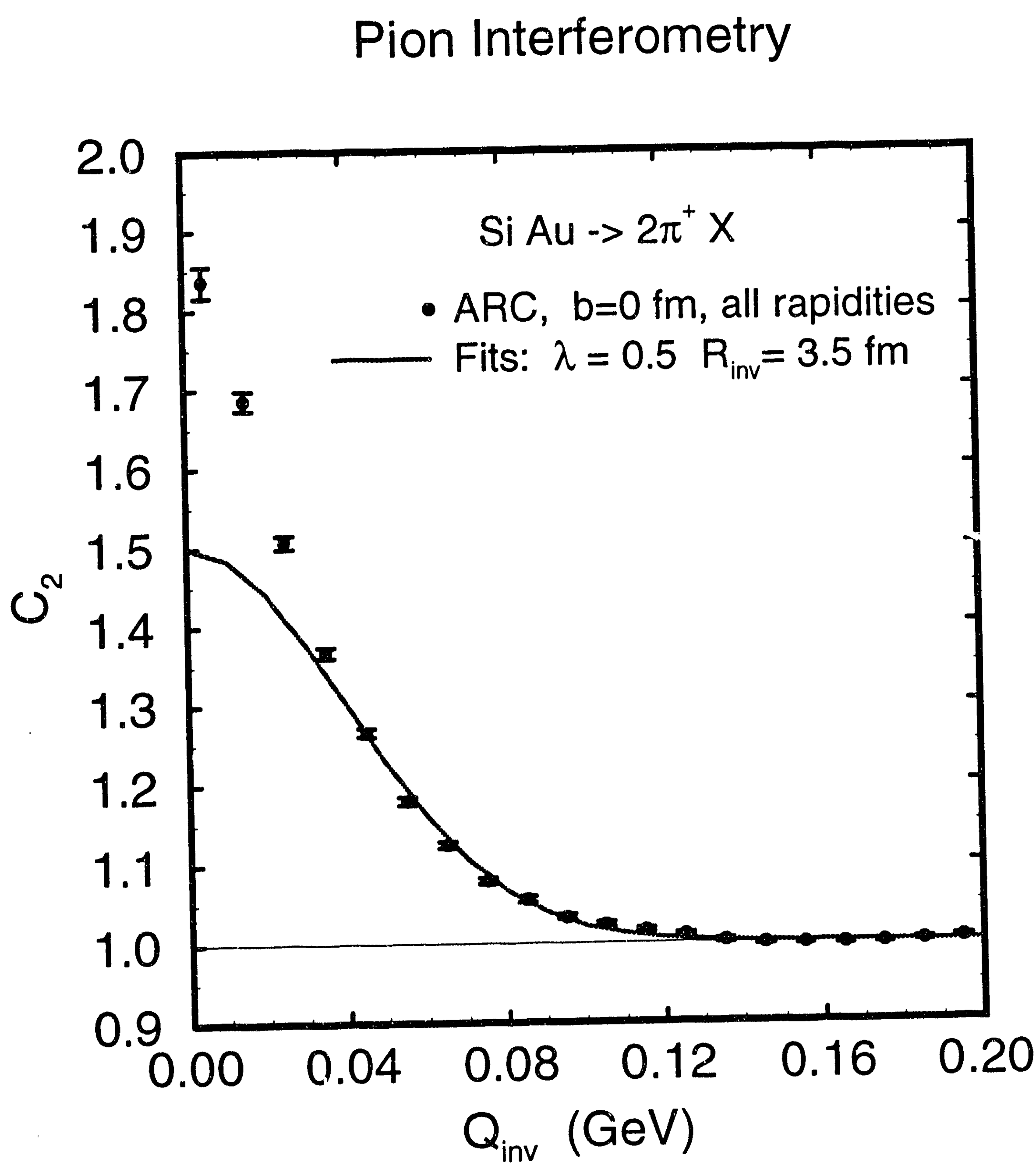
Pion Interferometry
Si Au -> 2π⁺ X
ARC, b=0 fm, all rapidities
Fits: λ = 0.5 R_inv = 3.5 fm
C_2
Q_inv (GeV)
2.0
1.9
1.8
1.7
1.6
1.5
1.4
1.3
1.2
1.1
1.0
0.9
0.00
0.04
0.08
0.12
0.16
0.20

Pion Interferometry

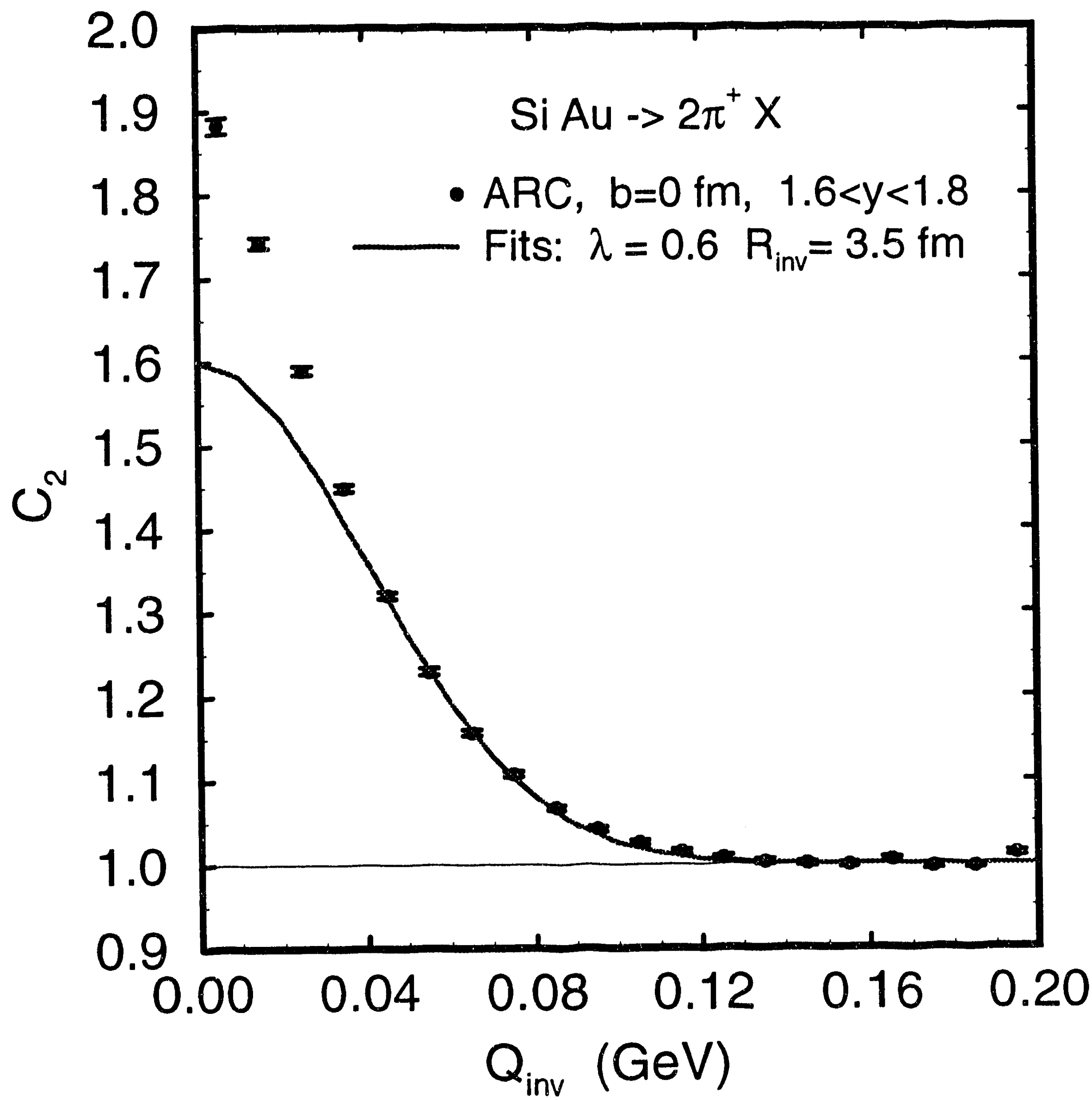

Pion Interferometry

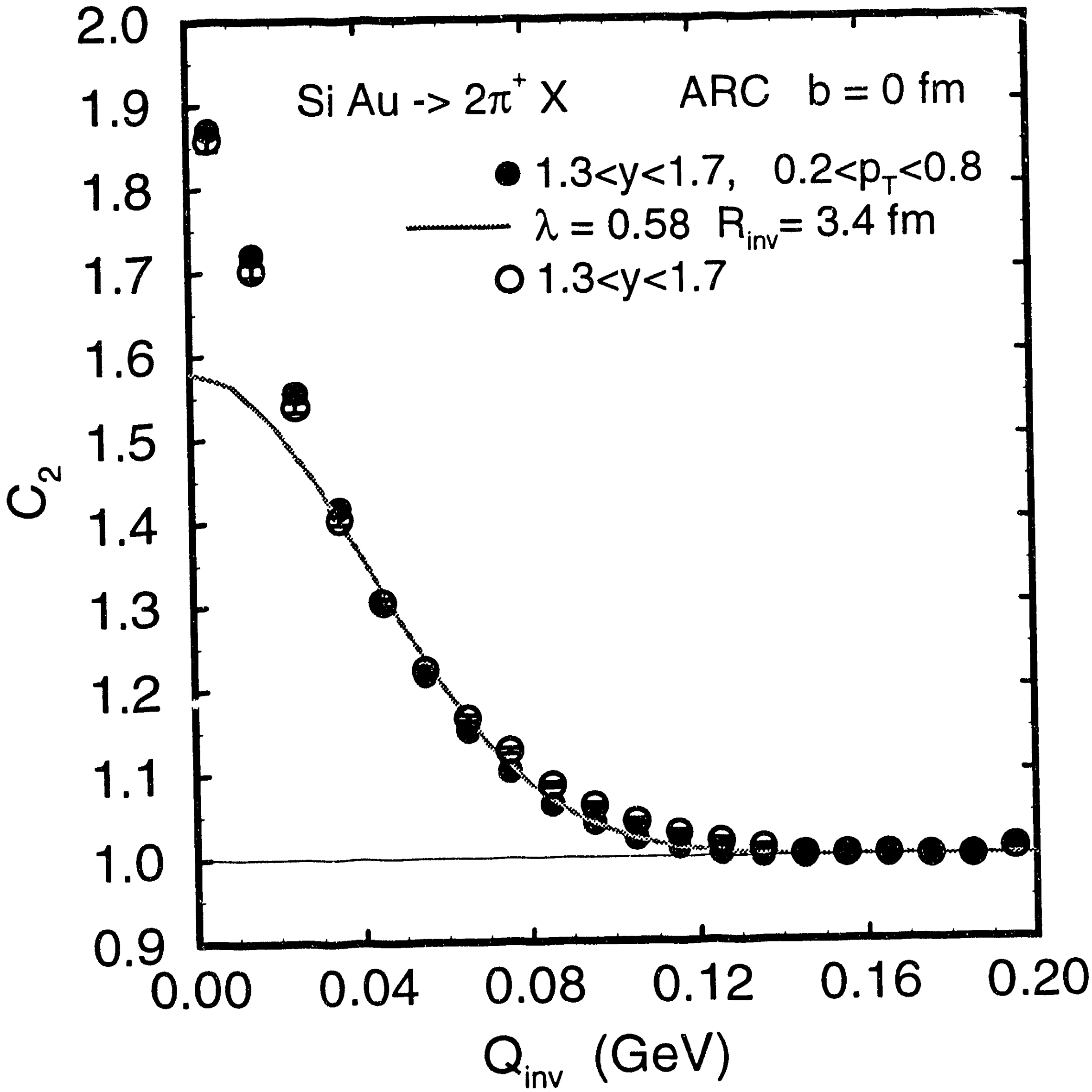

Three Pion Correlations

John Cramer
University of Washington

Three Particle Correlations

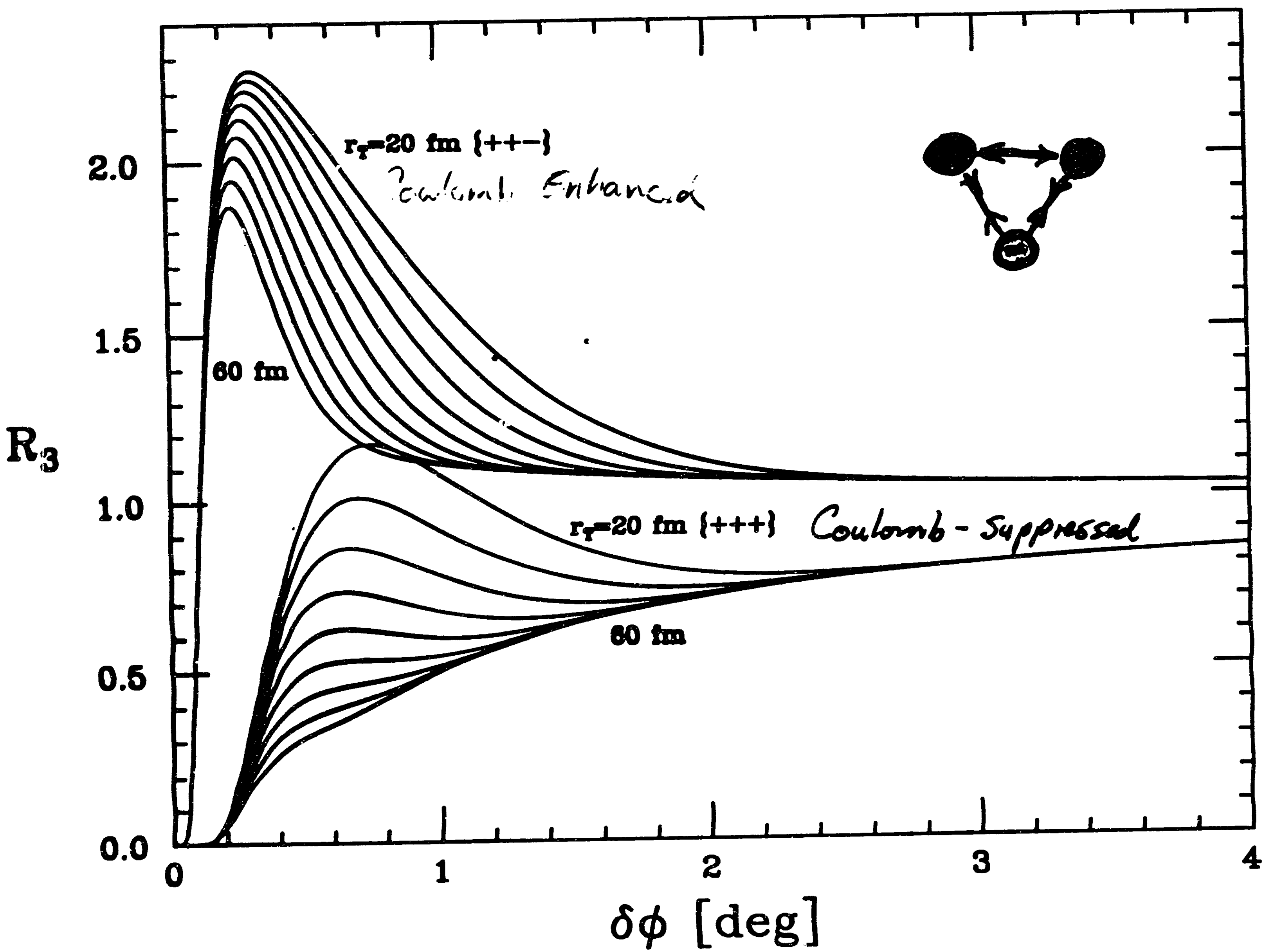

Two-Body Coulomb Corrections to Pion HBT Interferometry

Sommerfeld parameter

$$\eta_{ij} = z_i z_j \alpha / \beta_{ij}$$

α = *fine-structure constant* $\cong 1/137$

β_{ij} = *relative velocity between i and j*

z_i = *charge of* i^{th} *particle*

Gamow Penetrability

$$G(\eta_{ij}) = \frac{2\pi\eta_{ij}}{e^{2\pi\eta_{ij}} - 1}$$

Correction to HBT Correlation Function

$$C_{\text{Charge}}(\vec{q}_{ij}) = G(\eta_{ij}) C_{\text{Neutral}}(\vec{q}_{ij})$$

Three-Body Coulomb Corrections to Pion HBT Interferometry

- There is no general solution to the 3-body Coulomb problem.
- There are sophistocated numerical methods, but these have never been applied to the contunuum appropriate to HBT interferometry.
- However, exact analytic solutions can be obtained in high- and low-momentum limits:

Limit 1: $\eta_{12} \to 0,\ \eta_{23} \to 0,\ \eta_{31} \to 0$

Limit 2: $\eta_{12} \approx 1,\ \eta_{23} \to 0,\ \eta_{31} \to 0$

Limit 3: $\eta_{12} \to \infty,\ \eta_{23} \to \infty,\ \eta_{31} \to \infty$

Limit 4: $\eta_{12} \to \infty,\ \eta_{23} \to -\infty,\ \eta_{31} \to -\infty$
(z_3 *is negative*)

Limiting Cases of Three-Body Coulomb Corrections

Limit 1: $\eta_{12} \rightarrow 0,\ \eta_{23} \rightarrow 0,\ \eta_{31} \rightarrow 0$

$$G_3(\eta_{12},\eta_{23},\eta_{31}) \rightarrow 1 - \pi(\eta_{12}+\eta_{23}+\eta_{31})$$

Limit 2: $\eta_{12} \approx 1,\ \eta_{23} \rightarrow 0,\ \eta_{31} \rightarrow 0$

$$G_3(\eta_{12},\eta_{23},\eta_{31}) \rightarrow G(\eta_{12})$$

Limit 3: $\eta_{12} \rightarrow \infty,\ \eta_{23} \rightarrow \infty,\ \eta_{31} \rightarrow \infty$

$$G_3(\eta_{12},\eta_{23},\eta_{31}) \rightarrow \approx \eta^4 e^{-a\eta} \quad \textit{with } a \cong 6\pi$$

Limit 4: $\eta_{12} \rightarrow \infty,\ \eta_{23} \rightarrow -\infty,\ \eta_{31} \rightarrow -\infty$

(z_3 *is negative*)

$$G_3(\eta_{12},\eta_{23},\eta_{31}) \rightarrow \approx \eta^4$$

Ad Hoc "Candidates" for Three-Body Coulomb Corrections

$$F_1\text{(Riverside)}: \quad G_3(\eta_{12}, \eta_{23}, \eta_{31}) \cong G(\eta_{12})G(\eta_{23})G(\eta_{31})$$

$$F_2\text{(JGC)}: \quad G_3(\eta_{12}, \eta_{23}, \eta_{31}) \cong \tfrac{1}{3}[G(\eta_{12})G(\eta_{23}+\eta_{31}) + G(\eta_{23})G(\eta_{31}+\eta_{12}) + G(\eta_{31})G(\eta_{12}+\eta_{23})]$$

$$F_3\text{(JGC)}: \quad G_3(\eta_{12}, \eta_{23}, \eta_{31}) \cong G(\eta_{12}+\eta_{23}+\eta_{31})$$

Comparison of "Candidate" 3-Body Coulomb Corrections

Form of Candidate 3-Body Coulomb Correction	High Momentum Limits: $\eta \to 0$	High Momentum Limits: $\eta_{23} \to 0$, $\eta_{31} \to 0$	Low Momentum Limits: $\eta \to \infty$ +++	Low Momentum Limits: $\eta \to \infty$ +−+
$F_1 = G(\eta_{12})G(\eta_{23})G(\eta_{31})$	$1 - \pi(\Sigma\eta)$	$G(\eta_{12})$	$(2\pi\eta)^3 e^{-6\pi\eta}$	$(2\pi\eta)^3 e^{-2\pi\eta}$
$F_2 = \frac{1}{3}[G(\eta_{12})G(\eta_{23}+\eta_{31}) + G(\eta_{23})G(\eta_{31}+\eta_{12}) + G(\eta_{31})G(\eta_{12}+\eta_{23})]$	$1 - \pi(\Sigma\eta)$	$G(\eta_{12})$	$2(2\pi\eta)^2 e^{-6\pi\eta}$	$\frac{4}{3}\pi\eta$
$F_3 = G(\eta_{12}+\eta_{23}+\eta_{31})$	$1 - \pi(\Sigma\eta)$	$G(\eta_{12})$	$6\pi\eta\, e^{-6\pi\eta}$	$2\pi\eta$
$F_4 = 1 + C\left(\frac{1}{\eta_{12}^2} + \frac{1}{\eta_{23}^2} + \frac{1}{\eta_{31}^2}\right)^{-\frac{3}{2}}$	1	1	$C\eta^3$	$3^{-\frac{3}{2}} C\eta^3$
$F_5 = F_3 F_4$	$1 - \pi(\Sigma\eta)$	$G(\eta_{12})$	$6\pi C\eta^4 e^{-6\pi\eta}$	$2\pi C\, 3^{-\frac{3}{2}}\eta^4$
Desired Asymptotic Behavior (Preliminary)	$1 - \pi(\Sigma\eta)$	$G(\eta_{12})$	$\approx \eta^4 e^{-a\eta}$	$\approx \eta^4$

Note:

$G(\eta) = 2\pi\eta / (\exp(2\pi\eta) - 1)$

$\eta_{12} = z_1 z_2 \alpha / \beta_{12}$

$\Sigma\eta = \eta_{12} + \eta_{23} + \eta_{31}$

Conclusion:

Preferred *Ad Hoc*

Three-Body Coulomb Correction

$$F_4(\mathrm{JGC}):\ G_3(\eta_{12},\eta_{23},\eta_{31}) \cong$$

$$G(\eta_{12}+\eta_{23}+\eta_{31})\left[1 + C\left(\frac{1}{\eta_{12}^2}+\frac{1}{\eta_{23}^2}+\frac{1}{\eta_{31}^2}\right)^{-\frac{3}{2}}\right]$$

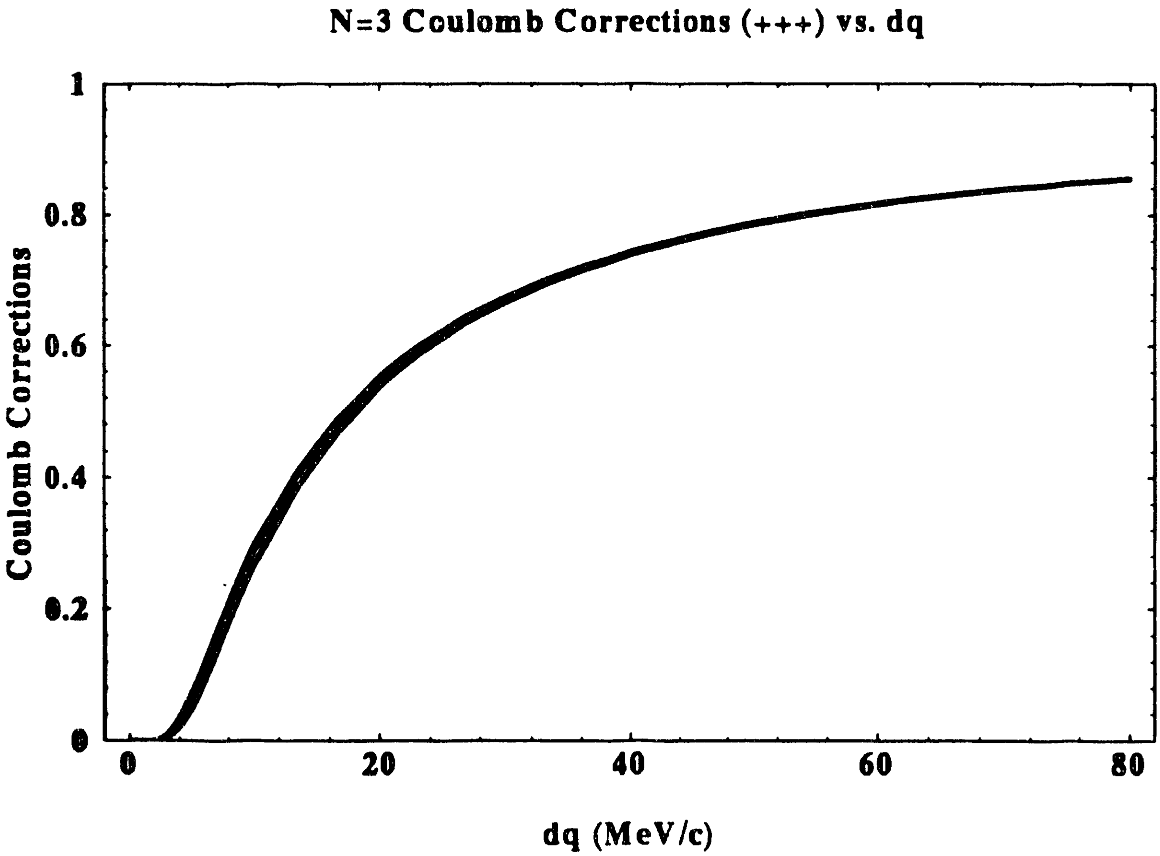
N=3 Coulomb Corrections (+++) vs. dq
Coulomb Corrections
1
0.8
0.6
0.4
0.2
0
0
20
40
60
80
dq (MeV/c)

N=3 Coulomb Corrections (+++) vs. dq

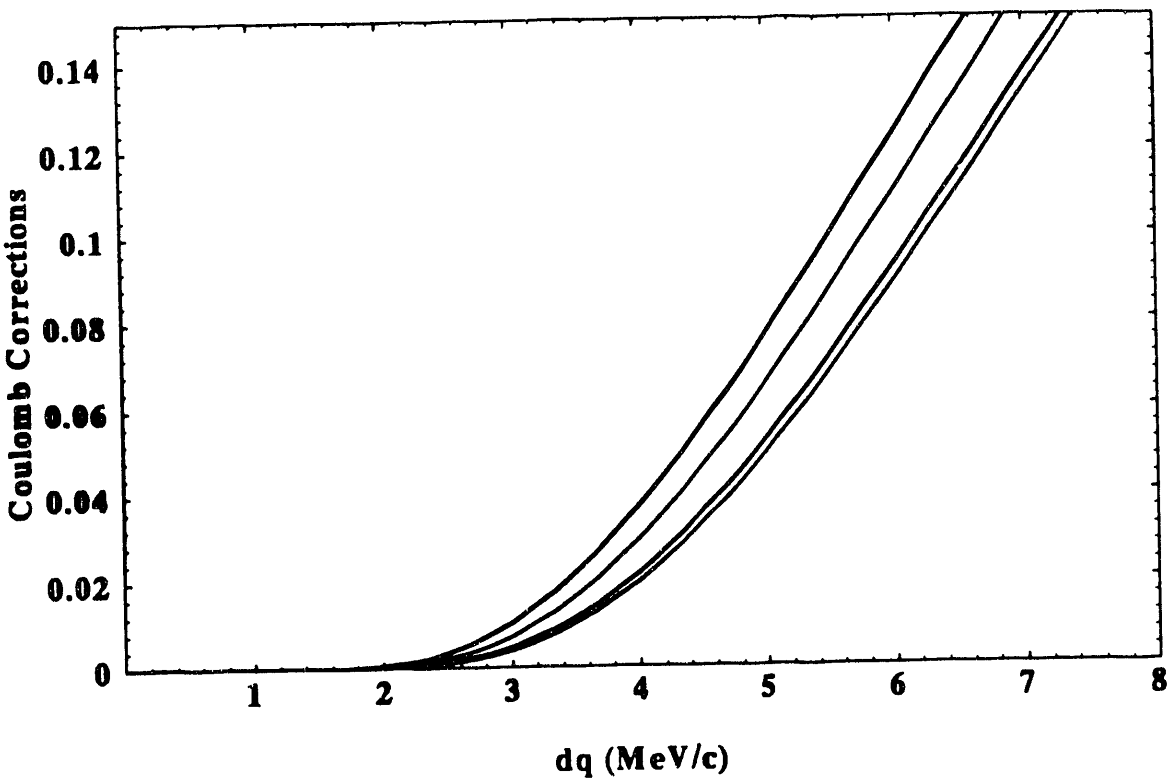

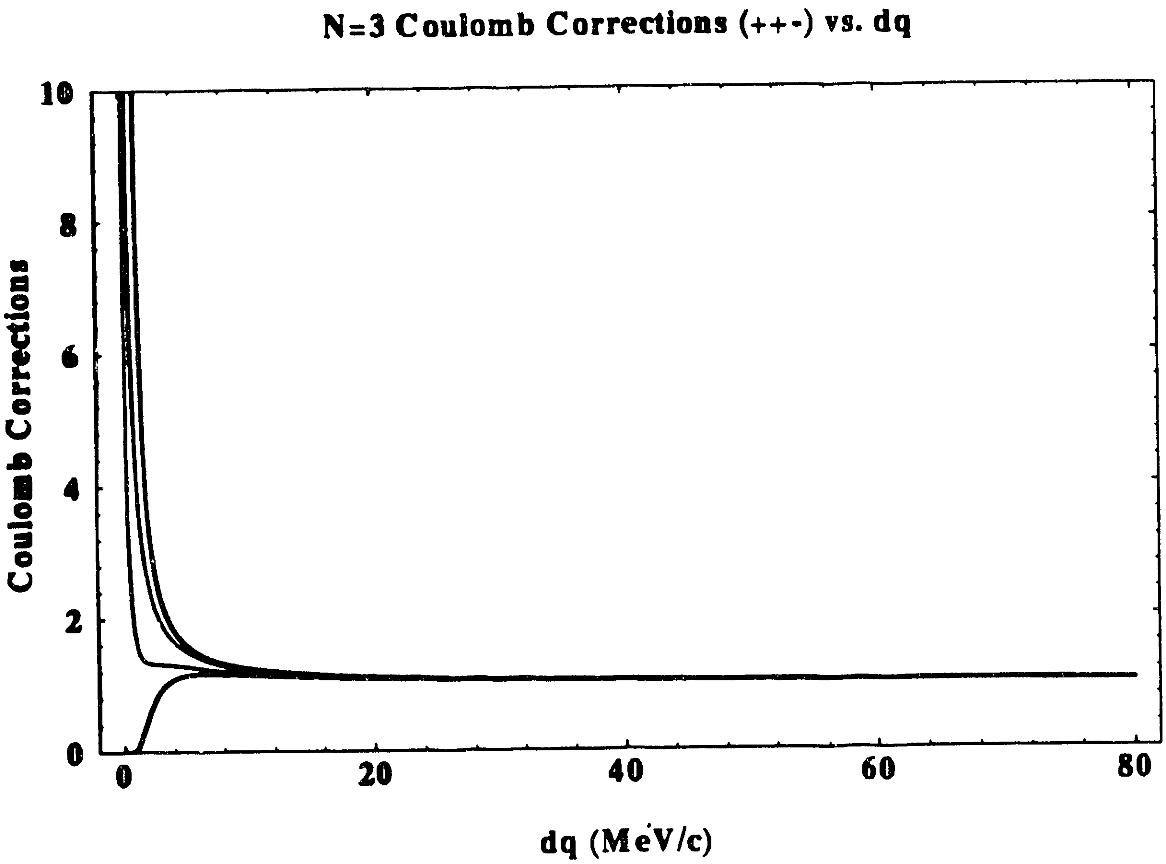
N=3 Coulomb Corrections (++-) vs. dq
Coulomb Corrections
dq (MeV/c)
0
2
4
6
8
10
0
20
40
60
80

Pion Correlations in Proton–induced Reactions at Relativistic Beam Energies

Wolfgang Bauer
Michigan State

Pion Correlations in Proton-Induced Reactions at Relativistic Beam Energies

Wolfgang Bauer
Michigan State University

- Collaborators:

  Pawel Danielewicz
  Dietrich Klakow (→ Erlangen)
  Bao-An Li (→ Berlin)

  } MSU

  Peter Schuck } Grenoble

J. Pluta et al. (DIOGENE): "Possible Observation of Medium Effects Using a Pion Correlation Technique" (submitted to NPA)

Basic idea: Medium modification in π-dispersion relation leads to build-up of σ strength

$\Rightarrow$ look for $\sigma \to \pi^+\pi^-$ by performing invariant mass analysis

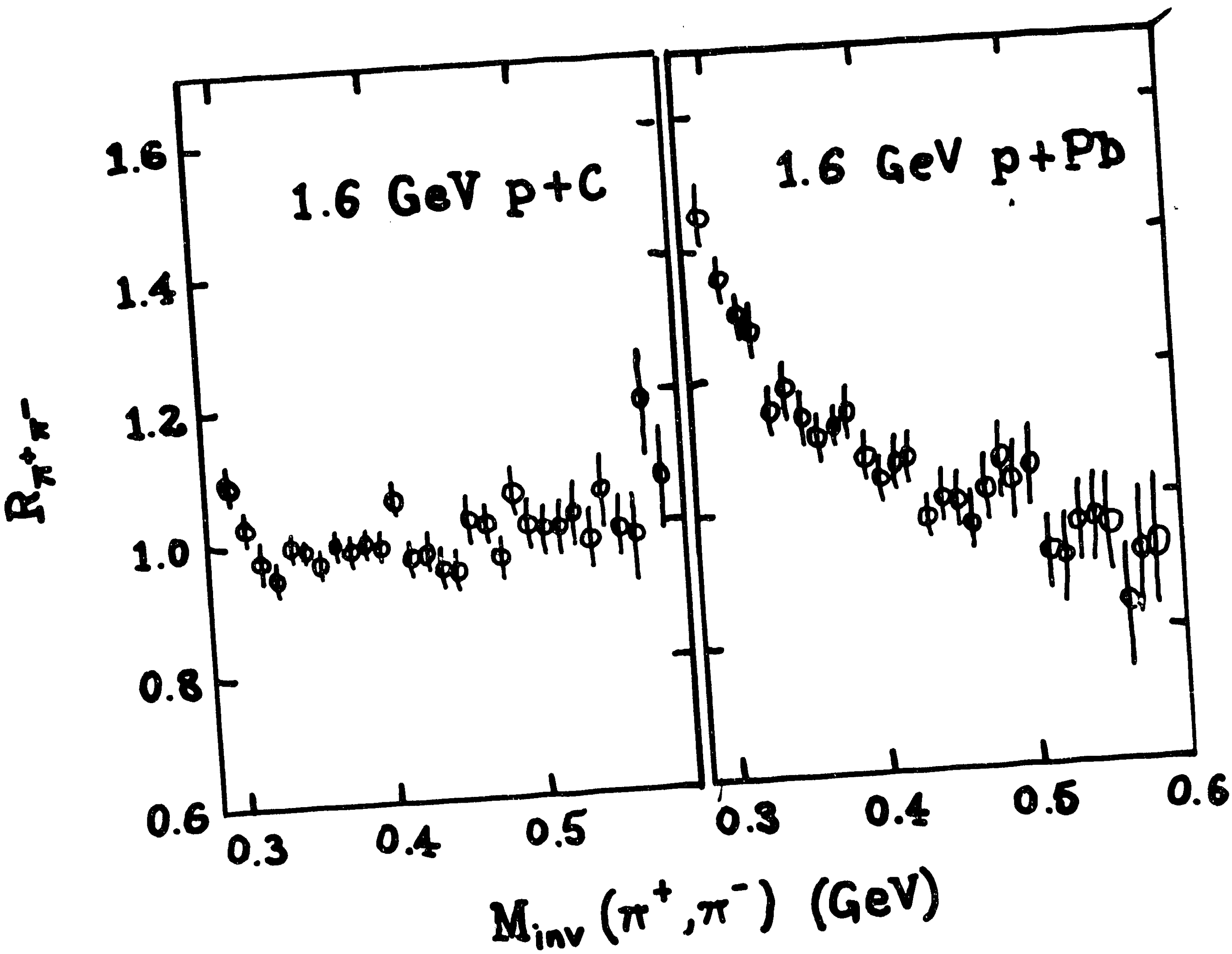

BUU Transport Theory for Relativistic Energies

- Propagation of: p, n, Δ, N^*, π
- Mean field
- Two body collisions

Basic Processes for π production and absorptio

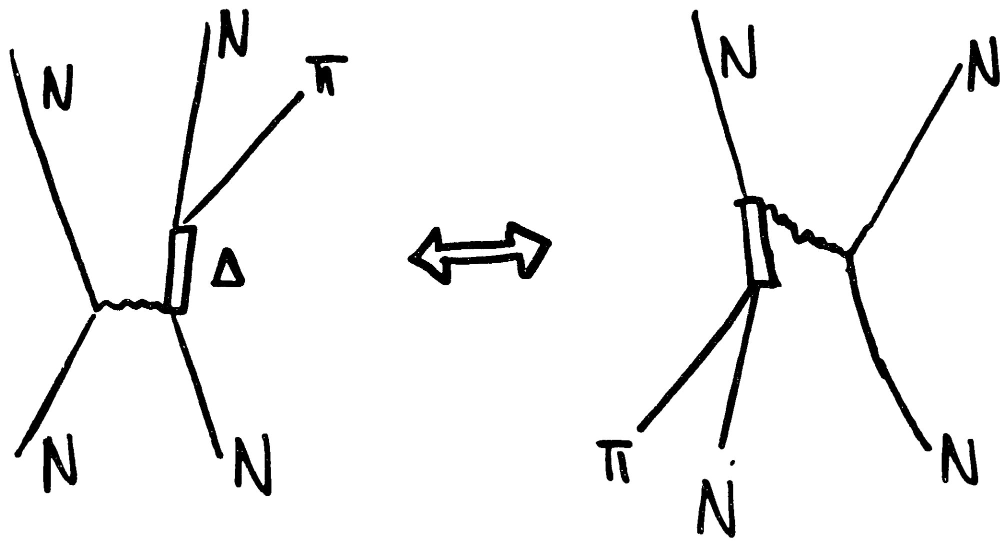

Detailed Balance (Danielewicz & Bertsch NPA 533, 712 (1991))

[Reference: B.A. Li & W.B., PRC 44, 450 (1991)]

Two Temperature Pion Spectra

- Explanation of concave shape of π-spectra from reaction dynamics:

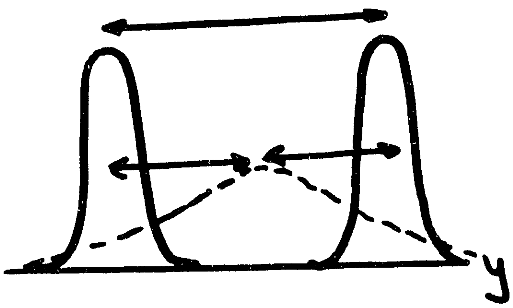

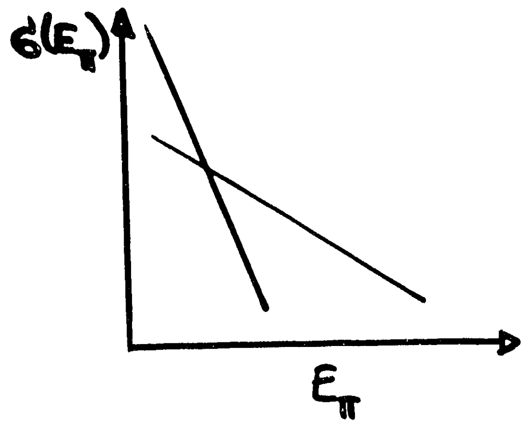

[B.A. Li & W.B., Phys. Lett. B 254, 335 (1991)]

Collective Pion Flow

Explained as due to rescattering and reabsorption of Δ's and π's in spectator matter

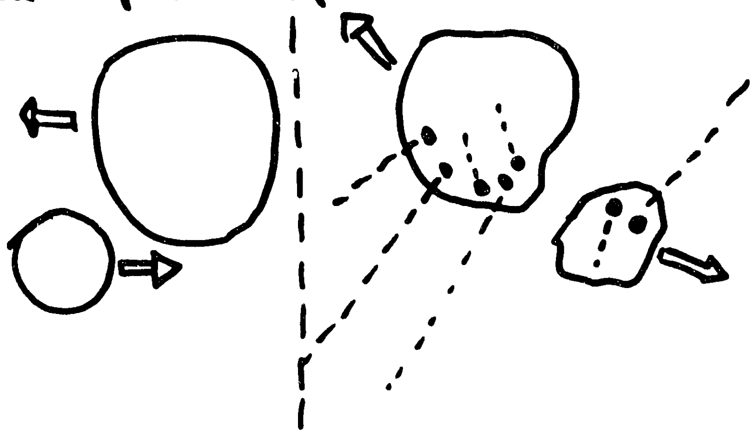

[B.A. Li, W.B., G. Bertsch, PRC 44, 2095 (1991)]

Calculations, B.A. Li, Nucl. Phys., in print

Data, Odyniec et al.

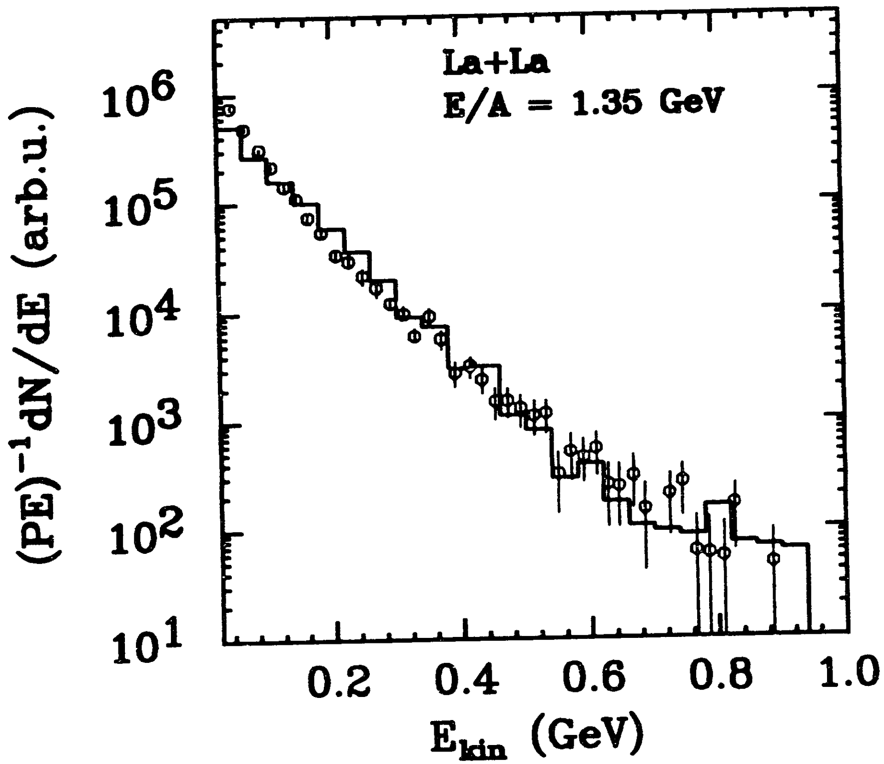

Calculations: B.–A. Li, Nucl. Phys., in print

Data: DIOGENE collaboration

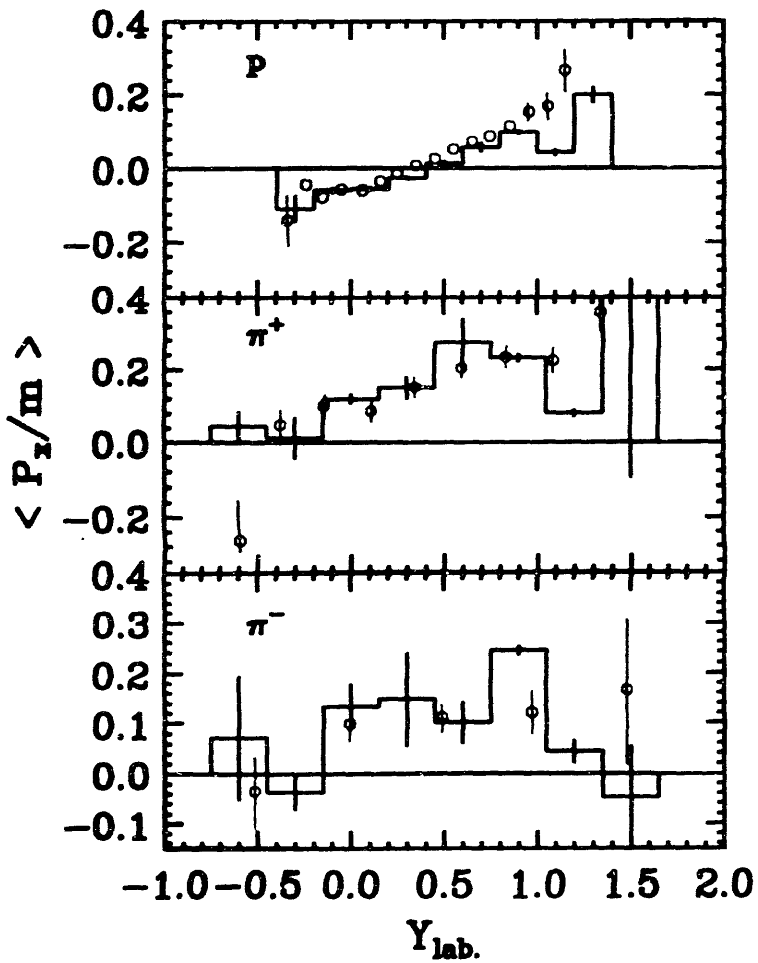

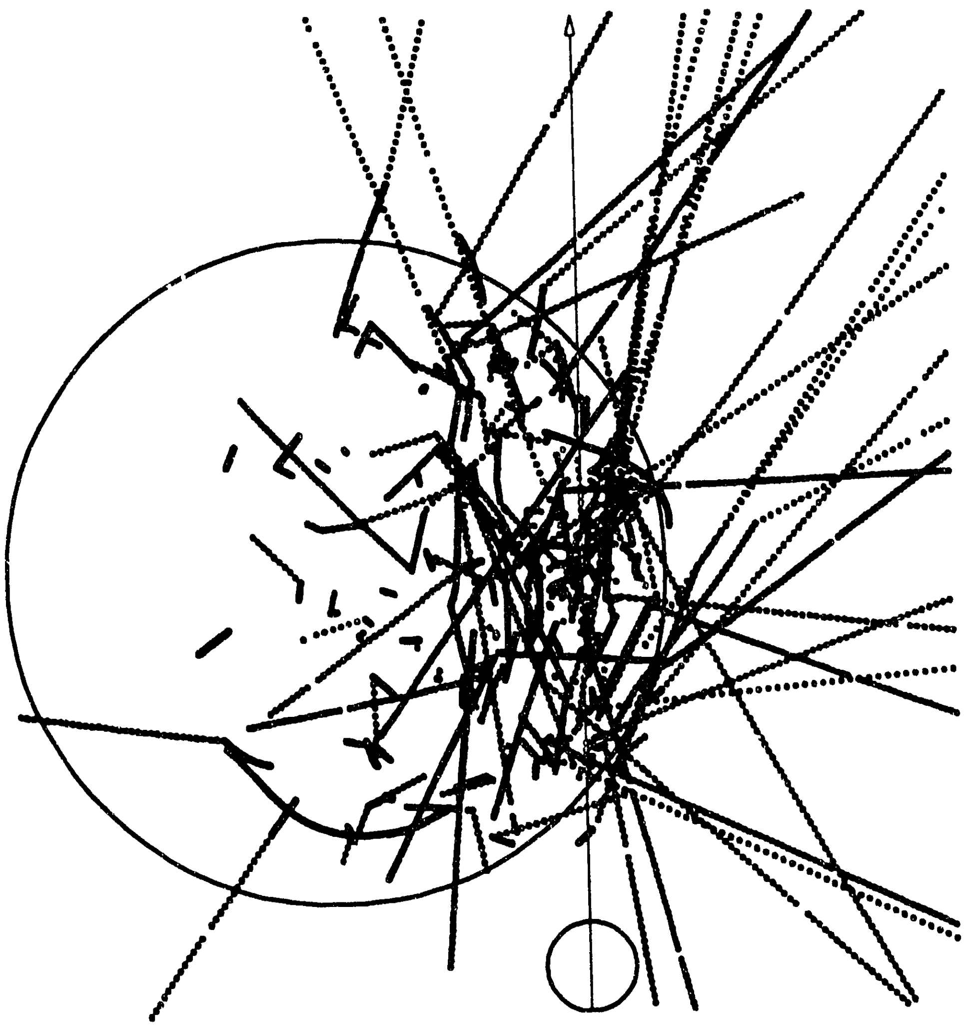

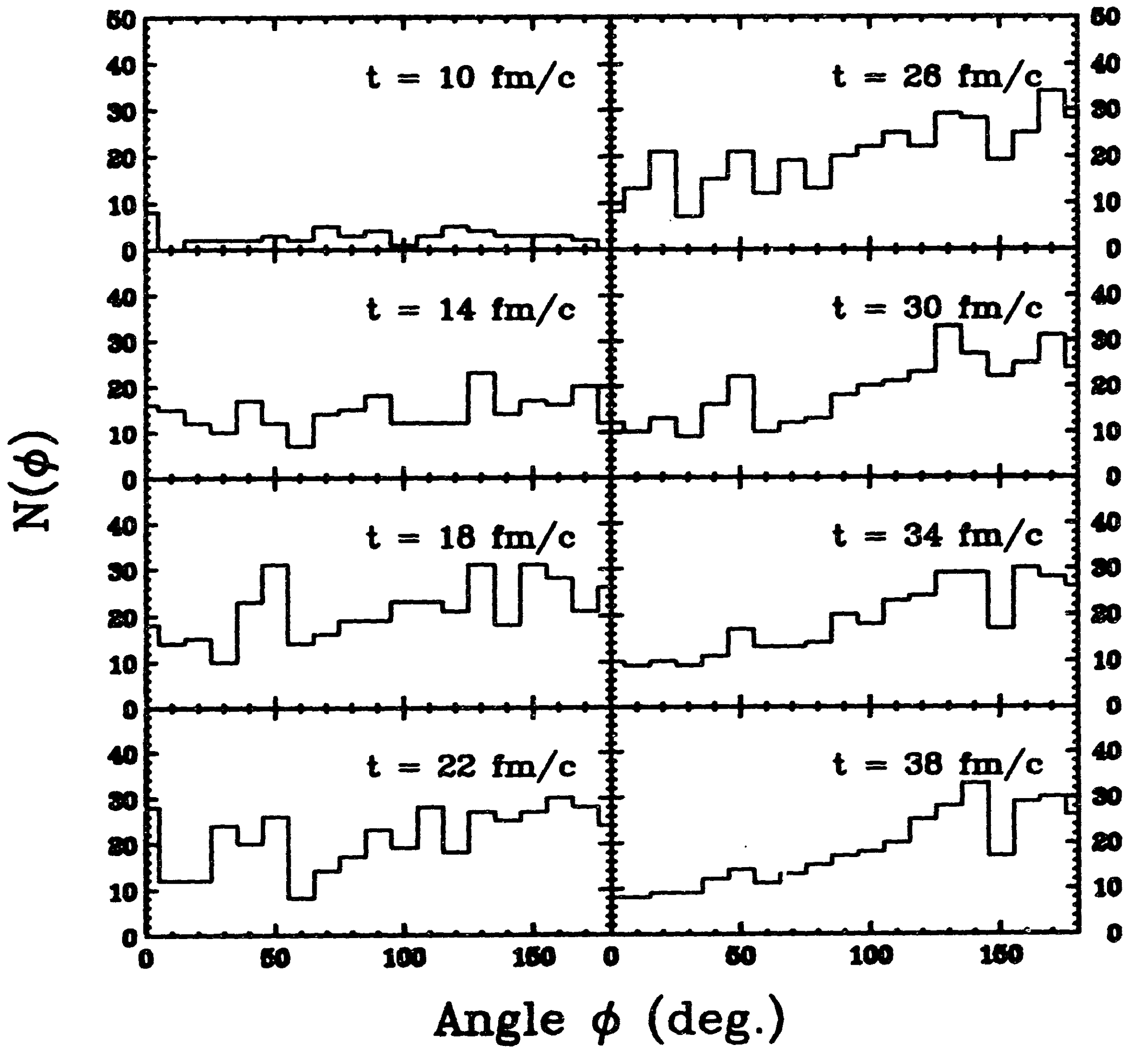

t = 10 fm/c
t = 14 fm/c
t = 18 fm/c
t = 22 fm/c
t = 26 fm/c
t = 30 fm/c
t = 34 fm/c
t = 38 fm/c
N(φ)
Angle φ (deg.)

Rotation of Reaction Plane

Experiment: • Numerator (Signal) → 2π's from same event ⇒ fixed reaction plane

• Denominator (Background) → 2π's from different events ⇒ random relative orientation of reaction plane

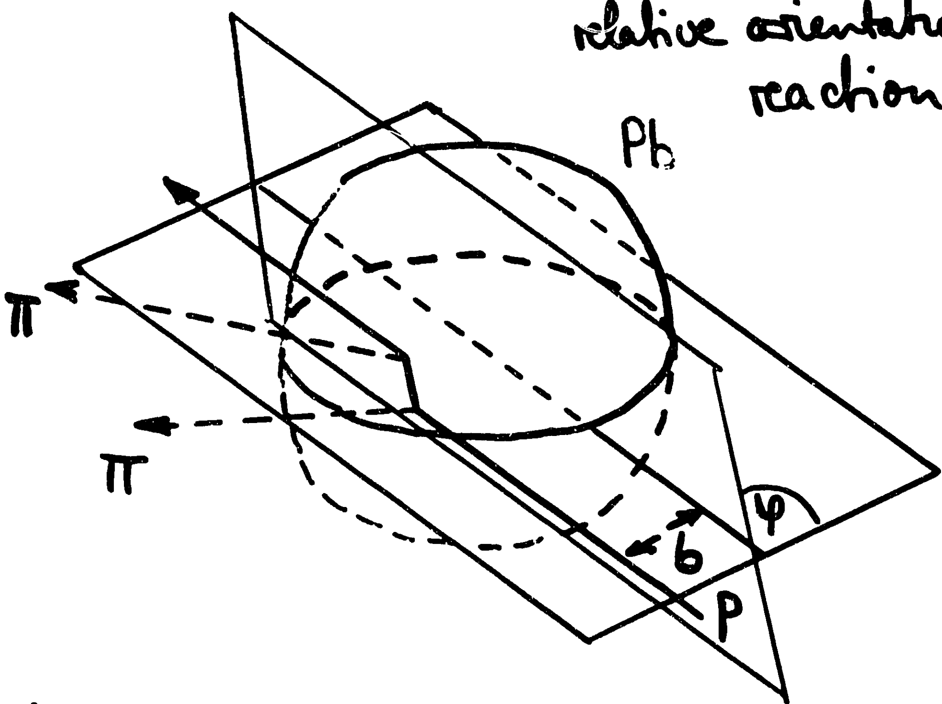

Calculation:

• Numerator: $M_{inv} = \sqrt{(E_1+E_2)^2 - (\vec{p}_1+\vec{p}_2)^2}$

• Denominator: $M_{inv,\varphi} = \sqrt{(E_1+E_2)^2 - (\vec{p}_1 + R(\varphi)\vec{p}_2)^2}$

$$\Rightarrow \boxed{R_{\pi^+\pi^-} = \frac{N(M_{inv})}{\langle N(M_{inv,\varphi})\rangle_\varphi}}$$

Impact Parameter Weighting (p+Pb)

1) Calculated 42000 events (2 cpu weeks, 4000-

2) $\langle n_\pi \rangle \sim 1$, $\sim 5\%$ 2π events
   $\Rightarrow$ 2000 true pairs, not enough for $R_{\pi^+\pi^-}$

3) Distinguish 1st and 2nd generated pions (kinematic constraints)

4) Combine all 1st with all 2nd for a given b

5) Problem: Combined pairs (b) $\not\propto$ real pairs (b)

6) Impact parameter weighting factors needed!

$$N(M_{inv}) = \int db\ \omega(b)\ N(M_{inv}, b)$$

$$\omega(b) = \frac{b}{N_{events}(b)} \cdot \frac{N_{\pi^+\pi^-}(b)}{N_{1,\pi^+}(b) \cdot N_{2,\pi^-}(b) + N_{1,\pi^-}(b) \cdot N_{2,\pi^+}(b)}$$

$N_{\pi^+\pi^-}(b)$ = # of true pairs

$N_{1,\pi^+}(b)$ = # of first generated π^+

$N_{2,\pi^+}(b)$ = # of second generated π^+

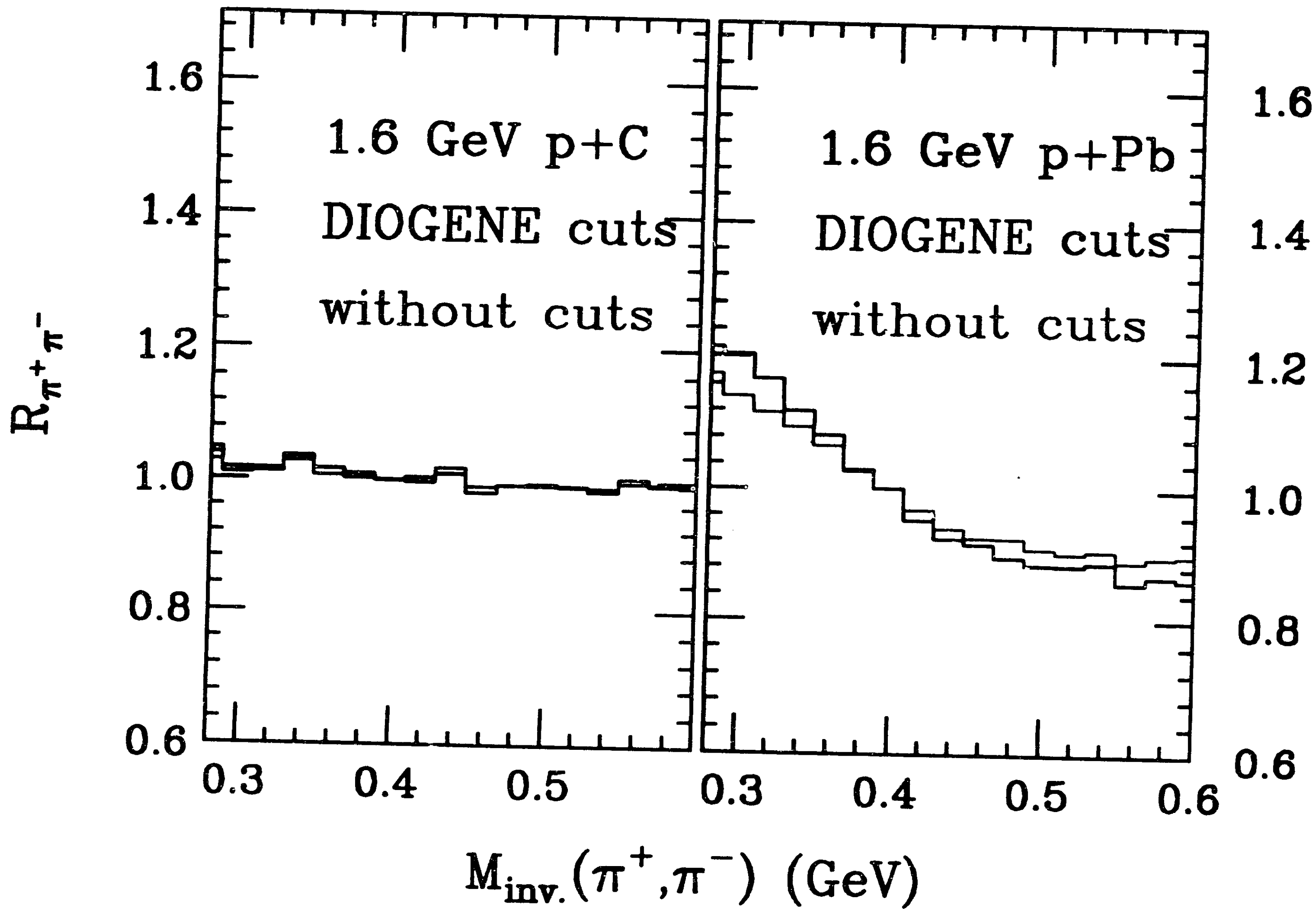
1.6 GeV p+C
DIOGENE cuts
without cuts
1.6 GeV p+Pb
DIOGENE cuts
without cuts
$R_{\pi^+\pi^-}$
$M_{inv.}(\pi^+,\pi^-)$ (GeV)
1.6
1.4
1.2
1.0
0.8
0.6
0.3
0.4
0.5
0.6

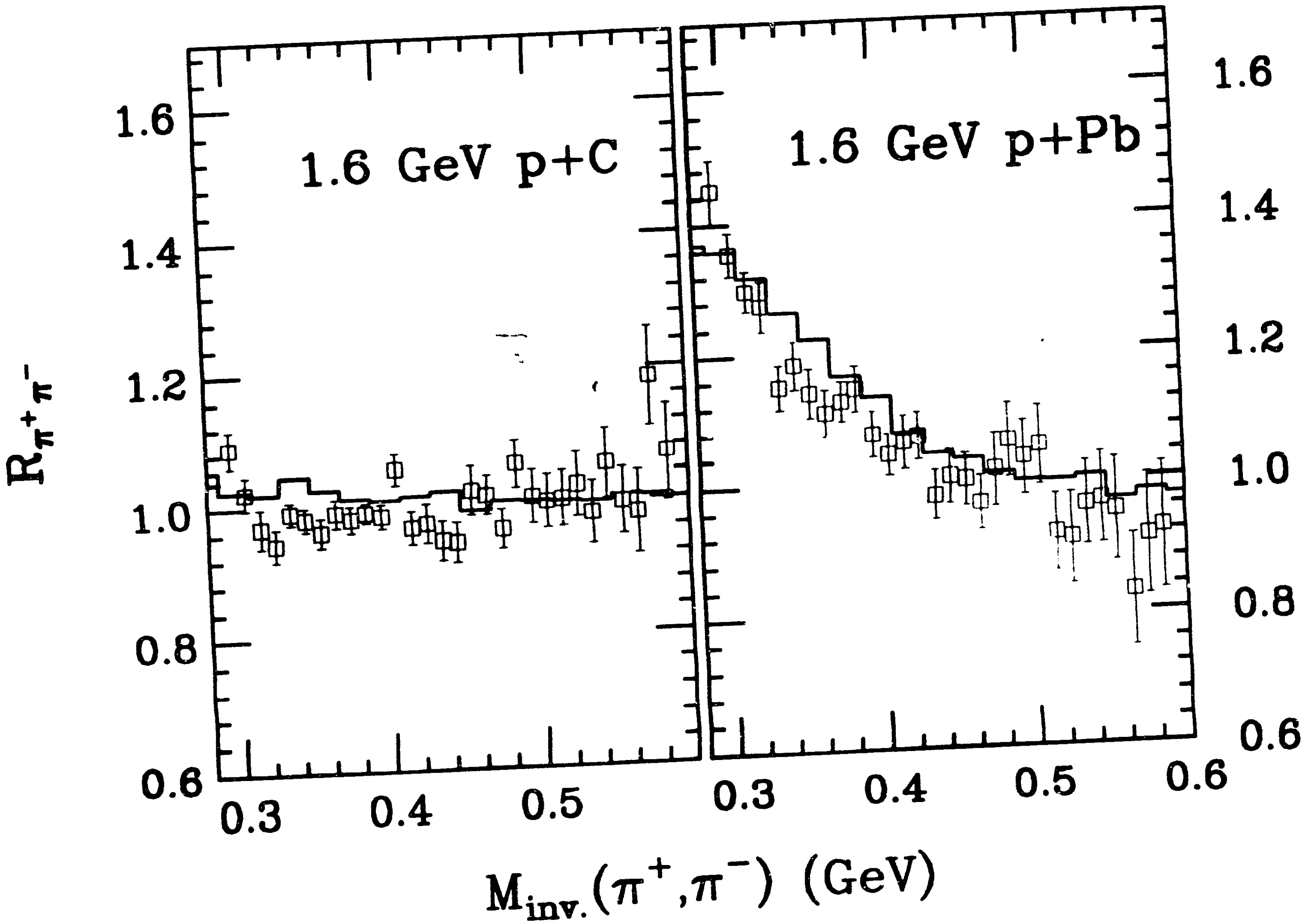
1.6 GeV p+C
1.6 GeV p+Pb
$R_{\pi^+\pi^-}$
0.6
0.8
1.0
1.2
1.4
1.6
0.3
0.4
0.5
0.6
$M_{inv.}(\pi^+,\pi^-)$ (GeV)

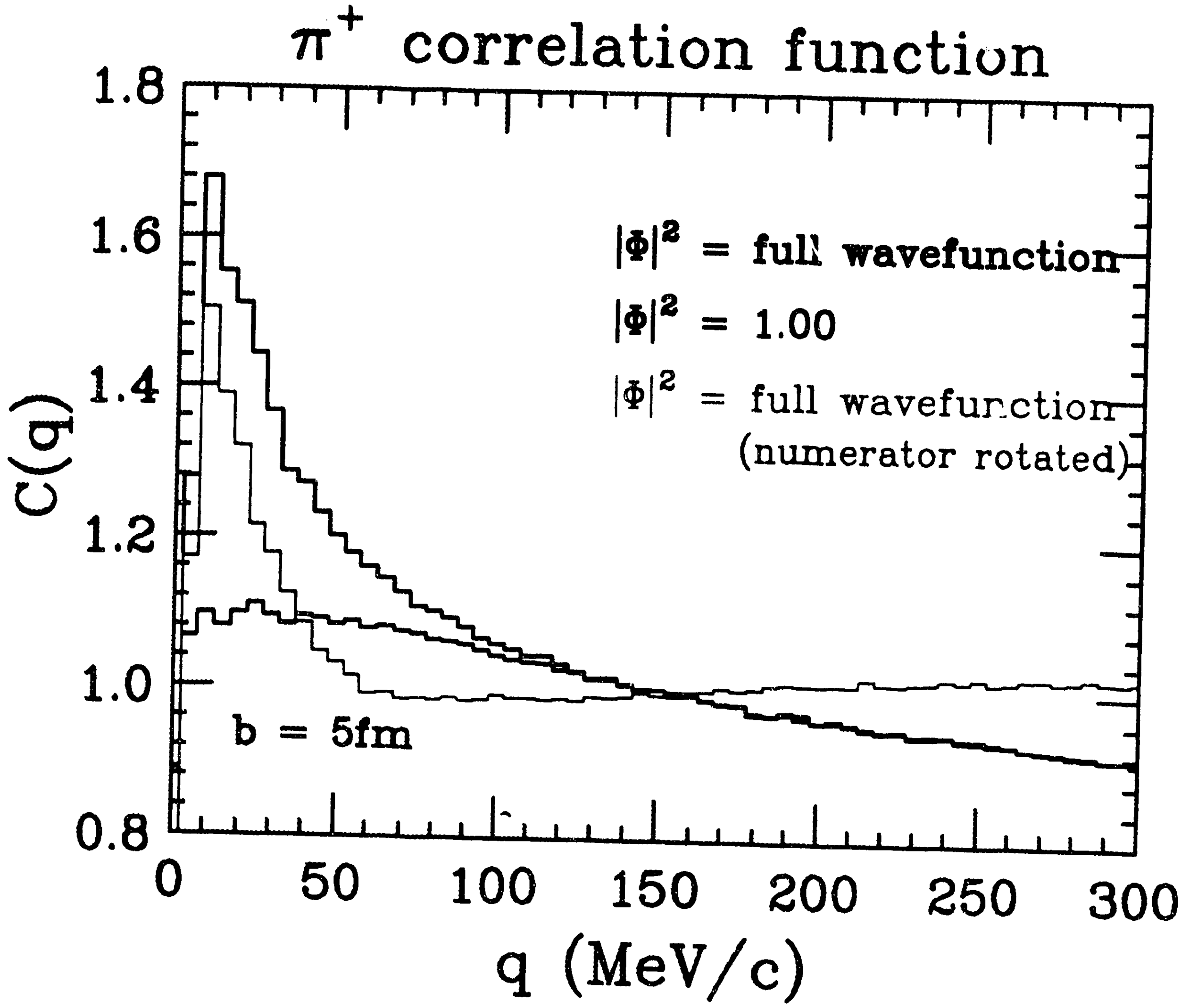

→ Catherine Mader

Anthony Baltz
Physics Department- 510A
Brookhaven National Laboratory
Upton, NY 11973
baltz@bnlcl1.bnl.gov

Wolfgang Bauer
NSCL
Michigan State University
East Lansing, MI 48824-1321
bauer@theo01.nscl.msu.edu

Dana Beavis
Physics Department- 510D
Brookhaven National Laboratory
Upton, NY 11973

George Bertsch
Department of Physics FN-15
University of Washington
Seattle, WA 98195
bertsch@uwaphast

Peter Braun-Munzinger
Department of Physics
SUNY/Stony Brook
Stony Brook, NY 11794
pbm@sb814a.physics.sunysb.edu

Larisa Bravina
Physics Department
University of Bergen
Allegaten 55, 5007
Bergen, Norway
larisa@kvart.fi.uib

Chellis Chasman
Physics Department- 510D
Brookhaven National Laboratory
Upton, NY 11973
chasman@bnldag

Vince Cianciolo
Mass. Inst. Tech.
Bldg. 26-402
77 Mass. Ave.
Cambridge, MA 02139
cianciolo@metal.mit.edu

John Cramer
Nuclear Physics Lab. GL-10
University of Washington
Seattle, WA 98195
cramer@phast.phys.washington.edu

Pawel Danielewicz
NSCL
Michigan State University
East Lansing, MI 48824
danielewicz@nscl.nscl.msu.edu

Gabor David
Physics Department-- 510C
Brookhaven National Laboratory
Upton, NY 11973
david1@bnldag

Jerry Dodd
Nevis Labs
P.O. Box 147
Irvington, NY 10533
dodd@nevis

Carl B. Dover
Physics Department- 510A
Brookhaven National Laboratory
Upton, NY 11973
dover@bnldag

Sean Gavin
Physics Department- 510A
Brookhaven National Laboratory
Upton, NY 11973
sean@nth1.phy.bnl.gov

Michel Gonin
Physics Department
Brookhaven National Laboratory
Upton, NY 11973
gonin@hi0.hirg.bnl.gov

Miklos Gyulassy
Physics Department
Columbia University
538 West 120th Street
New York, NY 10027
gyulassy@nt1.phys.columbia.edu

Michael Herrmann
INT
University of Washington
Seattle, WA 98195
herrmann@ben.npl.washington.edu

Byungsik Hong
Department of Physics
SUNY/Stony Brook
Stony Brook, NY 11794-3800
hong@sb814a.physics.sunysb.edu

Tom Humanic
Department of Physics
Ohio State University
Columbus, OH 43210
humanic@ohstpy

Barbara Jacak
MS D456
Los Alamos National Lab.
Los Alamos, NM 87545
jacak@p2vax.lanl.gov

Sid Kahana
Physics Department- 510A
Brookhaven National Laboratory
Upton, NY 11973
kahana@bnlcl1

Volker Koch
Physics Department
SUNY/Stony Brook
Stony Brook, NY 11794
vkoch@sunysbnp.bitnet

Shiva Kumar
Department of Physics
Yale University
New Haven, CT
shiva@alladin.physics.yale.edu

Catherine Mader
NSCL
Michigan State University
East Lansing, MI 48824-1321
mader@msunscl

Richard Morse
MS-50D
LBL
1 Cyclotron Road
Berkeley, CA 94720
rmorse@esa2.lbl.gov

Shoji Nagamiya
Columbia U., Nevis Labs.
P.O. Box 137
Irvington, NY 10533
nag@nevis.phys.columbia.edu

Tapan Nayak
Nevis Labs, Columbia U.
P.O. Box 137
Irvington, NY 10533
nayak@nevis

Craig Ogilvie
Bldg. 26-413
MIT
Cambridge, MA 02138
ogilvie@mitlns.mit.edu

Sandra S. Padula
Inst. de Fis. Teor. UNESP
Rua Pamplona, 145
01405-900 San Paulo - S.P.
Brazil
padula@192.160.128.1

Yang Pang
Physics Department- 510A
Brookhaven National Laboratory
Upton, NY 11973
pang@bnlnth.phy.bnl.gov

Serge Panitkin
Physics Department
SUNY/Stony Brook
Stony Brook, NY 11794

Max Potekhin
Physics Department, Pupin Lab
Columbia University
New York, NY 10027

Scott Pratt
NSCL
Michigan State University
East Lansing, MI 48824
pratt@msunscl

Louis Remsberg
Chemistry Dept.
Brookhaven National Laboratory
Upton, NY 11973
remsberg@bnldag

Thomas J. Schlagel
Physics Department- 510A
Brookhaven National Laboratory
Upton, NY 11973
schlagel@bnlnth.phy.bnl.gov

Ekkard Schnedermann
Physics Department- 510A
Brookhaven National Laboratory
Upton, NY 11973
schneder@nth3.phy.bnl.gov

Peter Schuck
Inst. des Sciences Nucleaires
53 Av Martyrs
38026 Grenoble, France
schuck@frcpn11

Sezgnei Sedykh
Department of Physics
SUNY/Stony Brook
Stony Brook, NY 11794
sedykh@sb814a.physics.sunysb.edu

Edward Shuryak
Physics Department
SUNY/Stony Brook
Stony Brook, NY 11794
shuryak@sunysbnp.bitnet

Ron Soltz
MIT, Rm. 26-402
77 Mass. Ave.
Cambridge, MA 02139
soltz@metal.mit.edu

Heinz Sorge
LANL
Los Alamos, NM 87545
sorge@lampf

George Stephans
Bldg. 26 Rm 415
MIT
Cambridge, MA 02138
gsfs@mitlns.mit.edu

Johanna Stachel
Physics Department
SUNY/Stony Brook
Stony Brook, NY 11794-3800
stachel@sunysbnp.bitnet

John Sullivan
MS D456
Los Alamos National Lab.
Los Alamos, NM 87545
sullivan@p2vax.lanl.gov

Michael Tannenbaum
Physics Department- 510C
Brookhaven National Laboratory
Upton, NY 11973
sapin@bnldag

Flemming Videbaek
Physics Department- 510D
Brookhaven National Laboratory
Upton, NY 11973
videbaek@hi0.hirg.bnl.gov

Ole Vossnack
Columbin Univ. Nevis Labs
P.O. Box 137
Irvington, NY 10533
vossnack@nevis

Yufeng Wang
Columbin Univ. Nevis Labs
P.O. Box 137
Irvington, NY 10533
wang1@nevis

Joseph Weneser
Physics Department– 510A
Brookhaven National Laboratory
Upton, NY 11973

Johannes Wessels
Physics Department
SUNY/Stony Brook
Stony Brook, NY 11794
wessels@sb814a.physics.sunysb.edu

Li Xiong
Physics Department
SUNY/Stony Brook
Stony Brook, NY 11794

Nu Xu
Physics Department
SUNY/Stony Brook
Stony Brook, NY 11794
xu@sb814e.physics.sunysb.edu

W.A. Zajc
Columbia Univ. Nevis Labs.
P.O. Box 137
Irvington, NY 10533
zajc@nevis.nevis.columbia.edu

Yingchao Zhang
Physics Department
SUNY/Stony Brook
Stony Brook, NY 11794

Fan Zhu
Physics Department– 510D
Brookhaven National Laboratory
Upton, NY 11973
zhu@hi0.hirg.bnl.gov

Chuan-Ming Zou
Department of Physics
SUNY/Stony Brook
Stony Brook, NY 11794
zou@sb814e.physics.sunysb.edu

DATE
FILMED
8/10/93

END